UNIVERSITY OF LIVERPOOL

An Investigation into the Role of the Hyperpolarisation-Activated Cyclic Nucleotide-Gated Ion Channels in Dorsal Root Ganglion Neurons in Rat Models of Chronic Inflammatory and Neuropathic Pain

Thesis submitted in accordance with the requirements of the University of Liverpool for the degree of Doctor in Philosophy

By Trevor Smith

September 2012

Acknowledgements

This work could not have been completed without the support and guidance of a number of people, primarily my principal supervisor, Dr. Laiche Djouhri. I am incredibly grateful for all of his advice, constant help, patience and support, as I have developed my career under his tutelage. I would also like to thank my secondary supervisor, Dr. Jean Sathish, for offering brilliant guidance throughout. Furthermore, I'd like to thank Dr. Richard Morris and Dr. Xiechuan Weng for, respectively, teaching me how to perform immunofluorescent and *in vivo* experiments. In addition I am grateful to Ms. Ailsa Dermody and Ms. Caroline Staunton, for their engaging discussions and help overcoming a multitude of challenges. Multiple support staff have been essential, particularly Mrs. Joanne Herriott, Mrs. Pam Pask, Mrs. Katherine Gittins, and Mr. Robert Galvin, in addition to all of the staff in the B.S.U., all of the staff in the Department of Pharmacology and many people in the Department of Physiology.

Personally, I'd like to thank my girlfriend Daiva, for her patience and support throughout this project, in addition to all of my family members, particularly my brother Steven, from the Smith, Buchert and Puriene families. In addition, this work would not have been completed without the support of my close friends, particularly Hannah, Dayani, Nesan and Rory.

Finally, I'd like to thank the funders of my work: the IMB consortium. Thanks to their generous financial backing, this costly, *in vivo* based project was able to proceed and contribute to elucidating the role of the HCN channels in chronic pain.

Table of Contents

Abbreviations of Key Words

CGRP = **C**alcitonin **G**ene **R**elated **P**eptide

cAMP = **c**yclic **A**denosine **M**ono**p**hosphate

CFA = **C**omplete **F**reund's **A**djuvant

COX-2 = **C**yclo**o**xygenase-**2**

CNS = **C**entral **N**ervous **S**ystem

CP = **C**hronic **P**ain

- **CIP** = **C**hronic **I**nflammatory **P**ain
- **CNP** = **C**hronic **N**europathic **P**ain

D-Hair = **D**own **Hair**

DAPI = 4',6-diamidino-2-phenylindole

DRG = **D**orsal **R**oot **G**anglion

G-Hair = **G**uard **Hair**

HCN = **H**yperpolarisation-Activated, **C**yclic **N**ucleotide-Gated Ion Channels

- **HCN1** = **HCN** Subunit **1**
- **HCN2** = **HCN** Subunit **2**
- **HCN3** = **HCN** Subunit **3**
- **HCN4** = **HCN** Subunit **4**

HTM = **H**igh-**T**hreshold **M**echanoreceptors

IB4 = **I**solectin-**B4**

I_h = Hyperpolarisation-Activated Current

IP = **I**nflammatory **P**ain

LTM = **L**ow-**T**hreshold **M**echanoreceptor

L3 – L6 = **L**umbar **3** – **L**umber **6** Spinal Nerves

mSHAM = **Sham** Operation Control for mSNA

mSNA = **M**odified **S**pinal **N**erve **A**xotomy

NP = **N**europathic **P**ain

PNS = **P**eripheral **N**ervous **S**ystem

RAdapt = **R**aidly **Adapt**ing Low Threshold Mechanoreceptor

SA = **S**pontaneous **A**ctivity

SAdapt = **S**lowly **Adapt**ing Low Threshold Mechanoreceptor

SFL = **S**pontaneous **F**oot **L**ifting

SN = **S**pinal **N**erve

SP = **S**pontaneous **P**ain

STT = **S**pino**t**halamic **T**ract

SubP = **Sub**stance **P**

Key Words Cut-Out

CGRP = **C**alcitonin **G**ene **R**elated **P**eptide

cAMP = **c**yclic **A**denosine **M**ono**p**hosphate

CFA = **C**omplete **F**reund's **A**djuvant

COX-2 = **C**yclo**o**xygenase-**2**

CNS = **C**entral **N**ervous **S**ystem

CP = **C**hronic **P**ain

- **CIP** = **C**hronic **I**nflammatory **P**ain
- **CNP** = **C**hronic **N**europathic **P**ain

D-Hair = **D**own **Hair**

DAPI = 4',6-diamidino-2-phenylindole

DRG = **D**orsal **R**oot **G**anglion

G-Hair = **G**uard **Hair**

HCN = **H**yperpolarisation-Activated, **C**yclic **N**ucleotide-Gated Ion Channels

- **HCN1** = **HCN** Subunit **1**
- **HCN2** = **HCN** Subunit **2**
- **HCN3** = **HCN** Subunit **3**
- **HCN4** = **HCN** Subunit **4**

HTM = **H**igh-**T**hreshold **M**echanoreceptors

IB4 = **I**solectin-**B4**

I_h = Hyperpolarisation-Activated Current

IP = **I**nflammatory **P**ain

LTM = **L**ow-**T**hreshold **M**echanoreceptor

L3 – L6 = **L**umbar **3** – **L**umber **6** Spinal Nerves

mSHAM = **Sham** Operation Control for mSNA

mSNA = **M**odified **S**pinal **N**erve **A**xotomy

NP = **N**europathic **P**ain

PNS = **P**eripheral **N**ervous **S**ystem

RAdapt = **R**aidly **Adapt**ing Low Threshold Mechanoreceptor

SA = **S**pontaneous **A**ctivity

SAdapt = **S**lowly **Adapt**ing Low Threshold Mechanoreceptor

SFL = **S**pontaneous **F**oot **L**ifting

SN = **S**pinal **N**erve

SP = **S**pontaneous **P**ain

STT = **S**pino**t**halamic **T**ract

SubP = **Sub**stance **P**

Thesis Abstract

Chronic **p**ain {**CP**} is a major health problem that affects about 20% of adults worldwide. Unlike acute, physiological pain, which resolves promptly once the painful stimulus is removed, CP can last for months, years or even a lifetime. CP, which includes **i**nflammatory **p**ain {**IP**} that is associated with both tissue injury and the accompanying inflammation and peripheral **n**europathic **p**ain {**NP**} that is a direct consequence of a lesion or disease affecting the **p**eripheral **n**ervous **s**ystem {**PNS**}, often is a constant burden, degrades peoples' quality of life, and costs billions of pounds. Patients with CP usually complain of either: a) continuous or intermittent spontaneous, un-provoked pain; or b) hypersensitivity, due to either increased pain from a stimulus that normally provokes pain or pain due to a stimulus that does not normally provoke pain. Successful therapy for CP, particularly NP, remains a challenge because the currently available drugs are largely ineffective and many result in adverse side effects. Therefore, there is a pressing need to understand the pathophysiology of CP, in order to devise appropriate palliative and curative strategies.

CP is believed to be due, at least partly, to increased excitability of normally quiescent **d**orsal **r**oot **g**anglion {**DRG**} neurons, which convey sensory information from the periphery to the **c**entral **n**ervous **s**ystem {**CNS**}. However, the underlying ionic and molecular mechanisms of this neuronal hyperexcitability and **s**pontaneous **a**ctivity {**SA**} are poorly understood. The aim of this research project was to examine the hypothesis that during peripheral CP states, hyperexcitability in DRG neurons could be due to increased expression of **h**yperpolarisation-activated **c**yclic **n**ucleotide-gated {**HCN**} channels, possibly in combination with a change in their activation properties. This is because these channels, which are composed of 4 subunits {**HCN1-4**}, produce an excitatory inward current, termed the hyperpolarisation-activated {I_h} current in neurons, that depolarizes the membrane potential toward the threshold of **a**ction **p**otential {**AP**} generation. To test this hypothesis, several integrated approaches,

including behavioural pharmacology, *in vivo* electrophysiology, and immunofluorescent staining, were used in two rat models of CP that were compared to appropriate controls. The rat models of CP were: a) **c**hronic **i**nflammatory **p**ain {**CIP**} model, which involved induction of hindlimb inflammation with **c**omplete **F**reund's **a**djuvant {**CFA**}; and b) **c**hronic **n**europathic **p**ain {**CNP**} model that involved L5 **s**pinal **n**erve {**SN**} axotomy, in addition to loose ligation of the L4 SN with neuro-inflammation inducing chromic gut, referred to as **m**odified **SN A**xotomy {**mSNA**}. The objectives of the current project were to:

- **(i)** evaluate, using behavioural pharmacology, the influence of modulating the HCN channels with the I_h-specific blocker, ZD7288, on pain hypersensitivity in both CIP and CNP.
- **(ii)** determine, using *in vivo* intracellular voltage and current recordings, the difference in AP parameters between normal and mSNA-treated L4 DRG neurons and the effect of ZD7288 on SA in the mSNA-treated L4 DRG neurons.
- **(iii)** determine, using immunofluoresence, the types of DRG neuron that express HCN1-HCN3 subunits in normal rats and whether expression of these subunits is altered in both CIP and CNP.

The results showed:

1. In both CIP and CNP, peripheral administration of ZD7288 resulted in significant attenuation of mechanical hypersensitivity and a non-significant absence of **s**pontaneous **p**ain {**SP**}.
2. In the L4 DRG neurons of mSNA-treated animals with CNP, ZD7288 had no effect on the frequency of SA from **l**ow-**t**hreshold **m**echanoreceptors {**LTM**} and induced changes in hyperpolarisation-associated AP parameters in Aα/β-fibre DRG neurons.
3. In both CIP and CNP, an increased proportion of small and medium sized DRG neurons express HCN2, but not HCN1 or HCN3, channel protein.

Taken together, the findings suggest that HCN channels, particularly HCN2, in specific sub-populations of DRG neurons contribute to the development of CIP and CNP.

Chapter 1 - Introduction

1.1. Abstract

The nervous system is a specialised biological system that is essential for protecting the body from noxious, or harmful, stimuli. Acute, short-lasting pain is essential to avoid injury, but persistent, **c**hronic **p**ain {**CP**} can be debilitating and life-ruining. Neuronal circuitry is extremely sensitive to changes and CP causes maladaptive changes, or plasticity, to this circuitry, partly by changing the expression of ion channel subunits that are embedded in the plasma membrane of highly specialised neurons. In peripheral CP, **d**orsal **r**oot **g**anglion {**DRG**} neurons undergo changes that alter their innate excitability, although there are many ion channels that could be implicated in this hyperexcitability. Despite efforts to characterise a vast number of ion channel subunits, the role of the **h**yperpolarisation-activated, **c**yclic **n**ucleotide-gated ion {**HCN**} channel subunits, of which there are four {**HCN1-4**} that form homo- or hetero-tetramers to mediate the hyperpolarisation-activated current {I_h}, are not clear. Therefore, it is possible that the expression of HCN1-4 in DRG neurons may play a pivotal contributory role to the development of CP states. HCN1-4 can be modulated by a variety of biological mediators and their exact physiological roles in CP are not clear. This thesis aims to examine their involvement in two rodent models of CP, both inflammatory pain {**IP**} and neuropathic pain {**NP**}, using three techniques.

1.2. Pain: Acute vs. Chronic

1.2.1. The Human Nervous System and Pain

The human body contains a series of highly specialised and interconnected biological systems that respond rapidly to noxious, or harmful, stimuli, and protects the body before long-lasting tissue damage occurs. By utilising a highly complex, sensory system, information from the periphery about a wide variety of stimuli, both noxious and non-noxious, is conducted to the brain, where the sensation of pain is first perceived (Woolf and Ma, 2007; Basbaum et al., 2009).

According to the International Association for the Study of Pain, pain is an unpleasant sensory and emotional experience associated with actual or potential tissue damage, or described in terms of such damage (Loeser). The ability to feel pain relies on a neuronal network with two parts: 1) the **p**eripheral **n**ervous **s**ystem {**PNS**}, which embodies all of the nerves outside the brain and spinal cord; and 2) the **c**entral **n**ervous **s**ystem {**CNS**}, which integrates information from the PNS in the brain and spinal cord to coordinate the body's activities.

1.2.2. Communication in the Nervous System

Sensory information is processed throughout the PNS and CNS in the form of an **a**ction **p**otential {**AP**}, which is a depolarisation of the neuron's electrical membrane potential {$\mathbf{E_m}$}, that is caused by a stimulus and is the code for neuronal communication. Ions, which are particles that have a net charge such as sodium {$\mathbf{Na^+}$}, potassium {$\mathbf{K^+}$}, and Calcium {$\mathbf{Ca^{2+}}$} (Faraday, 1834), utilise ionic concentrations that cause an electrical gradient across the neuron's membrane to alter the neuron's E_m (Nernst, 1888). Neurons rely on ion channels, which are pores in the membranes of neurons, to adjust the concentration of ions inside the neuron and this affects the generation of APs. Both the type and intensity of a stimulus determines the firing frequency of the neuron (Adrian and Zotterman, 1926) and this is relayed along the PNS to the CNS. Neuronal communication relies upon synapses, which are specialised structures that allow the passing of either electrical or chemical signals from the neuron to other types of cells. Ultimately, APs from the periphery reach the brain, which perceives pain (Woolf and Salter, 2000). By classifying pain according to the duration, there are two types: acute and chronic.

1.2.3. Acute Pain

Acute pain is beneficial and protective; warning the body of threats before severe tissue damage occurs. This type of pain typically originates from the skin and is proportional to the cause, lasting only for seconds (Millan, 1999). People

with hereditary disorders, such as deficiencies of the nerve growth factor receptor (Indo, 2001) or particular ion channels (Cox *et al.*, 2006), do not feel acute pain and experience extensive tissue damage through self-mutilation.

1.2.4. Chronic Pain

When pain is not transient, the result is **c**hronic **p**ain {**CP**} and this is normally a result of abnormal neuronal firing patterns (Wall and Gutnick, 1974), often in sensory neurons that continuously warn the body of threats that are no longer present. The burden of CP degrades the lives of people, whose peak number is 116 million adults in the U.S.A., which exceeds the combined number of victims suffering from heart disease, cancer, and diabetes (Pizzo *et al.*, 2011). One type of CP that is difficult to treat is **n**europathic **p**ain {**NP**}, with patients that are typically middle aged (Gagliese and Melzack, 1997) and female (Berkley, 1997). However, current pharmaceutical treatment is largely un-successful, chiefly due to a lack of understanding of the underlying physiological mechanisms (MacFarlane *et al.*, 1997).

1.2.5. Limitations with Current Chronic Pain Drug Therapy

Despite the substantial progress that has been made over the last decade to understand pathophysiological pain states, the current pharmacological treatment for CP is, at best, effective in 50% of cases (Arnér and Meyerson, 1988; Dworkin *et al.*, 2003; Rice and Hill, 2006; Dworkin *et al.*, 2007). Partly due to in-effective medication (Gaskin and Richard, 2012), the economic cost of CP runs into the hundreds of billions of pounds every single year (Turk, 2002; Pizzo *et al.*, 2011).

The main problems with current treatment regimes are the side effects as a result of secondary pharmacology, primarily in the CNS. Gabapentin, one of the first-line drug choices for NP, often causes dizziness, somnolence, peripheral odema and dry mouth (Attal *et al.*, 2006). Another treatment alternative is either

high (Chaney, 1995; Hempenstall *et al.*, 2005) or low (Arnér and Meyerson, 1988) dose intra-venous opioids, but these compounds have a narrow therapeutic index, making them difficult to use effectively. Selective and potent analgesics that act peripherally to avoid adverse side effects in the CNS are desperately required.

1.3. Pain Pathways

A noxious stimulus normally initiates an AP at the periphery in highly specialised neurons that are normally quiescent in the absence of a stimulus. This AP is normally conveyed to the brain along extremely complex 'pain pathways' that consist of billions of neurons, with ~20 billion neurons in the neocortex alone (Pakkenberg *et al.*, 2003). There are numerous 'pain pathways' in the mammalian nervous system, which are highly conserved across different species of mammals (Pennacchio *et al.*, 2006; Walters, 2007). However, inter-species differences have not been thoroughly investigated, primarily due to the difficulty in carrying out human studies. In general, nociceptive information is carried by several major ascending pathways, one of the most prominent is the **s**pino**t**halamic **t**ract {**STT**} [Fig.1.1], which was recognised in primates (Willis *et al.*, 1974; Besson and Chaouch, 1987) and in humans (Willis and Westlund, 1997).

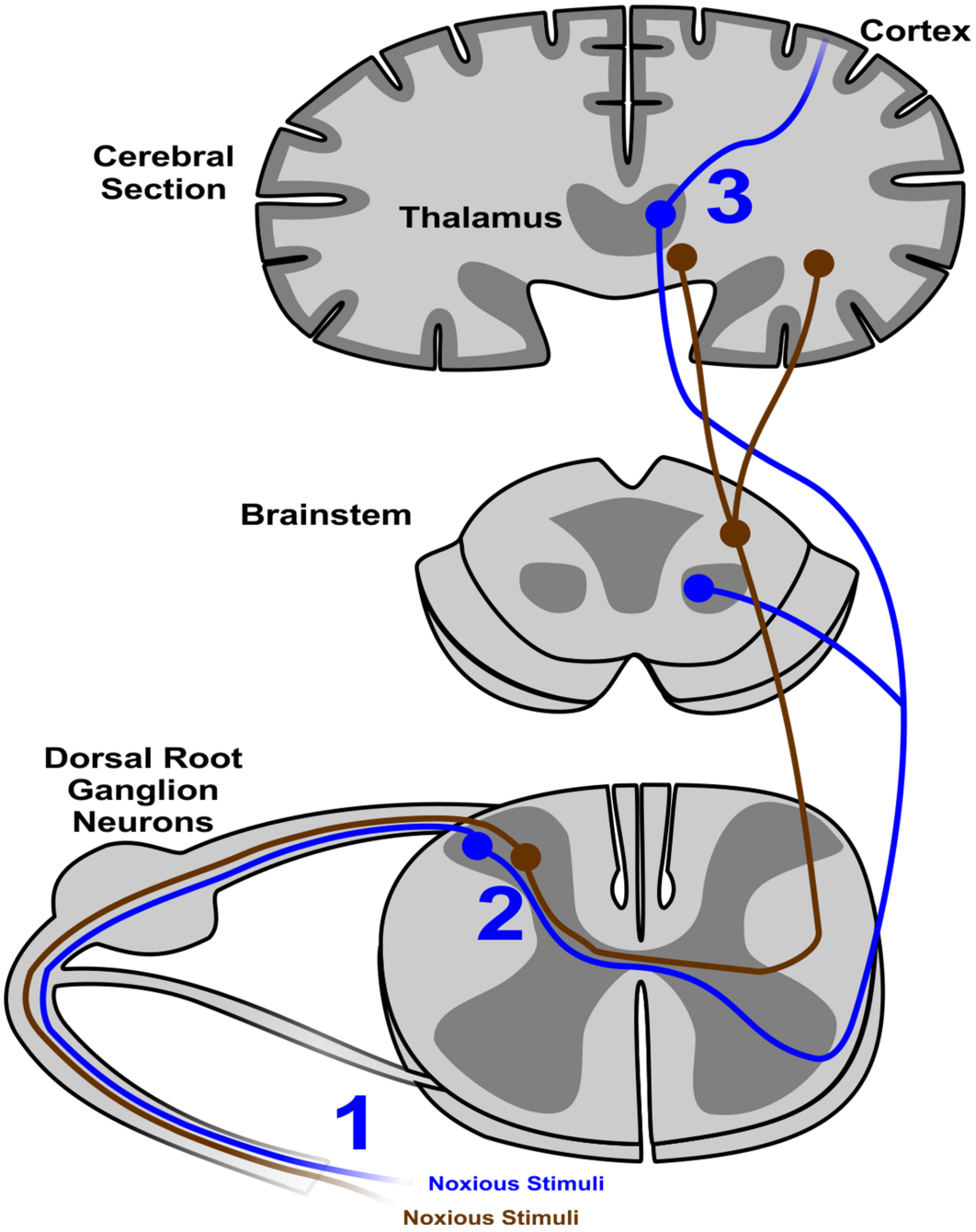

Figure 1.1: Mammalian Sensory Pathways, including the Nociceptive Spinothalamic Tract. Adapted from (Hunt and Mantyh, 2001; Lima, 2007; Costigan *et al.*, 2009), this schematic shows the principal neuronal circuitry in two nociceptive pathways: 1) the spinoparabrachial pathway, in dark brown; and 2) the STT tract, which conveys information regarding pain and temperature, in blue. Ascending sensory pathways typically consist of three orders of neurons: the 1st order neurons are primary afferent, or DRG, neurons, which link the periphery to the dorsal horn of the spinal cord; the 2nd order neurons in the

spinal cord ascend to the brain; and the 3rd order neurons terminate in different regions of the brain.

The STT begins in the periphery in neurons that respond to noxious heat and mechanical stimuli and these neurons terminate in the dorsal horn of the spinal cord onto, amongst others, both nociceptive and multi-receptive, or wide-dynamic range, neurons (Le Bars and Cadden, 2007). The dorsal horn in the spinal cord consists of different laminae, or layers, that contain synapses of specialised populations of neurons (Rexed, 1952), thought to be arranged primarily based on either the type of neuron or the amount of myelination (Millan, 1999). Along the STT, lamina I and the outer layer of lamina II of the spinal dorsal horn contain neuronal synapses and these relay sensory information, primarily regarding pain and temperature (Willis and Westlund, 1997; Kaas, 2004).

Another important type of neuron in the dorsal horn are inhibitory interneurons, which are densely populated in the superficial dorsal horn (Cook *et al.*, 1987). These neurons connect sensory neurons from the periphery to many other types of neurons, including motor neurons, to cause quick responses, in the spinal cord, before the brain receives the sensory information (Basbaum *et al.*, 2009).

Modern theories have advanced substantially from the gate control theory, which states that pain mechanisms are mediated by neuronal interactions in the dorsal horn with inhibitory interneurons having an important role (Melzack and Wall, 1965). However, all theories of peripheral pain perception rely on the sensory neurons that initiate the signalling cascade in response to stimuli in the periphery: DRG neurons.

1.4. DRG Neurons

1.4.1. Anatomy

The PNS consists of 31 pairs of dorsal root ganglia, each comprised of thousands of DRG neurons, that are located outside the blood-brain barrier (Drake *et al.*, 2009). Anatomically, the archetypal neuron consists of three distinct components: 1) dendrite, the recipient branch; 2) axon, the biochemically distinct transmission branch; and 3) cell body, the predominant site of protein synthesis that is responsible for the distribution of proteins, primarily ion channels (Basbaum *et al.*, 2009). However, DRG neurons differ, as they are pseudounipolar, meaning that the short axon divides into two branches: 1) a peripherally-terminating branch, which forms the dendrite and extends to the periphery; and 2) a centrally-terminating branch, which forms the axon and terminates in the dorsal horn (Lodish *et al.*, 2000; Basbaum *et al.*, 2009).

DRG neurons respond to a variety of stimuli and are normally quiescent in the absence of the stimulus. When stimuli are present, APs are generated in DRG neurons and the first signal processing occurs in the dorsal horn of the spinal cord. This thesis will focus primarily on the cell body, which represents the electrical properties of DRG neurons and is the protein-manufacturing centre.

1.4.2. Myelination

Using cell body size, which is correlated to axonal fibre thickness (Lawson and Waddell, 1991), DRG neurons can be divided into: large, medium and small. The amount of myelination around each neuronal fibre determines the **c**onduction **v**elocity {**CV**}, which is the distance travelled in **m**etres {**m**} divided by the time taken in **s**econds {**s**} and reflects the time it takes an AP to travel along the neuron. CVs are dependent on multiple factors: species, age, size, and neuronal type (Djouhri and Lawson, 2004), as CVs of myelinated afferent fibres increase

with age up to 300 days (Birren and Wall, 1956; Sato *et al.*, 1985). Myelination also maintains and promotes long-term survival of neurons (Nave, 2010).

Depending on the physiological type, DRG neurons, which are myelinated accordingly by glial cells in the PNS termed Schwann cells, consist of four types of fibres in three distinct categories: 1) Aα/β; 2) Aδ; and 3) C. Thick myelination, found in A-fibres, produces a fast CV, while smaller neurons are un-myelinated, C-fibres and have slower CVs (McCarthy and Lawson, 1990).

1.4.3. Neuropeptides

Additional classification of DRG neurons [Tab. 1.1] occurs according to whether neurons utilise neuropeptides, such as **sub**stance **P** {**SubP**} or **c**alcitonin-**g**ene **r**elated **p**eptide {**CGRP**}. These neuropeptides cause increased excitation (Woolf and Wiesenfeld-Hallin, 1986) and vasodilatation (Knibestöl, 1973), which promotes the recruitment of inflammatory mediators to the site of injury.

	Large	**Medium**	**Small**
Fibre Type	Aα/β	Aδ	C
Cell Diameter (Rat) (µm)	> 40	30 – 40	< 30
Conduction Velocity (Rat) (m/s)	> 4.5	1.2 – 4.5	< 1.2
Conduction Velocity (Human)(m/s)	~ 50 (Knibestöl, 1973; 1973)	9 (Kakigi *et al.*, 1991)	0.6 – 1.4 (Nordin, 1990; Schmidt *et al.*, 1995; Weidnar *et al.*, 1999)
% of Peptidergic Neurons	~ 0%	~ 20%	~ 50%
% of Nociceptors	~ 20% (Djouhri and Lawson, 2004)	~23% (Djouhri *et al.*, 2006)	~ 73% (Djouhri *et al.*, 2006)

Table 1.1: Characteristics of DRG Neurons. A table showing an assortment of characteristics for DRG neurons, as they have been divided into three general categories according to their cell body size: Large, Medium and Small.

1.4.4. Nociceptors

Furthermore, both within and superseding the categories according to myelination and the presence or absence of neuropeptides, there is a functionally important type of neuron known as a nociceptor. Charles Sherrington defined nociceptors as a specialised class of DRG neurons that respond to intense noxious stimuli (Sherrington, 1906). Nociceptors normally respond to three types of stimuli: mechanical, thermal, or chemical (Costigan *et al.*, 2009). Changes in the excitability of nociceptors play an essential role in the development of a variety of types of CP (Millan, 1999; Julius and Basbaum, 2001; Djouhri *et al.*, 2006).

The majority of small sized, C-fibre, and medium sized, Aδ-fibre, DRG neurons are nociceptors (Meyer *et al.*, 2005), with 45% responding to noxious heat (Julius and Basbaum, 2001). Furthermore, ~20% of large neurons are nociceptors (Djouhri and Lawson, 2004). There are a number of different types of nociceptor that develop specifically because of the concentrations of highly specific neuronal growth factors, or neurotrophins, that are present during embryological development and the early developmental period (Lallemend and Ernfors, 2012). Furthermore, nociceptors can be divided according to the stimuli that they respond to: 1) **H**igh-**t**hreshold **m**echanoreceptor {**HTM**}; 2) Thermal; 3) Chemical; and 4) Polymodal (Meyer *et al.*, 2005; Ringkamp and Meyer, 2007).

1.4.4.1. High-Threshold Mechanoreceptor

Strong mechanical stimulation, such as pinch, a pin-prick, or a cut, activate the high-threshold mechanoreceptors (Delmas *et al.*, 2011), which make up 32% of all DRG neurons with 12% being A-fibres and 20% being C-fibres (Lewin and Moshourab, 2004). Across mammalian species, the majority of A-fibre nociceptors are HTMs (Djouhri and Lawson, 2004).

Furthermore, there is a category of mechanically insensitive, or 'silent', nociceptors that were first observed in knee joints (Schaible and Schmidt, 1983a; 1983b), before being confirmed in the peroneal nerve of humans (Schmidt *et al.*, 1995). About 50% of Aδ-fibre nociceptors and 33% of C-fibre nociceptors are mechanically insensitive (Handwerker *et al.*, 1991; Meyer *et al.*, 1991). These nociceptors can be activated by second messenger systems that become active in the presence of inflammatory mediators, such as bradykinin (Dray *et al.*, 1988; Birrell *et al.*, 1993), protein kinases (Schepelmann *et al.*, 1993), prostaglandins (Schepelmann *et al.*, 1992; Birrell *et al.*, 1993), and finally, serotonin and histamine (Davis *et al.*, 1993). This can result in **s**pontaneous **a**ctivity {**SA**} and increased excitability to peripheral stimuli (Schabile and Schmidt, 1985), in both nociceptors and **l**ow-**t**hreshold **m**echanoreceptors {**LTM**} (Schaible and Schmidt, 1988). Currently, the role of these mechanically insensitive nociceptors is probably understated in states of CP (Gold and Gebhart, 2010).

1.4.4.2. Thermal

Subclasses of nociceptors respond to either, or possibly both, noxious heat and noxious cold (Julius and Basbaum, 2001). Furthermore, the noxious heat-activated nociceptors can be separated into two sub-classes with a majority that are activated at ≥ 43°C and a minority that are activated at ≥ 50°C (Cesare and McNaughton, 1996; Kirschstein *et al.*, 1997; Nagy and Rang, 1999; Leffler *et al.*, 2007). The noxious cold nociceptors are activated by either the application of cooling agents, such as menthol and eucalyptol (Hensel and Zotterman, 1951; Reid and Flonta, 2001), or temperatures ≤ 15°C (Tominaga and Caterina, 2004; Basbaum *et al.*, 2009). Furthermore, there is evidence that a single subclass of nociceptors could be responsible for both noxious temperature ranges (Dodt and Zotterman, 1952; Bautista *et al.*, 2005; Kobayashi *et al.*, 2005).

1.4.4.3. Chemical

This subclass of nociceptor, which responds to chemical stimuli including low pH, lactic acid and inflammatory mediators (Gold and Gebhart, 2010), is the least understood (Basbaum *et al.*, 2009). The presence of chemical irritants in the local microenvironment activates these neurons (Bautista *et al.*, 2006).

1.4.4.4. Polymodal

Polymodal nociceptors are the most common type of nociceptor and responds to different combinations of the three prinicipal noxious stimuli: mechanical, thermal and chemical (Bessou and Perl, 1969; Lynn and Carpenter, 1982; Perl, 1996). The most common type of polymodal nociceptor is activated by noxious thermal and mechanical stimuli (Meyer *et al.*, 2005; Gold and Gebhart, 2010). More mechanical- and heat-activated Aδ-, rather than C-, fibre polymodal nociceptors respond to chemical stimuli as well (Davis *et al.*, 1993).

1.4.5. Low-Threshold Mechanoreceptors

Although a few of the Aα/β-fibre DRG neurons respond to painful stimuli, 80% are LTMs and respond to light touch (Djouhri and Lawson, 2004). These neurons are largely responsible for propioception, or the essential ability to track the relative positioning of various body parts. There are many different types of LTMs, including: **R**apidly **Adapt**ing {RAdapt}, **S**lowly **Adapt**ing {**SAdapt**}, low threshold C-fibres and hair follicles (Delmas *et al.*, 2011).

1.4.5.1. Rapidly Adapting and Slowly Adapting DRG Neurons

RAdapt DRG neurons differ from SAdapt neurons according to their rates of adaptation to sustained, weak mechanical stimulation (Mountcastle, 1957). Different complexes mediate RAdapt, including Meissner's corpuscles, Pacinian corpuscles and longitudinal lanceolate endings (Iggo and Ogawa, 1977), while

SAdapt comprise Merkel discs and Ruffini receptors (Iggo and Muir, 1969; Chambers *et al.*, 1972; Paré *et al.*, 2002; Delmas *et al.*, 2011). These two types of LTM differentiate because of Ret signalling during the embryological stages of development (Luo *et al.*, 2009).

1.4.5.2. C-Fibre Mechanoreceptors

There is a small sub-population of LTMs that are C-fibres and are responsible for pleasant light touch (Olausson *et al.*, 2007). These particular DRG neurons have an important role in social interactions and exhibit interesting neurophysiological properties (Olausson *et al.*, 2010). Furthermore, there is compelling evidence that a specific sub-population of these DRG neurons that express vesicular glutamate transporter 3 might be responsible for mechanical hypersensitivity in states of CP (Seal *et al.*, 2009).

1.4.5.3. Hair Follicles

Generally, there are two types of hair depending on the fibre type: **G**uard **hair**s {**G-hair**} and **d**own **hair**s {**D-hair**}, which consist of Aα/β-fibres and Aδ-fibres, respectively (Brown and Iggo, 1967). These DRG neurons are typically RAdapt, but respond to light brushing (Delmas *et al.*, 2011), which some of the other LTMs do not respond to.

1.4.6. Speed of Pain

As different types of nociceptor possess various ranges of CVs, A-fibre nociceptors are culpable for the first, sharp pain that is initially perceived, while C-fibre nociceptors drive the slower, deeper pain [Fig. 1.2]. The primary way that different types of nociceptors affect the way pain is perceived is by changing the frequency of APs and this peripheral sensitisation is the underlying driver of CP (Costigan *et al.*, 2009; Hehn *et al.*, 2012). Current evidence indicates that although there are subtle changes to AP parameters during peripheral CP states,

these almost certainly affect the firing rate of DRG neurons (Djouhri and Lawson, 1999; Djouhri *et al.*, 2006), which is an important driver of central sensitisation.

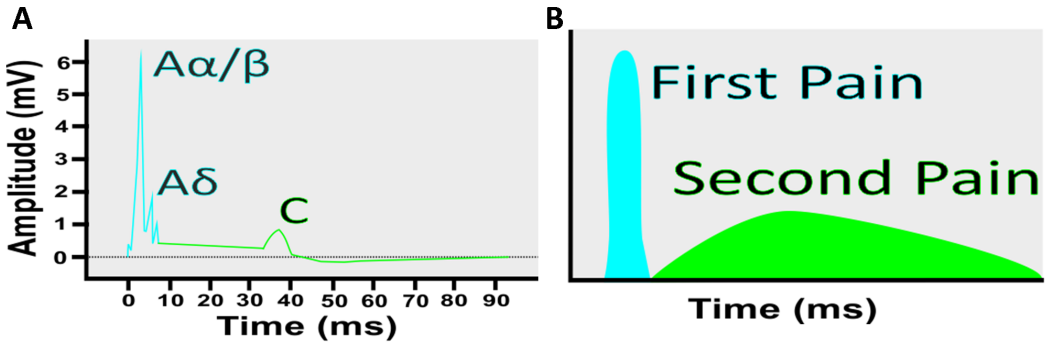

Figure 1.2: Different types of Fibres and their Response to Noxious Stimuli. A visual schematic, taken from (Julius and Basbaum, 2001; Perl, 2007), showing a compound AP [A], which indicates the different conduction velocities of DRG neurons using their response times. These different speeds indicate the two types of physiological responses that cause the first pain and the second pain [B].

1.5. Changes to Pain Pathways

While the evolutionary advantages of acute pain are beneficial, easing superficial wound healing by protecting the injured area, the same does not hold true for CP, which can persist for years and is currently poorly treated. CP possesses many diverse aetiologies, but this thesis will focus on two: IP and NP, which become **c**hronic **IP** {**CIP**} and **c**hronic **NP** {**CNP**} respectively.

1.5.1. Chronic Inflammatory Pain

IP is associated with inflammation, which is typically a result of tissue injury and the subsequent inflammatory response, but could also be due to an infection or irritation. Usually IP is resolved upon healing of the original tissue injury, however, in chronic inflammatory disorders, such as rheumatoid arthritis, the pain persists for as long as the inflammation is active (Wolfe and Hawley, 1985). Most of these inflammatory mediators act by changing the excitation properties

of DRG neurons, particularly chemically-activated and polymodal nociceptors, rather than activating them directly (Woolf and Costigan, 1999). CIP is typically due to changes in both the PNS and CNS, especially along the STT [Fig. 1.3] (Woolf and Salter, 2000; Hucho and Levine, 2007; Costigan *et al.*, 2009).

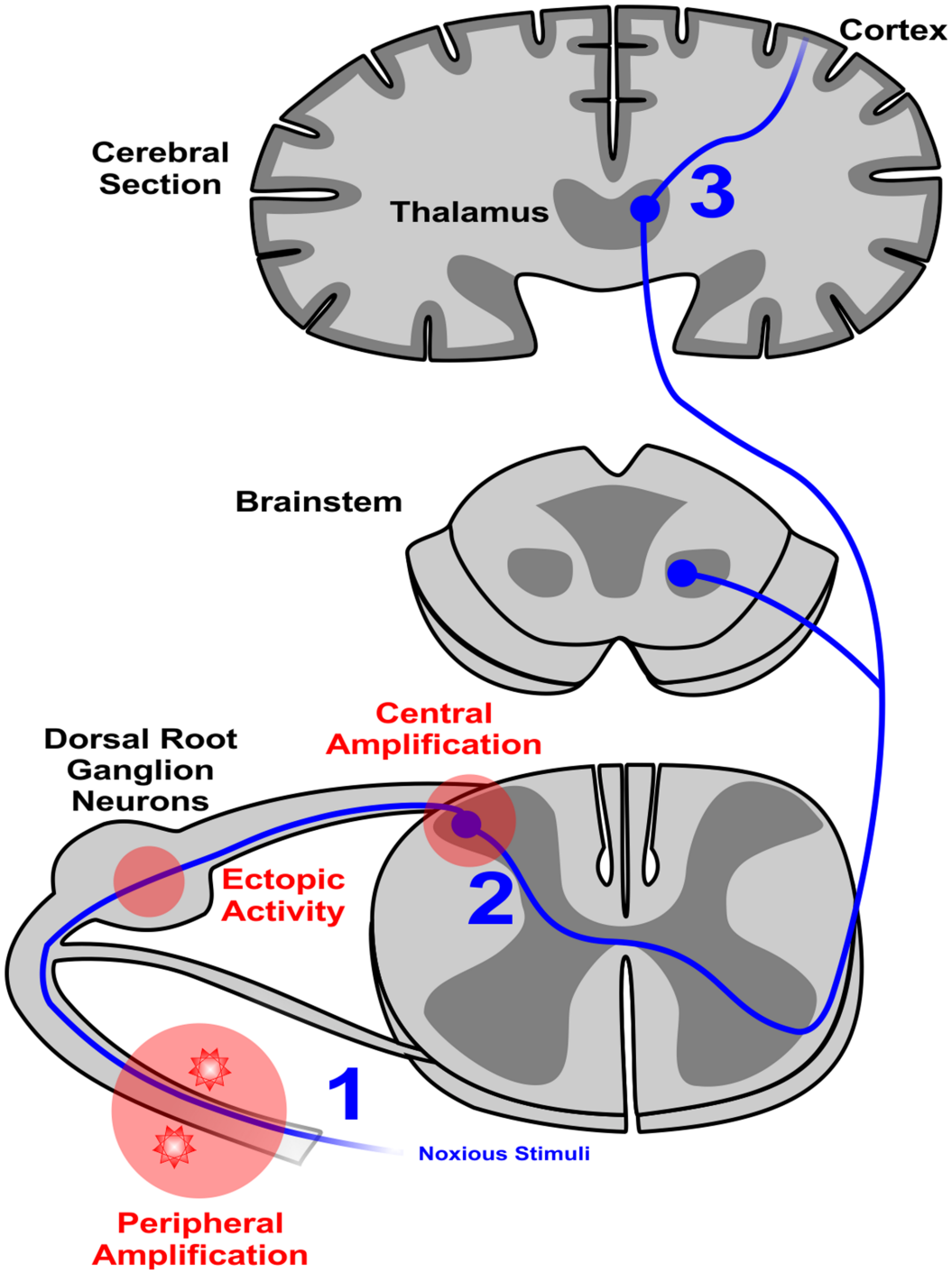

Figure 1.3: The Effects of Peripheral Inflammation on the Spinothalamic Tract. A diagram, taken from (Costigan *et al.*, 2009), showing the amplification in the PNS and CNS that occur along the STT as a result of peripheral CIP.

During inflammation, a wide variety of biological mediators known as an 'inflammatory soup' are produced (McMahon *et al.*, 2005b) and these trigger physiological changes, such as peripheral sensitisation and subsequently central sensitisation (Costigan *et al.*, 2009). The precise role of each inflammatory mediator is unclear, although not all are harmful, some have important roles in the healing process (Nathan, 2002). Growth factors, for example, are involved in guiding the re-growth of injured tissue and neurotrophins are the growth factors that aid the growth of neurons (Werner and Grose, 2003).

Some of these pro-inflammatory mediators act, either directly or indirectly, on the conducting, un-injured DRG neurons to cause increased excitability, through SA and hyperexcitability, and therefore sensitisation of the 2nd order neurons, which contributes to driving CP [Fig. 1.4]. Immune cells, particularly mast cells and macrophages, may release mediators that act directly or indirectly on DRG neurons to cause SA. Inflammatory mediators that induce APs could be **p**rostaglandin **E_2** {**PGE_2**} (England *et al.*, 1996) or TNF-α (Schäfers *et al.*, 2003). Furthermore, it has been shown that peripheral amplification, through the generation of SA, occurs at both the site of injury and the adjacent, conducting DRG neurons with their receptive fields still intact (Woolf and Salter, 2000; Costigan *et al.*, 2009). This SA in conducting DRG neurons has been shown in both monkey (Ali *et al.*, 1999) and rat (Djouhri *et al.*, 2006).

In addition, inflammation causes vascular permeability, the infiltration and activation of immunocompetent cells, and the synthesis and/or release of inflammatory mediators from immune cells and neurons (McCleskey and Gold, 1999). Furthermore, tissue acidosis contributes to the inflammatory milieu and may increase the excitability of DRG neurons (Mamet *et al.*, 2002; Krishtal, 2003).

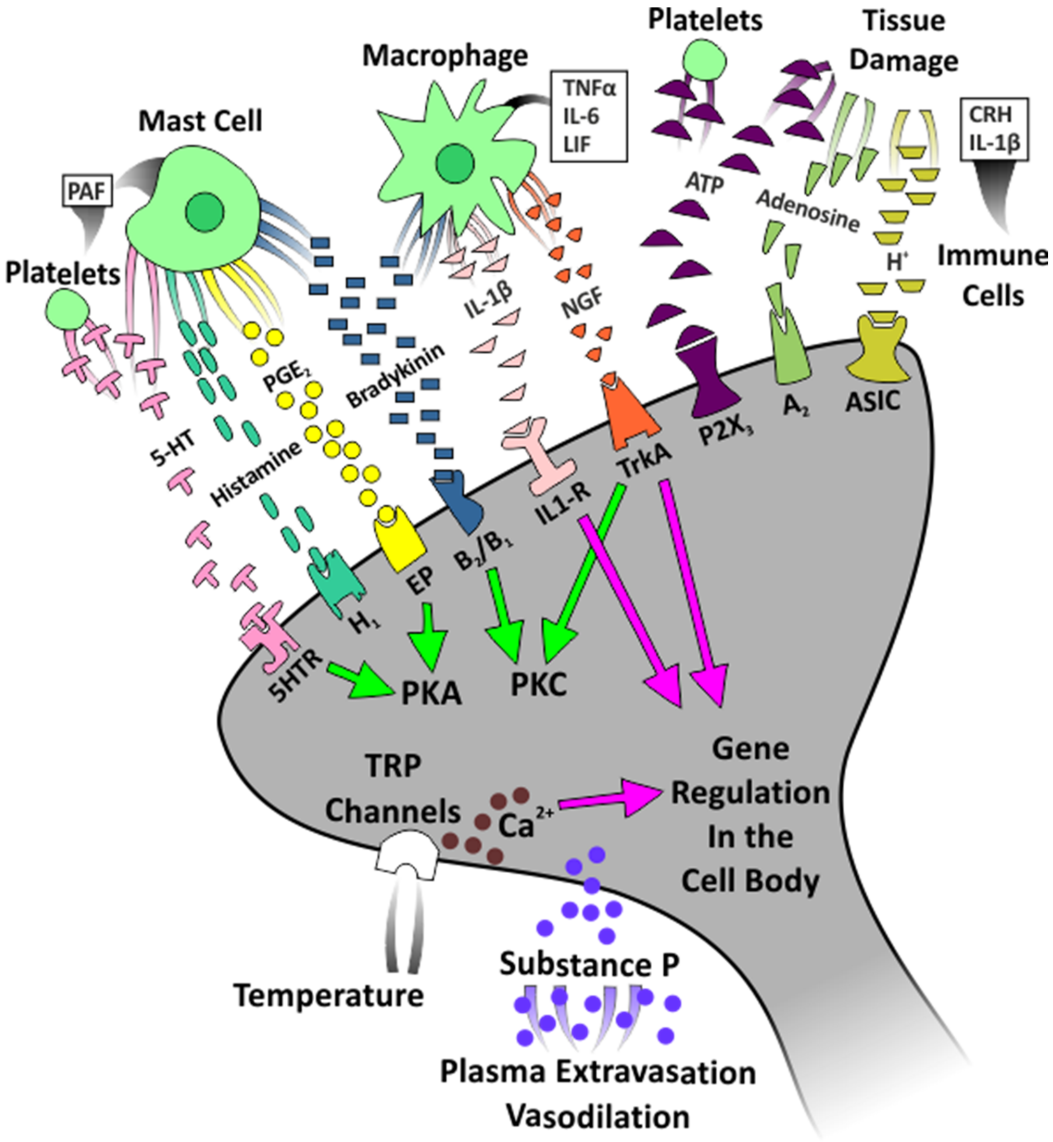

Figure 1.4: Inflammatory Mediators acting on a DRG Neuron. A schematic illustration, adapted from (Meyer *et al.*, 2005), that shows a variety of inflammatory mediators from various cells that could act on specific receptors at the terminals of DRG neurons to alter not only the firing properties of the neuron, but also a range of signalling pathways and further downstream, the regulation of genes. 5-HT, Serotonin; 5-HTR, Serotonin Receptor; ASIC, Acid-Sensing Ion Channels; ATP, Adenosine Triphosphate; B_2/B_1, Bradykinin Receptor 2/1; Ca^{2+}, Calcium; CRH, Corticotrophin Releasing Hormone; EP, E-Prostanoid Receptors; H^+, Hydronium Ions; H_1, Histamine Receptor 1; IL-1β, Interleukin-1β; IL1-R, Interleukin-1 Receptor; Interleukin-1β IL-6, Interleukin-6; LIF, Leukemia Inhibitory Factor; NGF, Nerve Growth Factor; PAF, Platelet Activating Factor; PGE_2, Prostaglandin E_2; PKA, Protein Kinase A; PKC, Protein Kinasae C; TNFα,

Tumour Necrosis Factor α; TrkA, High Affinity Nerve Growth Factor Recpetor; TRP, Transient Receptor Potential Ion Channel.

Both SA and increased excitability is thought to be a result of changes to ion channel subunits, either through altering their properties or expression levels. A better understanding of the neurophysiological changes during CIP is required to develop improved compounds that specifically block peripheral amplification.

1.5.2. Chronic Neuropathic Pain

1.5.2.1. Background

NP is defined as pain initiated or caused by a primary lesion or dysfunction in the nervous system (Treede *et al.*, 2008) specifically as a result of injury to pathways responsible for nociceptive pain (Kehlet *et al.*, 2006; Hehn *et al.*, 2012), particularly the STT (Boivie *et al.*, 1989). NP can be the result of a variety of physiological pathologies that injure neurons: physical injury, which is the focus of this thesis; viral infections, such as Herpes zoster; metabolic diseases, such as diabetes mellitus; vascular diseases, such as stroke; autoimmune diseases, such as multiple sclerosis; and damage caused by radiation or chemotherapy (Baron *et al.*, 2010). CNP is also driven by both peripheral and central sensitisation along 'pain pathways', as shown in the STT [Fig. 1.5] (Costigan *et al.*, 2009).

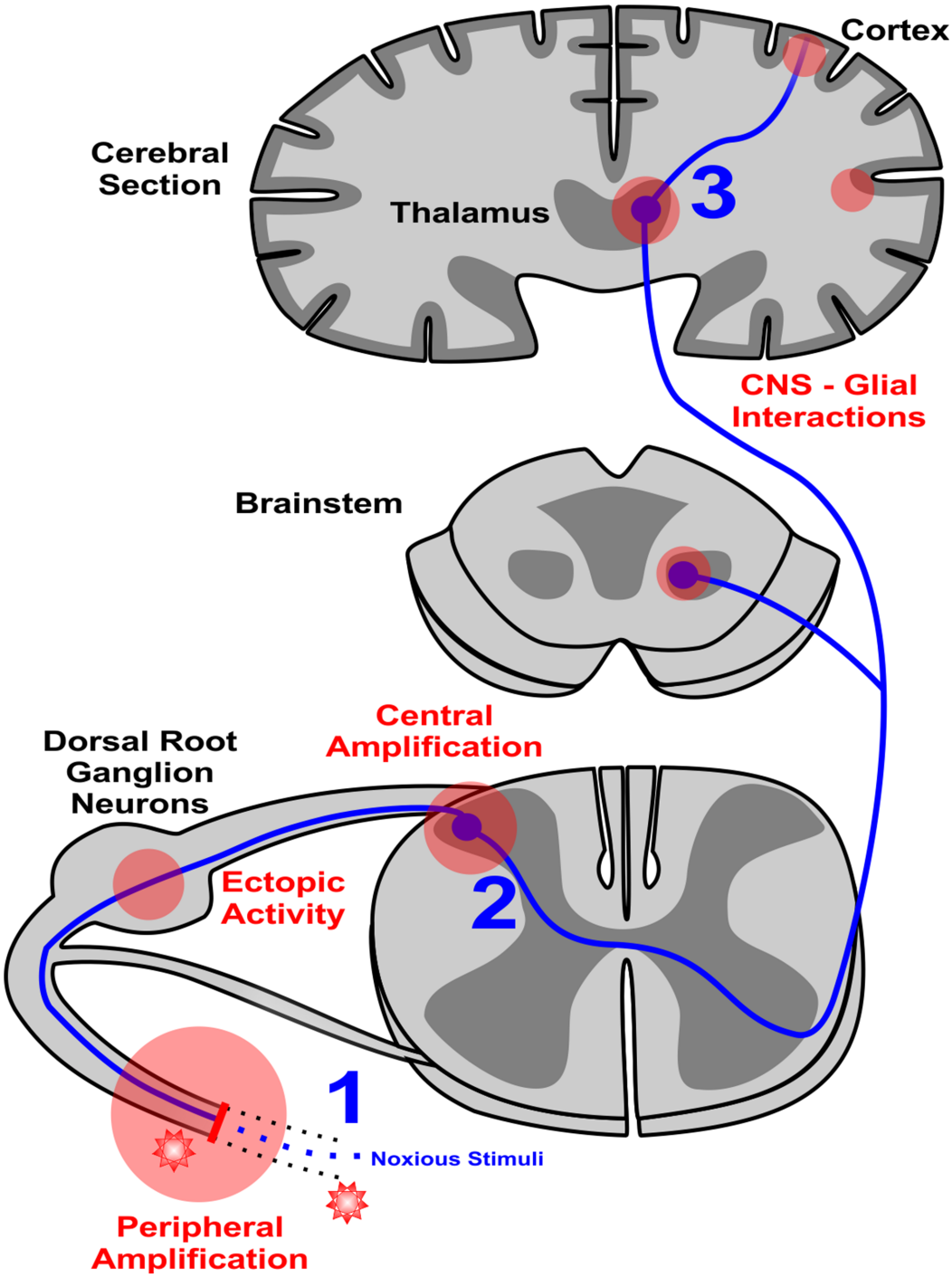

Figure 1.5: The Effects of Peripheral Nerve Injury on the Spinothalamic Tract. A diagram, taken from (Costigan *et al.*, 2009), showing the principal changes that occur to the STT as a result of peripheral nerve injury. These changes include peripheral and central sensitisation, which involves a change in the role of glial cells in the CNS.

When neuronal tissue injury occurs, a host of inflammatory factors are released by an assortment of cells and these mediators contribute to the hyperexcitability of DRG neurons. Multiple physiological changes occur during the development of peripheral NP in three areas, within both the PNS and the CNS, that undergo plasticity: 1) injured DRG neurons [Fig. 1.5.A]; 2) conducting DRG neurons with their receptive fields still intact [Fig. 1.5.B]; and 3) second order neurons in the dorsal horn of the spinal cord [Fig. 1.5.C] (Costigan *et al.*, 2009).

1.5.2.2. Injured DRG Neurons

Following peripheral nerve injury, a neuroma, or growth, forms at the site of injured neurons. Subsequently, the neuromas of different populations of DRG neurons become sensitised, or hyperexcitable, to mechanical, chemical and thermal stimuli, in addition to showing SA (Koschorke *et al.*, 1991; Boucher *et al.*, 2000; Liu *et al.*, 2000b; Amir *et al.*, 2005; Devor, 2005). Although Aβ-fibre DRG neurons immediately produce SA (Liu *et al.*, 2000a; Devor, 2009), injured C-fibre DRG neurons do not (Boucher *et al.*, 2000; Liu *et al.*, 2000a; 2000b), as SA takes time to develop (Devor, 2007). The APs from these injured DRG neurons partly contributes to changes in the expression profiles of hundreds of genes (Costigan *et al.*, 2002), particularly the up-regulation of genes that aid regeneration of both motorneurons (Brushart *et al.*, 2002) and sensory neurons (Udina *et al.*, 2008).

In addition, in a rodent model of NP, the direct application to the DRG of both lidocaine, a local anaesthetic (Sukhotinsky *et al.*, 2004), or tetrodotoxin, a neuronal blocker (Omana-Zapata *et al.*, 1997; Lyu *et al.*, 2000), attenuates mechanical hypersensitivity and DRG neuron hyperexcitability respectively. This may be due to reducing the barrage of activity from DRG neurons towards the CNS. Also, similar clinical trials in humans, although not always properly blinded, have relieved hypersensitivity associated with NP (Arnér *et al.*, 1990; Gracely *et al.*, 1992; Koltzenburg *et al.*, 1994). It is not clear, however, exactly which DRG neurons these drugs are acting on.

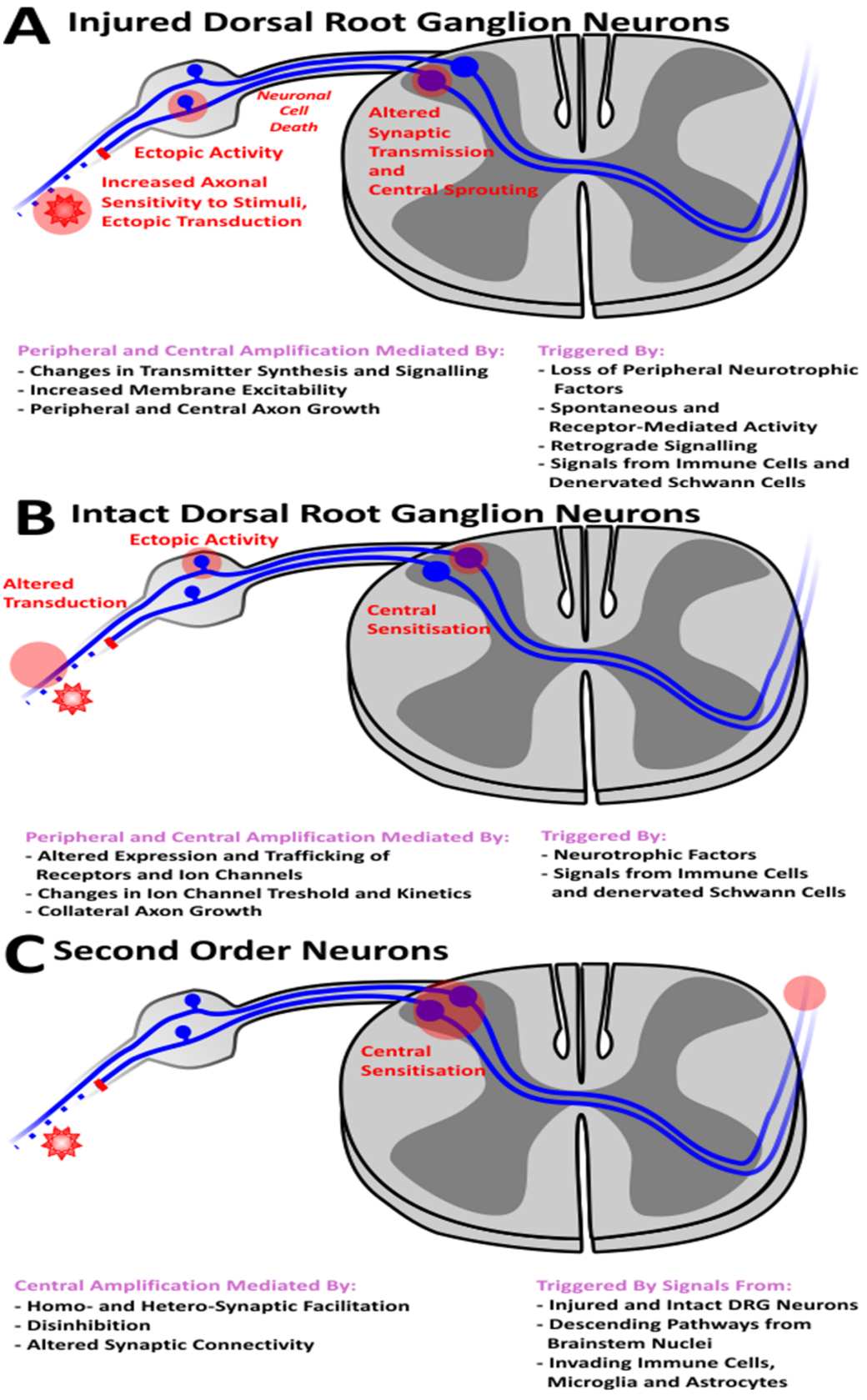

Figure 1.6: Three Sources of Plasticity Resulting in Sensitisation in States of NP.

This schematic representation, taken from (Costigan *et al.*, 2009), shows the

three main types of neuron affected by nerve injury: 1) Injured DRG neurons [A]; 2) intact, conducting DRG Neurons [B]; and 3) Second Order Neurons [C].

1.5.2.3. Conducting DRG Neurons with Receptive Fields Intact

Since injured DRG neurons are not connected to their receptive fields, tissue hypersensitivity could be due to either: 1) conducting, intact DRG neurons with their receptive fields intact; or 2) dorsal horn neurons in the CNS. Focussing on conducting DRG neurons, both A- and C-fibre DRG neurons display SA in models of NP (Ali *et al.*, 1999; Boucher *et al.*, 2000; Djouhri *et al.*, 2006). Furthermore, low-frequency electrical stimulation of C-fibres induces mechanical hypersensitivity in humans (Klede *et al.*, 2003) and rats (Wu *et al.*, 2002).

In addition, the excitability of these conducting neurons could be affected by neurotrophins that are released, principally by Schwann cells (Esper and Loeb, 2004), to aid re-growth of the injured DRG neurons (Campbell and Meyer, 2006). L4 and L5 DRG neurons have fibres that run adjacently, in the same peripheral nerve, in addition to sharing the same innervation territory and even the same Schwann cells (Campbell and Meyer, 2006). As a result, neurotrophins, from either inflammation or Wallerian degeneration in the injured neurons to aid regeneration, act on intact neurons as well. Although neurotrophins are protective and play a role in the regeneration of damaged sensory neurons, both nerve growth factor (Lewin *et al.*, 1994) and brain derived neurotrophic factor (Malin *et al.*, 2006) cause hypersensitivity, and nerve growth factor can also cause SA in neurons (Koltzenburg *et al.*, 1999).

The most persuasive piece of evidence for the key role of the intact DRG neurons is that some pain hypersensitivities can be alleviated by local injections of drugs, including: ZD7288 (Harris and Constanti, 1995; Chaplan *et al.*, 2003; Dalle and Eisenach, 2005); Mibefradil (Dogrul *et al.*, 2003); and JWH-133 (Elmes *et al.*, 2004). This is supported by the fact that capsaicin, which only affects nociceptors, can be applied to the site of injury to relieve **s**pontaneous **p**ain {**SP**}

(Campbell and Meyer, 2006). Furthermore, blocking peripheral sensitisation using anaesthetics prevented the development of mechanical hypersensitivity (LaMotte *et al.*, 1991).

1.5.2.4. Second Order Neurons

Both SA and hyperexcitability from both injured and un-injured DRG neurons have an effect on second order neurons in the dorsal horn that amplifies the signal from the periphery and causes central sensitisation (Gracely *et al.*, 1992; Yoon *et al.*, 1996; Costigan *et al.*, 2009). Central sensitisation can occur through two, possibly concurrent, principal mechanisms: 1) increased release of excitatory neurotransmitters, such as Glutamate, SubP, or CGRP; 2) enhanced synaptic efficacy (Woolf and Salter, 2000; Campbell and Meyer, 2006). Furthermore, glial cells in the CNS, both astrocytes and microglia, become activated and release a host of inflammatory mediators, such as the neurotrophin, brain-derived neurotrophic factor (Coull *et al.*, 2005), and IL-1β (Clark *et al.*, 2006), that contribute to central sensitisation (McMahon and Malcangio, 2009; Milligan and Watkins, 2009). While unquestionably there is evidence that the CNS is also involved in the pathophysiology of CP, the focus of this thesis is on the peripheral mechanisms.

1.5.3. Similarities Between Chronic Inflammatory and Neuropathic Pain

Although IP and NP have distinct aetiologies, they produce the same symptoms and share some mechanisms, including peripheral and central sensitisation.

1.5.3.1. Patients' Symptoms

Using patients' descriptions, there are many characteristics of CP, both CIP and CNP, with two particularly well-characterized clinical symptoms: SP and hypersensitivity to both thermal and mechanical stimuli (Costigan *et al.*, 2009). Patients predominantly complain of SP (Backonja and Stacey, 2004), which was

first characterised as severe burning pain (Mitchell, 1872). Unfortunately, as SP is stimulus independent and therefore un-avoidable, it is less manageable than pain due to hypersensitivity (Bennett, 2012). Furthermore, there is evidence that the physiological mechanisms responsible for SP (Bennett, 2012) and hypersensitivity are distinct (Djouhri *et al.*, 2006; Mogil, 2009).

1.5.3.2. Peripheral and Central Sensitisation

The mechanisms that drive pain during both CIP and CNP both reply upon combinations of peripheral and central sensitisation (Costigan *et al.*, 2009). DRG neurons are sensitised via selective physiological mechanisms that are activated by inflammatory mediators (Dray, 1995). This neuro-inflammation arises around DRG neurons in many different murine models of CP (Kim *et al.*, 1997; Honore *et al.*, 2000). Both neuro-inflammation, predominantly as a result of neuronal break-down, and the presence of pro-inflammatory mediators, act to sensitise DRG neurons via selective physiological mechanisms (Dray, 1995) in both CIP and CNP. Furthermore, both glial (McMahon and Malcangio, 2009; Milligan and Watkins, 2009) and immune cells (McMahon *et al.*, 2005a; 2005b; Stein and Machelska, 2011) appear to play an important role in the development of CP. One week after nerve injury, microglia in the dorsal horn are activated and this is thought to be localised at the central terminals of the injured DRG neurons (Scholz and Woolf, 2007). This contributes, in both models of CP, to central sensitisation. Therefore, a further understanding of the neurophysiological changes is important to develop selective compounds that act specifically to block the peripheral amplification that occurs at the site of injury and affects DRG neurons during states of peripherally originating CP.

1.5.4. Differences Between Chronic Inflammatory and Neuropathic Pain

1.5.4.1. Neuronal Injury

By definition, there are always injured DRG neurons in peripheral NP and these almost always express ATF-3, a transcriptional marker of neuronal injury (Tsujino *et al.*, 2000; Shortland *et al.*, 2006). However, in IP, the % of DRG neurons that express ATF-3 is either 2% (Boettger *et al.*, 2007) or 0% (Banchet *et al.*, 2009), depending upon the model used. This difference not only affects the inflammatory mediators in CIP and CNP, but also the length of time that the inflammation is present for.

1.5.4.2. Wallerian Degeneration

During CNP, an injured nerve is broken down through a process known as Wallerian degeneration (Gaudet *et al.*, 2011), which involves the controlled breakdown of injured neuronal fibres following injury through a modified apoptotic process (Finn *et al.*, 2000; Sievers *et al.*, 2003). This is primarily mediated by glial cells, known as Schwann cells and macrophages, that normally maintain homeostasis in the micro-environment, but struggle to preserve this balance in states of CP (McMahon *et al.*, 2005b; Scholz and Woolf, 2007). This process involves the recruitment of a myriad of cytokines (Finn *et al.*, 2000; Sievers *et al.*, 2003; Gaudet *et al.*, 2011). These cytokines, such as tumour necrosis factor α, interleukin 1-α and interleukin 1-β, recruit macrophages for myelin degradation (Shamash *et al.*, 2002) and cause the release of vaso-active neuropeptides, such as SubP and CGRP. These neuropeptides also recruit macrophages (Cheng *et al.*, 1995), which form a macrophage-centric inflammatory cellular filtrate (Scholz and Woolf, 2002), in addition to causing swelling and hyperemia (Zochodne *et al.*, 1999; Scholz and Woolf, 2007). The presence of these inflammatory mediators helps to cause hyperexcitability in specific DRG neurons through a variety of cellular pathways, such as increased adenylate cyclase, which increases cAMP (Cheng *et al.*, 1995).

1.6. Animal Models

To confirm these physiological pathways and how they are altered, experiments require careful design. Since human self-assessment of pain is extremely subjective, it is difficult to quantify (Jensen *et al.*, 1986), in addition to stringent ethical considerations. Therefore, to mirror human symptoms and test various hypotheses involving the physiological mechanisms of pain, a variety of animal models, each with strengths and weaknesses, have been developed. Most rodent models induce CP by altering, either surgically or chemically, the **L**umbar **4 – 6** {**L4-6**} DRG neurons, which innervate the hindpaw and hindlimb region. This allows behavioural testing on the dermatome of the affected neurons and quantification of the amount of pain in response to various stimuli.

1.6.1. Animal Models of Inflammatory Pain

The formalin test is widely used and displays similar symptoms in rats, cats (Dubuisson and Dennis, 1977), and primates (Alreja *et al.*, 1984). To develop models of arthritic pain, substances that activate the immune system were developed, including **c**omplete **F**reund's **a**djuvant {**CFA**} (Larson *et al.*, 1986), carrageenan (Kayser and Guilbaud, 1987), and urate crystals (Coderre and Wall, 1987), which all posses longer lasting, subtler effects than formalin. Finally, another alternative is the direct injection of a specific pro-inflammatory mediator, such as bradykinin, prostaglandins, or SubP (Rang *et al.*, 1991).

1.6.2. Animal Models of Neuropathic Pain

Several animal models of peripheral NP have been developed and significantly contributed to our current understanding of NP pathogenesis.

1.6.2.1. Chronic Constriction Injury

The chronic constriction injury model involves loose ligation of the sciatic nerve, the bundle of L3-L6 **s**pinal **n**erves {**SN**}, with 4 chromic gut, which is an absorbable suture, ligatures at intervals of 1-2 millimetres so that the epineurial vasculature is partly occluded to cause slight swelling of the nerve (Bennett and Xie, 1988; Cheng *et al.*, 1995; Kim *et al.*, 1997). The chromic gut induces an inflammatory response (Maves *et al.*, 1993).

1.6.2.2. Partial Nerve Ligation

The partial nerve ligation model of NP was developed after the chronic constriction injury model. This model is induced by ligating, using silk, one third to one half of the sciatic nerve (Seltzer *et al.*, 1990).

1.6.2.3. Spinal Nerve Ligation

The third model is the original SN ligation model, which involves axotomy of either the L5 SN or both the L5 and L6 SNs (Kim and Chung, 1992). This model results in the most mechanical hypersensitivity amongst all of the rodent models of NP (Kim *et al.*, 1997). Furthermore, this model evolved to nerve axotomy, which involves complete transection of the SN so there are no surviving neurons.

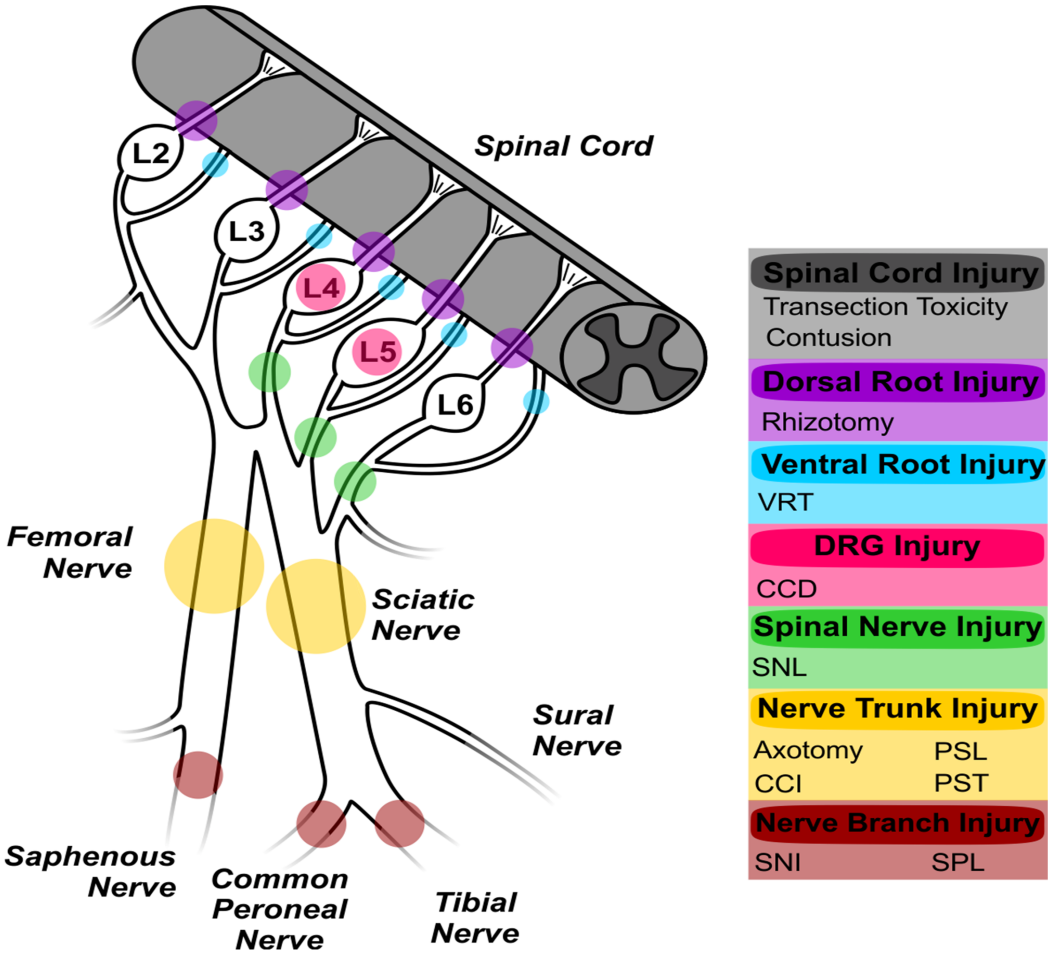

Figure 1.7: Different Models of Inducible Neuropathic Pain in Rodents. The figure, adapted from (Decosterd and Berta, 2007), shows various types of NP models: Starting from the top and moving down, this figure shows various spinal cord injuries, which can be due to transection, contusion or toxicity. The dorsal root injuries can selectively target various SNs with a rhizotomy. Furthermore, ventral root transection, VRT, can injure the ventral roots in isolation. Chronic compression of the DRG, CCD, can be used to study the effects of selective injury to the ganglia of SNs. Spinal nerve ligation, SNL, which involves tight ligation of the L4 and sometimes, the L6 SN, can also be used to study SNs in isolation. There are various types of nerve trunk injury: axotomy; chronic constriction injury, CCI; partial sciatic nerve ligation, PSL; partial sciatic nerve transection, PST. Finally, nerve branch injuries include spared nerve injury, SNI, and saphenous nerve partial ligation, SPL.

1.6.2.4. Modified Spinal Nerve Axotomy

The SN ligation model can be altered to become the **m**odified **s**pinal **n**erve **a**xotomy {**mSNA**}, which involves ligating and axotomising the L5 SN and loosely ligating the L4 SN with chromic gut (Lee *et al.*, 2003). Both this model and the SN ligation model are highly selective, allowing the investigation of either injured, L5 DRG neurons, or un-injured, L4 DRG neurons with their receptive fields intact, in states of NP. Within 1-2 days post-treatment, the mSNA model shows robust signs of hypersensitivity and **s**pontaneous **f**oot **l**ifting {**SFL**}, which lasts for at least 10 weeks. SFL, a correlate of SP (Bennett and Xie, 1988; Attal *et al.*, 1990; Djouhri *et al.*, 2006; Luo *et al.*, 2007; Abrahamsen *et al.*, 2008) is not reliably produced when only the L5 SN is injured (Djouhri *et al.*, 2006).

1.7. Role of Ion Channels

1.7.1. Ion Channel Evolution

CP partially results from the increased excitability of DRG neurons and ion channel subunits are the leading candidates for therapeutic intervention. Transcriptional channelopathies describe the change in ion channel subunit expression that subsequently changes the neuron's excitability (Waxman, 2001) and several of these changes occur in DRG neurons to drive CP. There are a multitude of ion channel families involved in the generation of each AP [Fig. 1.8] and many have already been investigated to further understand their role in CP.

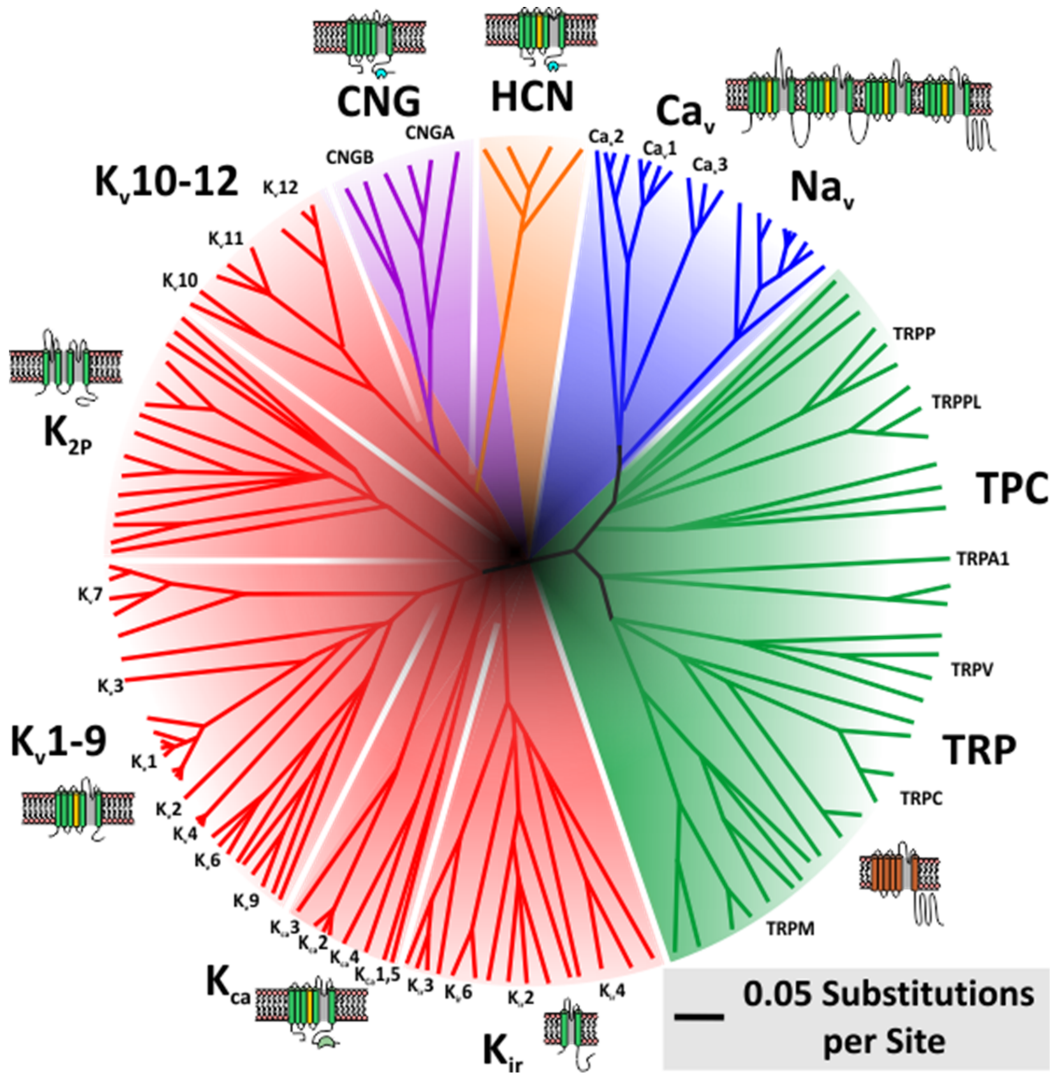

Figure 1.8: Phylogenetic Tree Representing the Amino Acid Relationship of the Minimal Pore Region of the Voltage-Gated Ion Channel Superfamily. Taken from (Yu et al., 2005), Ca_v and Na_v, which are four trans-membrane domain channels, are shown in blue, the TRP family are shown in green, the potassium-selective family are shown in red, the CNG family are in purple and the HCN channel family are in orange. Ca_v, voltage-gated calcium channel; CNG, cyclic nucleotide-gated cation channel family; K2P, two-pore potassium channel; K_{Ca}, calcium-activated potassium channel; K_{ir}, inwardly rectifying potassium family; K_v, voltage-gated potassium channel family; Na_v, voltage-gated sodium channel; TRP, transient receptor potential channel; TPC, two-pore calcium channel.

1.7.2. Sodium Channels

The voltage-gated Na^+ channels consist of 9 subunits, $Na_v1.1$ – $Na_v1.9$, and are responsible for the initiation of the AP through the rapid intake of Na^+ into the cell during the upstroke of the AP (Goldin *et al.*, 2000; Costigan *et al.*, 2009; Dib-Hajj *et al.*, 2009). These subunits are important contributors to pain pathophysiology (Dib-Hajj *et al.*, 2010) and can be categorised according to their response to tetrodotoxin: tetrodotoxin-sensitive or tetrodotoxin-resistant.

$Na_v1.8$ is a sensory-neuron specific subunit that was first identified in small DRG neurons in the rat (Jensen *et al.*, 1986; Akopian *et al.*, 1996; Sangameswaran *et al.*, 1996) and later in humans (Larson *et al.*, 1986; Rabert *et al.*, 1998). This subunit is found predominantly, but not exclusively, in small and large nociceptive neurons and mediates a tetrodotoxin-resistant current (Akopian *et al.*, 1996; Djouhri *et al.*, 2003; Shields *et al.*, 2012). Blocking $Na_v1.8$ using antisense oligonucleotides eliminates the generation of SA in a CFA-induced model of CIP (Jarvis *et al.*, 2007). Furthermore, $Na_v1.8$ antisense oligodeoxynucleotides attenuate hypersensitivities in the SN ligation model of NP (Porreca *et al.*, 1999). Another study used diphtheria toxin to selectively kill $Na_v1.8$-expressing-neurons to ablate IP and decrease sensitivity to noxious mechanical and cold, but not thermal stimuli or NP-induced hypersensitivities (Abrahamsen *et al.*, 2008).

In humans, a loss of function of $Na_v1.7$ results in insensitivity to noxious stimuli (Cox *et al.*, 2006; Ahmad *et al.*, 2007; Goldberg *et al.*, 2007). Using rodent studies, the expression profile of $Na_v1.7$ is not exclusive to nociceptors as it is present in LTM DRG neurons (Djouhri *et al.*, 2002). A double knock out of $Na_v1.7$ and $Na_v1.8$ did not affect L5 SN ligation induced NP (Nassar *et al.*, 2005). Although knock out techniques have improved recently, compensation from other proteins can interfere with the desired effect (Wolf and Woodside, 2005).

$Na_v1.9$ is a tetrodotoxin-resistant subunit that is expressed in small C-fibre DRG neurons (Cummins *et al.*, 1999). This subunit possesses unique, slow-activation properties (Cummins *et al.*, 1999; Gold and Caterina, 2007) and may have a profound effect on the resting membrane potential {$\mathbf{E_m}$} (Herzog *et al.*, 2001).

Finally, $Na_v1.3$ is tetrodotoxin-sensitive and has high expression levels in embryonic DRG neurons, but not adult DRG neurons (Waxman *et al.*, 1994), although up-regulation occurs following SN axotomy (Waxman *et al.*, 1994; Black *et al.*, 1999). A global knock-out in a mouse model of NP induced by L5 SN ligation did not affect mechanical hypersensitivity or SA (Nassar *et al.*, 2006).

1.7.3. Potassium Channels

The K^+ channels are primarily responsible for the repolarisation, or fall, of the AP and, predominantly, bring the membrane potential back towards the resting level. There are four main types of K^+ channel: 1) voltage-gated; 2) Ca^{2+}-activated; 3) inward rectifier; and 4) two-pore (Ocaña *et al.*, 2004).

The voltage-gated channels comprise the K_v1 to K_v12 families (Ocaña *et al.*, 2004) and although activators of the K_v7 family showed analgesic effects in a rat model of NP (Blackburn-Munro and Jensen, 2003; Passmore *et al.*, 2003), these compounds failed in clinical trials (Hehn *et al.*, 2012). The Ca^{2+}-activated group consists of $K_{Ca}1$ – $K_{Ca}8$, while the inward rectifier group consists of $K_{ir}1$ – $K_{ir}7$, of which two are particularly important for nociception: $K_{ir}3$ and $K_{ir}6$ (Ocaña *et al.*, 2004). Specific knockout of $K_{ir}3.1$ and $K_{ir}3.2$ from the CNS of normal animals caused hypersensitivity, particularly to heat (Marker *et al.*, 2004). The role of these subunits in the periphery is unclear. Finally, the two-pore channels consist of $K_{2P}1$ – $K_{2P}14$, but the physiological roles of the majority of this family are not well understood (Ocaña *et al.*, 2004). Currently, no potassium channel subunits have successfully been modified to alleviate CP, although research is on going.

1.7.3. Calcium Channels

The voltage-gated Ca^{2+} channels, in particular the T-Type, have been linked to CP. Intra-peritoneal (Barton *et al.*, 2005) or local (Dogrul *et al.*, 2003) injections of T-Type antagonists were shown to reverse acute and persistent pain behaviours.

1.7.4. Transient Receptor Potential Channels

Finally, the **T**ransient **R**eceptor **P**otential {**TRP**} family, of which 28 genes have been identified (Montell, 2005) and divided into 6 main sub-families (Stucky *et al.*, 2009) with almost all being non-selective cation channels (Wang and Woolf, 2005), are important in determining the excitability of DRG neurons. The TRP subunits have specific roles in thermosensation and are activated between highly specific temperature ranges (Dhaka *et al.*, 2006; Vay *et al.*, 2012): TRPV1, > 43°C; TRPV2, > 52°C; TRPV3 and TRPV4, 26-35°C; TRPM8, < 28°C; TRPA1, < 17°C (Lawson *et al.*, 2008; Talavera *et al.*, 2008).

TRPV1, a TRP ion channel subunit, responds to the active ingredient of chillies, capsaicin, noxious > 43°C temperatures, as it is essential for thermal hypersensitivity (Davis *et al.*, 2000), and low pH that is < 6.0 (Caterina *et al.*, 1997; 2000). In the presence of activators, such as capsaicin, TRPV1 allows an influx of Ca^{2+} into the neuron (Caterina et al., 1997; 2000). A TRPV1 knock out model of inflammation showed severely deficient responses to chemical and thermal stimuli (Caterina et al., 2000) and there is evidence that inflammatory mediators, such as neurotrophins or bradykinin (Cesare and McNaughton, 1996), act via TRVP1 (Tominaga *et al.*, 1998).

Two other important members of this family are TRPA1 and TRPM8. TRPA1, which is unique to mammals (Story et al., 2003; Stucky et al., 2009), is activated by noxious stimuli including cold temperatures, pungent natural compounds, and environmental irritants through covalent modification of cysteine residues

(Macpherson et al., 2007). TRPA1 functions as a cold sensor (Story et al., 2003) and a mechanical- and chemical-transducer (Kwan *et al.*, 2006). TRPM8 has been identified in both C- and Aδ-fibre DRG neurons (Takashima et al., 2007) and is activated by both menthol and a drop in temperature (McKemy et al., 2002; Peier et al., 2002), which is supported by *in vivo* experiments using knock-out techniques (Bautista et al., 2007; Colburn et al., 2007; Dhaka et al., 2007).

1.7.5. Ion Channels and Resting Membrane Potential

Research into the role of ion channel families in pain pathways has rapidly advanced the understanding of the somatosensory system and the development of CP. Despite this, a candidate that is up regulated during multiple types of CP and could account for the increased excitability and SA has not been found. For this reason, our lab focuses on two of the ion channel families that contribute to the resting E_m of the neuron: the HCN and KCNQ ion channel families, which act as an accelerator and a brake, respectively, on AP firing [Fig. 1.9]. As much as 85% of K^+ background currents in DRG are represented by two-pore K^+ channels: 1) TRESK, or $K_{2p}18.1$; and 2) TREK-2, or $K_{2p}10.1$ (Kang and Kim, 2006; Dobler et al., 2007) and there is evidence that mRNA levels of these proteins change during IP (Marsh et al., 2012), however, further work is required. Therefore, this thesis will focus exclusively on HCN1-4 (Ludwig et al., 1998).

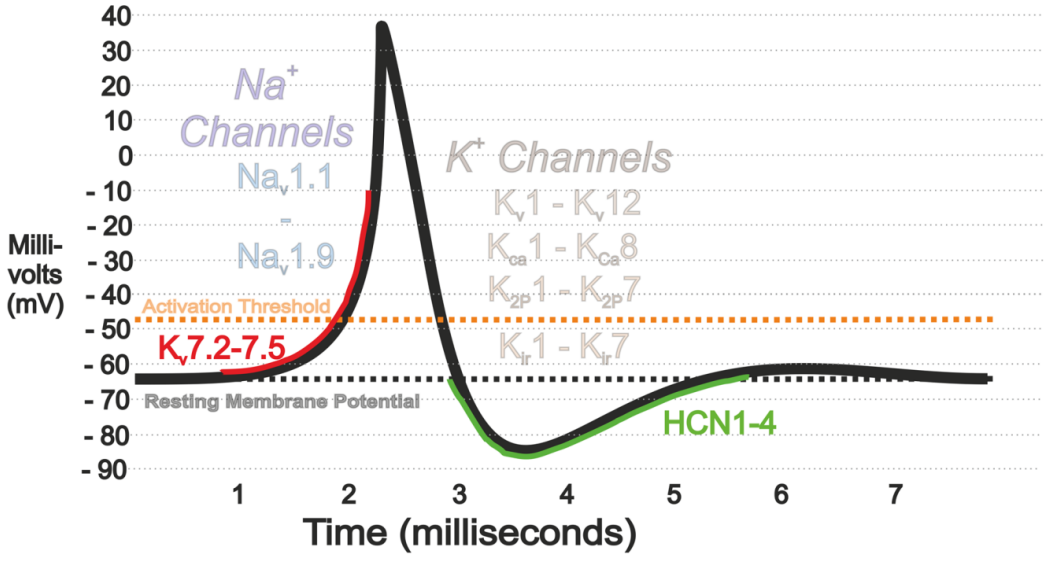

Figure 1.9: Ion Channel Families that Determine the Resting Membrane Potential. There are a multitude of ion channels that determine the resting E_m of the neuron, shown by the dashed black line, and this figure highlights two of them: HCN, in green, and K_v7, in red. The HCN channels drive the E_m from a hyperpolarised level back towards the resting level, acting as an accelerator, while the K_v7 channels act as a brake, driving the E_m back towards, or below, the resting potential to try and stop the neuron reaching the activation threshold, shown by the dashed orange line.

1.8. HCN Ion Channels

1.8.1. Evolution of HCN Channels

The HCN channel family emerged from voltage-gated potassium channels [Fig. 1.10.A]. There are four HCN channel subunits, HCN1-4, that mediate the I_h current, which is a mix of Na^+ and K^+ at a ratio of between 1:3 and 1:5 (Biel *et al.*, 2009). HCN subunits are highly selective as they are one of the only ion channel families that are able to distinguish Lithium from Na^+ (Biel et al., 2002).

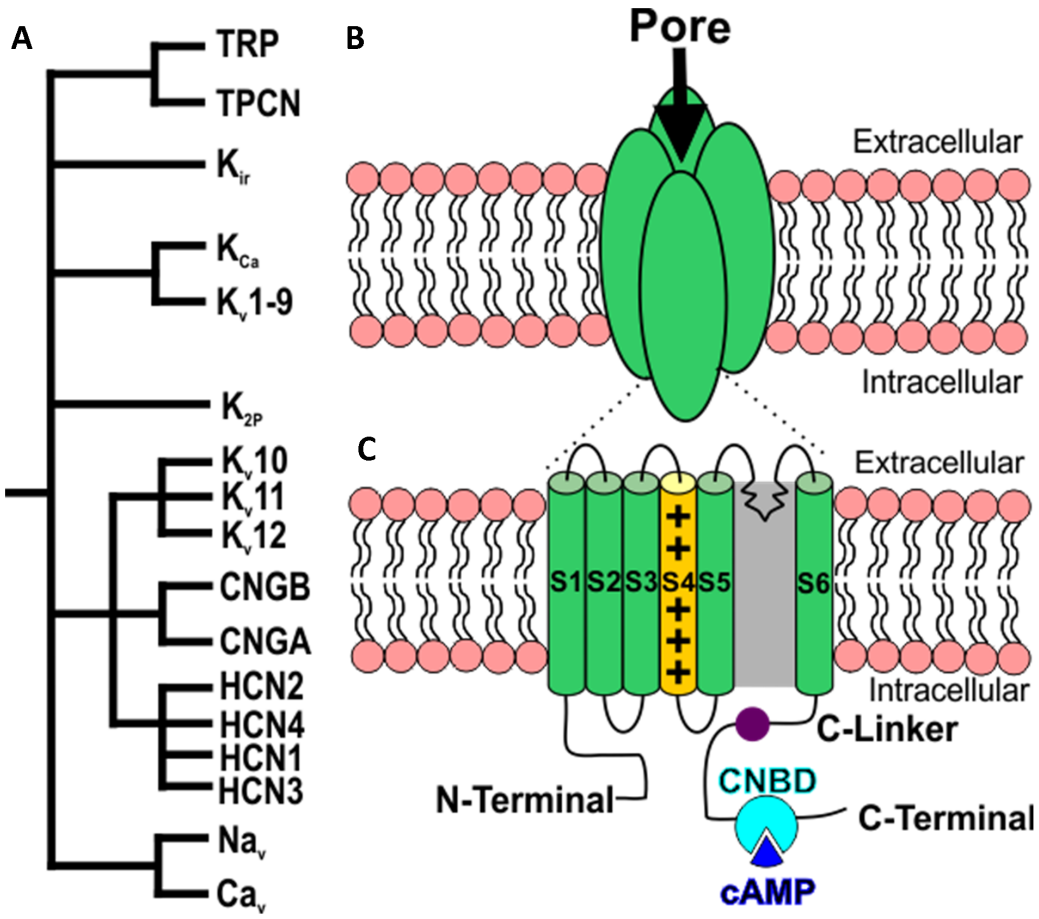

Figure 1.10: Phylogenetic Branches of Voltage-Gated Ion Channels and the HCN Channel Subunit Structure. [A] A schematic representation of the superfamily of pore loop cation channels, taken from (Postea and Biel, 2011). [B] A tetrameric channel formed by four HCN channel subunits, taken from (Postea and Biel, 2011). [C] The transmembrane topology of a single HCN channel subunit, taken from (Postea and Biel, 2011). The Cyclic Nucleotide Binding Domain, CNBD, which normally actively inhibits the pore and this inhibition is removed by the binding of a cyclic nucleotide, such as cAMP in blue. ZD7288, shown by the purple circle, binds intra-cellularly to the S6 domain to inhibit these subunits.

1.8.2. HCN Channel Subunits

1.8.2.1. HCN Channel Subunit Structure

Each HCN subunit [Fig. 1.10.C] contains three components: the trans-membrane core, the cytosolic NH_2-terminal and the COOH-terminal domains (Biel et al.,

2009). As a member of the pore-loop cation channel family, the molecular structure of a single subunit resembles a voltage gated K^+ channel subunit with six trans-membrane domains, including the voltage-sensing S4 domain (Biel et al., 2002; Yu et al., 2005).

1.8.2.2. Cyclic Nucleotide Binding Domain

The key difference between the voltage gated K^+ and HCN channels is the cyclic nucleotide binding domain, which confers selectively to different cyclic nucleotides, in particular **c**yclic **a**denosine **m**ono**p**hosphate {**cAMP**}, but also cyclic guanosine monophosphate (Zagotta et al., 2003). Cyclic nucleotides can be thought of as HCN channel co-agonists. Binding of cyclic nucleotides to the cyclic nucleotide binding domain enhances the voltage-gating characteristics at physiologically relevant membrane potentials, as the channel will open at more depolarised, or positive, voltages (Bobker and Williams, 1989; Pape and McCormick, 1989; Tokimasa and Akasu, 1990; Banks et al., 1993; Erickson et al., 1993; Larkman et al., 1995).

1.8.2.3. Mechanism of Cyclic Nucleotide Binding Domain

Although the CNBD's mechanism of action is debated, the predominant hypothesis is that it actively inhibits the HCN channels and the binding of cyclic nucleotides removes this inhibition (Wainger et al., 2001; Wang et al., 2001). X-ray crystallography showed that cAMP interacts directly with the highly-conserved arginine residues within the CNBD: arginine-591 in the HCN2 channel subunit (Chen et al., 2001; Zhou and Siegelbaum, 2007) and arginine-538 in the HCN1 channel subunit (Han et al., 2011). This interaction leads to allosteric changes coupled to gating (Zagotta et al., 2003), however, recent findings in the closely-related CNG channel family indicate that any changes in conformation are subtle (Taraska and Zagotta, 2007).

1.8.2.4. Cyclic Nucleotides and Activation Properties

Cyclic nucleotides, which play important physiological roles, are regulated by a variety of hormones, particularly in the heart where adrenaline acts through a cAMP-dependent mechanism on HCN4 (Brown et al., 1979; DiFrancesco and Tortora, 1991). Most drugs that affect heart rate, such as beta-blockers, affect cAMP concentrations and this affects HCN4 and the I_h current (Biel et al., 2002). In the presence of cAMP, both HCN4 and HCN2 experience shifts in their activation midpoint of up to 20 mV, meaning they are activated at more positive voltages (Chen *et al.*, 2001). In general, cAMP is 10-100 times more potent than cGMP (Gauss *et al.*, 1998; Ludwig *et al.*, 1998; Kaupp and Seifert, 2001; Biel *et al.*, 2009). Not all of the HCN channel subunits are affected by cyclic nucleotides, as the activation properties of HCN3 do not change in the presence of cyclic nucleotides (Stieber *et al.*, 2005).

1.8.2.5. Regulators of HCN Channel Subunits

The HCN channels' activation properties are regulated by a number of factors, including, but not limited to: 1) acidic lipids, such as **p**hosphatidyl**i**onositol 4,5-bis**p**hosphate {**PIP_2**} (Pian et al., 2006; Zolles et al., 2006); 2) intracellular (Munsch and Pape, 1999; Zong et al., 2001) and extracellular (Stevens et al., 2001) proton concentrations; 3) chloride, as extracellular concentrations exert a pronounced effect on HCN2 and HCN4 (Frace et al., 1992; Wahl-Schott et al., 2005); 4) tyrosine kinases of the src family (Wu and Cohen, 1997), with particularly pronounced effects on HCN2 and HCN4 (Zong et al., 2005); and 5) the serine/threonine p38-mitogen activated protein kinase (Poolos et al., 2006). All these different, highly specific modulatory actions allow for the possibility of physiologically specific roles for the HCN channel subunits.

1.8.2.6. HCN Channel Subunit Activation Speeds

Each HCN subunit boasts unique properties [Tab. 1.2]. HCN1 is the fastest subunit (Santoro et al., 2000; Ishii et al., 2001), requiring tens of **m**illi**s**econds {**ms**} to activate, followed by HCN2 (Ludwig et al., 1999), HCN3 and HCN4, which have speeds of hundreds of ms (Stieber et al., 2005). Different permutations of channel subunits, along with the physiological microenvironment, affect activation properties (Biel *et al.*, 2009).

	HCN1	**HCN2**	**HCN3**	**HCN4**
General DRG Neuronal Expression	Small and Large	Small and Large	All sizes	~2% of very Small
$V_{0.5}$ (mV)	-70 to -90	-70 to -100	-80 to -95	-70 to -100
Effect of cAMP on $V_{0.5}$ (mV) (Chen *et al.*, 2001)	2 to 7	0 to 20	0	0 to 20
Tau_{act} at -140 mV (ms)	30	150 to 200	250 to 400	> 400

Table 1.2: Activation Characteristics of the HCN Channel Subunits. For each HCN channel subunit, this table shows: 1) the general expression profile in DRG neurons; 2) the activation parameters $V_{0.5}$ is the voltage at which half of the channels are active; 3) the effect of cAMP; and 4) Tau_{act}, an activation time-constant showing the speed until full activation is accomplished.

1.8.2.7. HCN Channel Subunit Combinations

There is strong evidence that these four types of channel subunits come together *in vivo* to form hetero-tetramers of different permutations, specific to their required physiological role (Ulens and Tytgat, 2000; Chen et al., 2001; Xue et al., 2002; Altomare et al., 2003; Er et al., 2003; Much et al., 2003; Whitaker et al., 2007). This allows for increased physiological diversity to occur, since changes in

I_h could be a result of genetic changes that affects the heterogeneity of these functional ion channels.

1.8.3. HCN Channel Subunit / I_h Tissue Distribution

I_h was initially discovered in sinoatrial node cells in the heart around the late 1970s and early 1980s (Brown et al., 1977; Yanagihara and Irisawa, 1980; DiFrancesco, 1981a; 1981b), where it was referred to as I_f, before also being discovered in neurons, initially in the hippocampus (Halliwell and Adams, 1982; Maccaferri et al., 1993) and then in DRG neurons (Mayer and Westbrook, 1983).

Although the I_h current is widely expressed in tissue across the human body, with the exception of the heart and the nervous system, expression levels in these other tissues are relatively low (Biel *et al.*, 2009). In addition, HCN3 is neuronal specific, although it is only sparsely expressed throughout the nervous system (Biel et al., 2009). Of the four subunits, HCN3 showed the highest amounts of mRNA in small DRG neurons (Kouranova et al., 2008). Finally, HCN4 is predominantly found in the SA node of the heart, although, under normal conditions, this subunit is in just 2% of DRG neurons (Cho *et al.*, 2009b).

1.8.4. HCN Channels and Pharmacological Intervention

As the amount of research on the HCN channels and their role in CP has increased, it has become an increasingly important potential drug target (Postea and Biel, 2011). There are likely to be a number of suitable targets that act either on the channels themselves or directly up- or down-stream of the numerous signalling pathways that affect intracellular cyclic nucleotide concentrations. Currently, the most commonly used blocker of the HCN channels is ZD7288, which is not subunit selective, but is selective for the I_h current and seems to have an intracellular site of action that is irreversible in the sea urchin

homologue for the HCN channels (Shin et al., 2001) and possibly in mammalian HCN variants as well (Postea and Biel, 2011).

1.9. Hypothesis and Aims

Based on the literature reviewed above, a hypothesis can be formed where either CIP or CNP results from a change in the expression profiles of HCN channel subunits, primarily in the adjacent, conducting DRG neurons with their receptive fields still intact. This could result in an increase in the I_h current, which in turn increases the SA frequency that is responsible for driving the sensitisation of 2nd order neurons in the spinal cord and ultimately results in both types of CP.

Using two rodent models of CP to test this hypothesis, there were multiple aims, which included:

- Using behavioural tests to see whether peripherally blocking the I_h current affects SFL, in addition to mechanical and heat hypersensitivity.
- Using *in vivo* electrophysiology to examine whether there are changes in the AP parameters, excitability and I_h current in the intact L4 neurons following the induction of CNP when compared to sham-operated animals.
- Using immunofluorescence to determine, using quantification, which, if any, of the HCN channel subunits change their expression following the induction of models of CP.

Chapter 2 - Methods

2.1. Abstract

The principal aim of this PhD project was to examine the role of the **h**yperpolarisation-**a**ctivated, **c**yclic **n**ucleotide-**g**ated {**HCN**} channels and the current they mediate, the **h**yperpolarisation-activated current {I_h} in the excitability of **d**orsal **r**oot **g**anglion {**DRG**} neurons during **c**hronic **i**nflammatory **p**ain {**CIP**} and **c**hronic **n**europathic **p**ain {**CNP**} using reproducible and robust rodent models. In order to minimise animal suffering, both careful experimental design and the principles of the 3Rs were employed throughout. To investigate the principal hypothesis, three techniques were used: a) behavioural testing, to examine the effects of peripheral blockade of I_h on pain behaviours; b) *in vivo* electrophysiology, to record **a**ction **p**otential {**AP**} parameters and the I_h current from physiologically identified DRG neurons and determine whether the channels are involved in DRG neuronal hyperexcitability in CNP; and c) immunofluoresence, to determine which HCN channel subunits {**HCN1-3**} are expressed in DRG neurons and whether their expression changes during **c**hronic **p**ain {**CP**} states.

2.2. Animals Used

Young, female Wistar rats (180-280 g, Charles River, U.K.) were used for all types of experiment. Females were used since they are typically the most affected by CP (Berkley, 1997) and 79% of studies focussing on pain between 1996 and 2005 have used only male subjects, leading to a lack of knowledge about pain states in female strains (Mogil and Chanda, 2005; Greenspan et al., 2007). Furthermore, although controversial, there is strong evidence that the hormone cycles do not increase the variability of pain sensitivity in females (Mogil and Chanda, 2005).

Animals were housed in a room maintained at an ambient temperature, while under a 12-**h**our {**h**} dark and light cycle, with soft bedding and access to food and water *ad libitum*. All experimental procedures were carried out in

accordance with the 1986 UK Scientific Procedures Animals Act. In accordance with the 3Rs, which emphasise replacement, refinement and reduction, all efforts were made to utilise the best experimental design, so that the fewest number of animals possible would be used and suffering would be minimised. Based on their exploratory activity and weight gain, all rats appeared healthy throughout all of the experiments (Deacon, 2006). If rats showed any signs of ill health, such as sudden weight loss, they would have undergone an approved schedule 1 procedure [Appendix 1]. At the end of the experiment, animals were euthanized by an approved schedule 1 method.

2.2.1. Inflammatory Pain Model – Complete Freund's Adjuvant

To achieve a deep level of anaesthesia, the rat was placed in a sealed box and 3% isoflurane in oxygen and nitrous oxide, at 2 litres per **min**ute {**min**}, were administered. Nitrous oxide causes minimal cardiovascular and respiratory system depression to supplement the isoflurane, which rapidly induces anaesthesia and can be easily altered, as required (Flecknell, 2009). The high flow rates for these two gases are required because of the anaesthetic gas scavenging system, which ensured that nitrous oxide is ducted directly out of the room, so contamination does not occur.

Once deeply anaesthetised, two intra-dermal injections of **c**omplete **F**reund's **a**djuvant {**CFA**} (Sigma-Aldrich, U.K.), which induces changes in nociceptive thresholds (Larson *et al.*, 1986), were administered: one into the plantar surface of the left hind paw [Fig. 2.1.A] and the other into the lateral region of the left knee [Fig. 2.1.B]. Both injections were within the cutaneous receptive fields of the **L**umbar **3** - **5** {**L3-5**} DRG neurons (Takahashi et al., 1994) [Fig. 2.1.C-D]. The L4-L5 DRG neurons, which were used for the electrophysiological and immunofluorescent experiments, possesses dermatomes in rats (Takahashi et al., 1994) that corresponds to that of both humans (Keegan and Garret, 1948) and dogs (Fletcher and Kitchell, 1966).

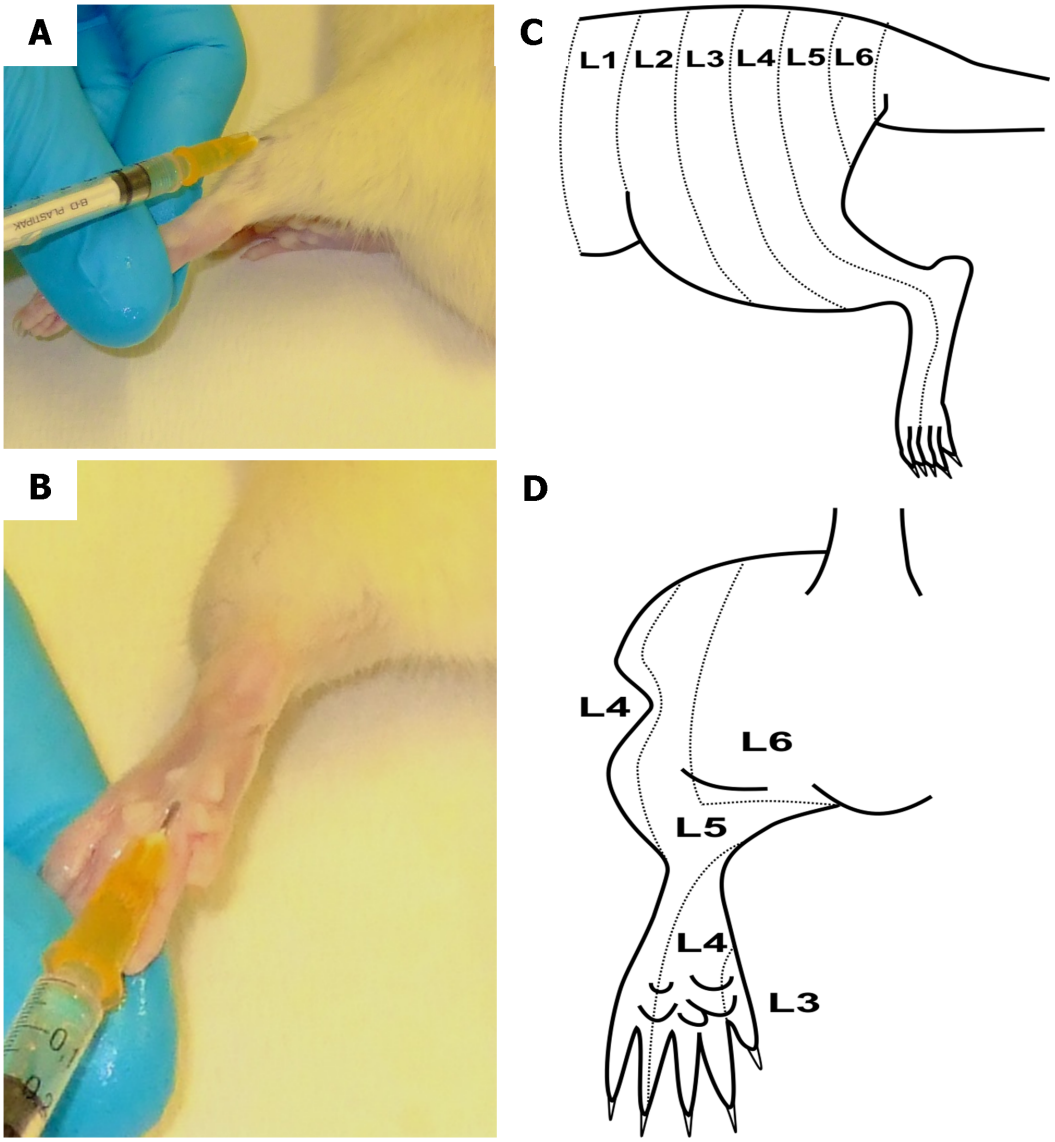

Figure 2.1: CFA Model and Dermatomes of L3-L6 Spinal Nerves. Pictures showing the intra-dermal [A] and intra-plantar [B] injections of CFA into the hindlimb and these injections affect the dermatomes of the L3 – L6, principally L4 and L5, DRG neurons [C-D] (Takahashi et al., 1994).

Each **m**illi**l**itre {**ml**} of CFA is composed of 1 **m**illi**g**ram {**mg**} of heat-killed and dried Mycobacterium tuberculosis (strain H37Ra, ATCC 25177), 0.85 ml paraffin oil and 0.15 ml of mannide monooleate (Sigma-Aldrich, 2010). CFA causes an inflammatory response by inducing dendritic cells to rapidly uptake adjuvant components, enhancing phagocytosis and the transudation of cytokines from mononuclear phagocytes, and temporarily activating $CD4_1$ lymphocytes. The mycobacteria within CFA causes the T lymphocytes to assume a Th1 profile,

which causes delayed-type hypersensitivity and initiates an inflammatory soup that results in pain behaviours developing in the afflicted hindpaw (Billiau and Matthys, 2001). For the immunofluorscent studies, the control groups received no CFA-treatment.

2.2.2. Neuropathic Pain Model – Modified Spinal Nerve Axotomy

Prior to the initiation of this procedure, animals were weighed and checked visually for good health. Efforts were made to keep the surgical conditions aseptic, which involved autoclaving the surgical tools, in addition to accessories, such as cotton buds and tissues, to minimise the risk of post-operative infection.

To achieve a surgical plane of anaesthesia, both isoflurane and nitrous oxide, were used, as described above for the CFA injections, and initially delivered via a sealed box before using a nose-piece during surgery. After shaving off back hair, viodine, a non-irritable and non-staining iodine that prevents skin infections due to anti-bacterial and anti-fungal properties, was applied.

After relocating to the operating table, an incision was made along the back to expose the muscles directly above the L4-L6 DRG. Then another incision was made in the muscle, which was approximately half the size of the incision in the skin, and the muscle was slowly removed to expose the lateral process of the L6 DRG [Fig. 2.2A]. If prolonged bleeding occurred, then sterilized cotton buds were applied until the bleeding stopped.

Once the L6 transverse process was exposed, it was chipped away to reveal a thin layer of muscle above the L5 and L4 **s**pinal **n**erves {**SN**} [Fig. 2.2.B]. After removing this tissue, the L5 SN was carefully lifted up using 45° angled forceps, ligated tightly with 5-0 silk and axotomised with small butterfly scissors, just distally to the suture with care to avoid damaging the spared L4 SN. A small piece of the L5 SN, distal to the initial axotomy, was removed to prevent regeneration.

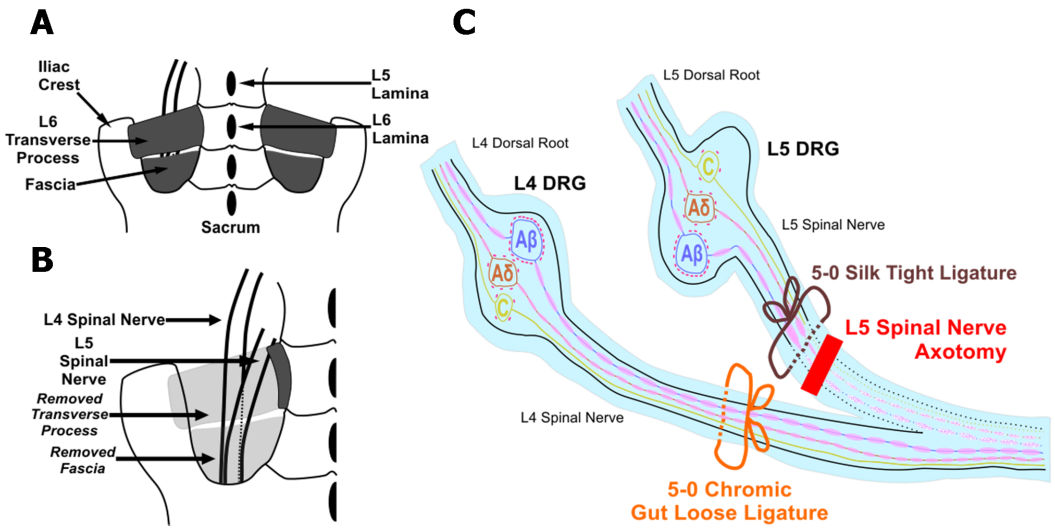

Figure 2.2: Modified Spinal Nerve Axotomy Model of Neuropathic Pain. A schematic diagram, modified from (Chung et al., 2004), showing the exposed skeletal section, which includes the L5 and L6 laminae, the iliac crest, the fascia and the L6 transverse process [A]. Once the fascia and L6 transverse process has been removed [B], the L5 and the L4 SN can be manipulated. A schematic [C], which is modified from (Djouhri *et al.*, 2006), shows the mSNA model of NP, which involves L5 SN ligation using 5-0 silk and axotomy, in addition to loose ligation of the L4 SN, which sits below the L5, with 5-0 chromic gut.

Underneath the L5 SN is the L4 SN, which was loosely ligated with 5-0 chromic gut (Look, Angiotech Pharmaceuticals, Canada) to cause enhanced neuro-inflammation (Maves *et al.*, 1993). The ligature around the L4 SN was double the nerve's diameter. In rats, Wallerian degeneration, a process of nervous tissue break-down that results in neuro-inflammation, occurs after just 24-h – 48-h (Miledi and Slater, 1970; Lubińska, 1977), as opposed to several days in primates (Gilliatt and Hjorth, 1972).

After this, the muscle was sewn together using 4-0 polysorb thread and a continuous intradermal pattern of stitching. Then, the skin was tightly sutured using either the slightly thicker 3-0 thread in a simple interrupted pattern, or an autoclaved skin stapler, to ensure that the wound would not be reopened by chewing or other behaviours.

No post-operative analgesics or antibiotics were applied as this was contraindicated in the project licence due to the possible effect on the complex physiological pathways that result in the development of CP. After transferring the rat to a recovery room kept at 25°C, physiological fluids (0.9% saline) were applied only if > 1 ml of blood was lost during the surgery or if the condition of the rat didn't dramatically improve following recovery from the anaesthesia.

For the immunofluorescent study, the control group received sham-treatment {**mSHAM**}, which involved performing the surgery to expose and lift up the L5 and L4 SNs, without inflicting any nerve damage. For the *in vivo* electrophysiology study, normal, un-treated animals were used for controls to compare with the L4 DRG neurons from the mSNA model of NP, as electrophysiological properties of DRG neurons after sham-operations used for L5 SN ligation were similar to the values from normal rats (Ma *et al.*, 2002).

2.3. Behavioural Tests

Prior to testing the thresholds of mechanical and heat stimuli, rats were allowed time to acclimatise in their chambers until exploratory and grooming behaviour ceased, which was typically more than 15-min. Then, experimental procedures were followed for all three tests, using three animals at a time, as described below. Habituation allows for more accurate and sensitive results (Taiwo *et al.*, 1989) and was done for 2-3 **d**ays {**d**} before the pre-treatment data point, which was taken 1-d before the induction of CP. Tests were also conducted before drug administration, known as the pre-drug time point, and then after drug administration, at 1-h, 3-h, 24-h and 48-h.

2.3.1. Spontaneous Foot Lifting

Spontaneous **p**ain {**SP**} is difficult to quantify (Mogil, 2009), so this study adopted a previously justified method for measuring SFL in animal models of CP (Bennett

and Xie, 1988; Attal et al., 1990; Yoon et al., 1996; Djouhri et al., 2006). Since SFL was not present before the induction of CP, data were only collected from the first time point post-treatment: Pre-Drug. Rats were placed in isolated compartments of a clear plastic chamber, measuring 22x18x14cm, on a glass floor [Fig. 2.3.A]. The animals were allowed to acclimatise to their boxes for approximately 15-min. Once acclimatised, the cumulative duration of time in **s**econds {**s**} that the ipsilateral hindpaw was lifted off the glass floor was recorded, over two 5-min periods, using a stopwatch for each hindpaw.

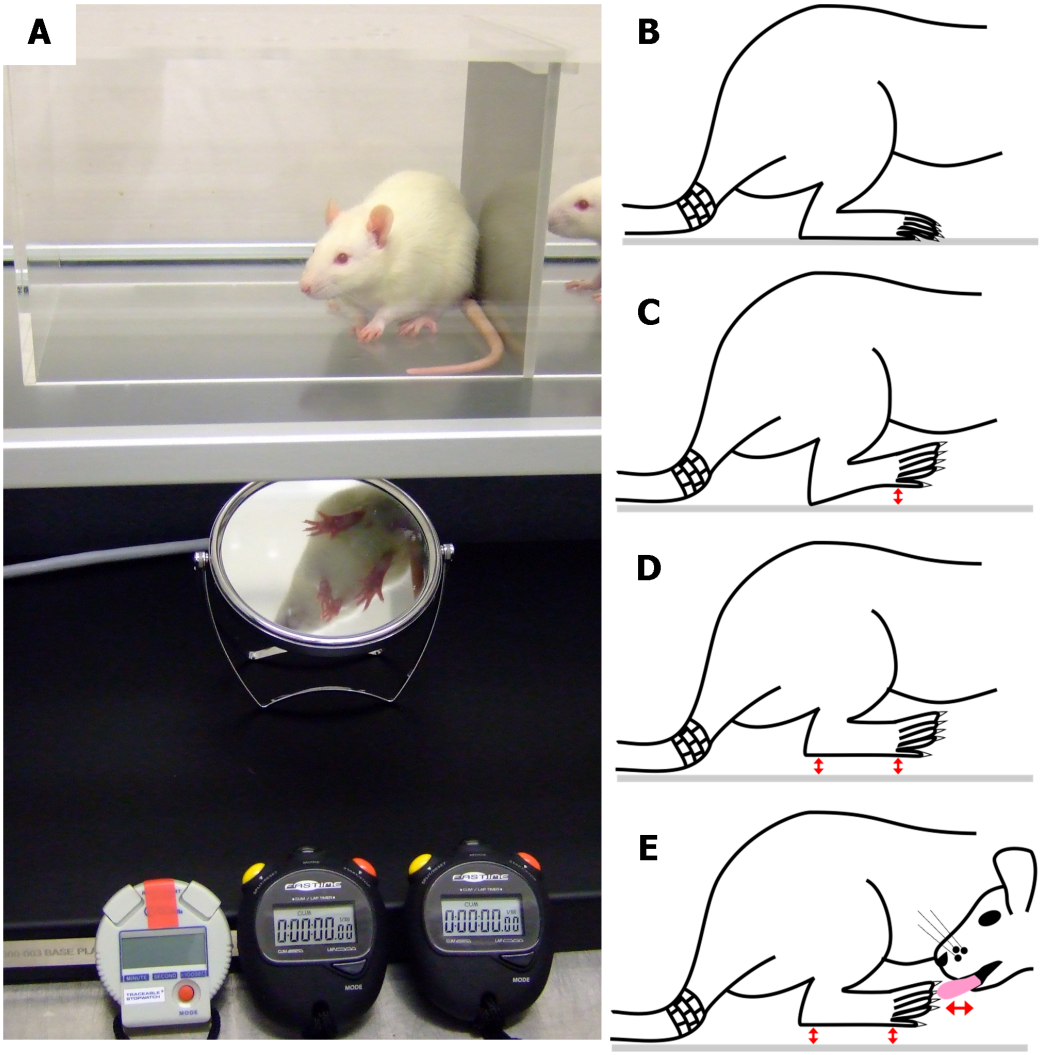

Figure 2.3: The Spontaneous Foot Lifting (SFL) Behavioural Test. All illustrations [B-F] were modified slightly from (Attal et al., 1990). [A] A photograph demonstrating how the SFL behavioural test was performed. Rats normally stand

with weight equally spread over both hinpdaws [A-B], but partial hindpaw lifting [C], complete hindpaw lifting [D], and foot licking [E] all demonstrated SP.

SFL was measured only when the animals were completely stationary [Fig.2.3.A-B], so that any lifting associated with locomotion or probing activities was excluded, due to the chance of the pain being evoked. SFL was recorded as either complete [Fig.2.3.C] or partial [Fig.2.3.D] stimulus-independent foot lifting or foot licking [Fig.2.3.E]. The total, cumulative duration of these abnormal behaviours were recorded over 5-mins. Foot lifting associated with grooming, locomotion, or body repositioning was excluded (Yoon *et al.*, 1996; Kim *et al.*, 1997). Furthermore, there is very little, if any, correlation between mechanical hypersensitivity, either static or dynamic, and SFL (Djouhri *et al.*, 2006; Bennett, 2012).

2.3.2. Withdrawal Threshold to Mechanical Stimulation

Prior to performing this test, rats were left in individual plastic chambers on top of a wire metal mesh floor [Fig.2.4.A] for 5-mins to allow for acclimatisation. A dynamic plantar aesthesiometer touch stimulator (Ugo Basile, Comerio, Italy) was used to apply pressure, through a blunt metal filament, to the mid-plantar surface of the hindpaw [Fig.2.4.C]. The force intensity increased from 0 – 50 **g**rams {**g**} over 15-s (Arévalo et al., 2003) to produce the paw withdrawal threshold, measured in g, which indicated the force required to cause hindpaw withdrawal from the stimulus. This was recorded after each test and decreased values infer mechanical hypersensitivity. Each rat received 1-min of rest in-between tests and 5-min in-between the same hindpaw. Tests were repeated four times to produce a mean and this was used for each time point for each rat.

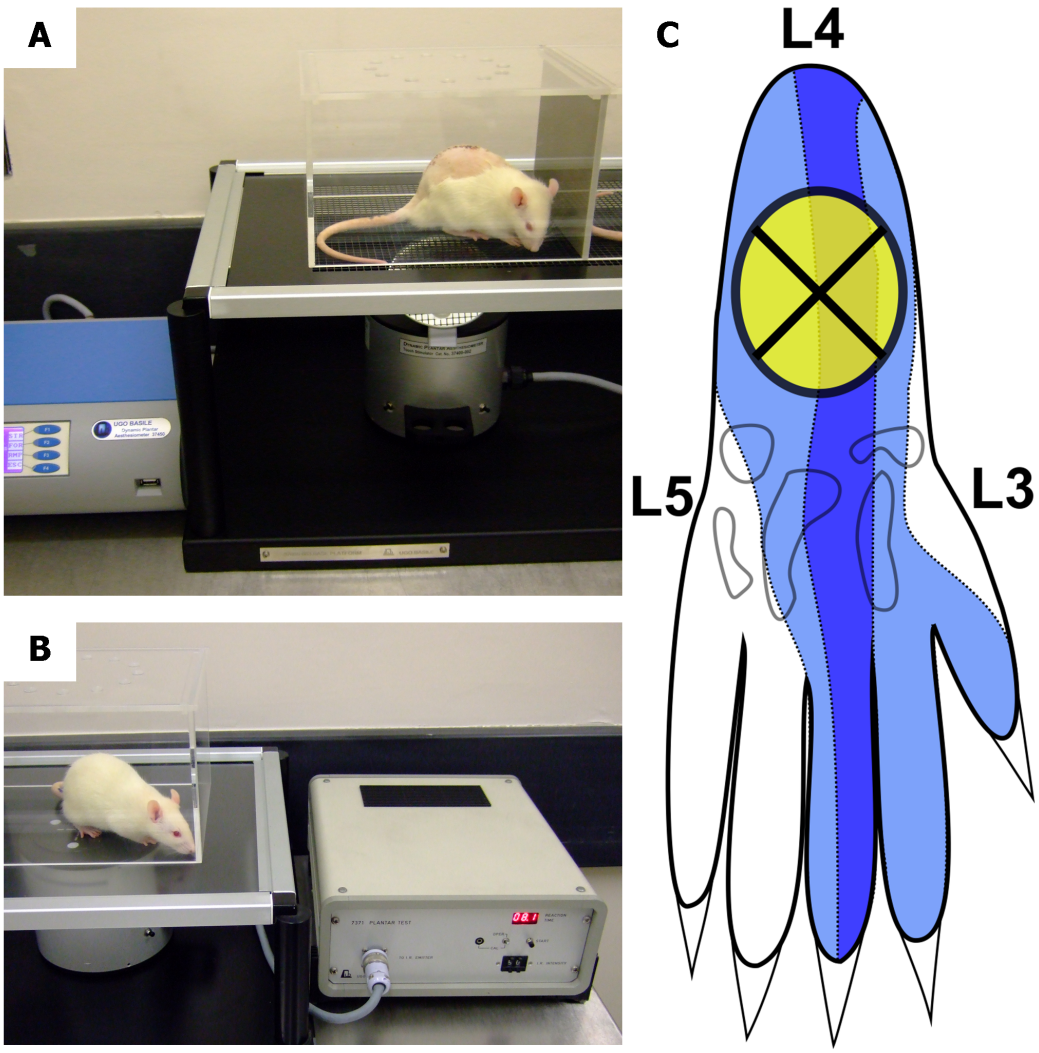

Figure 2.4: Plantar Aesthesiometer and Hargreaves Apparatus used for Behavioural Testing. These photographs show the apparatus used for the two evoked behavioural tests to test for mechanical [A] and thermal [B] hypersensitivity. The area tested is a part of the rat hindpaw that is made of up of L3-L5 SNs (Bajrović and Sketelj, 1998) and the area, in yellow, targeted during these behavioural tests. Overlapping lumbar spinal nerve regions are shown in light blue.

2.3.3. Withdrawal Latency to Noxious Heat

To assess heat hypersensitivity, the Hargreaves test, utilising a plantar analgesymeter (Ugo Basile, Comerio, Italy), which measures the latency, in s of

paw withdrawal to a noxious 50°C heat stimulus applied from a circular, 9-mm heat source placed underneath the rat's hindpaw, was used, as described previously (Nernst, 1888; Bennett and Xie, 1988; Hargreaves *et al.*, 1988; Allen and Yaksh, 2004; Djouhri *et al.*, 2006). 50°C activates both categories of heat-activated nociceptor: ≥ 43°C and ≥ 50°C (LaMotte and Campbell, 1978; Leffler *et al.*, 2007). In brief, rats were placed in plastic compartments on a 2 **m**illi-**m**etre {**mm**} thick glass floor [Fig.2.4.B] and allowed 5-mins to acclimatise. After positioning the equipment to target the same area for each test [Fig. 2.4.C], the noxious heat stimulus initiated, simultaneously starting a timer. The timer automatically ended when a photocell detected hindpaw withdrawal, although movement or grooming caused the test to be repeated. Heat hypersensitivity was inferred by decreased paw withdrawal latencies to the stimulus. Each hindpaw was tested four times to generate a mean, with 1-min of rest in-between tests on the same rat and 5-mins in-between the same hindpaw.

2.3.4. Drug Administration

The behavioural test experimenter was blind to drug treatment, which consisted of the I_h-specific blocker, ZD7288, or one of the positive controls, naproxen or gabapentin for CIP or CNP respectively. Prior to the CP studies, naïve animals were injected with these drugs to ensure there were no effects on pain sensitivity in normal conditions. For the CFA study, rats received: either an intra-plantar, into the hindpaw, injection of vehicle or ZD7288, or an inter-peritoneal, into the peritoneal cavity, injection of either naproxen. While for the mSNA study, this consisted of intra-plantar ZD7288, intra-plantar vehicle or inter-peritoneal gabapentin.

Vehicle (0.9% physiological saline) was used as a negative control. The rats received an intra-plantar injection of saline, at a dosing volume of 500 µl/Kg, into the ipsilateral hindpaw.

ZD7288 (Tocris Bioscience, U.K.) was diluted in 0.9% physiological saline to give a concentration of 100 µM. At a dose of about 15 µg/Kg, the rats received an intra-plantar injection of ZD7288, at a dosing volume of 500 µl/Kg, into the ipsilateral hindpaw. Furthermore, ZD7288 was injected intra-plantarly into the contralateral hindpaw, as a control for the local effects.

Naproxen (Sigma-Aldrich, U.K.), a non-steroidal anti-inflammatory drug, was diluted in 0.9% physiological saline and used as a positive control for the CFA model of IP. The compound was administered via an intra-peritoneal injection at a dose of 30 mg/Kg, using a dosing volume of 5 ml/Kg.

Gabapentin (Key Organics Ltd., U.K.), diluted in 0.9% physiological saline and injected inter-peritoneally at 10 mg/Kg, was used as a positive control for the mSNA model of NP. For this group, behavioural tests were performed at 4-h and 48-h post-administration, as gabapentin's half life is ~ 5-h – 7-h.

2.4. *In Vivo* Electrophysiology

2.4.1. Surgical Preparation

The preparation is based on a previously reported methodology (Fang *et al.*, 2005; Djouhri *et al.*, 2006). An intra-peritoneal injection, or injections if required, of sodium pentobarbital (50 mg/Kg) induced a surgical level of anaesthesia and after the first injection, due to the pentobarbital's hypothermic effects, the rat was artificially warmed (Lin, 1981). After shaving hair off of the back and hindlimb, the rat was placed on an electrical blanket and body temperature, which was maintained at about 36°C using a heat lamp, was monitored continuously using a rectal probe (Harvard Apparatus, U.K.).

Then, the trachea was intubated to allow artificial ventilation using a small animal ventilator (Harvard Apparatus, U.K.) and two cannulations were performed [Fig. 2.5.A-B]: the left external jugular vein and carotid artery, which,

respectively, enabled the administration of pentobarbital (10 mg/Kg) to maintain a surgical level of anaesthesia and monitoring of the blood pressure through a transducer connected to a neurlog pressure amplifier (NL 108, Digitimer, U.K.).

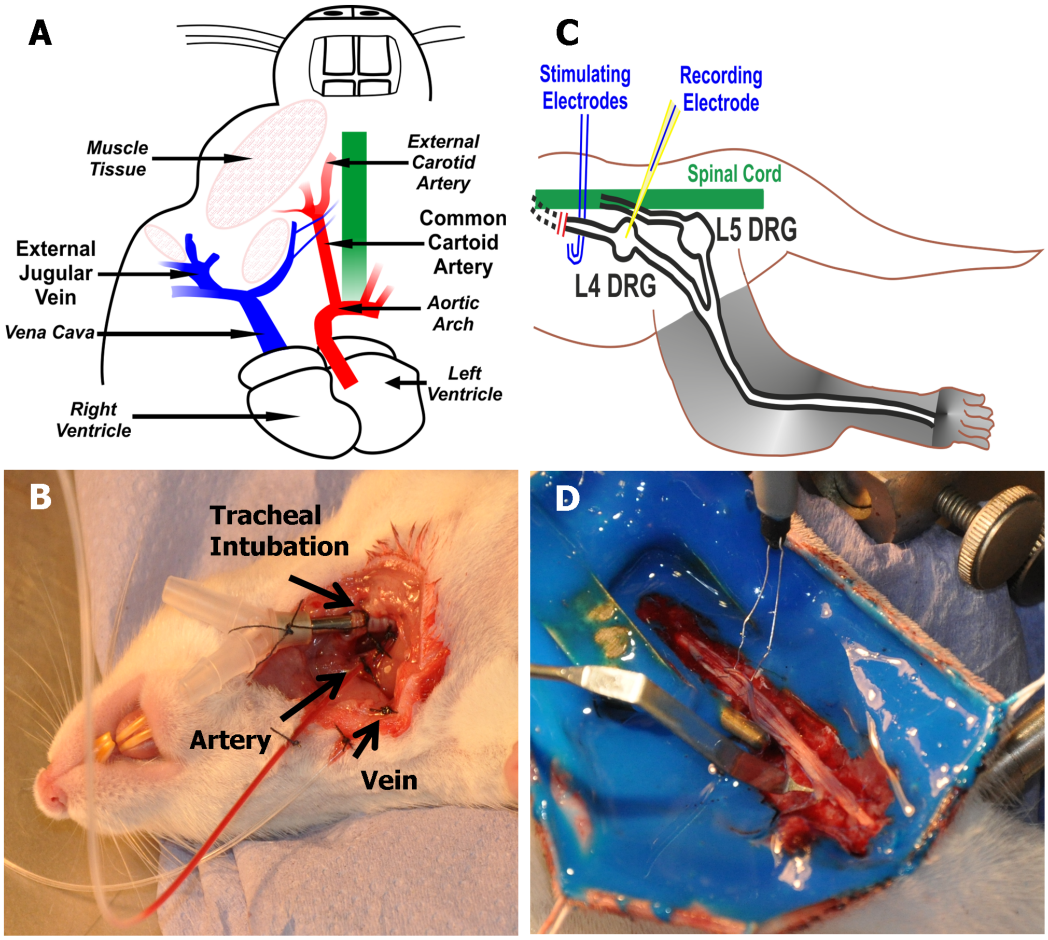

Figure 2.5: Preparation for *in vivo* Electrophysiology. A schematic diagram [A] showing the rat's external jugular vein and common carotid artery (Indo, 2001; Heisler, 2007) and a photograph showing these cannulations, together with the tracheal intubation, *in vivo* in an anaesthetised rat [B]. Then, the *in vivo* intracellular recording setup, which consists of a glass microelectrode placed on top of the L4 DRG to allow intracellular recording of somatic APs evoked anti-dromically by dorsal root electrical stimulation from a pair of bipolar platinum electrodes; shown schematically [C] and in a photograph [D].

Following laminectomy to expose the L4-L5 DRGs and their dorsal roots, a paraffin pool was formed, which was maintained throughout as close to body

temperature as possible, at ~ 30 ± 2°C, the dura matter was carefully peeled away using fine #7 dumont forceps. Then, the dorsal root, of the DRG under study, was cut near its entry point to the spinal cord and using polished glass, placed onto a pair of bipolar platinum electrodes [Fig. 2.5.C-D]. The left hindlimb was extended and fixed with superglue to a platform, with the glabrous hindpaw, facing upwards, to improve stability during sensory testing.

2.4.2. Electrophysiological Recordings

2.4.2.1. Finding a Neuron

Intracellular recordings were made from somata of either the ipsilateral L5 or L4 DRG, which both consist of thousands of neurons, estimated using the dissector method to be about 12,000 neurons in the L4 DRG (Arvidsson *et al.*, 1986; Tandrup, 1993; Cox *et al.*, 2006). Recordings were performed using borosilicate glass (1.2 mmOD, 0.69 mmID, Harvard Apparatus, Kent, U.K.) microelectrodes that were pulled with a programmable micropipette puller (P-97, Sutter Instrument Company, U.S.A.) with settings including pressure of 500, heat of 590, pull of 55, velocity of 90, and delay of 82. Then, the micropipette was filled with 1 Molar potassium chloride, which was used as it gives one of the lowest tip resistances (Axon Instruments Inc., 2003) and this generally ranged from 60 – 100 mega-ohms.

After attaching the microelectrode to a HS-9A headstage (Axon Instruments, CA, U.S.A.), DRG neurons were impaled by advancing the microelectrode in 1-µm steps into the DRG with a Patchstar micromanipulator (Scientifica, U.K.). A small capacitance buzz was applied until a membrane potential {$\mathbf{E_m}$} was recorded. Since two subunits that are responsible for I_h, HCN2 and HCN4, are particularly sensitive to cyclic nucleotides, the use of sharp electrode intracellular techniques may limit the patch electrode-induced cytoplasmic dialysis that can affect recordings (Wall and Gutnick, 1974; Hogan and Poroli, 2008).

2.4.2.2. Recording Spontaneous Activity

All APs were recorded using an Axoclamp 900A amplifier (Axon Instruments, CA, U.S.A.) in current clamp mode set to zero. Once the neuron's E_m stabilised and prior to sensory testing to avoid the influence of the experimenter, the neuron's voltage was recorded online for 1-min to observe any **s**pontaneous **a**ctivity {**SA**}. If the neuron displayed SA during this period, then the I_h-specific blocker, ZD7288, was applied and SA, indicated by 10 mV depolarisations, was recorded over 5-min periods for as long as the neuron was held. Data was obtained using a CED 1401 Mk II digitizer (Digitimer Ltd, Hertfordshire, U.K.) and Spike 2 software, version 6 (Cambridge Electronic Design, Cambridge, U.K.). Neuronal injury discharge, which is induced by microelectrode impalement, was excluded.

2.4.2.3. Recording the Action Potential

After allowing the initial 1-min period for recording SA to pass, APs were anti-dromically evoked by dorsal root stimulation through bipolar platinum electrodes with single, depolarising, rectangular pulses, which was typically 0.03 ms duration for faster units or 0.3 ms for slower units, with a Constant Voltage Isolated Stimulator DS2A Mk II. The lowest electrical threshold of activation was determined and recorded.

2.4.2.4. Identifying the Neuron

A variety of stimuli were applied to the hindlimb [Tab. 2.1] to physiologically identify the type of DRG neuron. This was done using hand held stimulators and applying them to the left hindlimb until the neuron's receptive field was found, as previously described in guinea-pig (Lawson *et al.*, 1997; Pizzo *et al.*, 2011) and rat (Gagliese and Melzack, 1997; Fang *et al.*, 2002; 2005). Non-noxious stimuli included a brush and blunt objects, to test for pressure-induced responses and the effects of light mechanical stimulation. Noxious stimuli included toothed forceps, sharp objects such as needles and hot water at temperatures > 50°C.

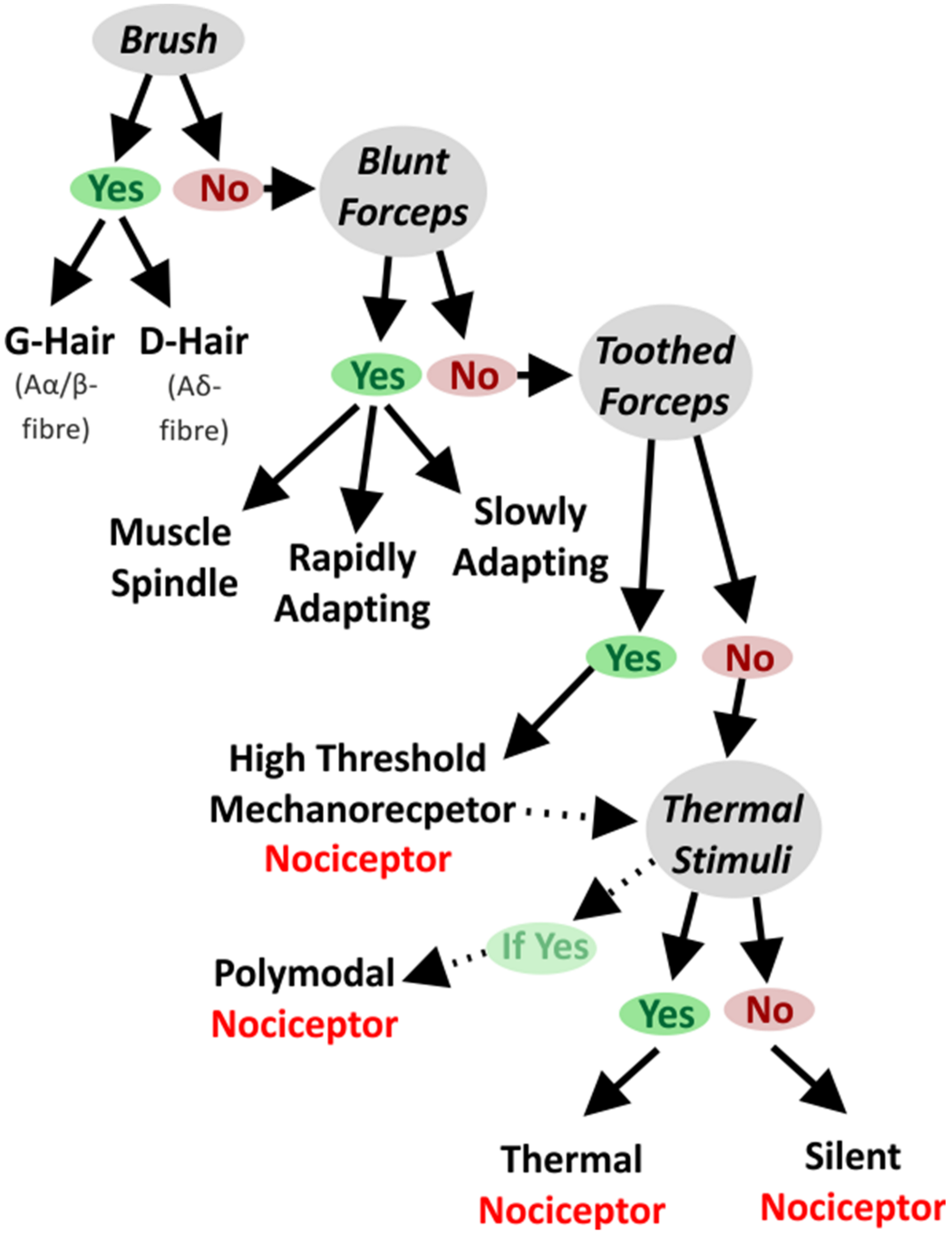

Figure 2.6: Physiologically Identifying Different Types of DRG Neurons. A figure that shows the various stimuli applied to the hindlimb to attempt to identify the various types of DRG neuron. If the neuron responds to the applied stimuli, then follow the green box to indicate what type of DRG neuron it is.

2.4.2.5. Limitations of Physiological Identification

Although most neurons were reliably identified, this preparation does have some shortcomings. All stimuli are applied to the exterior of the skin and therefore neurons with deeper receptive fields can be: 1) harder to access; 2) inaccessible, in the case of applying noxious heat; or 3) challenging to determine threshold. Finally, DRG neurons, particularly C-fibre nociceptors, can be lost as constantly probing for the receptive field can adversely affect the stability.

2.4.2.6. Recording the Current and Voltage Properties Related to I_h

After AP recordings and functional classification of each DRG neuron, a hyperpolarisation-activated depolarizing sag predominantly attributable to I_h (Scroggs *et al.*, 1994; Berkley, 1997; Villière and McLachlan, 2002) and the I_h current were recorded using Signal, version 5 (Cambridge Electronic Design Ltd., Cambridge, U.K.). Sag recordings were performed in discontinuous current clamp mode using a series of negative current injections, each lasting 100 ms and going from 0 to -4 **n**ano**a**mps {**nA**} in -0.5 nA step increments in discontinuous current-clamp mode. I_h was identified in these neurons by the presence of voltage sag of > 10% at the largest hyperpolarising current pulse, -4.0 nA.

Then, using the discontinuous single electrode voltage-clamp mode of the Axoclamp 900A amplifier, I_h was recorded, as previously described (Scroggs *et al.*, 1994; Hogan and Poroli, 2008; Momin *et al.*, 2008), from the L4-L5 DRG of normal and the L4 DRG of mSNA-treated animals. In brief, the membrane potential was clamped at -50 **m**illi**v**olts {**mV**} and a series of 1-s -10 mV hyperpolarising steps were run, with a return to -50 mV, from -60 mV until -130 mV was reached. Artefacts from other currents are a concern, but the administration of the barbituate, pentobarbital, can block some of the other, interfering currents, such as the potassium inward-rectifier (Gibbons et al., 1996). In addition, this current is only found in 4-15% of DRG neurons (Scroggs *et al.*, 1994; Wang *et al.*, 1997). Currents were filtered at 1 **k**ilo**H**ert**z** {**kHz**} in dSEVC

and DCC mode before being digitized for data acquisition by CED 1401 Mk II digitizers. I_h was sampled with a switching frequency of 7 kHz.

2.4.3. Analysis of Electrophysiological Variables

2.4.3.1. Conduction Velocity Classification

The speed that the AP travels along the neuron allows further categorization of the DRG neurons using the **c**onduction **v**elocity {**CV**}, which was calculated by dividing the conduction distance, typically 6-18 mm, by the latency to the onset of the evoked somatic AP. Neurons were then grouped by their CVs, with Aα/β-fibres having > 6.5 m/s, Aδ-fibres having 0.8 – 6.5 m/s and C-fibres having < 0.8 m/s, as previously established in the rat using compound AP recordings (Fang *et al.*, 2002). These values were quite low for reasons including use of the dorsal root for CV measurements (Waddell *et al.*, 1989), the high pool temperature of about 30°C and inclusion of utilisation time.

2.4.3.2. Action Potential Variables

For each neuron, the following variables were recorded, as previously described (Djouhri *et al.*, 2001): E_m, AP duration at base, AP rise time, AP fall time, AP overshoot, AP amplitude, **a**fter**h**yper**p**olarisation **a**mplitude {**AHPA**} and **a**fter**h**yper**p**olarisation time at **100%** E_m recovery {**AHP100%**}. These parameters were obtained post-experiment, using offline analysis and scripts created for use in Spike 2.

2.4.3.3. Sag and I_h Current Parameters

As I_h currents recorded in voltage-clamp mode have been contaminated by a rapidly decaying inward current (Scroggs et al., 1994; Yagi and Sumino, 1998; Komagiri and Kitamura, 2003), to remove this interfering current and to reveal 'pure' I_h, the steady state was subtracted from the instantaneous current using a

purpose built script in Signal. The initial I_h was measured 12 to 15 ms after the start of the voltage command to ensure that contamination from capacitative currents was excluded (Rodrigues and Oertel, 2006). Finally, due to the high microelectrode resistances used, the actual testing potentials were slightly different from the command potentials, but this was corrected using a Boltzmann equation and I_h was calculated at -100 mV.

2.5. Immunofluoresence

There are a number of techniques to examine, either directly or indirectly, the levels of protein in DRG neurons, with two most commonly used: 1) western blotting, which detects the amount of protein in tissue homogenates; and 2) immunofluorescence, which labels proteins with fluorescent markers and subsequently allows quantification and identification of cellular locations. Although immunofluorescence is not a flawless technique, this methodology reveals proteins' intra- and inter-cellular locations, which can then be quantified, and, therefore, was chosen to examine the hypothesis. Immunofluorescence requires highly specific, antibodies (Katikireddy and O'Sullivan, 2011), particularly when staining multiple antigens (Buchwalow and Böcker, 2010).

2.5.1. Antibodies Used

2.5.1.1. Primary Antibodies

The HCN1-4 antibodies used are all rabbit polyclonal antibodies (Alomone Laboratories, Jerusalem, Israel) raised against: the N-terminus amino acid residues 6-24 of rat HCN1; the N-terminus amino acid residues 147-161 of human HCN2; the C-terminus amino acid residues 727-744 of rat HCN3; and the amino acid residues 119-155 of human HCN4. These antibodies were chosen following an extensive literature search. The HCN1 antibody underwent pre-incubation with the control peptide and revealed no staining (Milligan et al., 2006), in addition to western blotting in rat (Lörincz et al., 2002), HEK293 cells

(Much *et al.*, 2003) and dogs (Han *et al.*, 2002), and extensive use (Lörincz et al., 2002; Much et al., 2003; Koch et al., 2004; Wells et al., 2007). The HCN2 antibody has been confirmed in at least four ways: 1) tested on human HCN2 expressed in HEK 293 cells (Luo et al., 2007); 2) omission of the primary HCN2 antibody resulted in lack of fluorescent signals (Meuth et al., 2006); 3) western blotting in both rats (Papp *et al.*, 2010) and dogs (Han *et al.*, 2002); and 4) extensive use (Wells et al., 2007). The HCN3 antibody showed a similar staining profile to other publications, as it is found primarily intra-cellularly (Hardel et al., 2008; Kouranova et al., 2008).

Furthermore, negative, positive and primary-omitted controls were performed for validation. Positive controls consisted of staining hippocampal sections to examine HCN staining in the CA3 region, as previously reported (Bender et al., 2001; Notomi and Shigemoto, 2004).

Interestingly, following these controls, the HCN4 antibody proved to be problematic, as the antibody we obtained did not produce staining to what was previously reported (Cho *et al.*, 2009b) and also our control experiments showed unexpected staining [data not shown]. Therefore, the HCN4 antibody was not used throughout this thesis.

2.5.1.2. Other Antibodies

To further elucidate the localisation of the HCN channels, marker were used: **I**solectin-**B4** {**IB4**} (1:100, Sigma-Aldrich, U.K.); **c**alcitonin-**g**ene **r**elated **p**eptide {**CGRP**} (1:500, Abcam, U.K.); and 4',6-diamidino-2-phenylindole {**DAPI**} (1:2500, Sigma-Aldrich, U.K.). IB4 preferentially stains non-peptidergic neurons (Kitchener *et al.*, 1993; Molliver *et al.*, 1997) over peptidergic DRG neurons, which utilise neuropeptides such as SubP and CGRP. DAPI stains DNA, allowing nuclear identification.

2.5.2. Methodology

For the immunofluorescent experiments, the exact methodology varied according to the type of the study: 1) Normal DRG neurons paired with CFA-treated DRG, in addition to nerve fibres of DRG neurons [Appendix 2]; 2) Normal lumbar enlargement of the spinal cord paired with CFA-treated lumbar enlargement of the Spinal Cord [Appendix 3]; 3) mSHAM-treated DRG neurons paired with mSNA-treated DRG neurons [Appendix 4]. In brief, rats were deeply anesthetized with a lethal dose of sodium pentobarbital (≥ 80 mg/Kg) and perfused transcardially with phosphate-buffered saline at pH 7.4, followed by Lana's Fixative, made of 4% paraformaldehyde in 0.1 M PBS at a final pH of 6.9. Lana's fixative is a slight modification of Zamboni's fixative, which has been commonly used over the last 50 years (Stefanini et al., 1967). L4-L5 DRGs and the lumbar enlargement of the spinal cord were extracted and fixed for a total of 1-h, before being kept in sucrose overnight and then rapidly snap-frozen the next day in a mixture of isopentane (Fischer-Scientific, U.K.) and liquid nitrogen (BOC, U.K.).

The tissue was then cut with either a cryostat (Leica CM1950, U.K.) or a freeze-knife microtome (Leica 2000R, U.K.) and sections from both control and treated animals were prepared on the same slide. Triple immunoflurescence was performed as follows: after washing the sections, non-specific staining was avoided by undertaking a blocking step, after which the tissue was permeabilised using a detergent. Then, primary antibodies were applied and incubated overnight at 4°C. The sections were then washed and incubated with the secondary antibodies for 2-h. The tissue was then washed again and incubated overnight with the primary antibody for antigen 2. Then, following another series of washes, the secondary antibody for antigen 2 was applied and left for 2-h. Then, the antibody for antigen 3 was applied and bound directly to the target antigen. Finally, a drop of vectashield (Vector Laboratories, U.S.A.) was applied to enhance and prolong the fluorescence.

2.5.3. Image Analysis

Using a Carl Zeiss M1 Imager with an AxioCam MRm attached (Carl Zeiss, Germany), labelled sections were examined and 3-4 images per slide, from a total of 9 slides (3 for each HCN subunit) were photographed at x200 magnification using Axiovision v4.7 software (Carl Zeiss, Germany). Then, DAPI staining was used to locate neurons that were cut through the nucleus. In brief, each image was only included if it contained at least one strongly positive {$^{+}$} HCN, HCN^{+}, and IB4, IB4^{+}, neuron, not necessarily the same neuron for each, and two neurons that were negative {$^{-}$} for both HCN and IB4 staining respectively. Weakly positive {$^{w+}$} neurons were overlooked at this stage of the analysis. In addition, if any artefacts or abnormal haze were present in any DRG neurons, then these were not analysed.

After circling all of the suitable neurons, analysis was performed to quantify the staining intensities of the three fluorophores: HCN, IB4 and DAPI [Fig. 2.7.A-B]. After this analysis was complete and normalised data was obtained, comparisons were made. The DRG neurons were categorised by their normalised values into: positive, $^{+}$, > 0.4; weakly positive, $^{w+}$, 0.2 - 0.4; or negative, $^{-}$, < 0.2 (Fang et al., 2006). Initially, each antibody's normalised intensity was plotted against diameter to reveal general staining patterns for both HCN1-3 and IB4 in control tissue. Furthermore, HCN normalised intensities were plotted against IB4 normalised intensities to further examine the relationship between the two antibodies and different sub-populations of DRG neurons. Finally, the percentage of HCN^{+} DRG neurons were examined for IB4-staining and compared across different categories between treatment groups.

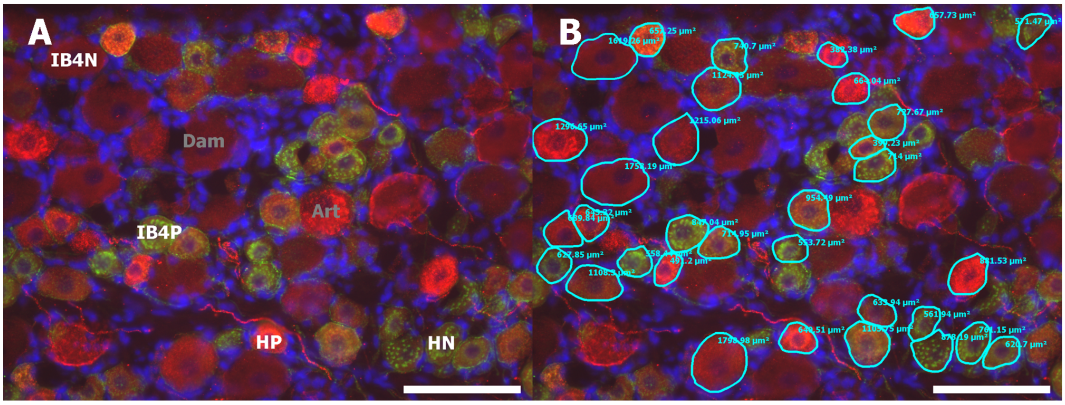

Figure 2.7: Densitometric Method of Analysis to Examine HCN Staining Intensity. A standard image [A] is checked for the following staining profiles: HCN-positive, HP; HCN-negative, HN; IB4-positive, IB4P; and IB4-negative, IB4N [A]. Neurons with damage, Dam, or artefacts, Art, are not included [A]. Then, all of the neurons that are suitable are circled to be included in the analysis [B].

Then, to compare this control tissue to CP tissue, the methodology was tested by plotting DAPI intensity against diameter, in micro-meters {**µm**}, for both of the treatment groups and fitting a line of linear regression. Then, the means of the normalised intensities of small diameter neurons, < 30 µm, were plotted against each other and tested for significance. If the graph of small DRG neurons revealed significance, then IB4 groups were examined to see if a sub-population showed an increased in HCN^+ DRG neurons following CP. Otherwise, HCN normalised intensities were plotted against IB4 normalised intensities with a trend line of linear regression to examine co-localisation profiles. The diameter was used to create 2.5 µm groups, from 17.5 – 40 µm to include both small- and medium-sized DRG neurons, showing the percentage of HCN^+ in each treatment group.

2.6. Statistical Analysis of Data

All of the statistical tests were performed using Graphpad Prism 5 (Graphpad Software, CA, U.S.A.) Statistical significance is indicated on graphs using: *, $P < 0.05$; **, $P < 0.01$; ***, $P < 0.001$. All data was tested for normality using the

Shapiro-Wilk normality test and if the data was normally distributed then the means were graphed, otherwise medians were used.

2.6.1. Behavioural Tests

The behavioural data are displayed as the mean ± standard error for each time point. Two-way repeated measures analyses of variance, with Bonferroni corrections to correct for the familywise error rate, between vehicle-treated hindpaws and the ipsilateral, Naproxen- and ZD7288-treated hindpaws, were performed to test for significance at various time-points.

2.6.2. *In Vivo* Electrophysiology

Most of the electrophysiologal data were not normally distributed, indicated by a Shapiro-Wilk text, and are therefore presented as medians. Furthermore, the p values are obtained using the nonparametric Mann-Whitney U test.

2.6.3. Immunofluorescence

To compare the scattergraph data, a method equivalent to analysis of covariance was used to reveal whether there was a significant difference between the two linear trendlines. To compare the percentage of positive neurons, the data was sorted into groups based on treatment and diameter, which was calculated from the cross-sectional area. Then, Fisher's Exact test was used to determine whether there was a significant difference between the two treatment groups. This data was graphed using the percentage of positive neurons for each treatment group.

Chapter 3 – Behavioural Tests

3.1. Abstract

Using animal models of **c**hronic **p**ain {**CP**}, which included the **c**omplete **F**reund's **a**djuvant {**CFA**} model of hindlimb inflammation and the surgically induced **m**odified **s**pinal **n**erve **a**xotomy {**mSNA**} model of **n**europathic **p**ain {**NP**}, we examined whether the **h**yperpolarisation-activated **c**yclic **n**ucleotide-gated {**HCN**} ion channels contribute to CP-related hypersensitivity. This involved assessing the effects of peripheral blockade of the HCN channels using a specific blocker, ZD7288, on three quantifiable behaviours, including two types of evoked pain, representing different aspects of CP: 1) **s**pontaneous **f**oot **l**ifting {**SFL**}, a sign of **s**pontaneous **p**ain {**SP**}; 2) Mechanical hypersensitivity; and 3) Heat hypersensitivity. In both models, intra-plantar, or local, administration of ZD7288 significantly reduced mechanical hypersensitivity and resulted in an absence of SFL. Heat hypersensitivity was un-affected in **c**hronic **i**nflammatory **p**ain {**CIP**}, but it did show a slight reversal trend in **c**hronic **n**europathic **p**ain {**CNP**}. Interestingly, ZD7288 was more effective in alleviating pain in these models than naproxen and gabapentin, the positive controls for CIP and CNP, respectively. The analgesic effects of ZD7288 are unlikely to be mediated by central mechanisms in at least the CIP model, as administration into the contralateral hindpaw had no effect on mechanical hypersensitivity. These findings suggest that HCN channels in DRG neurons are involved in both mechanical hypersensitivity and SP associated with both CIP and CNP.

3.2. Introduction

The ability to feel pain from the periphery is essential for survival and as a result, the physiological mechanisms have been conserved across species (Walters, 2007), including insects (Eisemann *et al.*, 1984). Pain causes alterations in behaviour to facilitate other fundamental biological functions, such as healing by maintaining tissue regeneration (Le Bars *et al.*, 2001; Correale and Villa, 2004). However, when the body's somatosensory system is compromised, as is the case

in states of CP, this can result in maladaptive pain behaviours that serve no useful function. The prevalence of mechanical and thermal hypersensitivity, or increased sensitivity in the areas affected by injury, among patients with NP is ~64% and ~38%, respectively, however, continuous, un-evoked SP is almost universal and is a reliable predictor of pain severity (Backonja and Stacey, 2004).

In this thesis, three behavioural signs, thought to represent different aspects of CP, were measured: 1) SFL, a correlate of SP (Bennett and Xie, 1988; Attal *et al.*, 1990; Yoon *et al.*, 1996; Djouhri *et al.*, 2006; 2006; Mogil, 2009); 2) mechanical hypersensitivity using a plantar aesthesiometer; and 3) thermal hypersensitivity using Hargreaves apparatus. Then, drugs were applied to examine the effect of peripheral blockade of HCN channels. In this chapter, the HCN channels / **h**yperpolarisation-activated current {$\boldsymbol{I_h}$} will be referred to as I_h, which is specifically blocked by ZD7288 (BoSmith *et al.*, 1993).

3.3. Results

3.3.1. Effects of ZD7288 on naïve Animals

ZD7288 was injected into the left hindpaws of un-treated, or naïve, animals. Post-ZD7288 injection, the paw withdrawal thresholds, for mechanical sensitivity [Fig. 3.1.A], and the paw withdrawal latencies, for heat sensitivity [Fig. 3.1.B], were measured at different time points. There was no significant difference between the pre-dug time point and any of the post-drug time points: 1-**h**our {**h**}, 3-h, 24-h and 48-h. Naïve animals do not display any behavioural signs of SFL, so this was not tested.

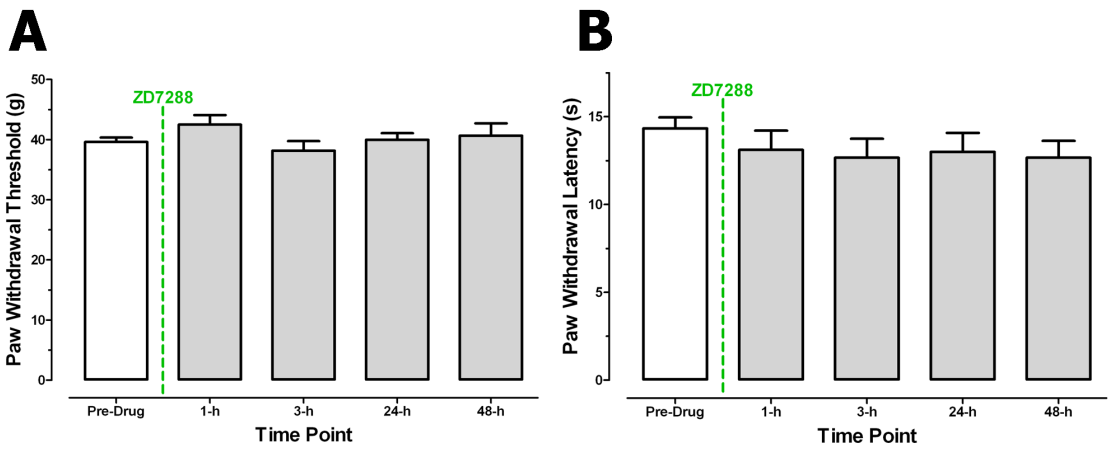

Figure 3.1: Effects of ZD7228 on Mechanical and Heat Pain Sensitivities in Naïve Animals. Intra-plantar administration of 100 µM ZD7288 had no effect on mechanical *(n = 8 rats)* [A] or thermal *(n = 9 rats)* [B] parameters at any of the time points tested: 1-h, 3-h, 24-h, and 48-h.

3.3.2. Complete Freund's Adjuvant

3.3.2.1. Effects of ZD7288 on CFA-Induced Spontaneous Foot Lifting

5-**d**ays {**d**} after hindlimb injections of CFA, animals display very little SFL, averaging less than 2-**s**econds {**s**} per 5-**min**utes {**min**} [Fig. 3.2.A], which makes it difficult to determine the effects of local administration of ZD7288 administration. However, peripheral administration of ZD7288 resulted in a temporary absence of SFL [Fig. 3.2.A], lasting for up to 3-h [Fig. 3.2.B], but disappearing by 48-h [Fig. 3.2.C]. Interestingly, naproxen, showed a slow-onset effect at 3-h, but this was transitory, as SFL returned by 24-h.

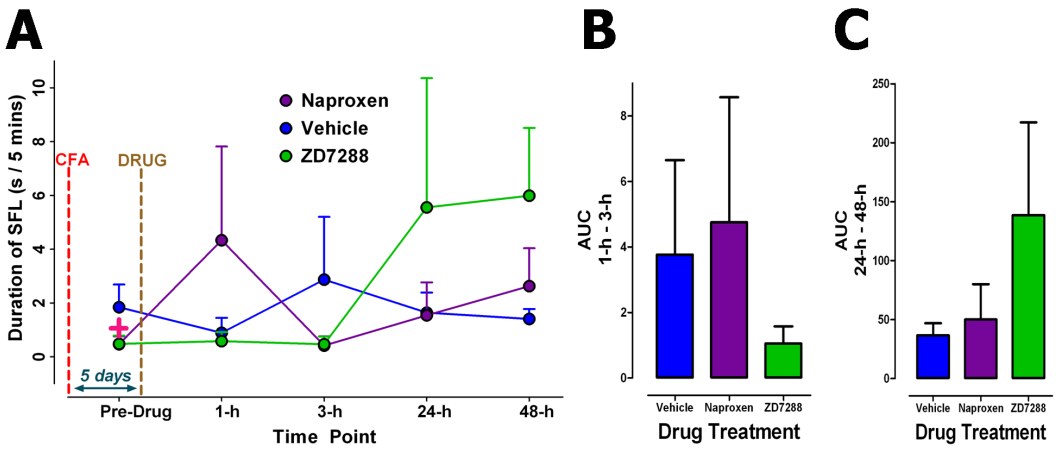

Figure 3.2: Effects of ZD7228 on CFA-Induced Spontaneous Foot Lifting. Intra-plantar administration of ZD7288 *(n = 6 rats)* transiently alleviated SFL, while intra-plantar administration of vehicle *(n = 6 rats)* had no effect, as shown by either an x-y scatter plot [A], or the area under the curve, AUC, at 1-h – 3-h [B] and 24-h – 48-h [C]. Intra-peritoneal administration of naproxen *(n = 5 rats)* reversed SFL at 3-h [A]. Dashed lines indicate CFA-treatment, in red, and drug treatments, in brown, with 5-d to allow CIP to develop. The pink sign, +, indicates the pre-drug average of all drug treatment groups [A].

3.3.2.2. Effects of ZD7288 on CFA-induced Mechanical Hypersensitivity

Mechanical hypersensitivity was studied by applying a normally innocuous mechanical stimulus, a blunt needle, to the plantar surface of the ipsilateral hindpaw and measuring the hindpaw withdrawal threshold in **g**rams {**g**}. 5-d after CFA-treatment, the mean paw withdrawal threshold significantly decreased, ***, $p < 0.001$ [Fig. 3.3.A] and in the absence of any drug treatment, this started at 1-d and persisted for 7-d [Fig. 3.3.B].

An intra-plantar injection of ZD7288 at 5-d post-CFA significantly increased the paw withdrawal threshold, indicating reduced mechanical hypersensitivity, at both 1-h, ***, and 3-h, ***, after dosing [Fig. 3.3.C]. ZD7288 was more effective than naproxen, the positive control, which also significantly increased, **, $p < 0.01$, the paw withdrawal threshold at 3-h after drug treatment. Vehicle treatment showed no significant changes at any time points.

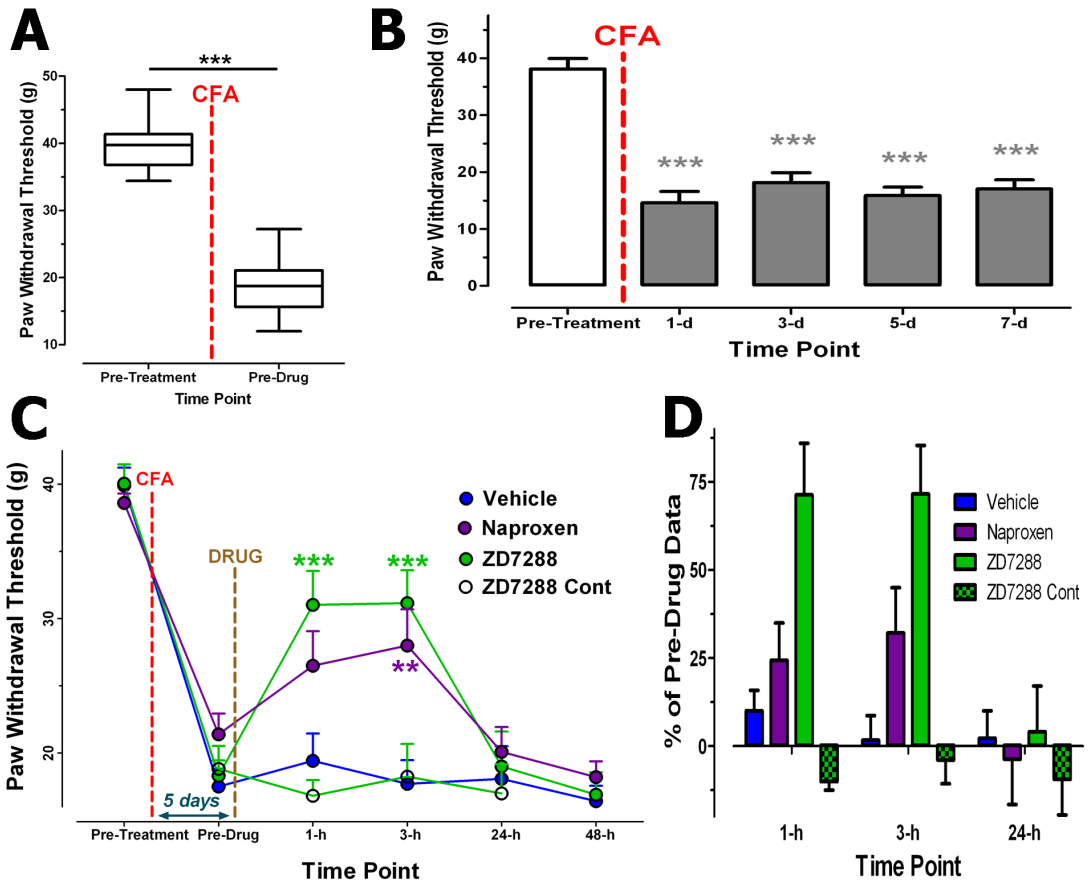

Figure 3.3: Effects of ZD7228 on CFA-Induced Mechanical Hypersensitivity. CFA-treatment significantly decreases mechanical thresholds at 5-d *(n = 20 rats)* [A]. A time course of CFA-induced mechanical hypersensitivity indicated highly significant decreases in the mean paw withdrawal threshold at all time points tested: 1-d, 3-d, 5-d, and 7-d *(n = 8 rats)* [B]. Compared with vehicle, in blue *(n = 9 rats)*, intra-plantar injection of ZD7288, in green *(n = 6 rats)*, significantly reduced mechancical hypersensitivity at both 1-h and 3-h post-drug treatment [C]. ZD7288 was more effective in alleviating mechanicaly hypersensitivity than than intra-peritoneal injection of the positive control, naproxen, in purple *(n = 5 rats)* [C]. Contralateral injection of ZD7288, shown in green lines with hollow circles, did not affect the paw withdrawal threshold in the ipsilateral paw [C-D]. Dashed lines indicate CFA-treatment, in red, and drug treatments, in brown, with 5-d to allow CIP to develop. The mean percentage difference between the various drug treatments and their pre-drug means quantifies the effects of the drugs [D]. Statistics used a Mann-Whitney U T-Test [A], in addition to either one-

way [B] or two-way [C] repeated measures ANOVA with either Tukey's or Bonferroni's post-tests: **, $p < 0.01$; ***, $p < 0.001$.

3.3.2.3. Effects of ZD7288 on CFA-Induced Thermal Hypersensitivity

Hypersensitivity to a normally noxious, 50°C, heat stimulus was indicated by a decrease in the hindpaw withdrawal latency, measured in **s**econds {**s**}. This was evident at 5-d [Fig. 3.4.A], but was also present at 1-d and persisted until 7-d [Fig. 3.4.B]. At 5-d post-CFA, intra-plantar administration of ZD7288 showed no alleviating effects, although naproxen significantly increased, *, $p < 0.05$, the paw withdrawal latency at 3-h post-drug injection [Fig. 3.4.C-D]. Vehicle treatment did not show any significance at any time point tested [Fig. 3.4.C-D].

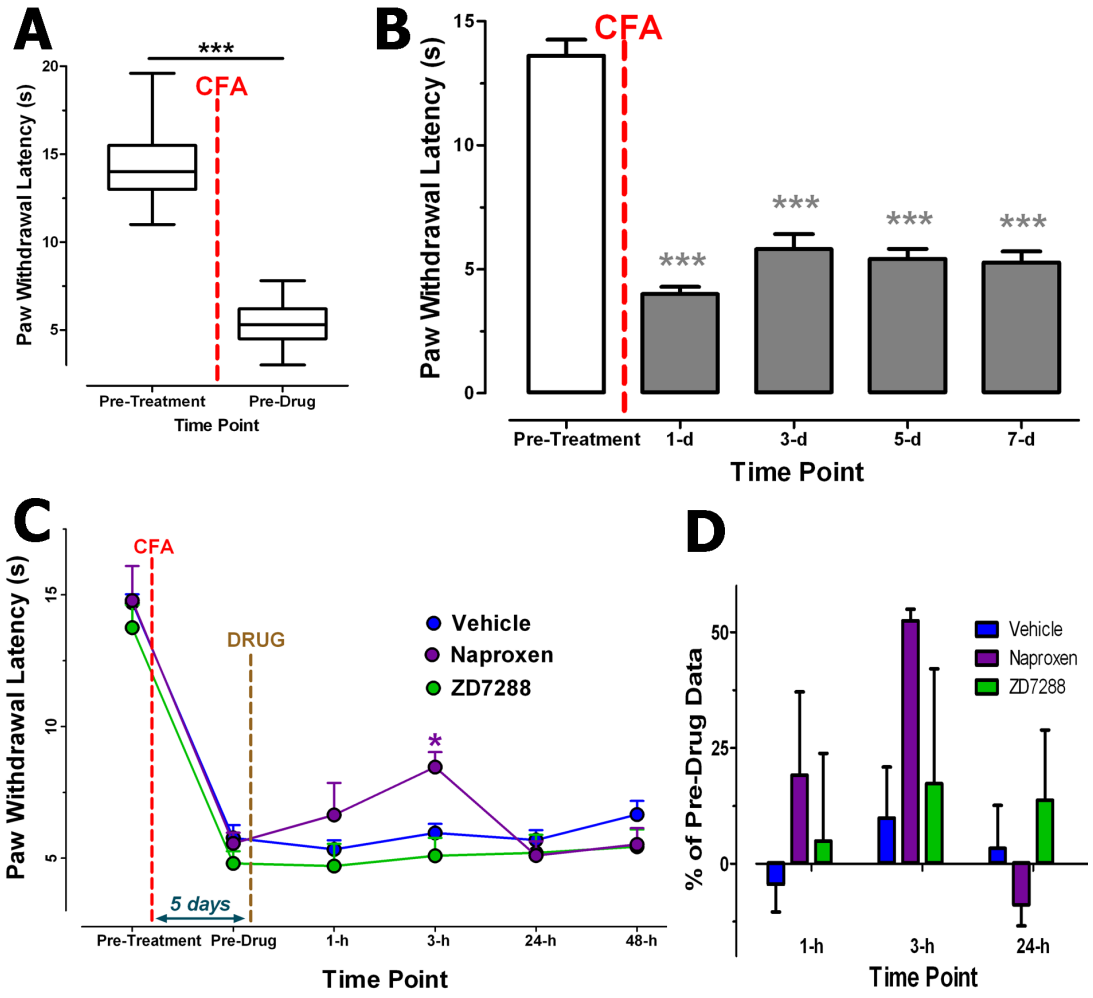

Figure 3.4: Effects of ZD7228 on CFA-Induced Heat Hypersensitivity. CFA-treatment significantly decreases heat thresholds at 5-d *(n = 23 rats)* [A]. A time-course of CFA-induced heat hypersensitivity indicated highly significant decreases in the mean paw withdrawal threshold at all time points tested: 1-d, 3-d, 5-d, and 7-d *(n = 8 rats)* [B]. Intra-plantar injection of either vehicle, in blue *(n = 9 rats)*, or ZD7288, in green *(n = 9 rats)* had no effect on paw withdrawal latencies at any time point [C]. Intra-peritoneal injection of the positive control, naproxen, in purple *(n = 5 rats)*, significantly increased the paw withdrawal latency, compared to control, at 3-h [C]. Dashed lines indicate CFA-treatment, in red, and drug treatments, in brown, with 5-days to allow CIP to develop. The mean percentage difference between the various drug treatments and their pre-drug means show the effect of the drugs [D]. Statistics used a Mann-Whitney U T-Test [A], in addition to either one-way [B] or two-way [C] repeated measures ANOVA with Tukey's or Bonferroni's post-tests: *, $p < 0.05$; ***, $p < 0.001$.

3.3.3. Modified Spinal Nerve Axotomy

3.3.3.1. Effects of ZD7288 on mSNA-Induced Spontaneous Foot Lifting

7-d after surgical induction of the mSNA model of NP, animals show SFL in the injured, ipsilateral, hindlimb [Fig. 3.5.A], but not the contralateral hindlimb [data not shown]. Intra-plantar administration of ZD7288 almost completely blocked SFL at 1-h post-drug and resulted in a non-significant decrease of SFL after 4-h [Fig. 3.5.A]. However, the effect of ZD7288 was transient [Fig 3.5.B] and disappeared completely by 24-h [Fig. 3.5.C]. Compared to vehicle, the effects of ZD7288 on SFL at 1-h was better than the positive control, gabapentin, which was observed at 4-h post-drug treatment [Fig. 3.5.A].

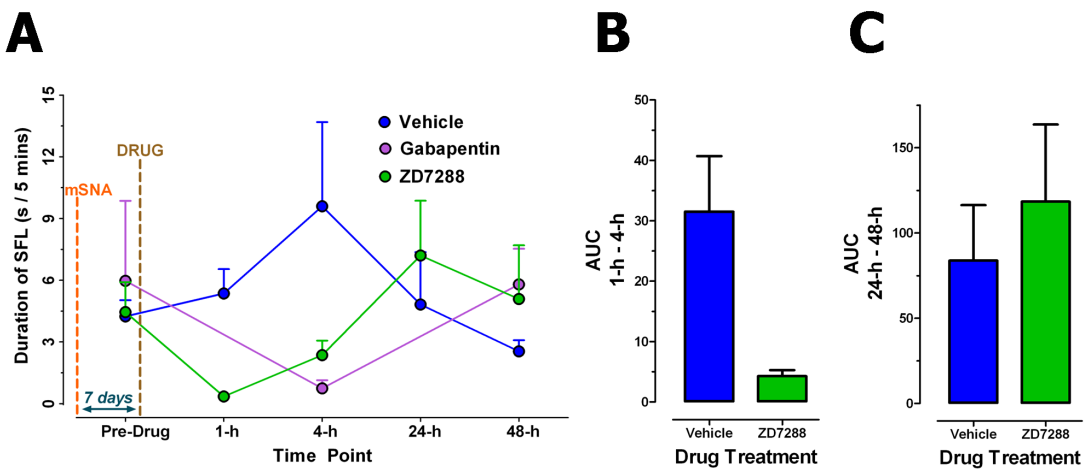

Figure 3.5: Effects of ZD7228 on mSNA-Induced Spontaneous Foot Lifting. Intra-plantar administration of vehicle, in blue *(n = 5 rats)*, had no effect, while intra-plantar administration of ZD7288, in green *(n = 11 rats)*, transiently alleviated SFL at 1-h and 4-h [A]. In addition, intra-peritoneal injection of gabapentin, in purple *(n = 5 rats)*, reversed SFL at 4-h [A]. Dashed lines indicated mSNA-treatment, in orange, and drug treatments, in brown, with 7-d to allow CNP to develop. Analysing the area under the curve, AUC, at 1 – 4 h [B] and 24 – 48 h [C] showed the transient effects of ZD7288.

3.3.3.2. Effects of ZD7288 on mSNA-Induced Mechanical Hypersensitivity

Mechanical hypersensitivity was present 7-d after mSNA surgery, shown by a significant decrease, ***, in paw withdrawal threshold [Fig. 3.6.A]. Peripheral administration of ZD7288 significantly increased the paw withdrawal theshold, at both 1-h, ***, and 4-h, **, after dosing [Fig. 3.6.B]. Gabapentin, the postive control, also increased the paw withdrawal threshold, at 4-h, although this was not significant [Fig. 3.6.B]. Vehicle treatment resulted in no significant deviation at any time point [Fig. 3.6.B] and this is shown when data are compared to the pre-drug values [Fig. 3.6.C].

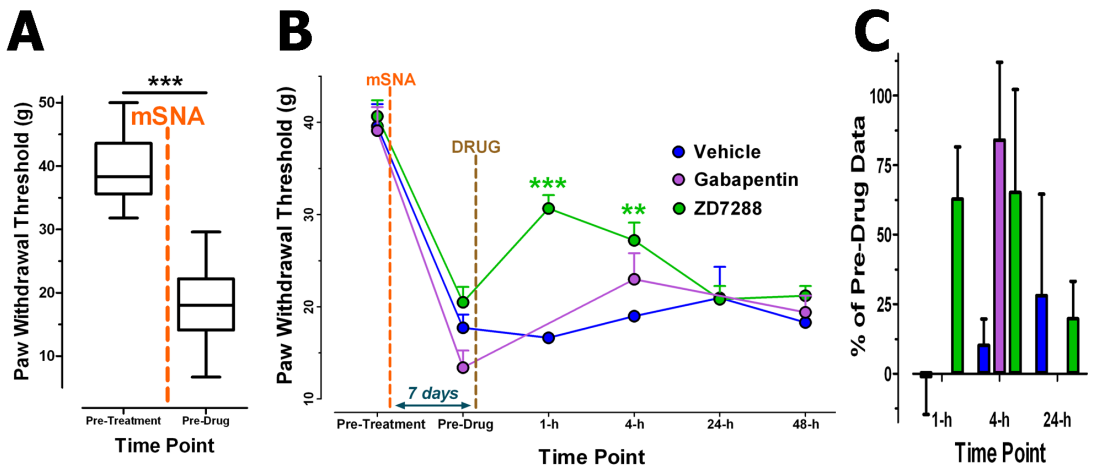

Figure 3.6: Effects of ZD7228 on mSNA-Induced Mechanical Hypersensitivity. mSNA-treatment significantly decreases mechanical thresholds at 7-d *(n = 19 rats)* [A]. Compared with vehicle, in blue *(n = 5 rats)*, intra-plantar injection of ZD7288, in green *(n = 11 rats)*, significantly reduced mechancical hypersensitivity at both 1-h and 4-h post-drug treatment [B]. Dashed lines indicate mSNA treatment, in orange, and drug treatments, in brown, with 7-d to allow CNP to develop. ZD7288 was as effective, at alleviating mechanicaly hypersensitivity, as the positive control, gabapentin, in purple *(n = 5 rats)*, shown by graphing the mean percentage difference between the various drug treatments and their pre-drug means [C]. Statistics was performed using either a Mann-Whitney U T-Test [A] or two-way repeated measures ANOVA with Bonferonni post-tests [B]: **, $p < 0.01$; ***, $p < 0.001$.

3.3.3.3. Effects of ZD7288 on mSNA-Induced Heat Hypersensitivity

Heat hypersensitivity was confirmed by comparing the paw withdrawal latencies prior to treatment with mSNA to those after 7-d, revealing a significant decrease, *** [Fig. 3.7.A]. Peripheral administration of ZD7288 did not have any effect, at any time point, on paw withdrawal latencies [Fig. 3.7.B]. Gabapentin only slightly increased the hindpaw withdrawal latency [Fig. 3.7.B]. Vehicle treatment showed no significant deviation at any time point and this is clear when data are compared to the pre-drug values [Fig. 3.7.C].

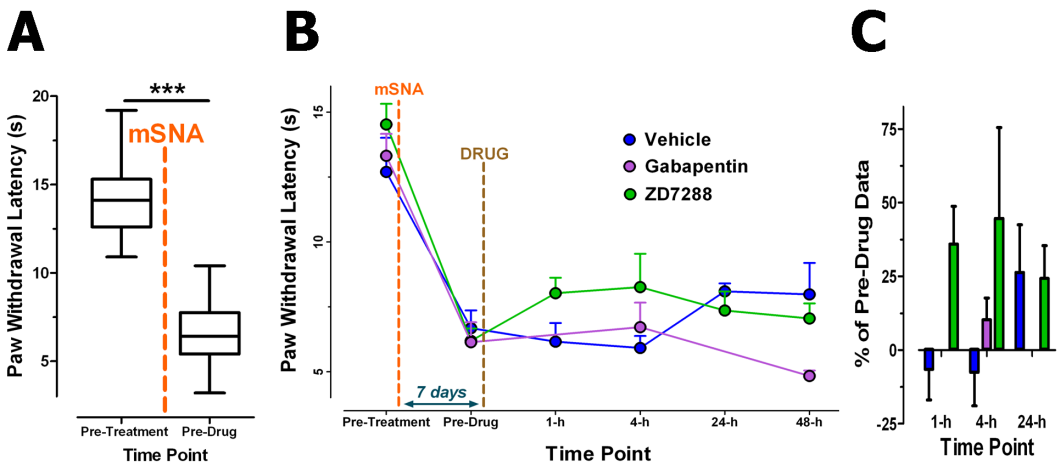

Figure 3.7: Effects of ZD7228 on mSNA-Induced Heat Hypersensitivity. mSNA-treatment significantly decreases heat thresholds at 7-d *(n = 21 rats)* [A]. Intra-plantar injections of vehicle, in blue *(n = 5 rats)*, and ZD7288, in green *(n = 11 rats)*, showed no significant effects at any time point post-drug treatment [B]. Intra-peritoneal injection of gabapentin, in purple *(n = 5 rats)*, only showed a small effect [B]. Dashed lines indicate mSNA-treatment, in orange, and drug treatments, in brown, with 7-d to allow CNP to develop. This is also shown by graphing the mean percentage difference between the various drug treatments and their pre-drug means [C]. Statistics was performed using either a Mann-Whitney U T-Test [A] or two-way repeated measures ANOVA with Bonferonni post-tests [B]: ***, $p < 0.001$.

3.4. Discussion

3.4.1. Summary of Results

Our results showed that, in the CFA model of CIP and the mSNA model of CNP, peripheral blockade of I_h, using ZD7288, significantly attenuated mechanical hypersensitivity and showed an absence of SP, especially in the mSNA model of CNP. Additionally, in CIP, ZD7288 was more efficacious than the positive control: naproxen. While in CNP, the effects of ZD7288 were comparable to the positive control: gabapentin. Furthermore, in CNP, ZD7288 showed a trend for the reversal of heat hypersensitivity, although this was not significant. We also found

that in CIP, administration of ZD7288 into the contralateral paws had no effects on mechanical hypersensitivity in the ipsilateral paws. This finding suggests that the analgesic effects of ZD7288 are un-likely to be mediated by central mechanisms, at least in the CFA-model. Collectively, these findings largely support recent data suggesting that the I_h current plays a critical role in both CIP and CNP (Emery *et al.*, 2011).

3.4.2. SFL

3.4.2.1. SFL and ZD7288

Using SFL to measure SP, peripheral blockade of the I_h current, with ZD7288, in both CIP and CNP, transiently minimised the amount of SFL. This is supported by data, from a model of IP induced by formalin, that demonstrated that ZD7288 had a significant, dose-dependent effect, lasting for at least an hour, on reducing, but not abolishing, the duration of licking, biting or lifting of the hindpaw (Emery *et al.*, 2011). The short-lasting effects might be due to ZD7288's half-life of 1.9 ± 0.1 h (Chaplan *et al.*, 2003).

The amount of SFL is correlated to SA from un-injured DRG neurons in the mSNA model of NP (Djouhri *et al.*, 2006). There is increasing evidence that I_h contributes to this SA, as recordings made extra-cellularly, *ex vivo*, from DRG neurons that had previously undergone L4 or L6 axotomy to induce NP exhibited SA, which was reduced upon ZD7288 application (Chaplan *et al.*, 2003). Furthermore, there is evidence that clonidine, thought to act by inhibiting I_h (Knaus *et al.*, 2007), administration can reduce the amount of SP in the **s**pinal **n**erve {**SN**} ligation model of NP (King *et al.*, 2009).

3.4.2.2. SP and Current Treatment

Although the two positive controls, naproxen and gabapentin for CIP and CNP respectively, showed a reversal of SP, neither offers a viable long-term treatment

option. Although naproxen is the safest of all of the non-steroidal anti-inflammatory drugs (Trelle *et al.*, 2011), there are still cardiovascular-associated problems (Ray *et al.*, 2002; McKellar *et al.*, 2007). Similarly, gabapentin, the drug of choice for NP, is limited by marginal efficacy and significant CNS side effects, including drowsiness and dizziness (Dworkin *et al.*, 2003).

3.4.3. Effects of ZD7288 on Mechanical Hypersensitivity

Peripheral blockade of I_h resulted in significant attenuation of mechanical hypersensitivity in both models of CP. The transient effect was slightly surprising, given the irreversible binding of ZD7288 to HCN channels, but could be explained by the rapid turn-over of ion channel subunits, as witnessed with other K^+ channels (Levitan and Takimoto, 1998).

3.4.3.1. Effect of ZD7288 on Mechanical Hypersensitivity in CIP

In CIP, the effects of ZD7288 were greater than those of naproxen, which has previously been shown in a CFA-induced model of IP to attenuate mechanical hypersensitivity (Clarke *et al.*, 1994). Studies using $Na_v1.8$ specific HCN2-knock out mice produced contrasting results, as one study showed an attenuation of mechanical hypersensitivity in the CFA-induced model of IP (Schnorr *et al.*, 2012) and the other revealed no change in a **p**rosta**g**landin **E_2** {**PGE_2**}-induced model of IP (Emery *et al.*, 2011). $Na_v1.8$ is largely, but not completely, sensory neuron specific (Djouhri *et al.*, 2003; Shields *et al.*, 2012), yet these studies don't clarify whether blocking the I_h current in the injured or intact DRG neurons is critical for driving CIP.

3.4.3.2. Effect of ZD7288 on Mechanical Hypersensitivity in CNP

While ZD7288's analgesic effects in a model of CIP is relatively novel, attenuation of NP-induced mechanical hypersensitivity with ZD7288 implicate I_h in mechanical hypersensitivity and are in agreement with previous work showing

that: 1) systemic, but not intra-thecal, administration of ZD7288 reduced mechanical hypersensitivity in the spinal nerve ligation model of NP (Chaplan *et al.*, 2003); 2) peri-neural administration of ZD7288 has also been shown to alleviate mechanical hypersensitivity in the partial sciatic nerve injury model of NP (Dalle and Eisenach, 2005) and in the chronic constriction model of NP (Jiang *et al.*, 2008); and 3) the effect of knocking out the HCN2 subunit from $Na_v1.8^+$ DRG neurons resulted in an ablation of mechanical hypersensitivity in the chronic constriction injury of NP (Emery *et al.*, 2011) and the spinal nerve ligation model of NP (Schnorr *et al.*, 2012). These results suggest that the conducting, intact DRG neurons with receptive fields intact are crucial to mechanical hypersensitivity as a result of CNP. Finally, ZD7288's efficacy is comparable to Gabapentin.

3.4.4. Effects of ZD7288 on Heat Hypersensitivity in CP

In this study, ZD7288 had no significant effect, at any time points, on heat hypersensitivity in both models of CP, although there was a slight reversal trend in CNP. These observations are consistent with previous findings showing a lack of suppression of heat hypersensitivity in both the chronic constriction model of NP (Jiang *et al.*, 2008) and in a model of acute pain induced by mild thermal injury (Luo *et al.*, 2007). However, there is evidence that the mechanisms that underlie acute and chronic inflammation differ (Trowbridge and Emling, 1997a; 1997b). Also, clonidine, which could act via I_h (Yagi and Sumino, 1998), reversed heat hypersensitivity in the CFA model of CIP (Lin *et al.*, 2002).

However, in CIP and CNP, neuronal-specific genetic knock-out studies have proved inconclusive, as using the $Na_v1.8$ HCN2 knock-out mentioned earlier, one group found a reversal of heat hypersensitivity in CIP and CNP (Emery *et al.*, 2011), while another group found the same results in CNP, but not CIP (Schnorr *et al.*, 2012), which mirrored the findings of this study.

For the positive controls, naproxen showed a significant alleviation of heat hypersensitivity at 3-h in the CFA-model of CIP. However, in CNP, gabapentin had no effect at any time-point.

3.4.5. Possible Physiological Mechanisms for ZD7288

3.4.5.1. Pharmacokinetics of ZD7288

ZD7288 has a plasma half-life of 1.9 ± 0.1 h (Chaplan *et al.*, 2003) and binds irreversibly (Shin *et al.*, 2001) to the S6 domain of HCN channels (Shin *et al.*, 2001; Cheng *et al.*, 2007). At extremely hyperpolarized membrane potentials, there is a profound relief of this irreversible blockade (Wickenden *et al.*, 2009).

3.4.5.2. Physiological Site of Action for ZD7288

In this study, ZD7288's physiological location of action implicates peripheral terminals of DRG neurons, in particular, the intact DRG neurons that still possess receptive fields. However, the site of action could be the injured DRG neurons, but it is unlikely to be **c**entral **n**ervous **s**ystem {**CNS**} neurons, as contralateral administration resulted in no change in CFA-induced mechanical hypersensitivity. Another study, also showed that contralateral hindpaw administration of ZD7288 had no effect on ipsilateral paw withdrawal thresholds in a partial sciatic nerve injury model of NP (Dalle and Eisenach, 2005).

In addition, ZD7288 is believed to be unable to cross the blood-brain barrier (Chaplan *et al.*, 2003; Lee *et al.*, 2005). ZD7288 administered to the spinal cord through an intra-thecal injection had no effect on mechanical hypersensitivity in NP due to SN injury (Chaplan *et al.*, 2003; Brown *et al.*, 2004). Finally, electrophysiological studies have also implicated I_h at the terminals of DRG neurons and not central neurons in the CNS (Takasu *et al.*, 2010). These findings all indicate ZD7288's analgesic effects are at a localized, peripheral site of action: DRG neurons. Since DRG neurons lie outside the blood-brain barrier (Olsson,

1968; MacFarlane *et al.*, 1997), they are exciting drug targets, as their peripheral blockade would result in minimal CNS related side-effects, which compromise the current first line treatments for NP, such as gabapentin (Attal *et al.*, 2006).

3.4.5.3. ZD7288 and T-Type Calcium Channels

It should be noted that the possibility that the analgesic effects of ZD7288, observed in the present experiments, were mediated by inhibition of T-Type **ca**lcium {**Ca^{2+}**} channels can not be excluded. ZD7288, at the same concentration used in these experiments, 100 µM, reversibly inhibited ~50% of low-threshold, T-type, Ca^{2+} channels (Felix *et al.*, 2003). These Ca^{2+} channels have been implicated in nociception (Altier and Zamponi, 2004; Bourinet *et al.*, 2005) and CP states, such as the diabetic model of peripheral neuropathy (Messinger *et al.*, 2009) and the SN ligation model of NP (Dogrul *et al.*, 2003). However, peri-neuronal administration of ZD7288, at 50 µM, a concentration that minimally affects T-Type Ca^{2+} channels, has been shown to block SA from DRG neurons in the chronic constriction injury model of NP (Jiang *et al.*, 2008). As SA plays a critical role in CP development (Campbell and Meyer, 2006; Djouhri *et al.*, 2006), these findings imply that the more likely target to exert analgesic effects for ZD7288 is the HCN, and not the T-Type Ca^{2+}, channels.

3.4.6. Complications with Behavioural Tests

3.4.6.1. SFL as a Behavioural Sign of SP

The majority of human sufferers of CNP complain of SP (Backonja and Stacey, 2004) and although animals are unable to verbally communicate their feelings, they do show behaviours of evoked pain that are believed to represent those reported by CP patients (Bennett and Xie, 1988; Attal *et al.*, 1990; Yoon *et al.*, 1996). However, the extent of pain, particularly SP, is difficult to quantify and has resulted in the attempt to use several behaviours thought to represent SP: audible and ultrasonic vocalisations, conditional place avoidance, excessive

grooming, and self-mutilation of a limb (Mogil and Crager, 2004). However, these are rarely used because rats often use vocalisations in social situations (Calvino *et al.*, 1996), which makes this behaviour an inappropriate correlate of SP (Jourdan *et al.*, 2002). While not perfect, SFL is a robust, quantifiable behaviour that is present in both of these models of CP (Djouhri *et al.*, 2006).

3.4.6.2. Methodology

Two of the three of these behavioural tests rely on evoked withdrawal responses, which do not actually measure pain, but peripheral hypersensitivity that frequently accompanies pain (Mogil, 2009). Methodologies for quantifying the degree of pain an animal is experiencing must continue to improve to further enhance the ability to design novel analgesics. Additionally, although transgenic technology has revolutionised pain research, there are a number of interpretational complexities (Lariviere *et al.*, 2001), as elegant knock-out techniques allow the study of individual proteins in specific populations of neurons, but behavioural data are more difficult to obtain as the majority of nociceptive behavioural assays were initially designed for the larger rat (Wilson and Mogil, 2001). Furthermore, there remains a debate about the validity of using rodents to study human models of pain (Blackburn-Munro, 2004). However, until technology improves, rodent models are the best available, which is reinforced by their ability to provide robust backward validation for compounds that have shown analgesic efficacy in humans (Mogil, 2009).

3.4.6.3. Variability of Results

Several factors may account for the discrepancies between various behavioural test studies: 1) species differences; 2) types of injury, particularly in CIP, which relies upon various chemical compounds; 3) duration of injury; 4) route of ZD7288 administration; and 5) the sub-types of DRG neurons that respond to various chemical stimuli, particularly in CIP.

Behavioural responses are the culmination of two main phenomena: 1) the activation of highly specific DRG neurons, pre-dominantly nociceptors; and 2) neuronal pathways in the CNS. Focussing on DRG neurons, there are many different sub-types that respond to highly specific stimuli. In addition to the mechanical and heat hypersensitivity observations, I_h has been found to play a key role in cold-responsive small DRG neurons, but not the small neurons that respond to heat (Luo *et al.*, 2007). To support this finding, an HCN1 KO mouse strain showed less cold hypersensitivity after partial sciatic nerve ligation, while mechanical and heat hypersensitivity appeared un-affected (Momin *et al.*, 2008). Although it is tempting to hypothesize that the I_h current is either not expressed or not critical to the hyperexcitability in the subset of DRG neurons that are activated by noxious heat, this remains controversial, primarily because of the wide-ranging role of polymodal nociceptors that respond to multiple types of noxious stimuli. Therefore, further work is required to elicit the exact mechanisms that result in heat hypersensitivity.

3.4.7. Conclusion

The present behavioural data provides strong evidence implicating the I_h current in peripheral DRG neurons in mechanical hypersensitivity, and possibly SP, in both CIP and CNP. Although, it is not clear exactly which DRG neurons, injured or un-injured, are responsible for hypersensitivity during CP. Furthermore, given that the I_h current is mediated by four HCN channel subunits, HCN1-4, these studies are not able to determine the precise subunits that are involved, although other groups have implicated HCN2 (Emery *et al.*, 2011). Therefore, to elucidate the precise role of the HCN channel subunits, it will be essential to further develop HCN-subunit selective drugs (Postea and Biel, 2011) and possibly even specific neuronal-selective compounds.

Chapter 4 – *In Vivo* Electrophysiology

4.1. Abstract

The excitability of **d**orsal **r**oot **g**anglion {**DRG**} neurons is critical for relaying sensory information to the brain. Voltage-gated ion channels, such as the **h**yperpolarisation-activated **c**yclic **n**ucleotide-gated {**HCN**} channels that mediate the **h**yperpolarisation-activated {I_h} current, play a vital role in regulating neuronal excitability. The I_h current has been implicated in DRG neuronal hyperexcitability associated with a number of **c**hronic **p**ain {**CP**} conditions and in the generation of **s**pontaneous **a**ctivity {**SA**} in injured DRG neurons in the L5 **s**pinal **n**erve {**SN**} ligation model of **n**europathic **p**ain {**NP**}. However, whether the HCN channels contribute to the excitability and SA of adjacent L4 DRG neurons, whose receptor fields are still intact, has not been examined. Using *in vivo* electrophysiology, comparisons of the electrophysiological properties were made between normal L4-L5 DRG neurons from control rats and the ispsilateral L4 DRG neurons from rats with the **m**odified **s**pinal **n**erve **a**xotomy {**mSNA**} model of NP, which involves axotomy of the L5 SN and loose ligation of the L4 SN with neuro-inflammation causing chromic gut. The results revealed that the hyperpolarisation properties of **a**ctions **p**otentials {**AP**} from L4 neurons do change, particularly in nociceptors, possibly implicating the HCN channels. We also found that administration of the I_h-specific blocker, ZD7288, at a dose of 10 mg/Kg, given intra-venously blocked the I_h current, although this had no significant effects on the rate of SA in a subpopulation of **l**ow-**t**hreshold **m**echanoreceptive {**LTM**} L4 DRG neurons. This suggests that these HCN channels do not contribute to SA generation, at least in this subpopulation of DRG neurons.

4.2. Introduction

Conserved across mammalian species (Walters, 2007), the sensation of pain is a result of a complex network of neurons relaying information to high levels of the **c**entral **n**ervous **s**ystems {**CNS**} for processing. Current knowledge of neuronal

signalling to warn of noxious, or harmful, stimuli is a result of a tremendous amount of work throughout history (Perl, 2007). It is well established that the body's periphery is innervated by a variety of DRG neurons, which convey somatosensory information as APs to the CNS. DRG neurons are one of two main types: 1) non-nociceptive neurons that respond to non-noxious stimuli; and 2) nociceptive neurons that respond to noxious stimuli (Lumpkin and Caterina, 2007; Gold and Gebhart, 2010), including mechanical (Delmas et al., 2011), thermal (Dhaka et al., 2006), and chemical. DRG neurons are heterogenous in their **c**onduction **v**elocities {**CV**}, receptor properties, electrical properties and AP firing rates (Lawson, 2002; Delmas *et al.*, 2011), and somatic AP configuration (Fang *et al.*, 2005). Injury or insult to DRG neurons results in peripheral NP (Jensen *et al.*, 2011).

One of the causes of **c**hronic **p**ain {**CP**} is transcriptional channelopathies (Waxman, 2001), or changes in the expression of ion channel subunits. One such ion channel family is the HCN, of which there are 4 subunits {**HCN1-4**} that form channels consisting of either homo- or hetero-tetramers that mediate I_h. Changes in ion channel subunit expression have dramatic consequences on the generation of APs from DRG neurons. Each ion channel subunit contributes, sometimes passively, using feedback loops to determine the membrane voltage, which is the common control variable of feedback loops for the voltage gated superfamily of ion channels (Lai and Jan, 2006; Geffeney and Goodman, 2012).

In states of CP, APs are spontaneously generated and this aberrant firing is believed to drive regeneration in the injured DRG neurons (Mandolesi et al., 2004; Abe and Cavalli, 2008; Rishal and Fainzilber, 2010). However, un-injured DRG neurons, whose receptive fields are still intact, also show SA (Ali *et al.*, 1999; Djouhri *et al.*, 2006) and appear to play a key role in the development of CP (Costigan *et al.*, 2009). The aim of this chapter was to examine the electrophysiological changes in intact, un-injured L4 neurons after the mSNA model of NP. An additional aim was to examine the effect of blocking the HCN

channels with ZD7288, an I_h specific blocker, on the electrophysiological properties, particularly the SA, of these un-injured DRG neurons.

4.3. Results

Electrophysiological recordings were made from L4-L5 DRG neurons in 30 normal, un-treated rats and from ipsilateral L4 neurons in 18 mSNA-treated rats, 7-**d**ays {**d**} post-operation. In both control and mSNA rats, neurons were classified according to their dorsal root CVs as C-, Aδ-, or Aα/β-fibre units. Thicker myelination produces faster CVs and correlates to a larger cell body and the three fibre types correlate to various cell body diameters (Lawson and Waddell, 1991): 1) C-fibre, or small DRG neurons with diameter < 30 micro-metre {**µm**}; 2) Aδ-fibre, or medium DRG neurons with diameters between 30 – 40 µm; 3) Aα/β-fibre, or large DRG neurons with diameters > 40 µm. The AP parameters were measured for the different neurons and changes in these variables after mSNA are described in the following sections.

4.3.1. Action Potential Parameters

4.3.1.1. Aα/β-Fibre DRG Neurons

The only electrophysiological variables that significantly, *, $p < 0.05$, changed in Aα/β-fibre DRG neurons from the L4 of mSNA rats were the increased AP fall time and the decreased **a**fter **h**yper**p**olarisation **a**mplitude {**AHPA**} [Tab. 4.1]. Indeed, the medians of CV, membrane potential {$\mathbf{E_m}$}, AP Risetime, AP overshoot, and the **a**fter-**h**yper**p**olarisation time to reach **100%** {**AHP100%**} were not significantly different between normal and mSNA rats.

Type	**n**	**CV** (m/s)	**E_m** (mV)	**Rise-time** (ms)	**Over-shoot** (mV)	**Fall-time** (ms)	**AHP Ampli-tude** (mV)	**AHP 100%** (ms)
Norm	87	17.5 *(14.53 – 25.88)*	-55.10 *(-62.85 – -49.53)*	0.38 *(0.33 – 0.48)*	12.48 *(5.6 – 20.43)*	0.55 *(0.4 – 0.73)*	9.28 *(6.2 – 12.29)*	14.99 *(6.4 – 30.46)*
mSNA	58	17.7 *(11.69 – 22.19)*	-58.48 *(-62.34 – -52.37)*	0.40 *(0.33 – 0.53)*	10.06 *(3.61 – 19.5)*	0.63 * *(0.48 – 1.10)*	8.11 * *(3.84 – 10.24)*	19.55 *(9.99 – 41.96)*

Table 4.1: Action Potential Variables in Aα/β-fibre L4 DRG Neurons 5 – 9 Days after mSNA. This table shows the median of a variety of AP parameters, with the 25% and 75% percentile values given in italics underneath. Significant differences are shown by coloured boxes, with blue boxes resembling a significantly smaller value in the normal cohort and orange boxes detailing a significantly smaller value in the mSNA data set. Statistics was performed using Mann Whitney U tests: *, $p < 0.05$.

The Aα/β-fibre DRG neurons can be separated into twelve different groups (Lawson et al., 1997) and this thesis combined a few of those groups to result in eight different groups, of which the majority fell into one of five groups [Methods Chapter]. One of these are the **h**igh-**t**hreshold **m**echanoreceptors {**HTM**}, which are a subclass of nociceptors, and mSNA-treatment caused a significant decrease, *, in the AHPA [Fig. 4.1.F]. Examples of AP traces from these DRG neurons are shown from normal [Fig. 4.1.A] and mSNA [Fig. 4.1.B] treated L4 DRG neurons. Meanwhile, the resting E_m [Fig. 4.1.C], AP Amplitude [Fig. 4.1.D] and AHP100% [Fig. 4.1.E] showed no significant differences.

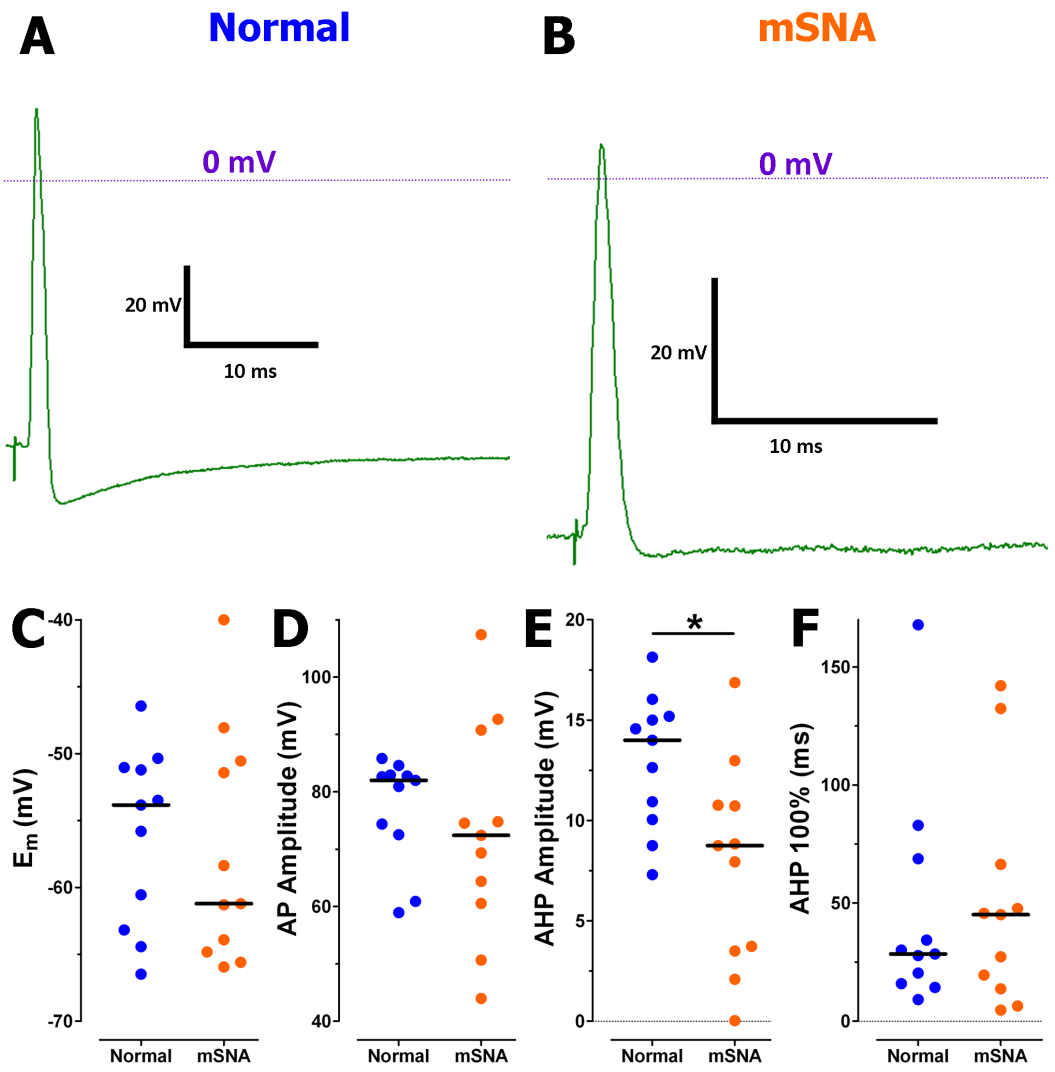

Figure 4.1: Changes in AP Variables in Aα/β-Fibre HTM L4 DRG Neurons 5 – 9 Days after mSNA. Examples of HTM AP traces are shown for normal [A] and mSNA [B]. The median AHP Amplitude in mSNA *(n = 11 neurons)* was significantly smaller, *, than in control *(n = 11 neurons)* [E]. In contrast, there were no significant differences in the medians of E_m [C], AP Amplitude [D] and AHP100% [F]. Mann-Whitney U tests compared normal and mSNA values: *, $p < 0.05$.

Another type of Aα/β-fibre DRG neuron is the **G**uard **Hair** {**G-Hair**}, which is a type of LTM, and sample AP traces are shown below for normal [Fig. 4.2.A] and mSNA [Fig. 4.2.B] treated animals. Following mSNA, G-hairs from the L4 DRG did not show any significant differences in either E_m [Fig. 4.2.C], AP Amplitude [Fig. 4.2.D], AHPA [Fig. 4.2.E] or AHP100% [Fig. 4.2.F]. Although AHPA decreased in

the mSNA DRG neurons, it was not significant. Furthermore, the AHP100% of G-hairs [Fig.4.2.D] was much faster than that of the HTMs [Fig.4.1.D].

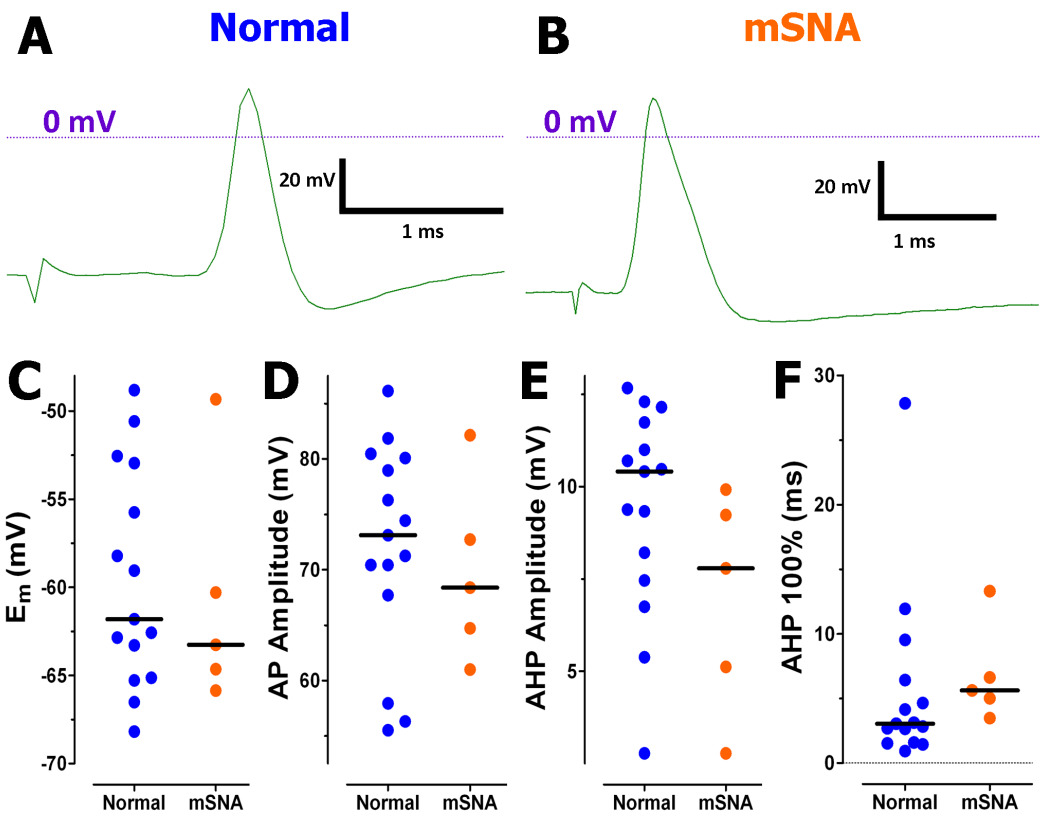

Figure 4.2: Changes in AP Variables in Aα/β-Fibre G-Hair L4 DRG Neurons 5 – 9 Days after mSNA. Examples of G-Hair AP traces are shown for normal [A] and mSNA [B]. There were no significant differences between normal *(n = 15 neurons)* and mSNA *(n = 5 neurons)* for E_m [C], AP Amplitude [D], AHPA [E] and AHP100% [F], as shown by the medians in the graphs. Mann-Whitney U tests were used to compare normal and mSNA values.

Another type of Aα/β-fibre LTM DRG neuron is the **r**apidly **adapt**ing {**RAdapt**} and sample AP traces are shown below for normal [Fig. 4.4.A] and mSNA [Fig. 4.4.B] treated neurons. Induction of the mSNA model of NP resulted in no changes in AP parameters between normal and mSNA, in E_m [Fig. 4.3.A], AP amplitude [Fig. 4.3.B], AHPA [Fig. 4.4.C] and AHP100% [Fig. 4.4.D].

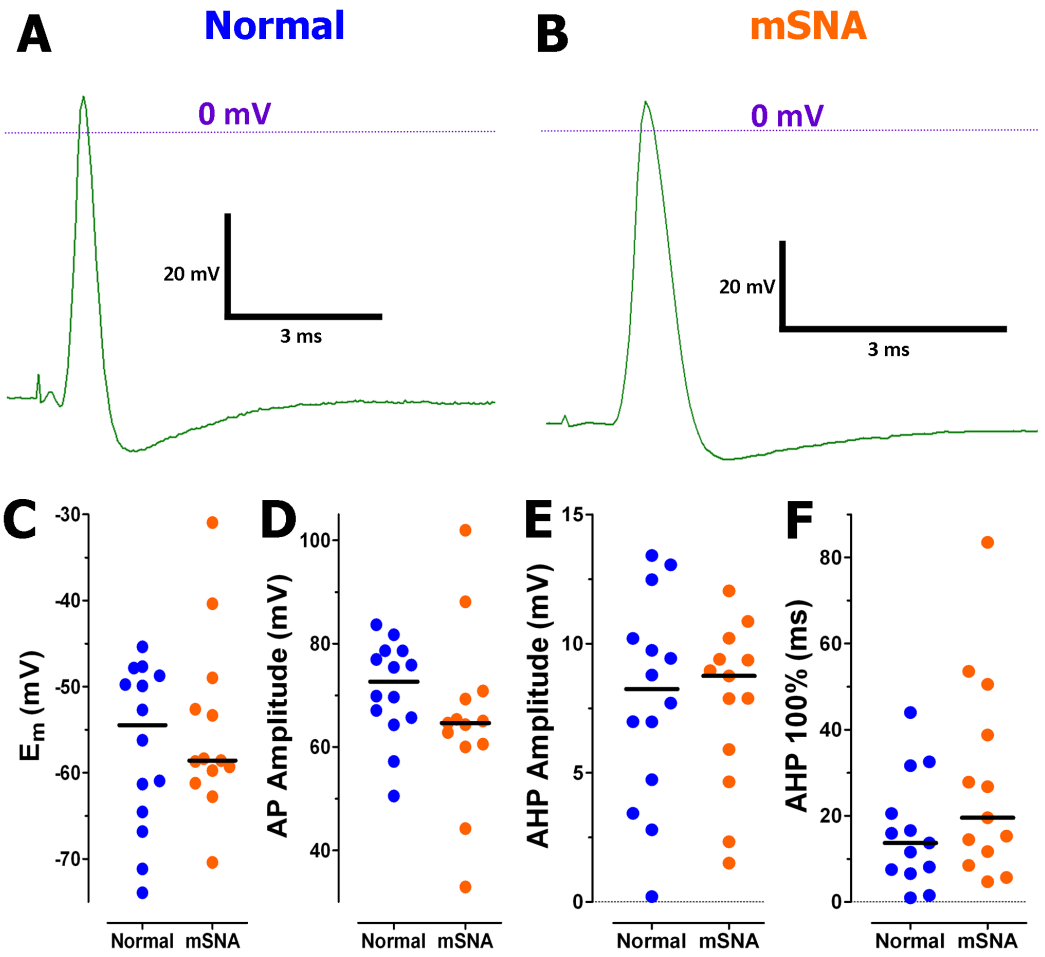

Figure 4.3: Changes in AP Variables in Aα/β-Fibre RAdapt L4 DRG Neurons 5 – 9 Days after mSNA. Examples of G-Hair AP traces are shown for normal [A] and mSNA [B]. There were no significant differences between normal *(n = 14 neurons)* and mSNA *(n = 13 neurons)* for E_m [C], AP Amplitude [D], AHPA [E] and AHP100% [F], as shown by the medians in the graphs. Mann-Whitney U tests were used to compare normal and mSNA values.

4.3.1.2. Aδ-Fibre DRG Neurons

Aδ-fibres are thinly myelinated and therefore have CVs, ranging from 0.8 – 6.5 m/s, inbetween small, C-fibre, and large, Aα/β-fibre DRG neurons. Sample AP traces are shown following normal [Fig. 4.4.A] and mSNA [Fig. 4.4.B] treated DRG neurons.

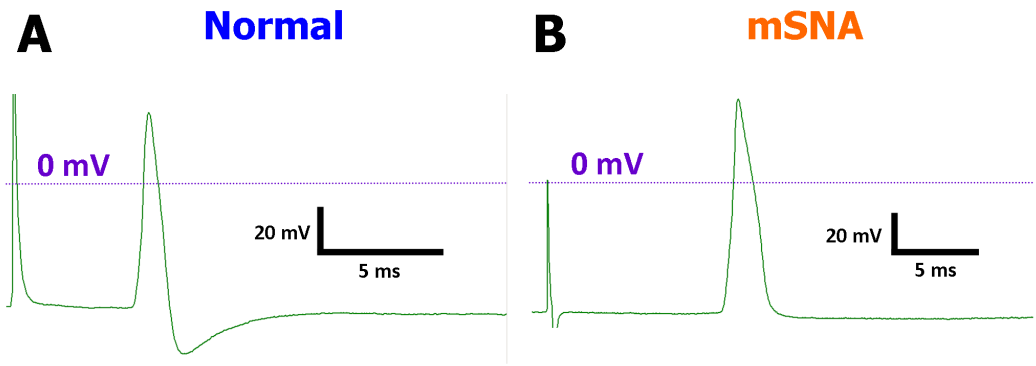

Figure 4.4: AP Traces from Aδ-Fibres from L4 DRG Neurons 5 – 9 Days after mSNA. AP traces are shown for normal [A] and mSNA [B].

Following mSNA-treatment, the Aδ-fibre DRG neurons showed a significant decrease, *, in AHPA, and significant increases, *, in risetime and falltime. No changes were observed for CV, E_m, overshoot of the AP and AHP100% [Tab.4.2].

Type	**n**	**CV** (m/s)	**E_m** (mV)	**Rise-time** (ms)	**Over-shoot** (mV)	**Fall-time** (ms)	**AHP Ampli-tude** (mV)	**AHP 100%** (ms)
Norm	7	1.93 *(1.17 – 5.13)*	-54.30 *(-63.76 – -46.95)*	0.4 *(0.28 – 0.60)*	11.14 *(5.62 – 28.78)*	0.40 *(0.33 – 0.88)*	12.55 *(10.03 – 16.21)*	15.35 *(6.33 – 43.38)*
mSNA	3	1.22 *(0.93 – 6.07)*	-65.57 *(-79.59 – -40.75)*	0.9 * *(0.63 – 1.08)*	35.10 *(0.0 – 42.69)*	2.45 * *(1.58 – 4.45)*	2.98 * *(2.35 – 3.04)*	39.27 *(11.38 – 40.90)*

Table 4.2: Action Potential Variables in Aδ-Fibre L4 DRG Neurons 5 – 9 Days after mSNA. This table shows the median of a variety of AP parameters, with the 25% and 75% percentile values given in italics underneath. Significant differences are shown by coloured boxes, with blue boxes resembling a significantly smaller value in the normal cohort and orange boxes detailing a significantly smaller value in the mSNA data set. Mann-Whitney U tests compared normal and mSNA values: *, $p < 0.05$.

4.3.1.3. C-Fibre DRG Neurons

C-fibre DRG neurons are un-myelinated and therefore have the slowest CVs of less than 0.8 m/s. Examples of AP traces are shown below for normal [Fig. 4.5.A] and mSNA [Fig. 4.5.B] treated DRG neurons.

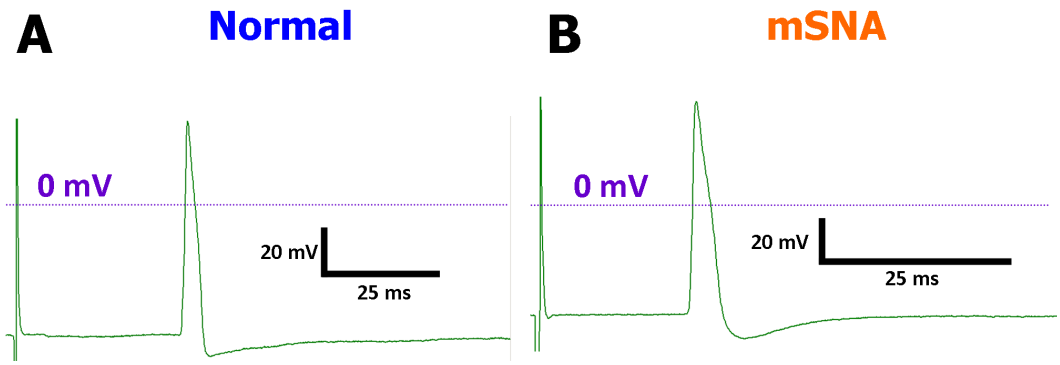

Figure 4.5: AP Traces from C-Fibres from L4 DRG Neurons 5 – 9 Days after mSNA. AP traces are shown for normal [A] and mSNA [B].

Following mSNA-treatment, there were no significant differences in parameters [Tab.4.3]. Trends did reveal that there was a decrease in AHPA and AHP100%, which contrasted with increases in both risetime and falltime [Tab.4.3]. Interestingly, a few DRG neurons showed a more positive E_m, which raised the median, although not significantly [Tab.4.3].

Type	**n**	**CV** (m/s)	**E_m** (mV)	**Rise-time** (ms)	**Over-shoot** (mV)	**Fall-time** (ms)	**AHP Ampli-tude** (mV)	**AHP 100%** (ms)
Norm	10	0.70 *(0.54 – 0.71)*	-55.83 *(-62.36 – -51.22)*	0.78 *(0.45 – 0.96)*	18.76 *(6.75 – 36.71)*	0.90 *(0.58 – 2.10)*	7.89 *(6.68 – 9.39)*	39.46 *(15.48 – 103.6)*
mSNA	10	0.67 *(0.56 – 0.77)*	-51.97 *(-63.45 – -44.49)*	0.74 *(0.56 – 1.04)*	28.61 *(16.58 – 37.99)*	2.10 *(1.37 – 2.49)*	6.34 *(2.83 – 10.74)*	24.01 *(5.39 – 124.1)*

Table 4.3: Action Potential Variables in C-Fibre DRG Neurons 5 – 9 Days after mSNA. This table shows the median of a variety of AP parameters, with the 25% and 75% percentile values given in italics underneath.

4.3.2. ZD7288

4.3.2.1. Effects of ZD7288 on Electrophysiological Parameters

Prior to ZD7288, the current- [Fig. 4.6.A] and voltage-clamp [Fig. 4.6.D.] protocols resulted in robust sag [Fig. 4.6.B] and I_h [Fig. 4.6.E] recordings. However, administration of ZD7288 blocked both sag [Fig. 4.6.C] and a current that is primarily attributable to I_h [Fig.4.6.F]. Furthermore, when AP parameters were compared for values before and after ZD7288 administration, E_m [Fig. 4.6.G] and AHPA [Fig. 4.6.H] showed no difference following ZD7288 administration, although AHP100% showed a non-significant increase [Fig. 4.6.I].

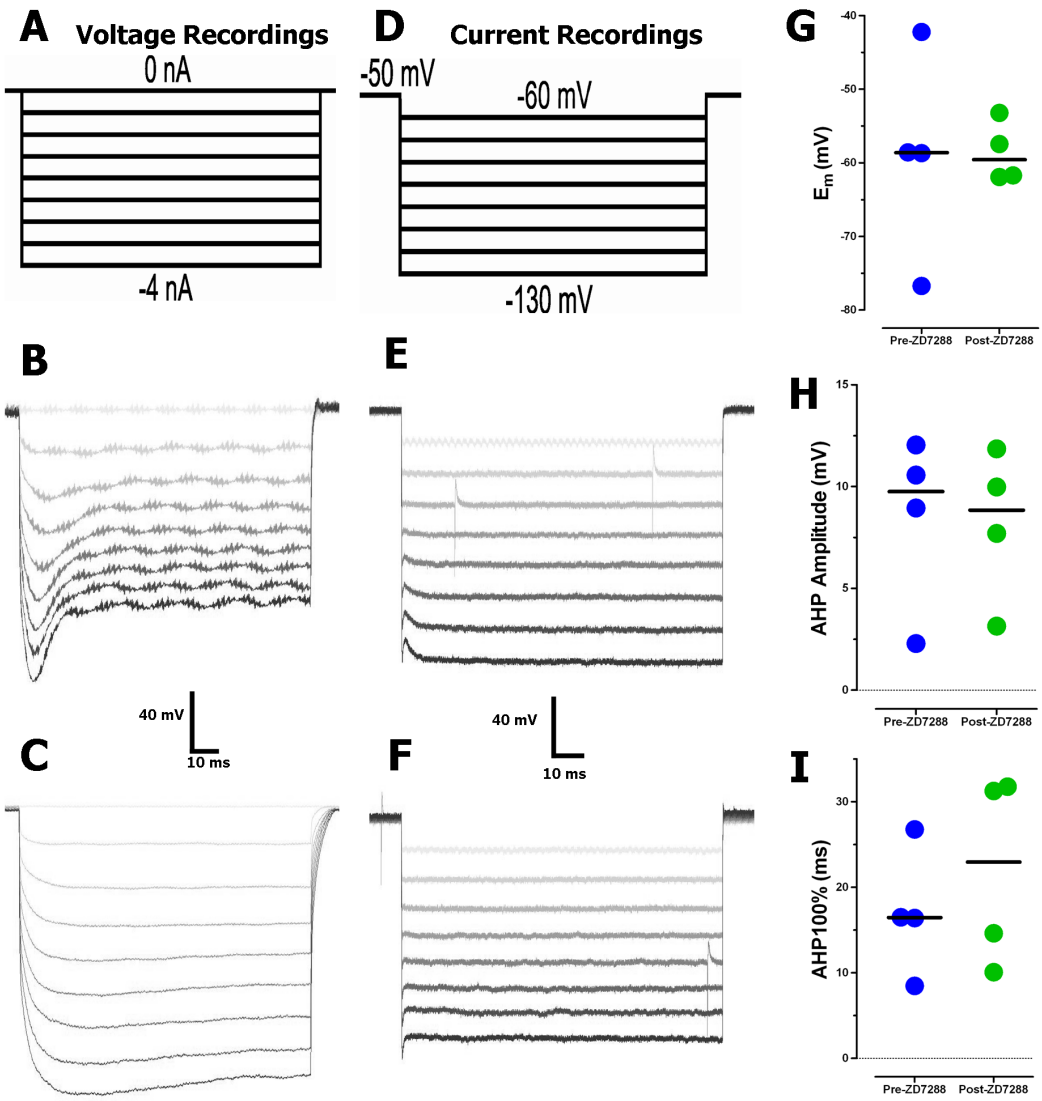

Figure 4.6: Effects of ZD7288 on Electrophysiological Parameters in DRG Neurons. Physiologically identified DRG neurons were current clamped using a protocol [A] to elicit a depolarising sag [B], which was blocked with ZD7288 administration (10 mg/Kg) [C]. Also, voltage clamp [D] produced an identifiable current that was activated at hyperpolarised membrane potentials [E] and this was blocked with ZD7288 administration (10 mg/Kg) [F]. Furthermore, in neurons with ZD7288 *(n = 4 neurons)*, the blocker had no effect pre-ZD7288 values for E_m [G] and AHPA [H], although AHP100% showed a non-significant increase [I].

4.3.2.2. Spontaneous activity

ZD7288 was administered to four LTM Aα/β-fibre DRG neurons and the AP firing frequency was calculated to examine the effect of blocking I_h. These four

neurons, recorded at the same time-points, consisted of two RAdapt, one **s**lowly-**adapt**ing {**SAdapt**}, and one G-hair, which is shown at various time-points as an example below [Fig.4.7.A-D]. ZD7288 administration had no significant effect on the firing rates of these DRG neurons, even transiently increasing the rate in one of the RAdapt [Fig.4.7.E].

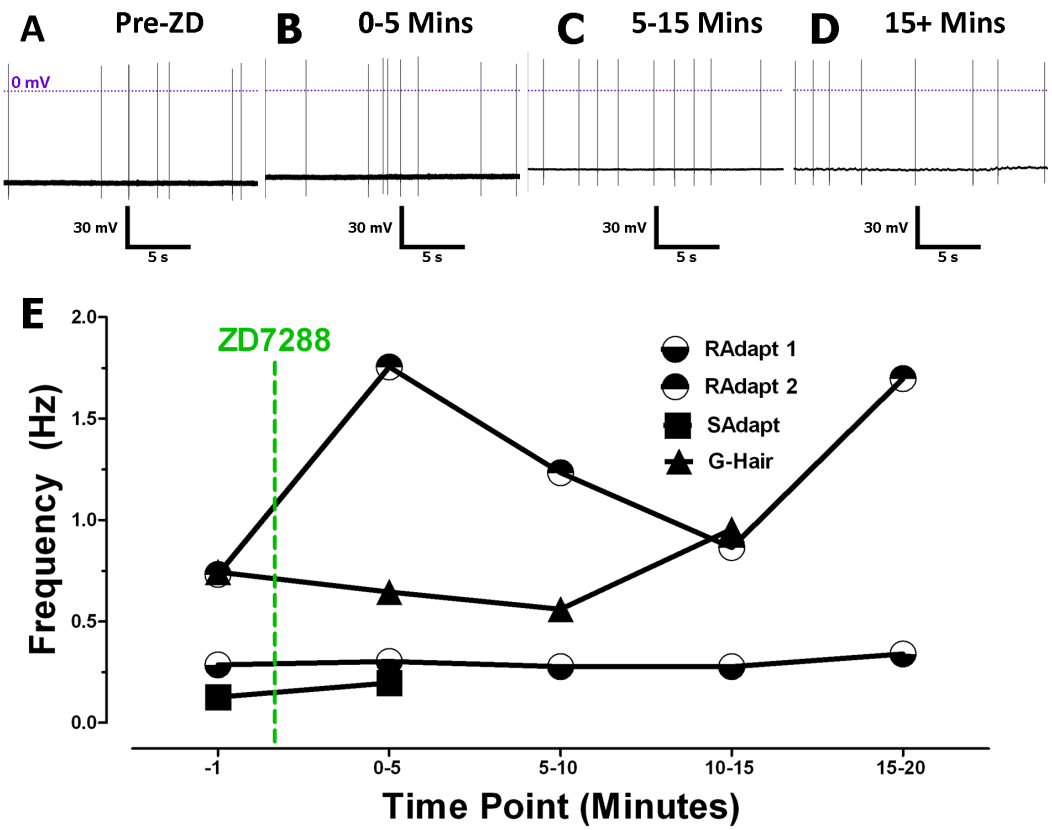

Figure 4.7: ZD7288's Effect on SA in LTM DRG Neurons. A specific example of the SA rate of a G-hair unit, both pre- [A] and post-ZD7288, at 0-5 mins [B], 5-15 mins [C] and 15+ mins [D]. [E] The effects of ZD7288 on SA frequency in four LTM DRG neurons, including the G-hair LTM neuron [A-D].

4.4. Discussion

4.4.1. Summary of results

The primary aim of these *in vivo* electrophysiological experiments was to examine the impact of the mSNA model of peripheral NP on electrophysiological

properties of DRG neurons with intact receptive fields. The term intact refers to DRG neurons that haven't been injured by axotomy, as the loose ligature in the NP model is only intended to alter the neuro-inflammation, although depending on the experience of the surgeon, up to 50% of DRG neurons express ATF3 (Djouhri *et al.*, 2006), which is a specific marker of nerve injury (Tsujino *et al.*, 2000) that enhances peripheral nerve regeneration (Seijffers *et al.*, 2007).

An additional aim was to determine, using pharmacological blockade of the HCN channels with the specific blocker, ZD7288, whether these channels contribute to the electrophysiological changes in DRG neurons associated with CP. The results show that changes in AP parameters were highly dependent upon the type of DRG neuron, with the most prominent difference being a reduction in AHPA in A-fibre DRG neurons, particularly HTM, but not G-Hairs or RAdapt. In addition, blockade of HCN channels with ZD7288 did not reduce the SA rate from Aα/β-fibre LTM DRG neurons.

4.4.2. Action Potential Variable Changes

4.4.2.1. Membrane Potential

The resting E_m of neurons is important for the excitability of neurons (Catterall, 1984), particularly during states of CP. One hypothesis is that E_m oscillations cause the increased excitability of DRG neurons (Amir *et al.*, 1999), particularly with the generation of SA occurring in the soma (Djouhri *et al.*, 2012). Across all of the A-fibre DRG neurons, there was no significant difference between E_m, which had previously been reported in the mSNA model of NP (Djouhri *et al.*, 2012). Furthermore, this thesis did not see any significant differences in various subtypes, including HTM, G-hairs and RAdapt DRG neurons.

4.4.2.2. Risetime

A change in AP risetime is typically a result of changes in sodium {**Na^+**} channel subunit expression (Renganathan *et al.*, 2001; Dib-Hajj *et al.*, 2010). No changes were found in Aα/β-fibre or C-fibre DRG neurons, although surprisingly, following mSNA-treatment, Aδ-fibres showed a significant increase. The Aα/β-fibre data confirmed another study that also found no changes in AP risetime of Aα/β-fibre L4 DRG neurons following mSNA surgery (Djouhri *et al.*, 2012).

4.4.2.3. After-Hyperpolarisation Amplitude

This observation of a decrease in AHPA in Aα/β-fibre HTM DRG neurons offers a mechanism for the increased excitability of nociceptors. This decrease in AHPA could be explained by I_h being activated at physiological membrane voltages, possibly due to mediators that are present as a result of the mSNA model of NP, in particular, the neuro-inflammation around the conducting, intact L4 DRG. Other models of NP have noticed an increase in I_h: 1) I_h amplitude increased in the chronic compression of DRG model (Yao *et al.*, 2003); and 2) I_h density increased in the SN ligation model of NP in injured DRG neurons (Chaplan *et al.*, 2003). Furthermore, increases in both I_h density and amplitude have been reported in DRG neurons following **c**omplete **F**reund's **a**djuvant {**CFA**} induced **c**hronic **i**nflammatory **p**ain {**CIP**} (Weng *et al.*, 2012).

4.4.2.4. After-Hyperpolarisation 100%

Despite the changes in AHPA, AHP100% was not different between any groups of DRG neurons when comparing the control to the mSNA. This is surprising since I_h could affect the time it takes for the membrane to return to E_m.

4.4.3. Spontaneous Activity

4.4.3.1. Importance in Dorsal Root Ganglion Neurons

Nerve-injury induced SA in DRG neurons was originally thought to halt neuronal growth, due to experiments in mice (Fields et al., 1990) and snails (Cohan and Kater, 1986). However, recently, SA has been suggested to be essential for initiating the growth capacity of neurons after axotomy (Hanz and Fainzilber, 2006; Abe and Cavalli, 2008; Rishal and Fainzilber, 2010; Allodi et al., 2012).

In the mSNA model of NP, there are many mediators that can cause SA in L4 DRG neurons, such as increases in the intracellular concentration of **c**yclic **a**denosine **m**ono**p**hosphate {**cAMP**} (Udina et al., 2008). cAMP is able to shift the activation kinetics of HCN2 and HCN4, but not HCN1 or HCN3, to voltages that are 20 mV more positive (Wainger et al., 2001). In DRG neurons, cAMP might be required for the maintenance of CP (Zheng *et al.*, 2007). Additionally, in the CNS, cAMP is critical for regeneration after injury (Hannila and Filbin, 2008). This is relevant as the HCN channels have been widely implicated in the generation of SA in DRG neurons, although it is not entirely clear which subpopulation is responsible (Chaplan *et al.*, 2003; Emery *et al.*, 2011; Weng *et al.*, 2012). This study provided provisional evidence that LTM in the intact DRG neurons are not responsible for the analgesic effects of ZD7288.

In addition, there are many inflammatory mediators and cytokines associated with Wallerian degeneration of the L5 SN (Gaudet *et al.*, 2011). One proinflammatory cytokine, tumour necrosis factor α, has been shown to cause increased SA in C-fibre DRG neurons (Schäfers *et al.*, 2003). Finally, a neurotrophic factor, nerve growth factor, has also been implicated in SA in C-fibre DRG neurons (Djouhri *et al.*, 2001) and concentrations are increased in these intact DRG neurons after L5 SN axotomy (Shamash *et al.*, 2002).

4.4.3.2. SA and ZD7288

In these experiments, ZD7288 had no effect on the rate of SA in a small number of LTM, including two RAdapt, one SAdapt, and one G-Hair. These findings suggest that the HCN channels do not play a significant role in the generation of SA in this subpopulation of intact DRG neurons, after nerve-injury to adjacent DRG neurons. Unfortunately, our attempts to examine the effects of ZD7288 on SA in C-fibre and A-fibre nociceptive DRG neurons were un-successful, as many neurons were lost during the recording stage, because it is much more difficult to penetrate, stably maintain, and electrophysiologically record from smaller neurons. Thus, it remains to be determined whether or not HCN channels contribute to SA generation in L4 nociceptors following L5 SN injury.

There is partial evidence implicating I_h in nociceptors in a model of CIP, as results obtained using *in vivo* electrophysiology showed that a greater % of C-fibre nociceptors show an increased I_h current (Weng et al., 2012), possibly suggesting that I_h may contribute to the increased SA (Djouhri *et al.*, 2006) and hyperexcitability of DRG neurons in CIP. Additionally, HCN2 knock-out from $Na_v1.8$ specific DRG neurons, of which 85% are nociceptors (Coward *et al.*, 2000; Djouhri *et al.*, 2003; Shields *et al.*, 2012), resulted in an ablation of PGE_2 induced SA, in addition to peripheral hypersensitivity to mechanical and chemical stimuli (Emery *et al.*, 2011).

Other groups have observed SA from these large DRG neurons following CP, however, the physiological purpose is not entirely clear. There is evidence that A-fibre, and not C-fibre, activation of injured DRG neurons drives tactile, mechanical hypersensitivity (Liu *et al.*, 2000a; Song *et al.*, 2012), although this precise mechanism is controversial (King *et al.*, 2011). However, mechanical hypersensitivity could be due to hyperexcitability from both Aδ- and Aα/β-fibre DRG nociceptors. This mechanism does not provide an explanation for the contribution of SA from the adjacent, un-injured DRG neurons in CP.

Peripheral sensitisation initiates and maintains changes in the CNS (Gracely et al., 1992) and an early and prolonged block of this initial electrical activity can prevent the development of NP (Xie et al., 2005). The ability of DRG neurons, particularly nociceptors, to sensitise, or increase their excitability, is important during states of CP (Gold and Gebhart, 2010). Many C-fibres discharge at rates of 1–10 impulses per second because of either inflammation or nerve injury (Puig and Sorkin, 1995). Furthermore, low-frequency electrical stimulation of C-fibers can lead to behavioural signs of hypersensitivity in humans (Klede et al., 2003) and rats (Wu et al., 2002). This low frequency stimulation of DRG neurons in spinal cord slices could also cause the release of the neurotransmitter, **sub**stance **P** {**SubP**}, while high frequency stimulation of 100 hertz {**Hz**} causes the release of excitatory neurotrophins, such as brain-derived neurotrophic factor (Lever *et al.*, 2001). The responses of central neurons to different frequency stimulation from DRG neurons provides possibilities for the existence of highly specific neuronal circuitry that is reliant upon the firing rate of DRG neurons.

With peripheral injury or insult, DRG neurons become hyperexcitable and this drives changes in both gene expression in the cell body and modifications in the CNS. This hyperexcitability also aids neuronal regeneration, which sometimes takes years, of the injured neurons and is partly guided by intracellular cAMP (Neumann et al., 2002), which is also a potent modulator of the HCN channels.

4.4.3.3. Significance of SA in Other Neurons:

SA is an important physiological phenomena, particularly in neurons, as it has a key role in early neuronal development (Spitzer, 2006), which was shown using *in vivo* imaging to govern axonal growth in the thalamocortical neurons of mice (Mire et al., 2012). Furthermore, there is evidence that SA modulates the direction of the growth cone (Ming et al., 2001) and this is reliant upon intracellular concentrations of both calcium and cAMP (Ming et al., 1997).

Nerve injury initially results in an influx of sodium {**Na^+**} and calcium {**Ca^{2+}**} ions into the neuron, as this is also what occurs in the CNS following axotomy (Mandolesi et al., 2004), where cAMP controls the ability of axons to regenerate, although this decreases with age (Cai et al., 2001). This initial SA allows the initiation of chromatolytic changes, or the dissolution of Nissl bodies, such as the endoplasmic reticulum, in the cell body to allow the break-down of the neurons and this is also mediated by raised intracellular Ca^{2+} and cAMP (Allodi et al., 2012). Finally, SA has been shown to be imperative for the maintenance of olfactory neurons (Yu *et al.*, 2004).

4.4.4. Physiological Mechanism of ZD7288

After ZD7288 application to DRG neurons produced an increase in the AHP100%, which implies that I_h expedites the return of DRG neurons to their resting E_m. Although AHPA showed a significant decrease in the mSNA-treated Aα/β-fibre HTM DRG neurons, in neurons that were administered ZD7288, AHPA was not changed. However, no nociceptors were found, which showed more profound changes in hyperpolarisation properties than LTMs.

4.4.5. Relationship Between I_h and Other Ion Channels

4.4.5.1. TRPA1

There are a number of voltage-gated ion channels that are regulated by feedback loops that are dependent upon the cell's voltage, or E_m (Geffeney and Goodman, 2012). Less hyperpolarisation alters the activation properties of other ion channels, such as the TRPA1 ion channel subunit, which is subject to hyperpolarisation-dependent inactivation (Nagata et al., 2005). TRPA1 is expressed in small- and medium-sized DRG neurons (Story et al., 2003; Nagata et al., 2005), which matches the immuno-flourescent expression profile of $HCN2^+$ primarily peptidergic DRG neurons (Weng et al., 2012). TRPA1 is expressed in a sub-population of $TRPV1^+$ C-fibre DRG neurons, but not co-localised with TRPM8

(Story et al., 2003). Furthermore, TRPA1 is activated by cold (Karashima et al., 2009; del Camino et al., 2010), chemical (Jordt et al., 2004; Bautista et al., 2006) and specific mechanical (Kwan et al., 2009) stimuli, although TRPA1 is not the sole transducer of mechanical sensitivity (Vilceanu and Stucky, 2010). Furthermore, isotonic solutions activate TRPA1, partly due to lowering of the membrane potential, to increase the excitability of DRG neurons (Zhang et al., 2008). TRPA1 antagonism prevented SA induced by CFA (Andrade et al., 2012). In NP due to L5 SN ligation, the intact L4 showed increased TRPA1 expression (Obata et al., 2005). As HCN channel subunits and TRPA1 are expressed in similar DRG neuronal sub-populations, changes in I_h, and therefore hyperpolarisation, can alter TRPA1's activation profile.

4.4.5.2. $Na_v1.9$

A specific sodium channel subunit that is found in 80% of small and medium, in addition to a few large DRG neurons, is $Na_v1.9$ (Amaya *et al.*, 2000; Fjell *et al.*, 2000). Almost all of these small and medium $Na_v1.9^+$ DRG neurons are nociceptors, some of which are thought to be activated by chemical stimuli (Fang *et al.*, 2002). These ion channels are slowly activated at hyperpolarised potentials of -70 mV (Cummins *et al.*, 1999) and so with I_h causing less hyperpolarisation, maintaining the resting E_m around $Na_v1.9$'s activation voltage, $Na_v1.9$ could contribute to the hyperexcitability of DRG neurons during states of CP.

4.4.6. Possible Modulators of HCN Channels during Chronic Pain

4.4.6.1. Cyclic Adenosine Monophosphate

Intracellular cAMP has a profound effect on HCN2 and HCN4, but not HCN1 or HCN3, causing the activation of HCN2 and HCN4 to shift to voltages that are 20 mV more positive (Wainger et al., 2001). Furthermore, cAMP is required for the maintenance of the DRG compression model of NP (Song et al., 2006). This provides a means for cAMP to exert an effect on I_h to maintain NP, although the

possibility of inhibition of the inward rectifying potassium current by cAMP can not be completely excluded (Evans et al., 1999).

4.4.6.2. Phophatidylinositol 4,5-bisphosphate

The presence of PIP_2 effects the activation kinetics of the HCN channel subunits, especially HCN2, by causing the activation voltage to occur at +20 **m**illi-**v**olts {**mV**} from their normal range, which brings them into physiologically-relevant ranges (Pian et al., 2006; Zolles et al., 2006). A change in concentration of PIP_2, which also affects other ion channel subunits, could be responsible for the increase in excitability seen in states of CP and this is supported by evidence that both thermal and mechanical hypersensitivity can be reduced by prostatic acid application to inhibit the phospholipase-C mediated depletion of PIP_2 (Sowa et al., 2010).

4.4.7. HCN Channel Rundown

When performing electrophysiology, channel rundown, which consists of a rapid decrease of activity, can be a problem, as HCN channels experience a shift in activation voltage of up to a rate of -0.5 milli-volts per minute (Wickenden et al., 2009). However, only in the ZD7288 application experiments, when recording times went up to 30 minutes, or -15 milli-volts, would this have been an issue. In this study, the administration of ZD7288 blocked I_h in only a few minutes.

Chapter 5: Immunofluorescence

5.1. Abstract

Immunofluorescence was used to examine whether protein expression of the **h**yperpolarisation-activated, **c**yclic-**n**ucleotide gated {**HCN**} ion channel subunits {**HCN1-4**} changed in **d**orsal **r**oot **g**anglion {**DRG**} neurons following **c**hronic **p**ain {**CP**},. DRG neurons were extracted from animal models of **c**hronic **i**nflammatory **p**ain {**CIP**}, induced by **c**omplete **F**reund's **a**djuvant {**CFA**}, or **c**hronic **n**europathic **p**ain {**CNP**}, surgically caused by the **m**odified **s**pinal **n**erve **a**xotomy {**mSNA**} procedure. Tissue was sectioned onto slides and paired with appropriate controls. Immunofluorescence was performed to triple stain the tissue with antibodies for HCN1-3, **I**solectin **B4** {**IB4**}, and 4',6-diamidino-2-phenylindole {**DAPI**} to examine whether the inter- and intra-cellular expression profiles of the HCN channel subunits changes in CP. 7-**d**ays {**d**} after the induction of **i**nflammatory **p**ain {**IP**} and **n**europathic **p**ain {**NP**}, in both models there was a significant increase in HCN2 in both the normalised intensity in small neurons and also the percentage of **HCN2** positive {$^{+}$} small, < 30 micro-metres {**µm**} DRG neurons, which are predominantly nociceptors. Interestingly, this increase occurred in all types of IB4-neurons, although the highest percentage of $HCN2^{+}$ neurons was seen in the IB4 negative {$^{-}$} neurons. HCN1 also showed a significant increase in small neurons after mSNA and highly specific changes in expression at only a few diameters in both models, while HCN3 did not show any change, at any diameter, in either model. These changes were mirrored in other tissues associated with DRG neurons, such as the dorsal horn of the lumbar enlargement and axonal fibres. Therefore, HCN2 appears to be an important subunit in the development of CP, especially as the expression profile indicates that HCN2 may contribute to the hyperexcitability of DRG neurons, which drives CIP and CNP.

5.2. Introduction

To relay sensory information through the nervous system, neurons depend upon the generation of **a**ction **p**otential {**APs**}. Each AP is a result of many factors, such

as the composition of ion channel subunits, each of which possesses extremely specific inter-cellular expression profiles that are a result of post-translational modifications and also have specialised gating mechanics. Over the last decade, these factors have identified the importance of transcriptional channelopathies, which occur in states of disease due to changes in the expression of non-mutated ion channels genes, and therefore, subunits (Waxman, 2001). Due to the large number of different ion channel subunit permutations, it is challenging to identify those that are responsible for **s**pontaneous **a**ctivity {**SA**} in DRG neurons in states of CP. HCN1-4 may undergo transcriptional channelopathies that occur during states of CP (Chaplan *et al.*, 2003).

Different ion channel subunits are regulated according to the types of physiological stimuli that DRG neurons respond to. During embryological stages of development, all DRG neurons rely on nerve growth factor to survive, 7.5-d after birth, a population of these neurons switch to rely upon glial cell line-derived neurotrophic factor for survival (Molliver *et al.*, 1997; Lallemend and Ernfors, 2012) and become a population of non-peptidgeric nociceptors, primarily marked by the expression of IB4 binding (Stucky and Lewin, 1999). These neurons display functional differences from peptidergic DRG neurons, which utilise neuropeptides such as **sub**stance **P** {**SubP**} and **c**alcitonin **g**ene-**r**elated **p**eptide {**CGRP**}, and still rely on nerve growth factor (Nagy and Hunt, 1982; Silverman and Kruger, 1990; Molliver *et al.*, 1997). Electrophysiologically, $IB4^+$ neurons typically have higher AP thresholds, longer AP durations, larger tetrodotoxin-resistant currents (Fang *et al.*, 2006), and smaller heat-sensitive currents (Stucky and Lewin, 1999). Furthermore, $IB4^+$ and $IB4^-$ nociceptors express different **t**ransient **r**eceptor **p**otential {**TRP**} ion channel subunits in their plasma membranes to create physiologically distinct types of neurons that respond to different stimuli (Basbaum *et al.*, 2009). This is probably partially responsible for the different neuro-anatomical pathways, as $IB4^+$ nociceptors typically terminate in inner lamina II of the dorsal horn, while $IB4^-$ nociceptors terminate in lamina I and outer lamina II (Zylka *et al.*, 2005; Basbaum *et al.*, 2009).

To elucidate the HCN channel subunits' neuro-anatomy, this chapter explored the relationship of HCN1-3 and IB4, especially as this has not been examined at 7-d post-injury in these models of CP. Using immunofluorescence, followed by densitometric analysis, this was aimed at examining the hypothesis that the expression profiles of HCN1-3 increase in DRG neurons following hindlimb inflammation, for CIP, and surgically induced **s**pinal **n**erve {**SN**} injury, for CNP.

5.3. Results

5.3.1. Expression of HCN1-3 in Control Dorsal Root Ganglia

In control tissue from un-treated animals, HCN1-3 showed distinct staining profiles. Furthermore, each subunit was found in DRG populations that possessed different levels of IB4 binding.

5.3.1.1. HCN1 Immunoreactivity

HCN1-**i**mmuno**r**eactivity {**IR**} was primarily in the vast majority of large DRG neurons, in clear ring staining around the perimeter, known as ring staining [Fig. 5.1.A,D]. In addition, HCN1-IR revealed cytoplasmic staining in a subpopulation of small DRG neurons. IB4 binding [Fig. 5.1.B,E] in these DRG neurons revealed that these small, $HCN1^{+}$ DRG neurons also bind IB4 [Fig. 5.1.C], revealing a strong correlation [Fig. 5.1.F] to indicate HCN1 staining is in small, non-peptidergic DRG neurons.

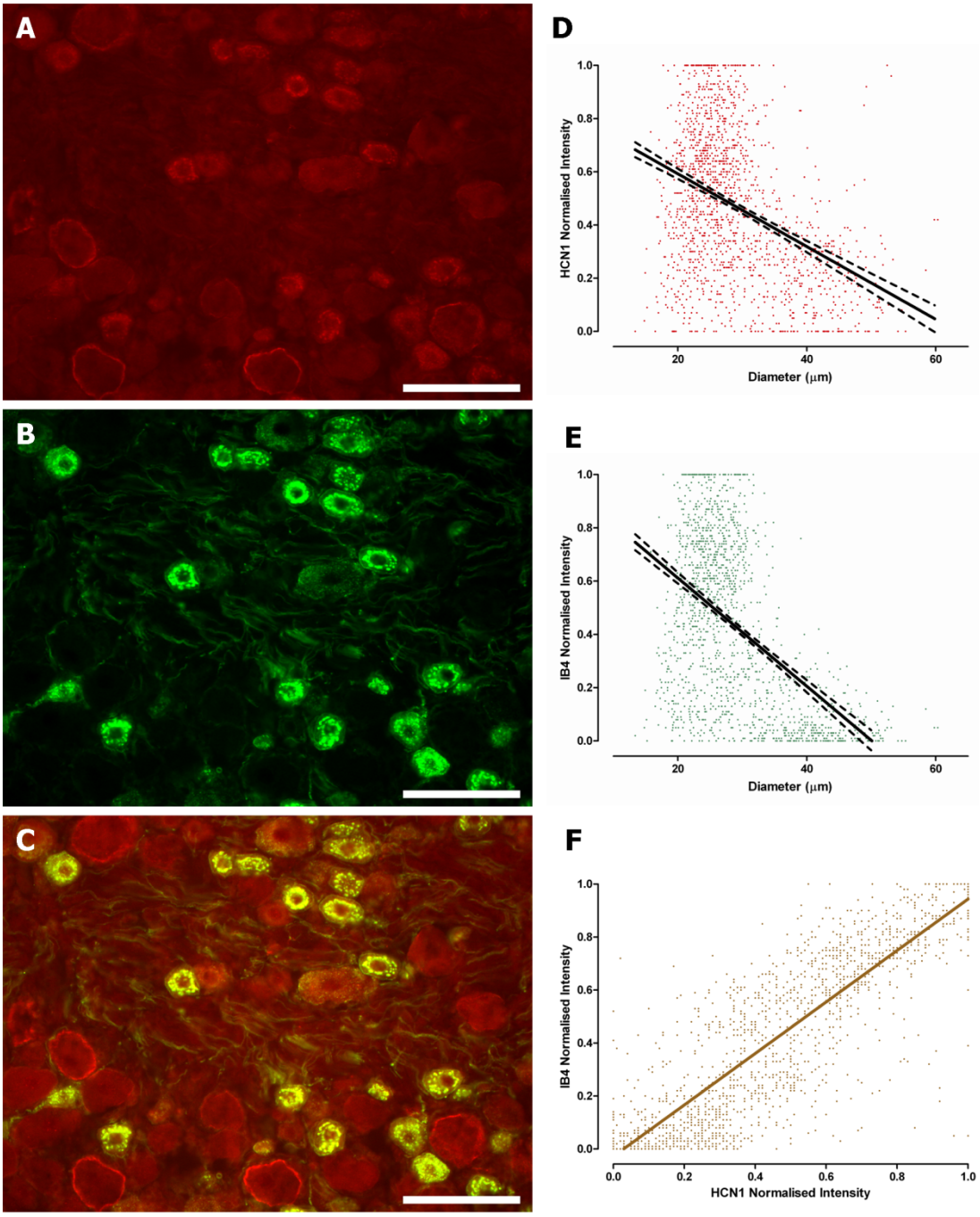

Figure 5.1: HCN1 and IB4 Expression in Naïve L4/L5 DRG Tissue. Photomicrographs of HCN1-IR [A], IB4-IR [B] and the two images overlayed [C]. Following normalisation, densitometric analysis was performed to show the normalised values against neuronal diameter (µm) for HCN1 [D] and IB4 [E] (*n = 1515 neurons*), with the dashed lines showing 95% confidence intervals. Finally, a graph of each neuron's HCN1's normalised intensity was plotted against IB4's normalised intensity to reveal the extent of co-localisation [F]. Scale Bars [A-C] represent 100 µm.

5.3.1.2. HCN2 Immunoreactivity

HCN2-IR in DRG neurons revealed some similarities to HCN1-IR, as both showed ring staining of large DRG neurons and HCN2-IR was also in a subpopulation of small DRG neurons [Fig. 5.2.A,D]. However, in stark contrast to HCN1-IR, HCN2-IR was not in the majority of large DRG neurons and was in a different subpopulation of small DRG neurons, where it was much brighter. When examining HCN2-IR with IB4-IR [Fig. 5.2.B,E], co-localisation revealed two separate populations [Fig. 5.2.C,F], as 62% of $HCN2^{+}$ small neurons were $IB4^{-}$, while only a small population were $HCN2^{+}$ and $IB4^{+}$. Finally, $HCN2^{+}$ DRG neurons included a subpopulation of medium sized neurons, which was not evident in the $HCN1^{+}$ neurons.

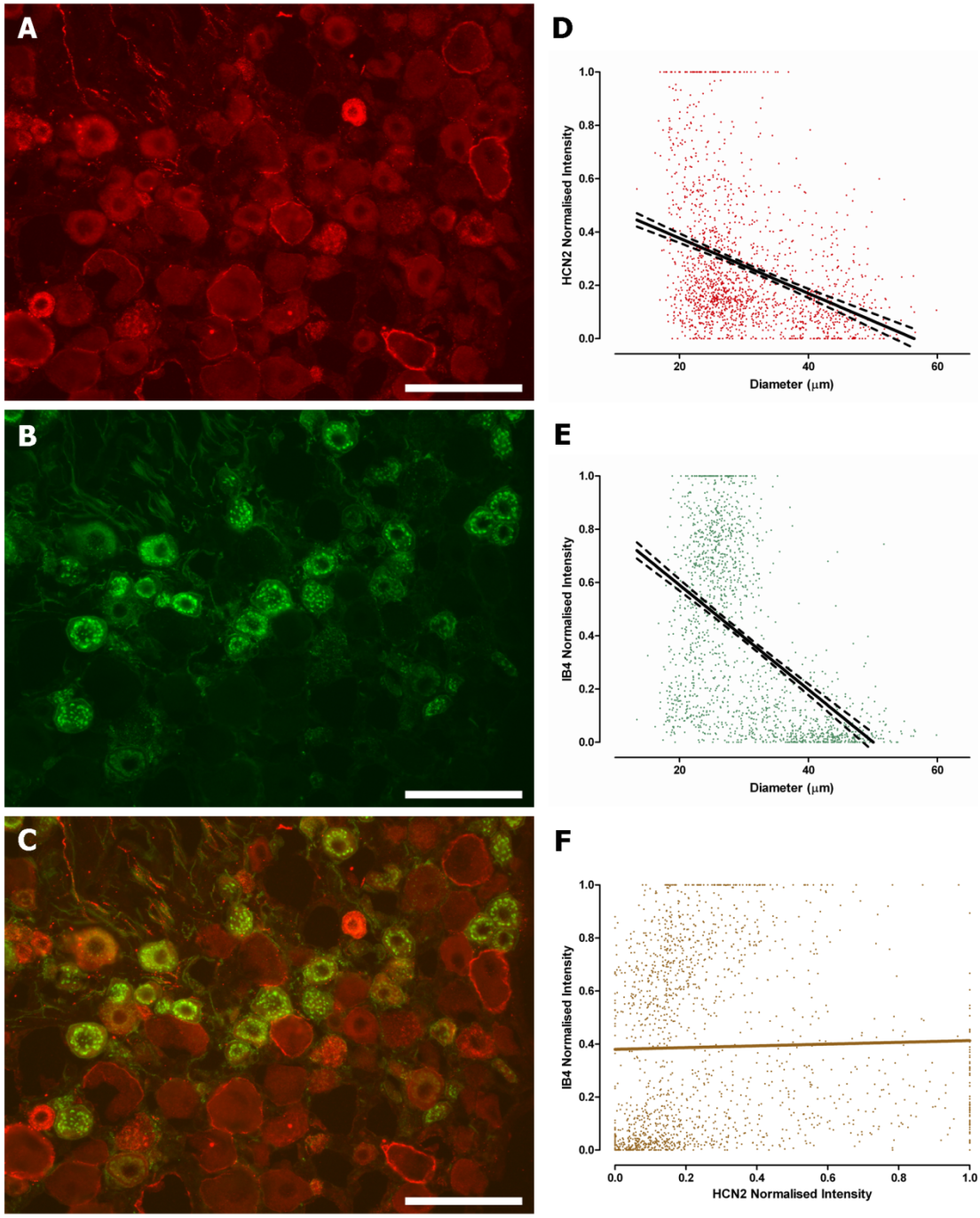

Figure 5.2: HCN2-IR and IB4-IR in Naïve L4/L5 DRG Tissue. Photomicrographs of HCN2-IR [A], IB4-IR [B] and the two images overlayed [C]. Following normalisation, densitometric analysis was performed to show the normalised values against diameter (µm) for HCN2 [D] and IB4 [E] (*n = 1662 neurons*), with the dashed lines showing 95% confidence intervals. Finally, a graph of each neuron's HCN2 normalised intensity was plotted against IB4 normalised intensity to reveal the extent of co-localisation [F]. Scale Bars [A-C] represent 100 µm.

5.3.1.3. HCN3 Immunoreactivity

HCN3-IR was found intra-cellularly in all sizes of DRG neurons, although in the large neurons ring staining was present [Fig. 5.3.A,D]. When cross-examining the HCN3 staining with IB4 [Fig. 5.3.B,E], HCN3 appears in both $IB4^+$ and $IB4^-$ small neurons, with a preference for $IB4^+$ neurons [Fig. 5.3.C] and this was reflected in the scatter plot of the two sets of normalised intensities [Fig. 5.3.F].

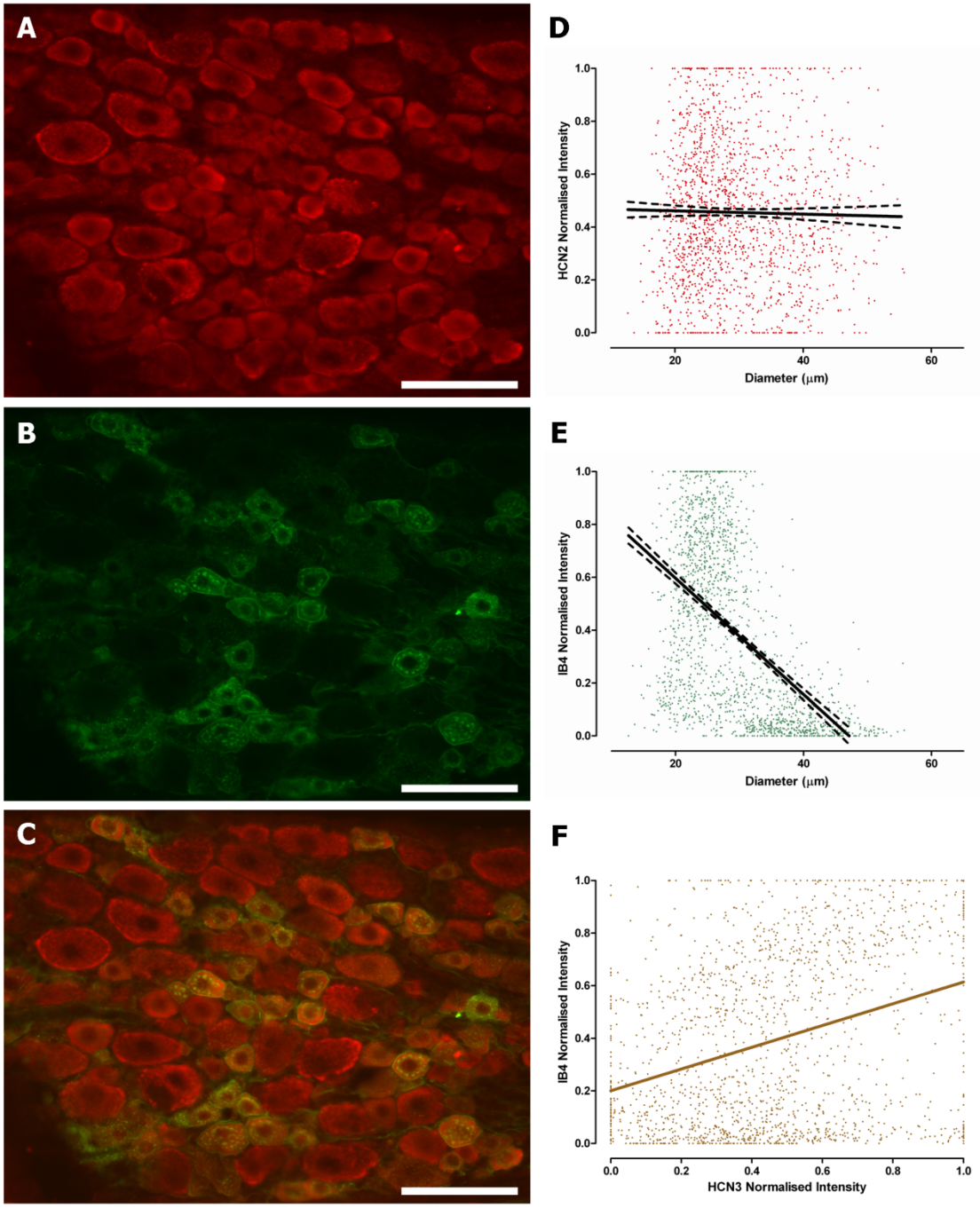

Figure 5.3: HCN3-IR and IB4-IR in Naïve L4/L5 DRG Tissue. Photomicrographs of HCN3-IR [A], IB4-IR [B] and the two images overlayed [C]. Following normalisation, densitometric analysis was performed to show the normalised values against neuronal diameter (µm) for HCN1 [D] and IB4 [E] (*n = 1670 neurons*), with the dashed lines showing 95% confidence intervals. Finally, a graph of each neuron's HCN3 normalised intensity was plotted against IB4 normalised intensity to reveal the extent of co-localisation [F]. Scale Bars [A-C] represent 100 µm.

5.3.2. Effect of Chronic Inflammation on HCN Expression

5.3.2.1. HCN1 in DRG Neurons

7-d after CFA-induced inflammation, HCN1-IR [Fig. 5.4.D-F] showed a staining profile that was not very different from control tissue [Fig. 5.4.A-F]. In addition, the HCN1-IB4 co-localisation scatter plot [Fig. 5.4.H] did not change from control [Fig. 5.1.F]. To confirm both sets of tissue had the same treatment conditions, DAPI, a DNA marker, was used as a control [Fig. 5.4.G]. In small DRG neurons, putative nociceptors, CFA did not increase the normalised staining intensity [Fig. 5.4.I]. The percentage of $HCN1^{+}$ DRG neurons was compared across 2.5 µm diameter increments from 17.5 – 40 µm [Fig. 5.4.J] and revealed a significant decrease, *, $p < 0.05$, at 20.0 – 22.5 µm and a significant increase, *, at 27.5 – 30.0 µm.

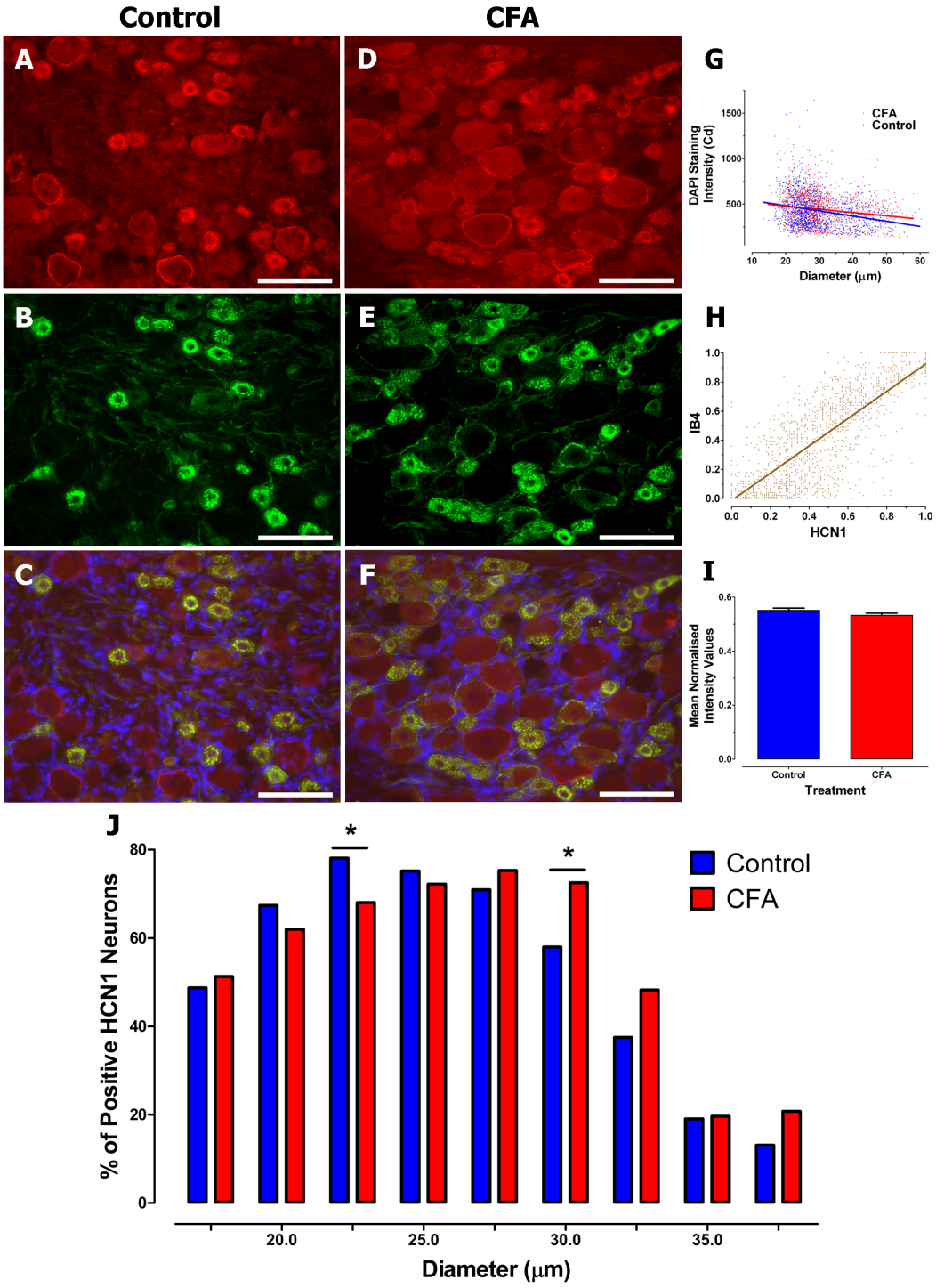

Figure 5.4: Effects of CFA After 7-Days on HCN1 Expression in L4 and L5 DRG Neurons. Photomicrographs of DRG tissue from control [A-C] and CFA [D-F], immunolabelled with HCN1 [A,D], IB4 [B,E], and the two images overlayed [C,F], showing no obvious differences in HCN1-IR. HCN1-IR is expressed mainly in small, $IB4^+$ DRG neurons and the membranes of large DRG neurons. The staining intensity of DAPI, a DNA stain, is used as a control, showing no difference in staining between control, in blue (*n = 1515 neurons*), and CFA, in red (*n = 1489*

neurons) [G]. Normalised HCN1 is plotted against normalised IB4 [H] to explore the co-localisation relationship. Mean normalised HCN1 values are plotted for control (*n = 1012 neurons*) and CFA (*n = 897 neurons*) of small DRG neurons, with a diameter < 30 µm [I]. The percentage of $HCN1^+$ small and medium sized control (*n = 1295 neurons*) and CFA (*n = 1255 neurons*) DRG neurons were compared at various diameters [J]. Scale bars [A-F] represent 100 µm. Statistics relied upon the Mann Whitney U test [I] and Fisher's Exact test [J]: *, $p < 0.05$.

5.3.2.2. HCN2 in DRG Neurons

In contrast to HCN1-IR, HCN2-IR showed noticeable changes, following 7-d of CFA [Fig. 5.5.D-F], compared to control [Fig. 5.5.A-C] in the expression profile of the HCN2 subunit in small and medium DRG neurons. DAPI showed no difference between control and CFA [Fig. 5.5.G]. Following CFA-treatment, the normalised intensity of small DRG neurons significantly increased, **, $p < 0.01$ [Fig. 5.5.H]. These small neurons were separated according to their IB4 normalised values, although all of these subpopulations revealed an increase [Fig. 5.5.I]. Finally, the percentage of $HCN2^+$ neurons were classified by their diameter to reveal significant increases after CFA in a number of groups: 25.0 – 27.5 µm, ***, $p < 0.001$; 27.5 – 30.0 µm, ***; 30.0 – 32.5 µm, ***; 32.5 – 35.0 µm, **, $p < 0.01$; 35.0 – 37.5, *.

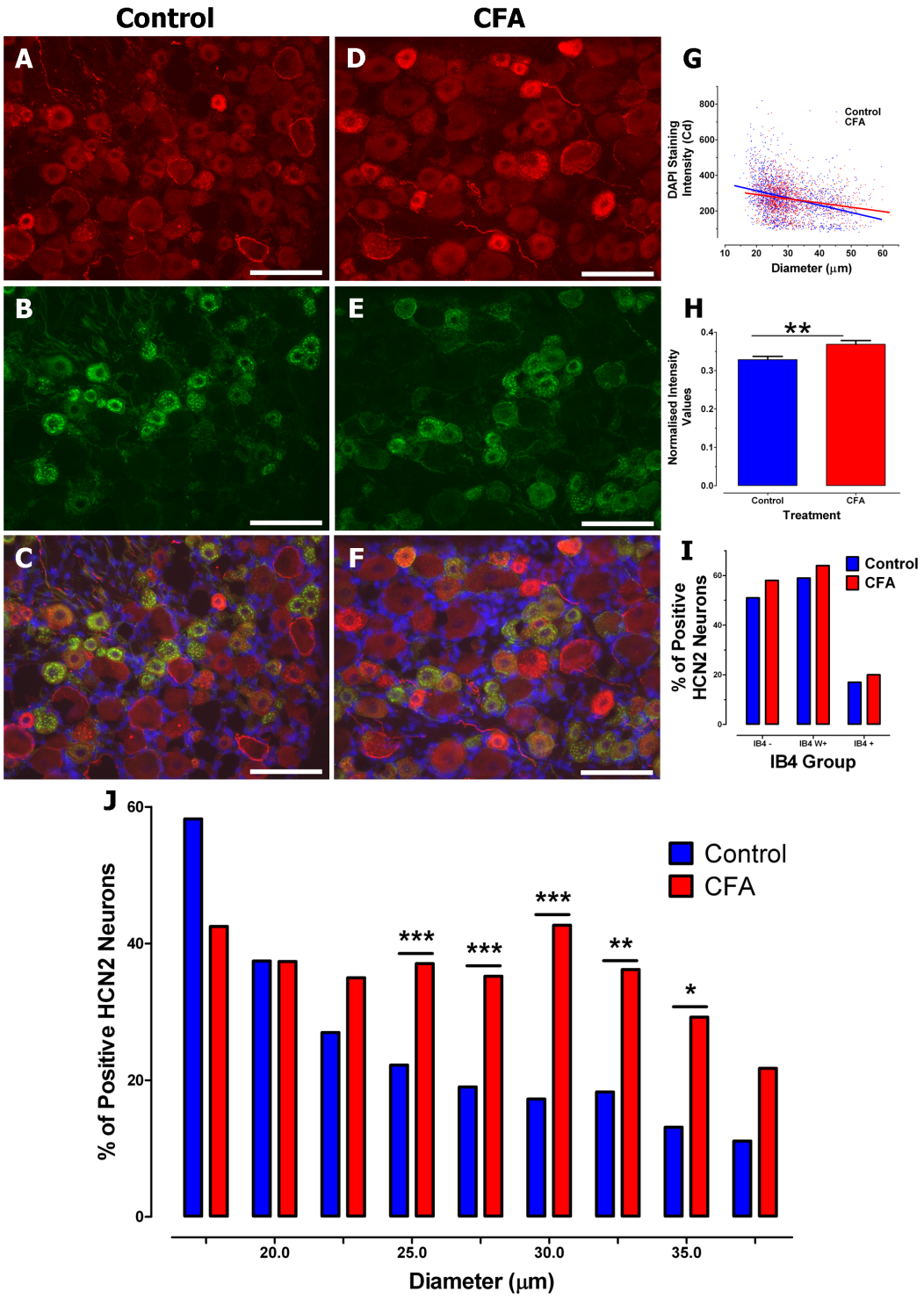

Figure 5.5: The Effects of 7-Days of CFA on HCN2 Expression in L4 and L5 DRG Neurons. Photomicrographs of DRG tissue from control [A-C] and CFA [D-F], immunolabelled with HCN2 [A,D], IB4 [B,E], and the two images overlayed [C,F]. HCN2-IR is expressed mainly in small, $IB4^-$ DRG neurons and the membranes of a subpopulation of large DRG neurons. The staining intensity of DAPI [G] is used as a control, showing no difference in staining between control, in blue (*n = 1662*

neurons), and CFA, in red (*n = 1413 neurons*). Mean normalised HCN2 values are plotted for control (*n = 1014 neurons*) and CFA (*n = 813 neurons*) of small DRG neurons, with a diameter < 30 µm, revealing a significant increase, **, following CFA [H]. These small neurons were separated by their IB4 staining: IB4 negative, $IB4^{-}$; IB4 weakly positive, $IB4^{w+}$; IB4 positive, $IB4^{+}$ [I]. The percentage of $HCN2^{+}$ small and medium sized DRG neurons were compared between control (*n = 1356 neurons*) and mSNA (*n = 1188 neurons*) at different diameters [J]. Scale bars [A-F] represent 100 µm. Statistics relied upon the Mann Whitney U test [H-I] or Fisher's Exact test [J]: *, $p < 0.05$; **, $p < 0.01$; ***, $p < 0.001$.

5.3.2.3. HCN3 in DRG Neurons

HCN3-IR revealed no significant changes after CFA [Fig. 5.6.D-F], with a similar staining profile to control tissue [Fig. 5.6.A-C]. DAPI did not differ between treatment groups [Fig. 5.6.G] and the HCN3 normalised intensity was plotted against IB4 [Fig. 5.5.H] to reveal a similar staining profile to control tissue. Furthermore, there was no change in the normalised intensity of HCN3 in small DRG neurons [Fig. 5.6.I] or the percentage of $HCN3^{+}$ DRG neurons, when categorised by diameter [Fig. 5.6.J].

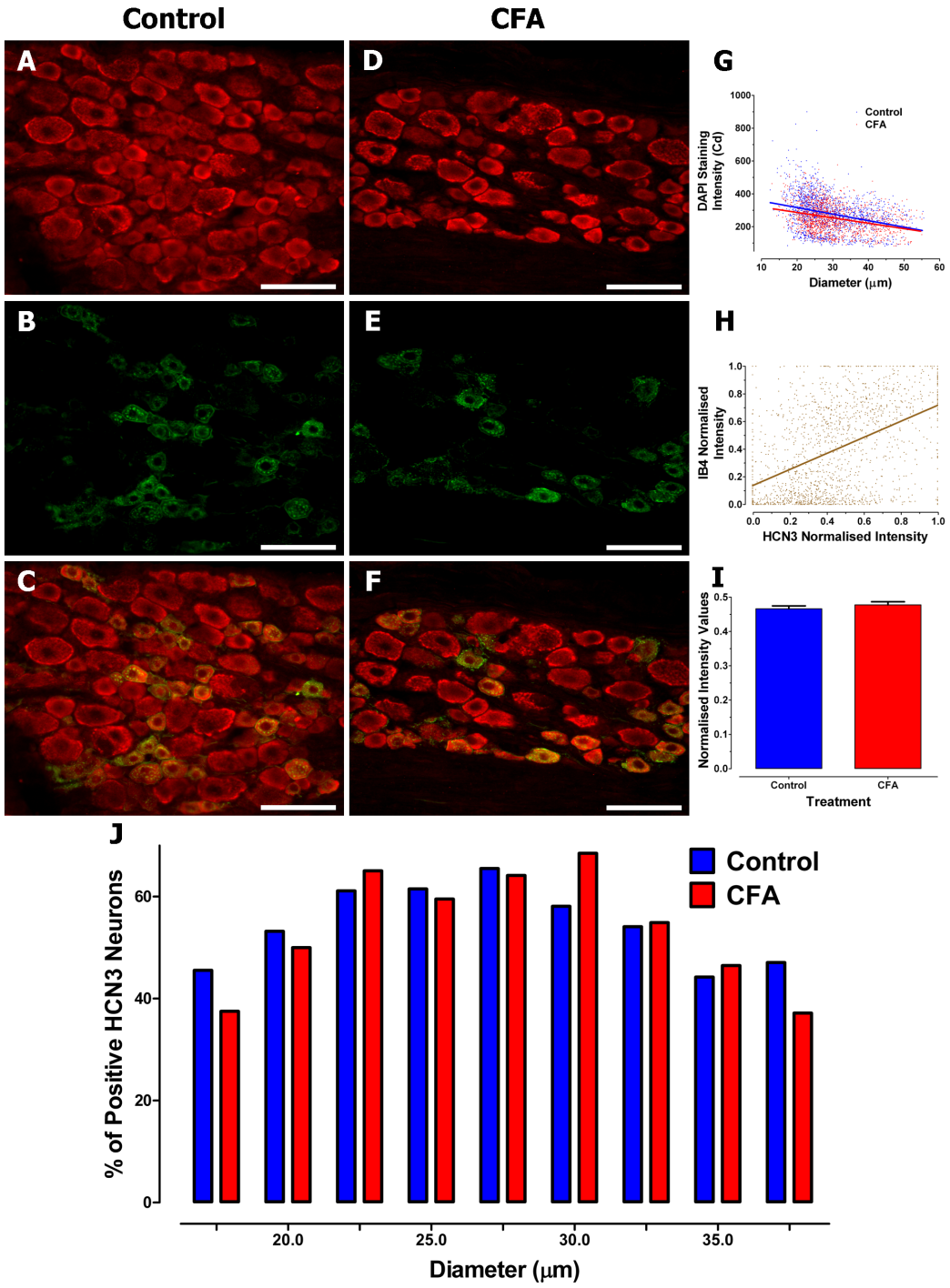

Figure 5.6: The Effects of 7-Days of CFA on HCN3 Expression in L4 and L5 DRG Neurons. Photomicrographs of DRG tissue from control [A-C] and CFA [D-F], immunolabelled with HCN3 [A,D], IB4 [B,E], and the two images overlayed [C,F], showing no obvious differences in HCN3-IR. HCN3-IR is expressed in all sizes of DRG neuron. The staining intensity of DAPI [G] is used as a control, showing no difference in staining between control, in blue (*n = 1670 neurons*), and CFA, in red (*n = 1504 neurons*). Normalised HCN3 is plotted against normalised IB4 [H] to

explore the co-localisation relationship. Mean normalised HCN3 values are plotted for control (*n = 1017 neurons*) and CFA (*n = 876 neurons*) of small DRG neurons, with a diameter < 30 µm [I]. The percentage of $HCN3^+$ small and medium sized control (*n = 1419 neurons*) and CFA (*n = 1245 neurons*) DRG neurons were compared at different diameters [J]. Scale bars [A-F] represent 100 µm. Statistics used the Mann Whitney U test [I] and Fisher's Exact test [J].

5.3.2.4. HCN1 and HCN3 in Spinal Cord

The lumbar enlargement of the spinal cord, where the lumbar DRG neurons terminate, was also examined for HCN1-3 and IB4 staining. HCN1-IR was not pronounced in control tissue [Fig. 5.7.A-C] and this did not change 7-d after CFA [Fig. 5.7.D-F]. In control tissue [Fig. 5.7.G-I.], HCN3-IR was found in motor neurons in the ventral horn of the lumbar enlargement, but revealed no positive staining in the dorsal horn in control tissue. CFA, after 7-d, did not result in any changes in the expression profile of HCN3 [Fig. 5.7.J-L].

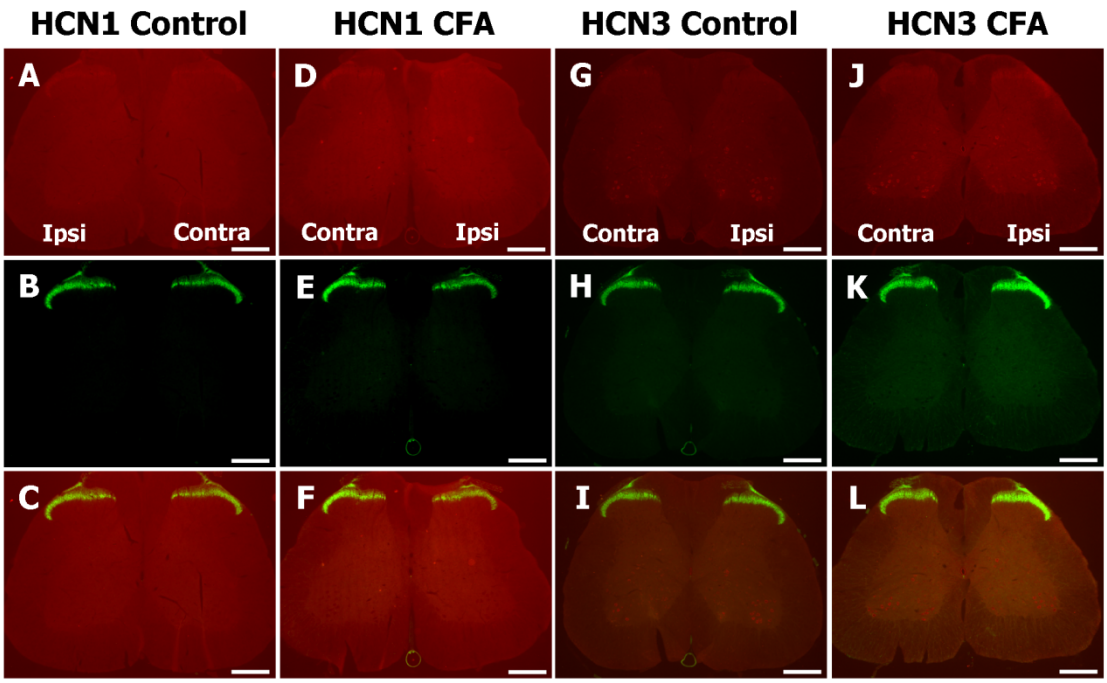

Figure 5.7: The Effects of 7-Days of CFA on HCN1 and HCN3 Spinal Cord Expression. Photomicrographs of the spinal cord's lumbar enlargement from

control [A-C & G-I] and CFA [D-F & J-L], immunolabelled for HCN1 [A-F], HCN3 [G-L], and IB4 [B,E,H,K]. The images are shown with HCN [A, D, G, J], IB4 [B, E, H, K] and the overlays at the bottom [C, F, I, L]. Contra = contralateral, un-injured, side; Ipsi = ipsilateral, injured, side. Scale bars [A-L] = 500 µm.

5.3.2.5. HCN2 in Spinal Cord

However, in control tissue, HCN2-IR was found in lamina I and outer lamina II of the dorsal horn of the spinal cord's lumbar enlargement, while IB4-IR was found in inner laminae II [Fig. 5.8.A-C]. HCN2-IR was only slightly co-localised with IB4 [Fig. 5.8.G-I], but HCN2 was almost completely co-localised with the neuropeptide, CGRP [Fig. 5.8.J-L]. Furthermore, following 7-d post-CFA, there was a dramatic up-regulation of HCN2 in the injured, or ipsilateral, side of the lumbar enlargement [Fig. 5.8.D-F], which remained co-localised with CGRP, but only partially co-localised with IB4 [Fig. 5.8.F].

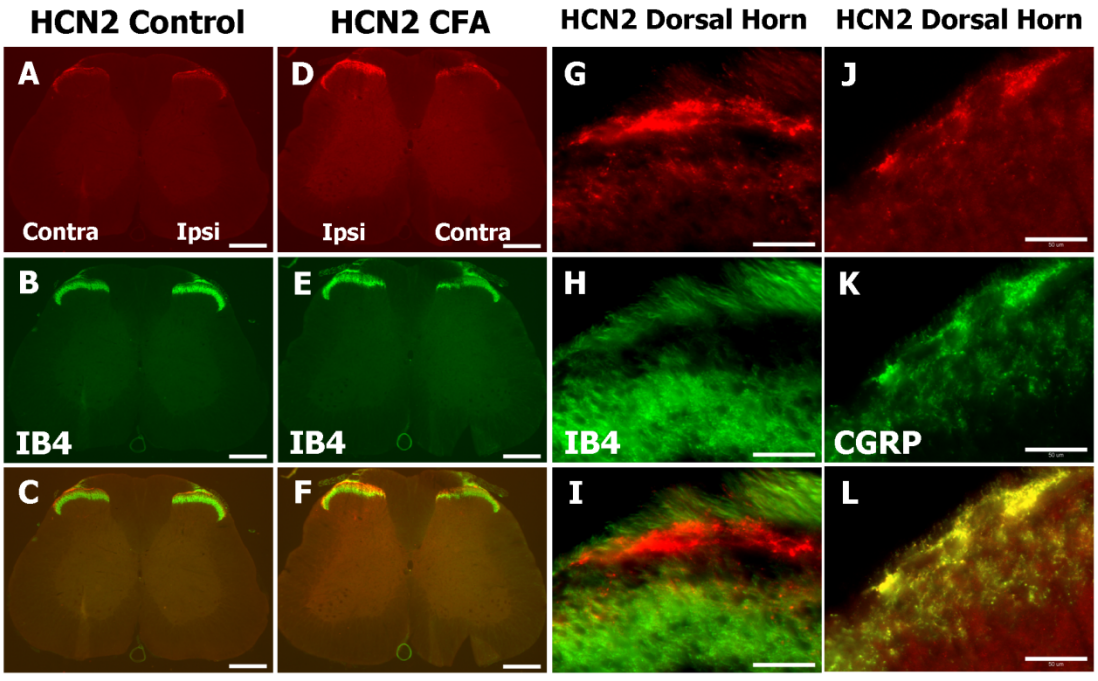

Figure 5.8: The Effects of 7-Days of CFA on HCN2 Spinal Cord Expression in DRG Neurons. Photomicrographs of the spinal cord's lumbar enlargement from control [A-C & G-L] and CFA [D-F], immunolabelled for HCN2 [A, D, G, J], IB4

[B,E,H] and CGRP [K]. Contra = contralateral, un-injured, side; Ipsi = ipsilateral, injured, side. Scale bars: [A-F] = 500 µm, [G-L] = 50 µm.

5.3.2.6. HCN2 Expression in Nerve Fibres

Following this observation in the central terminals of DRG neurons, axonal fibres, which bifurcate from the DRG to innervate the periphery and terminate in the dorsal horn, were examined. There was no observable difference between control and CFA-treated in the two types of axonal fibres: ventral, which occupy the DRG to the periphery [data not shown]; and distal, which occupy the DRG to the dorsal horn [Fig. 5.9.A-C]. In distal DRG neuronal fibres, HCN1-IR and HCN3-IR were faint [data not shown], while HCN2-IR revealed slight staining in control tissue [Fig. 5.9.D-F] and although this appeared to co-localise with IB4, upon examination at higher magnification, this was not the case [data not shown]. 7-d post-CFA, this staining appeared to increase slightly [Fig. 5.9.G-I].

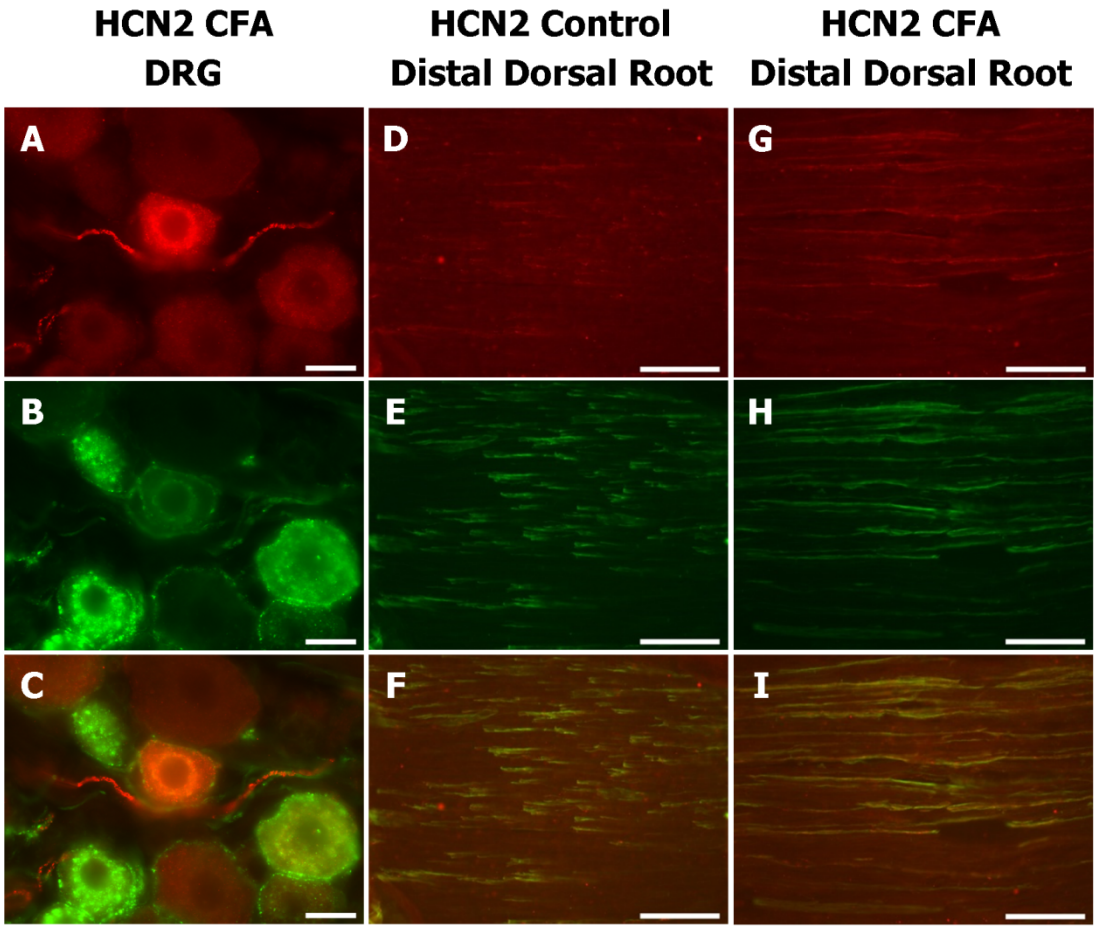

Figure 5.9: The Effects of 7-Days of CFA on HCN2 Staining in Axonal Fibres of DRG Neurons. After observing a bifurcation of a brightly positive $HCN2^{+}$ [A], but $IB4^{-}$ [B-C], DRG neuron, distal dorsal roots were stained in tissue from control [D-F] and 7-d post-CFA [G-I]. The tissue was stained for HCN2 [A,D,G] and IB4 [B,E,H} with the overlays shown at the bottom [C,F,I]. Scale bars [A–I] represent 100 µm.

5.3.3. Effect of Nerve Injury on HCN Expression

5.3.3.1. HCN1 in DRG

To compare tissue in the mSNA model of NP, mSHAM tissue was used, which involved performing the surgery and lifting up the L5 and L4 SN without damaging them. Following mSNA surgery, the L4 DRG was stained [Fig. 5.10.D-F] and both HCN1-IR and IB4-IR showed a similar staining profile to mSHAM tissue [Fig. 5.10.A-C]. This matched the original control, with HCN1-IR showing ring staining in the membranes of most large neurons and cytoplasmic staining in small, $IB4^{+}$ neurons. The extent of co-localisation between normalised HCN1 and IB4 revealed minimal changes between mSHAM and mSNA [Figure 5.10.H]. Surprisingly, DAPI revealed a big increase in mSNA [Fig. 5.10.G]. The normalised intensities in small DRG neurons indicated a significant increase, * [Fig. 5.10.I]. Furthermore, there were significant increases in the % of $HCN1^{+}$ DRG neurons across a few, highly specific diameter profiles: 20.0 – 22.5 µm, *; and 32.5 – 35.0 µm, *** [Fig. 5.10.J].

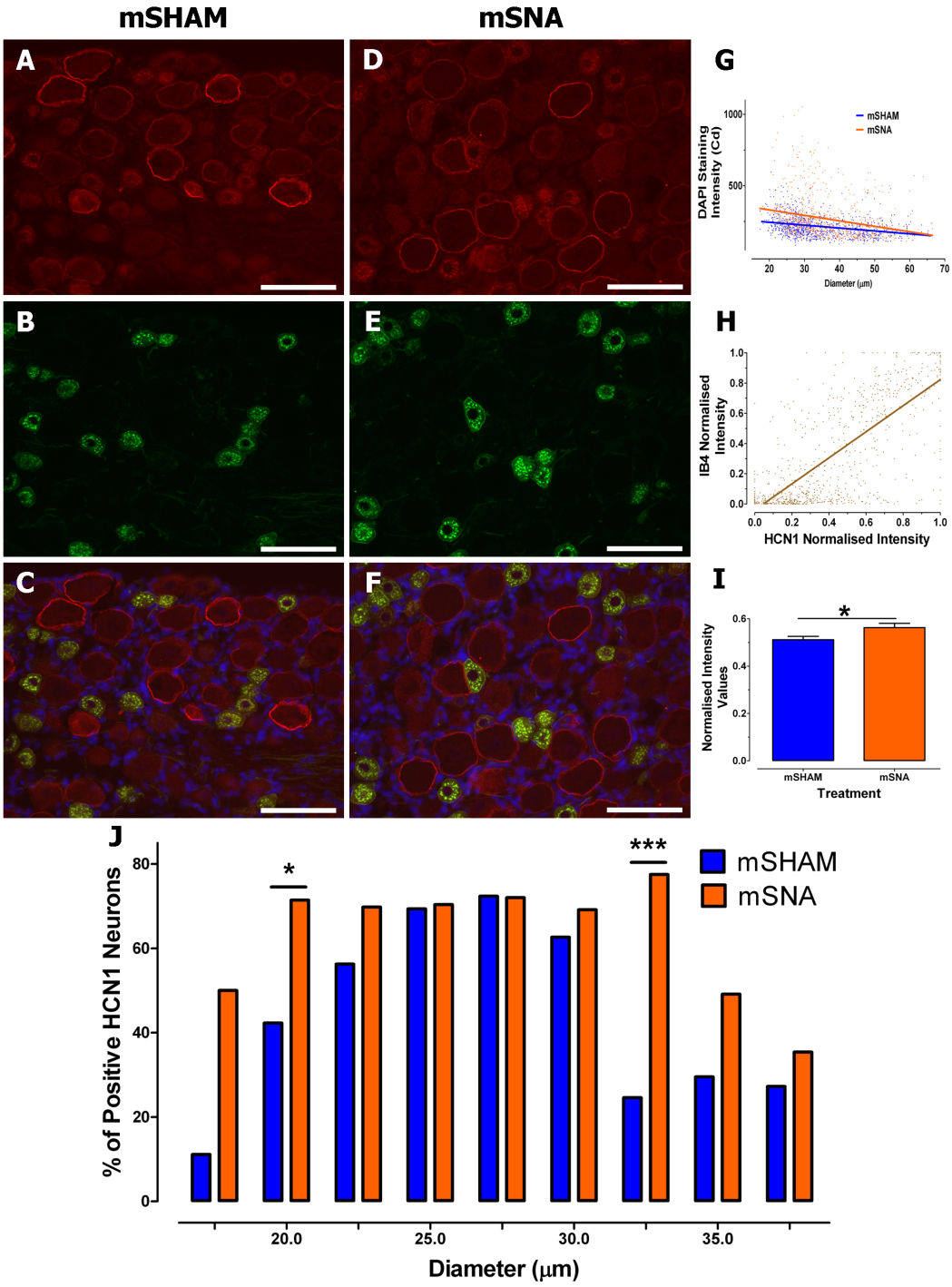

Figure 5.10: HCN1-IR in L4 DRG Neurons 7-Days after Induction of the mSNA Model of NP Compared to mSHAM. Photomicrographs of DRG tissue from mSHAM [A-C] and mSNA [D-F], immunolabelled with HCN1 [A,D], IB4 [B,E], and the two images overlayed [C,F], showing no obvious differences in HCN1-IR. HCN1-IR is expressed mainly in small, $IB4^{+}$ DRG neurons and the membranes of large DRG neurons. The staining intensity of DAPI, a DNA stain, is a control, showing brighter staining in the mSNA, in orange (*n = 782 neurons*), compared to

the mSHAM, in blue (*n = 902 neurons*) [G]. Normalised HCN1 is plotted against normalised IB4 [H] to explore the co-localisation. Mean normalised HCN1 values of small, diameter < 30 µm, DRG neurons, are plotted for mSHAM (*n = 393 neurons*) and mSNA (*n = 251 neurons*), showing a significant increase, * [I]. The percentage of $HCN1^+$ small and medium sized DRG neurons were compared between mSHAM (*n = 630 neurons*) and mSNA (*n = 530 neurons*) at diameter intervals [J]. Scale bars [A-F] represent 100 µm. Statistics used the Mann Whitney U test [I] and Fisher's Exact test [J]: *, $p < 0.05$; ***, $p < 0.001$.

5.3.3.2. HCN2 in DRG

In the mSHAM tissue [Fig. 5.11.A-C], HCN2-IR and IB4-IR resembled control tissue. In all photomicrographs, including the mSNA tissue [Fig. 5.11.D-F], HCN2-IR was found cytoplasmically in small, $IB4^-$ DRG neurons and with ring staining in a subpopulation of large DRG neurons. DAPI revealed no difference between mSNA and mSHAM [Fig. 5.11.G]. When examining the small DRG neurons, the normalised intensity showed a significant increase, * [Fig. 5.11.H]. Furthermore, all populations of normalised IB4 revealed an increase in the percentage of $HCN2^+$ DRG neurons [Fig. 5.11.I]. When classifying according to diameter [Fig. 5.11.J], the following groups revealed a significant increase: 17.5 – 20 µm, *; 22.5 – 25 µm, *. A solitary group, 37.5 – 40 µm revealed a significant decrease, *.

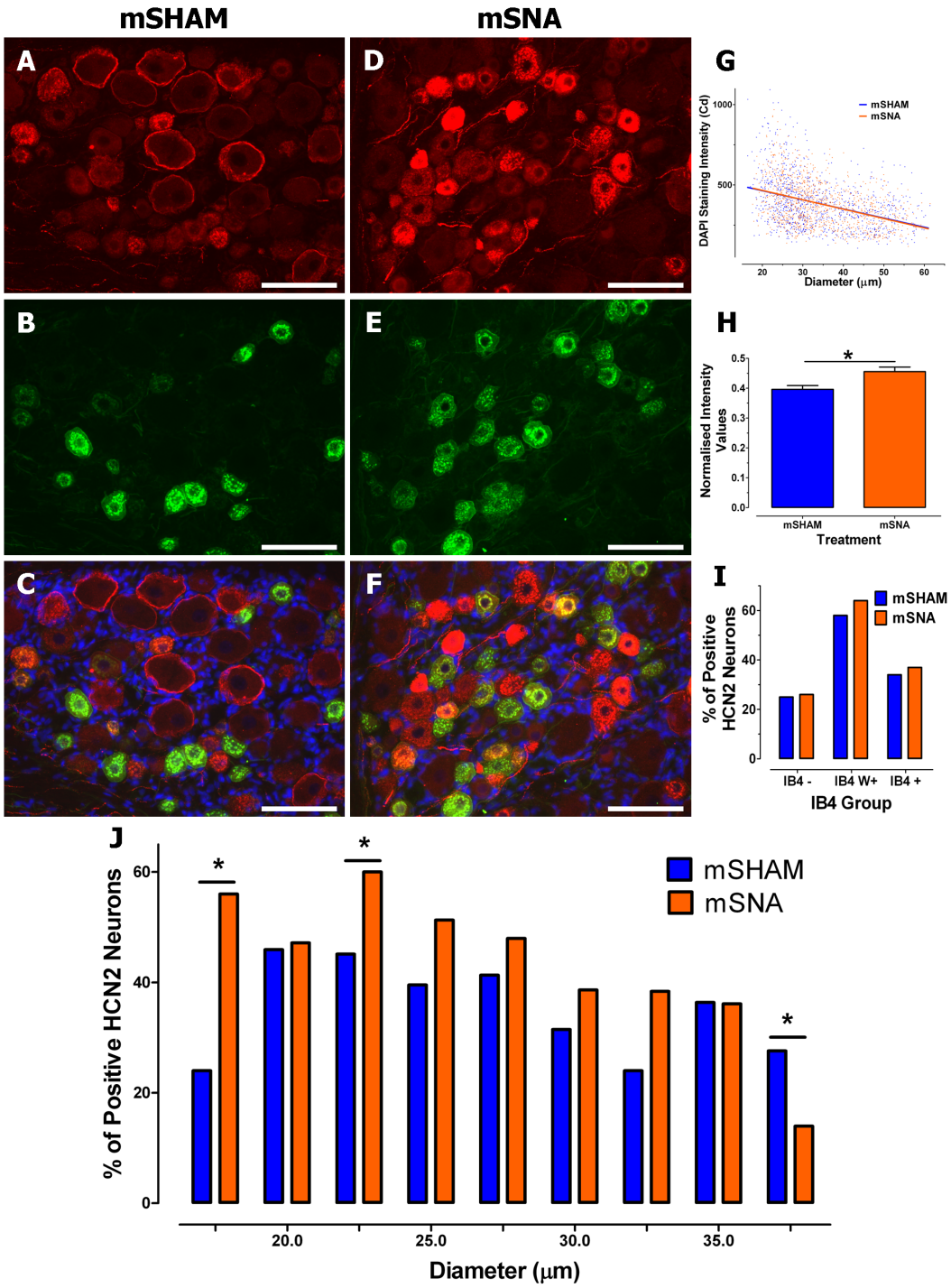

Figure 5.11: HCN2-IR in L4 DRG Neurons from the mSNA Model of NP after 7-Days Compared to mSHAM. Photomicrographs of DRG tissue from mSHAM [A-C] and mSNA [D-F], immunolabelled with HCN2 [A,D], IB4 [B,E], and the two images overlayed [C,F]. HCN2-IR is expressed mainly in small, $IB4^-$ DRG neurons and the membranes of a small subpopulation of large DRG neurons. The staining intensity of DAPI [G] is used as a control, showing no difference in staining between mSHAM, in blue (*n = 1110 neurons*), and mSNA, in orange (*n = 1043*

neurons). Mean normalised HCN2 values are plotted for mSHAM (*n = 518 neurons*) and mSNA (*n = 419 neurons*) of small DRG neurons, with a diameter < 30 µm, revealing a significant increase, *, following mSNA [H]. These small neurons were compared after being broken into categories according to their IB4 staining: IB4 negative, $IB4^-$; IB4 weakly positive, $IB4^{w+}$; IB4 positive, $IB4^+$ [I]. The percentage of $HCN2^+$ small and medium sized mSHAM (*n = 814 neurons*) and mSNA (*n = 752 neurons*) DRG neurons were compared at different diameters [H]. Scale bars [A-F] represent 100 µm. Statistics were performed using the Mann Whitney U test [H-I] and Fisher's Exact test [J]: *, $p < 0.05$.

5.3.3.3. HCN3 in DRG

In this rodent model of CNP, both HCN3-IR and IB4-IR revealed similarities in the inter-cellular staining profile between control [Fig. 5.3.A-C] and mSHAM tissue [Fig. 5.12.A-C] and this did not change following the induction of the mSNA model [Fig. 5.12.D-F]. The DAPI stain revealed no difference between the two methodologies for each treatment group [Fig. 5.12.G]. The plot of the normalised intensity of HCN3 against IB4 [Fig. 5.12.H] revealed no difference from control tissue. Finally, small DRG neurons did not reveal any significant differences [Fig. 5.12.I] and after categorising the DRG neurons by their diameter [Fig. 5.12.J], there were still no significant differences.

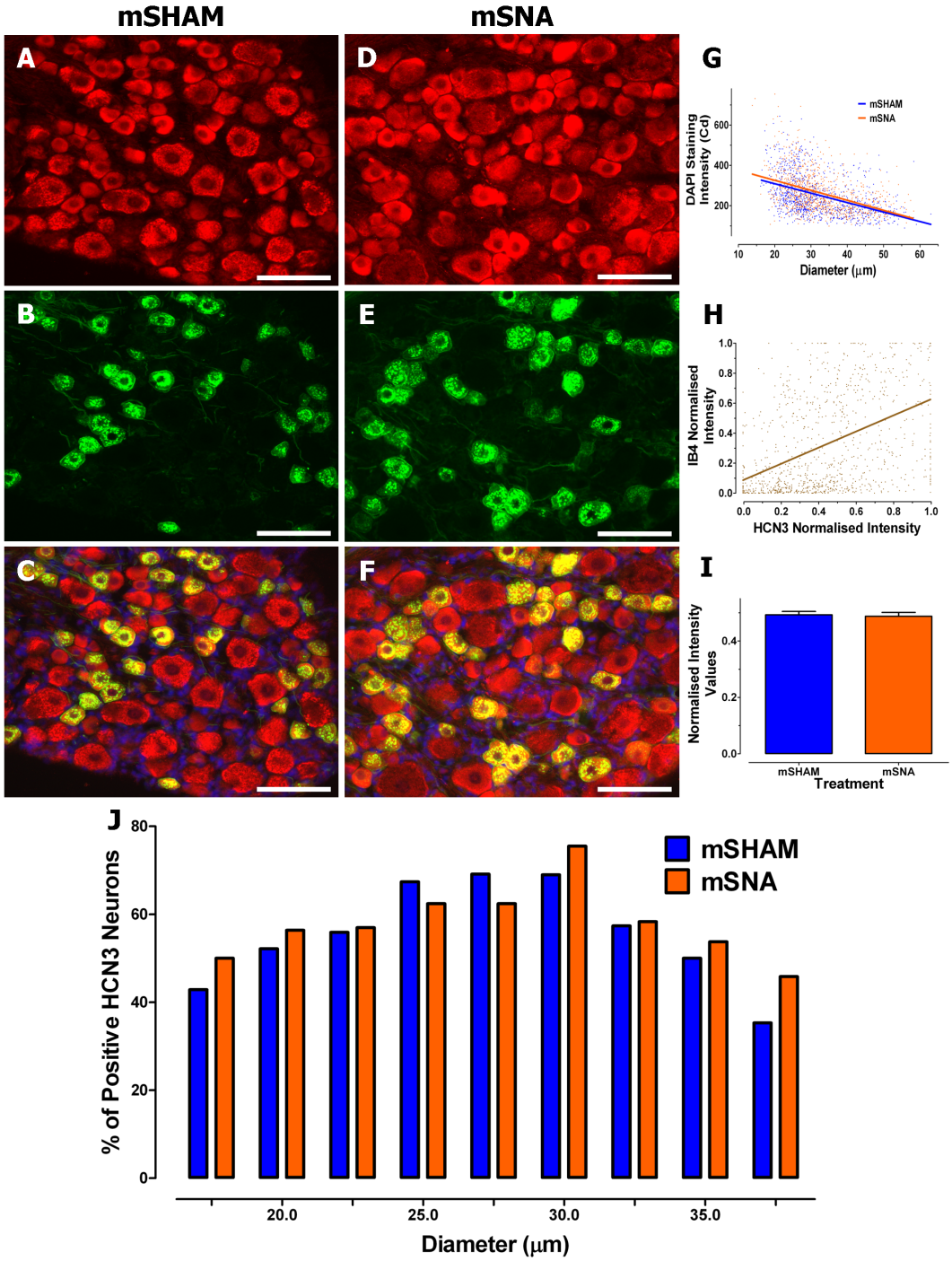

Figure 5.12: HCN3-IR in L4 DRG Neurons 7-Days after Induction of the mSNA Model of NP Compared to mSHAM. Photomicrographs of DRG tissue from control [A-C] and CFA [D-F], immunolabelled with HCN3 [A,D], IB4 [B,E], and the two images overlayed [C,F], showing no obvious differences in HCN3-IR. The staining intensity of DAPI [G] is used as a control, showing no difference in staining between mSHAM, in blue (*n = 1064 neurons*), and mSNA, in orange (*n = 943 neurons*). Normalised HCN3 is plotted against normalised IB4 [H] to explore

the co-localisation relationship. Mean normalised HCN3 values are plotted for mSHAM (*n = 579 neurons*) and mSNA (*n = 449 neurons*) of small DRG neurons, with a diameter < 30 µm [I]. The percentage of $HCN3^{+}$ small and medium sized mSHAM (*n = 836 neurons*) and mSNA (*n = 714 neurons*) DRG neurons were compared at different diameters [H]. Scale bars [A-F] represent 100 µm. Statistics used the Mann Whitney U test [I] and Fisher's Exact test [J]

5.4. Discussion

5.4.1. Summary

Cumulatively, this immunofluorescent data, showing the expression of HCN1-3 in DRG neurons during states of CP, supports and strengthens the majority of the literature, while adding a previously unpublished observation: the increase in the percentage of $HCN2^{+}$ DRG neurons in rodent models of CP, both CIP and CNP. HCN2, and not HCN1 or HCN3, appears to experience a change in inter-cellular expression profile and this occurs all along the neuron in the axonal fibres and possibly the central terminals. Furthermore, the importance of the HCN2 channel subunit is reinforced by another study that used genetic knock-out techniques to remove HCN2 from $Na_v1.8^{+}$ nociceptors and this subsequently abolished SA from cultured, nociceptive DRG neurons, as well as returning both heat and mechanical sensitivies to normal levels in mouse models of CIP and CNP (Emery *et al.*, 2011).

5.4.2. Previous Studies Examining HCN Expression in DRG Neurons

The expression of HCN1-3 expression in various neurons, particularly DRG neurons, has been widely explored, using both these, and other, antibodies. Unfortunately, not all of the results have corroborated one another [Tab. 5.1].

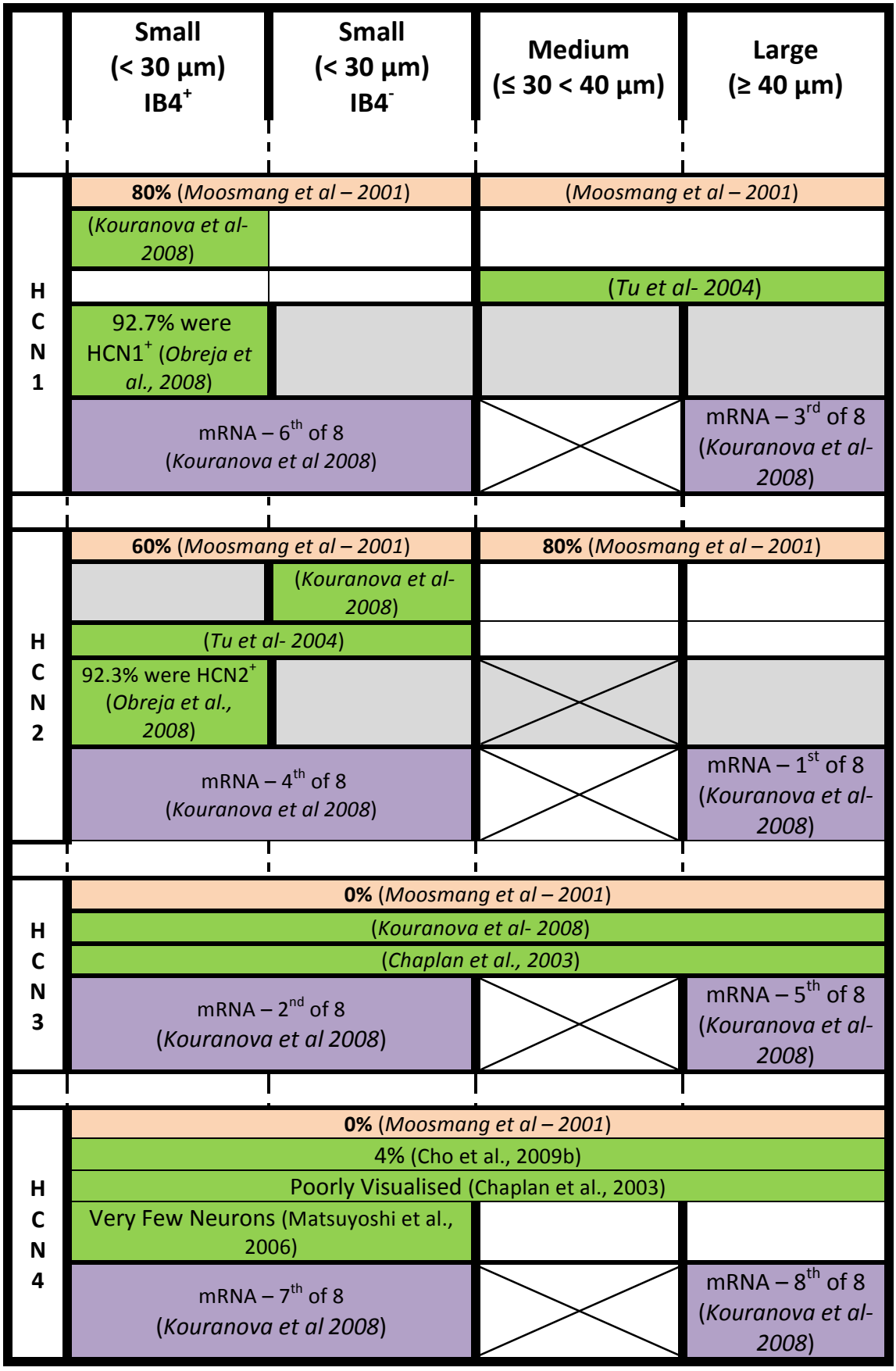
Small (< 30 µm) IB4+
Small (< 30 µm) IB4-
Medium (≤ 30 < 40 µm)
Large (≥ 40 µm)
HCN1
80% (Moosmang et al – 2001)
(Moosmang et al – 2001)
(Kouranova et al- 2008)
(Tu et al- 2004)
92.7% were HCN1+ (Obreja et al., 2008)
mRNA – 6th of 8 (Kouranova et al 2008)
mRNA – 3rd of 8 (Kouranova et al- 2008)
HCN2
60% (Moosmang et al – 2001)
80% (Moosmang et al – 2001)
(Kouranova et al- 2008)
(Tu et al- 2004)
92.3% were HCN2+ (Obreja et al., 2008)
mRNA – 4th of 8 (Kouranova et al 2008)
mRNA – 1st of 8 (Kouranova et al- 2008)
HCN3
0% (Moosmang et al – 2001)
(Kouranova et al- 2008)
(Chaplan et al., 2003)
mRNA – 2nd of 8 (Kouranova et al 2008)
mRNA – 5th of 8 (Kouranova et al- 2008)
HCN4
0% (Moosmang et al – 2001)
4% (Cho et al., 2009b)
Poorly Visualised (Chaplan et al., 2003)
Very Few Neurons (Matsuyoshi et al., 2006)
mRNA – 7th of 8 (Kouranova et al 2008)
mRNA – 8th of 8 (Kouranova et al- 2008)

Table 5.1: A Compilation of Previously Reported Studies Looking at the Expression of HCN Channel Subunits in DRG Neurons. This table shows a synopsis of studies looking at the expression levels of HCN channel subunits in different sizes of DRG neurons using a variety of direct or indirect techniques: Immunofluorescence, in green; In Situ Hybridisation, in pink; and Northern Blot, in purple.

5.4.3. HCN2

5.4.3.1. HCN2 in the Cell Body of the DRG Neurons

HCN2's staining profile in both models of CP reveals significant increases in small C-fibre, primarily $IB4^-$, DRG neurons and particularly in the percentage of $HCN2^+$ small and medium sized DRG neurons. This appears to be due to either: 1) *de novo* protein synthesis in a sub-population of DRG neurons, possibly nociceptors that are normally silent; or 2) increased expression in previously either $HCN2^{w+}$ or $HCN2^-$ DRG neurons.

Despite the majority of $HCN2^+$ DRG neurons being $IB4^-$, the CP induced increase in $HCN2^+$ DRG neurons occurred across all populations of IB4. IB4 is a marker of a subpopulation of non-peptidergic neurons, predominantly nociceptors (Stucky and Lewin, 1999). Furthermore, IB4 is found in different subpopulations of nociceptor, including a population of potentially heat sensitive $TRPV1^+$ DRG neurons (Obreja *et al.*, 2008). In addition, amongst the $IB4^+$, but $TRPV1^-$, DRG neurons there is a class that express G protein-coupled receptors belonging to the Mrg family, with members such as MrgA, which are localised in specific sup-populations of DRG neurons (Dong *et al.*, 2001). Furthermore, another subtype, Mrgprd, specifically innervate the stratum granulosum layer of the epidermis, indicating the spatial segregation of peptidergic and non-peptidergic DRG neurons (Zylka *et al.*, 2005) and their different neuro-anatomical pathways to the brain (Bráz *et al.*, 2005). Therefore, this provides evidence for the high degree of specialisation amongst the numerous different sub-types of DRG neurons.

5.4.3.2. HCN2 in Axonal Fibres of DRG Neurons

Protein synthesis occurs in the DRG and is translocated along axonal fibres to control the neuron's excitatory properties (Perry and Wilson, 1981). After CFA, there is an increase in HCN2 in the axonal fibres and this supports evidence that in control tissue, HCN2 stains the axelomma, or the cell membrane surrounding the axon, of c-fiber DRG neurons (Jiang *et al.*, 2008). In addition, at the terminals of DRG neurons, both HCN2 and HCN1 was expressed in Meissner's corpuscles, a type of **R**apidly **Adapt**ing {RAdapt} **L**ow-**T**hreshold **M**echanoreceptor {**LTM**}, and furthermore, HCN2 was also expressed in nerve fibres of the dermal layer, presumably c-fibre nociceptors (Luo *et al.*, 2007).

5.4.3.3. HCN2 in the Dorsal Horn of the Lumbar Enlargement

The $HCN2^{+}$ staining in peptidergic neurons in the outer laminae of the dorsal horn in the spinal cord's lumbar enlargement corroborates previous findings (Matsuyoshi *et al.*, 2006). Our study, at 7-d post-CFA, supported the finding that, at 3-d post-CFA, HCN2 increases in peptidergic, $SubP^{+}$ (Papp *et al.*, 2010) and $CGRP^{+}$ (Antal *et al.*, 2004), but $IB4^{-}$ (Antal *et al.*, 2004), neurons located in lamina I-IIo of the spinal dorsal horn. The observed increased in a peptidergic population of neurons in the ipsilateral side of the dorsal horn is not a novel post-inflammation observation (Papp *et al.*, 2010), but it is novel at this time-point.

Although these results alone can not determine if this increase in HCN2 is at the terminals of DRG neurons, 2^{nd} order neurons, or interneurons, there is evidence using both fluorescence and electron microscopy (Antal *et al.*, 2004), in addition to electrophysiology (Takasu *et al.*, 2010) that this staining in the dorsal horn of the spinal cord consists primarily of the axon terminals of DRG neurons. This is supported by the absence of HCN2 staining in the dorsal horn following dorsal rhizotomy of the L2-S1 segment (Antal *et al.*, 2004).

5.4.3.4. Cumulative Importance of HCN2's Results

The increase in HCN2 could be responsible for the electrophysiological changes that occur following CIP (Weng *et al.*, 2012): 1) the increase in % of neurons with I_h > 200 pico-amps, with 15.1% in control against 50% post-CFA; and 2) the increase in I_h current amplitude and density observed in C-fibre nociceptors. These electrophysiological changes in I_h may correlate to the increase in C-fibre DRG neurons that show SA, with 25% and 35% of conducting c-fibre units, with their receptive fields intact displayed SA at 4-d post-CFA and 7-d post-mSNA (Djouhri *et al.*, 2006).

Currently, it is not clear which somatosensory types of these conducting DRG neurons are experiencing this change in the HCN2, as there is evidence that although it is pre-dominantly C-fibre DRG neurons that are responsible for the barrage of activity from the periphery, many different types of DRG neurons show an increase in SA (Djouhri *et al.*, 2006). In particular, HCN2 has been implicated in $Na_v1.8^+$ small neurons in SA caused by the presence of forskolin, an inflammatory mediator that raises cAMP concentrations, using knock-out techniques and *in vitro* electrophysiology (Emery *et al.*, 2011).

5.4.4. HCN1 and HCN3

5.4.4.1. HCN1 and HCN3 in the Cell Bodies of DRG Neurons

In control DRG neurons, these results matched the established expression profiles that show HCN1 has been reported in the membranes of large DRG neurons, showing ring staining, while HCN3 has been reported to show an intra-cellular staining profile in all sizes of DRG neurons (Biel *et al.*, 2009). During states of CIP and CNP, the only change involved a significant increase in HCN1 in small DRG neurons following CNP. However, the control for this comparison, DAPI, also showed drastic differences between the two treatment groups.

To examine the physiological role of HCN1 in somatosensation, a global HCN1 knock-out only revealed a phenotype displaying hypersensitivity to cold temperatures following a partial sciatic nerve ligation model of NP (Momin *et al.*, 2008). The excitability of cold-sensitive DRG neurons is affected by I_h, which is largely driven by HCN1 (Orio *et al.*, 2009). The role of HCN1 in large DRG neurons appears to be expressed in LTMs, as it has been seen in the terminals of what are suspected Meissner's corpuscles, a subtype of RAdapt DRG neuron, and Merkel disc complexes, a subtype of **s**lowly **adapt**ing {**SAdapt**} (Luo *et al.*, 2007). HCN3, which is neuronal specific (Stieber *et al.*, 2005), did not show any changes in either model and this subunit could be responsible for the contributing to various permutations of hetero-tetramers. Furthermore, this subunit is possibly responsible for the slow-gating I_h in small DRG neurons (Kouranova *et al.*, 2008).

5.4.4.2. HCN1 and HCN3 in Axonal Fibres of DRG Neurons

In the axonal fibres, neither HCN1 nor HCN3 showed a staining profile in control or following CIP. Other studies have shown that HCN1 stains the axelomma in A-fibres, which contrasts HCN2's staining of C-fibre axelommas (Jiang *et al.*, 2008).

5.4.5. Dimerisations of HCN Subunits

The 4 HCN channel subunits form tetramers to create functional ion channels and different permutations of HCN channel subunits may occur during CP. Homo-tetramers possess profoundly different activation kinetics in model cell systems (Ludwig *et al.*, 1998; Santoro *et al.*, 1998; Ishii *et al.*, 1999; Ludwig *et al.*, 1999; Seifert *et al.*, 1999), but there is also evidence that hetero-tetramers are formed *in vivo*, both in the brains of mice (Much *et al.*, 2003) and in the heart, where it is essential for cardiac pacing (Xue *et al.*, 2002; Er *et al.*, 2003). One common permutation involves HCN1/HCN2 subunits (Brewster *et al.*, 2005) for which there is evidence that a change in stoichiometric proportions is responsible for the changes in activation kinetics (Chen *et al.*, 2001), although by

retaining HCN2, **c**yclic **a**denosine **m**ono**p**hosphate {**cAMP**} sensitivity is preserved (Ulens and Tytgat, 2000; Chen *et al.*, 2001).

Different subunit expression for functional channel formation in various neuronal types is also essential for other ion channel families, such as a wide variety of K^+ channels (Levitan and Takimoto, 1998), with one example being the K_v7 family that relies heavily on $K_v7.2$ and $K_v7.3$ (Hadley *et al.*, 2003). Interestingly, using immunofluorescence to study expression in HEK293 cells, HCN2/3 did not appear to form functional ion channels, which was indicated by reduced electrophysiological current recordings (Much *et al.*, 2003). Although this requires further exploration in DRG neurons *in vivo*, where the integration of subunits and the presence of binding partners is complex.

5.4.6. Intra-cellular Staining Profiles of HCN Channel Subunits

Given the necessity of ion channels to be embedded in the plasma membrane, it was surprising to see such a large amount of protein located intra-cellularly, especially in small neurons. However, this is not the first family of ion channels to reveal this staining pattern in DRG neurons, as it was also seen in the K_v1 family of ion channels: $K_v1.1$, $K_v1.2$, and $K_v1.4$ (Rasband *et al.*, 2001). It is most likely that this pattern of staining is a result of recently synthesized HCN proteins that are being processed through both the rough endoplasmic reticulum and the golgi apparatus on the way to the plasma membrane (Kouranova *et al.*, 2008). Furthermore, it is plausible that there is an incredibly rapid re-location of this protein to the plasma membrane based upon a specific stimulus, as this has been shown with the protein kinase C-ε, which is normally located intra-cellularly, but upon application of bradykinin, localises to the plasma membrane within 5 seconds (Cesare *et al.*, 1999). It is important to remember that IF is an extremely variable technique and only reveals a snapshot of the very dynamic inner workings of the neuron.

5.4.7. Role of Binding Partners in HCN Channel Expression

One important binding partner for the HCN channel subunits is tetratricopeptide repeat-containing Rab8b-interacting protein, which is an accessory subunit that binds to HCN channel subunits in almost a 1:1 ratio (Zolles *et al.*, 2009) and is an important modulator of cell-surface expression and intra-neuronal trafficking (Han *et al.*, 2011; Piskorowski *et al.*, 2011). Interacting with a conserved tripeptide sequence in the C-terminal of HCN channel subunits (Santoro *et al.*, 2004) and also with the cyclic nucleotide binding domain (Bankston *et al.*, 2012), these interactions affect the trafficking of vesicles to their final targets (Zerial and McBride, 2001). Furthermore, the presence of tetratricopeptide repeat-containing Rab8b-interacting protein is suggested to prevent cyclic nucleotides exerting their maximal effect on HCN2 and HCN4 (Lewis *et al.*, 2009; Santoro *et al.*, 2009; Zolles *et al.*, 2009). Another important process for intra-cellular tracking is N-linked glycosylation, which appears to play a critical role in functional HCN ion channel formation, as it is required for normal HCN channel surface expression (Santoro *et al.*, 1997; Much *et al.*, 2003).

5.4.8. Role of Glial Cells

Glial cells play an important role in maintaining the nervous system and in the PNS, a specific type of glial cell, Schwann cells, forms myelin, ensheathes synaptic junctions and bundles small diameter neurons together (Fields and Stevens-Graham, 2002). This is interesting, as HCN1 and HCN2 staining on large DRG neurons might have also been partly due to IR in the Schwann cells that surround the DRG neurons. However, confocal scanning microscopy showed that HCN1 and HCN2 did not co-localise with glial fibrillary acidic protein, a marker of glial cells (Cho *et al.*, 2009a). However, there is increasing evidence that glial cells maintain the environment around neurons of both the PNS and the CNS and their signalling roles include regulating ion fluxes, neurotransmitters, cell adhesion molecules, and specialised signalling molecules (Fields and Stevens-Graham, 2002), all of which can affect DRG neuronal excitability. Furthermore,

stimulation of efferent, motor neurons, which emanate from the CNS to control muscles, causes Ca^{2+} responses in a specialised type of terminal Schwann cell (Reist and Smith, 1992; Lev-Ram and Ellisman, 1995) and this could be done through the release of prostaglandins (McMahon *et al.*, 2005b). This same mechanism could act on nociceptors, when a number of pro-inflammatory prostaglandins are present.

Chapter 6: Discussion

6.1. Contribution of This Thesis

6.1.1. Summary of Results

Chronic **p**ain {**CP**} is a difficult disease to treat, partly because the underlying mechanisms are poorly characterised. In cases of peripheral injury, the increased excitability of **d**orsal **r**oot **g**anglion {**DRG**} neurons is believed to play a critical role (Costigan *et al.*, 2009). The underlying ionic and molecular mechanisms of DRG neuronal hyperexcitability are variable and not thoroughly understood (Hehn *et al.*, 2012). Therefore, there is a pressing need to understand the pathophysiological processes so that alleviative treatments can be developed. The main aim of the present research was to test the hypothesis that the **h**yperpolarisation-activated **c**yclic **n**ucleotide-gated {**HCN**} ion channel subunits, of which there are four {**HCN1-4**}, are involved in the pathophysiology of **c**hronic **i**nflammatory **p**ain {**CIP**} and **c**hronic **n**europathic **p**ain {**CNP**}. The HCN channels are tonically active near the resting membrane potential {$\mathbf{E_m}$} and mediate the hyperpolarisation-activated current {$\boldsymbol{I_h}$}, which, if increased, could be responsible for the increased number of **a**ction **p**otentials {**AP**}. Therefore, changes in the expression or function of HCN1-4 may render DRG neurons more excitable, which is observed during CP states. To test the hypothesis, two rodent models of CP were subjected to three different techniques: 1) behavioural pharmacology; 2) *in vivo* electrophysiology; and 3) immunofluorescence. Each finding supports the role of the HCN channels in CIP and CNP. Furthermore, immunofluorescent data indicated that HCN2 appears a promising target for a novel analgesic.

6.1.2. Behavioural Tests

The behavioural tests revealed that intra-plantar administration into the ipsilateral hindpaw of ZD7288, a selective blocker of I_h, significantly reversed mechanical hypersensitivity and alleviated **s**pontaneous **p**ain {**SP**} in rodent models of CIP and CNP. ZD7288 showed a non-significant reversal of heat

hypersensitivity in the **m**odified **s**pinal **n**erve **a**xotomy {**mSNA**} model of CNP, but not in the **c**omplete **F**reund's **a**djuvant {**CFA**} model of CIP. The site of action of ZD7288 was believed to be the terminals of the un-injured DRG neurons with their receptive fields intact, because contralateral injections of the compound had no effect on pain hypersensitivity in the ipsilateral hindpaw.

6.1.3. *In Vivo* Electrophysiology

Recording intra-cellularly from ipsilateral L4 DRG neurons with receptive fields intact in the mSNA model of NP showed that Aα/β-fibre DRG neurons, particularly **h**igh-**t**hreshold **m**echanoreceptor {HTM} nociceptors, exhibited a significant decrease in the **a**fter-**h**yper**p**olarisation **a**mplitude {**AHPA**}. This change in AHPA could explain the mSNA-induced mechanical hypersensitivity. 7-**d**ays {**d**} post-mSNA in the L4 DRG neurons, blocking I_h in a few Aα/β-fibre **l**ow-**t**hreshold **m**echanoreceptors {**LTM**} had no effect on their rate of **s**pontaneous **a**ctivity {**SA**}.

6.1.4. Immunofluorescence

In CIP this increase in HCN2 is also seen in the dorsal horn of the spinal cord, most likely at the terminals of the DRG neurons, implying that this increase in HCN2 is along all parts of the neuron. HCN4 was not examined due to problems with the specificity of the antibody. There is an increased percentage of small, putative nociceptive, HCN2 positive {$^+$} DRG neurons in both CIP and CNP. HCN1$^+$ neurons were mostly large DRG neurons showing ring staining, with a population of small, **I**solectin-**B4**$^+$ {**IB4**}, DRG neurons. HCN3 was found in both IB4$^+$ and IB4$^-$ neurons DRG neurons of all sizes. The expression profiles of HCN1 and HCN3 did not change in models of CIP or CNP, although HCN1 increased significantly in sub-populations of DRG neurons following CNP and this significantly increased HCN1 in small DRG neurons. Therefore, this immunofluorescent study strongly implicates HCN2, rather than HCN1 or HCN3, as the critical subunit responsible for enhancing the contribution of I_h in states of CIP and CNP.

6.1.5. Conclusion

Together, these results suggest that HCN2, in specific sub-populations of conducting DRG neurons with their receptive fields still intact may contribute significantly to hypersensitivity associated with CP. Therefore, blocking HCN2 specifically in these subpopulations of DRG neurons, possibly excluding the Aα/β-fibre LTMs, may provide a novel class of analgesics.

6.2. Unifying Cellular Pathway for CIP and CNP

Pain pathophysiology is complex and CP is caused by numerous physiological changes in the nervous system (Basbaum *et al.*, 2009; Costigan *et al.*, 2009), so determining where and how to pharmacologically intervene is a major challenge. Over the past decade there has been increasing evidence for the pivotal role of I_h in controlling the excitability of neuronal cells, particularly DRG neurons, during states of CP (Chaplan *et al.*, 2003; Biel *et al.*, 2009), and HCN2 could be the subunit responsible (Emery *et al.*, 2011; Weng *et al.*, 2012). Until recently, the cellular mechanism that implicates HCN2 in both CIP and CNP has not been described, although both seem to be partly driven by increased **p**rostaglandin **E_2** {**PGE_2**} (Emery *et al.*, 2012). It is critically important to understand cellular pathways so novel analgesics will not be compromised by adverse side effects.

6.2.1. Macrophages

Macrophages are physiologically important for the body's defence and in states of CP, macrophage activation and recruitment occurs at both sites of inflammation (Nathan, 2002) and nerve injury (Scholz and Woolf, 2007) around the affected DRG neurons (Stoll *et al.*, 1989). Macrophages, which are also present in human conditions of neuropathy (Said and Hontebeyrie-Joskowicz, 1992), serve important physiological roles to aid healing, particularly during

Wallerian degeneration, by controlling pathogens and digesting cellular debris (Perry *et al.*, 1987; Watkins and Maier, 2002).

In states of **i**nflammatory **p**ain {**IP**} [Fig. 6.1.B], adjuvants, such as **c**omplete **f**reund's **a**djuvant {**CFA**}, activate the toll-like receptors (Aderem and Ulevitch, 2000; Akira *et al.*, 2001; Billiau and Matthys, 2001) and cause monocytes, of which macrophages are a specialised type, to release adenosine tri-phosphate (Piccini *et al.*, 2008). *In vivo* studies revealed that adenosine triphosphate binds to the extra-cellular domain (Kawate *et al.*, 2009) of $P2X_4$ receptors on macrophages and, via a **c**yclo**ox**ygenase-**2** {**COX-2**} mediated mechanism, releases PGE_2 (Ulmann *et al.*, 2010). In response to both CFA and carrageenan, mice deficient in $P2X_4$ showed no development of mechanical hypersensitivity, but CFA still produced heat hypersensitivity (Ulmann *et al.*, 2010). Furthermore, the second phase of the behavioural responses induced by formalin was not observed in the $P2X_4$ knock-outs (Ulmann *et al.*, 2010). These results display strong similarities to the behavioural data showed in this thesis and indicate a common cellular pathway.

In **n**europathic **p**ain {**NP**} [Fig. 6.1.C], galectin-1, which is expressed in both a subset of DRG neurons (Regan *et al.*, 1986; Hynes *et al.*, 1990; Horie *et al.*, 1999) and Schwann cells (Horie *et al.*, 2004), is released following nerve injury and peaks at 3-**d**ays {**d**} post-axotomy (Gaudet *et al.*, 2009). Galectin-1 activates macrophages and promotes axonal regeneration (Horie *et al.*, 1999) through a macrophage-exclusive mechanism (Horie *et al.*, 2004). Around the injured nerves in these recruited macrophages, whose absence delays Wallerian degeneration (Bisby and Chen, 1990), COX-2 is dramatically up-regulated (Ma and Eisenach, 2002). This macrophage recruitment is facilitated by the breakdown of the blood-nerve barrier, which occurs within 48 hours and lasts for a prolonged period of time: beyond 14 weeks in a rodent NP model involving nerve transection (Bouldin *et al.*, 1991). Although these changes are driven by injured DRG neurons, adjacent DRG neurons, whose receptive fields are intact, become susceptible to these inflammatory mediators that are released to aid axonal

regeneration of the injured DRG neurons (Li *et al.*, 2000; Thacker *et al.*, 2007; Gaudet *et al.*, 2011).

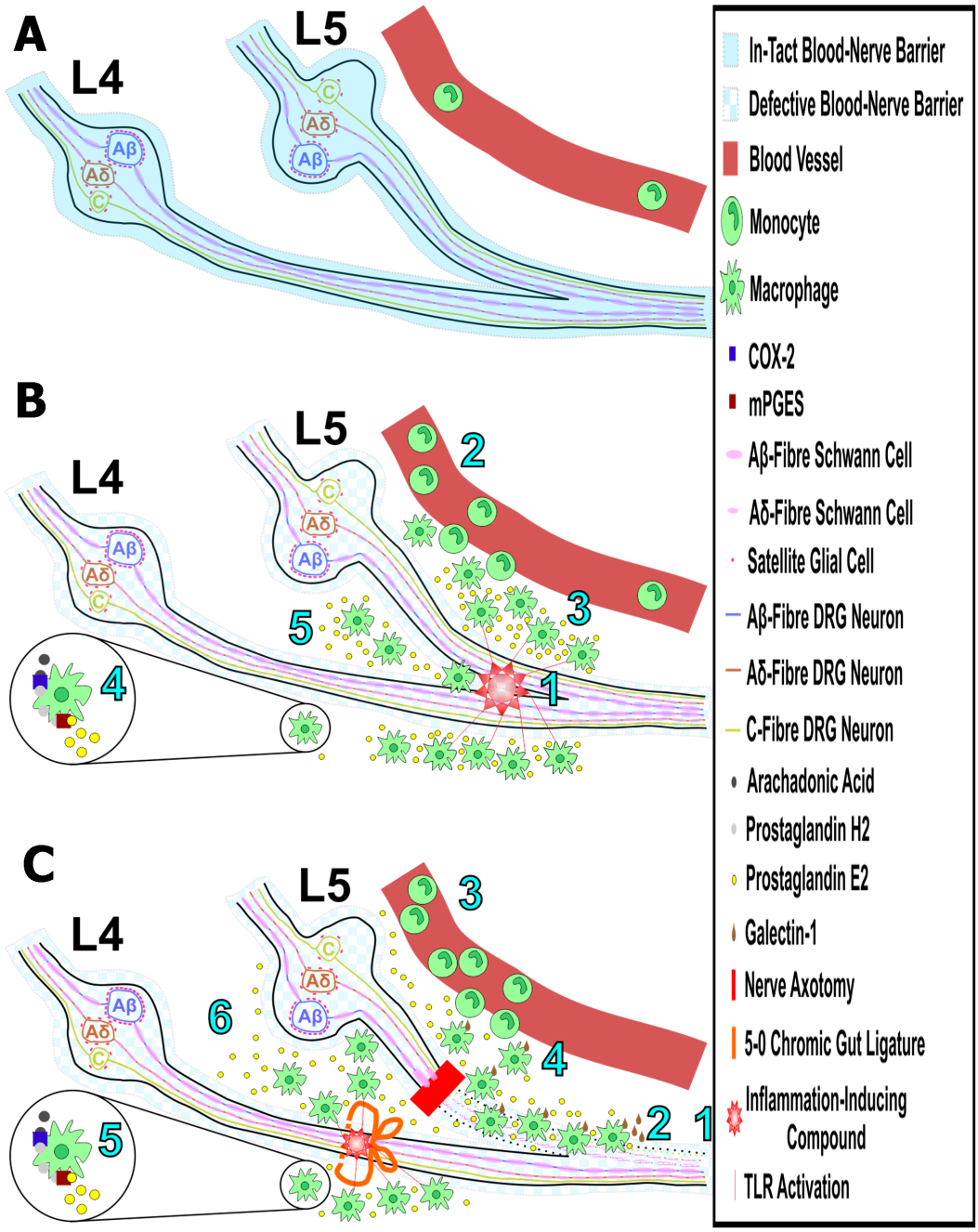

Figure 6.1: Common Cellular Responses of CIP and CNP. [A] This schematic diagram shows the normal conditions around the L5 and L4 DRG neurons, with the blood-nerve barrier still intact. [B] Following inflammation, macrophages are recruited through activation of toll-like receptors and the release of adenosine triphopshate, ATP, that acts on PGX_4 receptors on macrophages and they are

shown by the thin red lines. Through COX-2, arachadonic acid is converted to PGH_2 and then through PGES, PGH_2 is converted to PGE_2. [C] Following nerve injury, galectin-1 is released from the injured nerve and recruited due to neuro-inflammation in response to the loose chromic gut ligature, which also contributes to the recruitment of macrophages that produce PGE_2 via the COX-2 mediated pathway.

6.2.2. Cyclooxygenase-2

In these recruited macrophages and native Schwann cells (Takahashi *et al.*, 2004), but not DRG neurons (Broom *et al.*, 2004; Amaya *et al.*, 2009), there is a potent, but local, induction of COX-2 (Vane *et al.*, 1998). In models of NP, COX-2 up-regulation persists for years in humans and months in rats (Durrenberger *et al.*, 2006). The physiological role of COX-2 involves converting arachadonic acid to Prostaglandin H_2, which is converted to a different prostanoid, such as PGE_2, depending upon the type of prostaglandin synthase enzyme (Vane *et al.*, 1998).

6.2.3. Microsomal Prostaglandin E2 Synthase

PGE_2 is biologically activated from its precursor by three distinct PGE synthases (Hara *et al.*, 2010), one of which, microsomal PGE Synthase 1, has been implicated in the inflammatory cascade associated with both NP (Mabuchi *et al.*, 2004) and normal pain responses (Trebino *et al.*, 2003), resulting in antagonists being explored for their therapeutic value (Samuelsson *et al.*, 2007). Microsomal PGE Synthase 1 antagonists need to be carefully reviewed (Koeberle and Werz, 2009) as they may have un-desired side effects, such as impaired healing of bone fractures (Yamakawa *et al.*, 2008).

6.2.4. Prostaglandin E2

PGE_2 is a potent pro-inflammatory mediator that functions in an autocrine and paracrine fashion (Hamberg and Samuelsson, 1971) with a self-sustaining feedback loop, which could explain the persistent and maladaptive nature of CP (Díaz Muñoz *et al.*, 2012) since post-inflammation levels rise several-fold in affected regions (Jakobsson, 2010). PGE_2 has a half life of about 30 seconds, probably due to the compound's potent ability to increase neuronal excitability (Funk, 2001).

COX-2 and the resulting PGE_2 released around injured nerves can last for up to 18 months after nerve injury and maintains NP (Ma *et al.*, 2010). Blocking PGE_2 using a neutralising antibody in models of carrageenan-induced inflammation results in an ablation of both heat hypersensitivity and paw edema (Portanova *et al.*, 1996). PGE_2 evokes different physiological responses by binding to various G-protein coupled receptors known as EP receptors, of which are there are 4: EP1-4 (Sugimoto and Narumiya, 2006). Of these four types, EP2 and EP4 result in increases in intracellular **c**yclic **a**denosine **m**ono**p**hosphate {**cAMP**} (Sugimoto and Narumiya, 2006), while EP1 and EP4 antagonists raise evoked-pain thresholds (Ma *et al.*, 2012). Furthermore, specifically EP3C or EP3B, and not EP3A or EP3D (Namba *et al.*, 1993), could also be responsible for the rise in intracellular cAMP (Southall and Vasko, 2001).

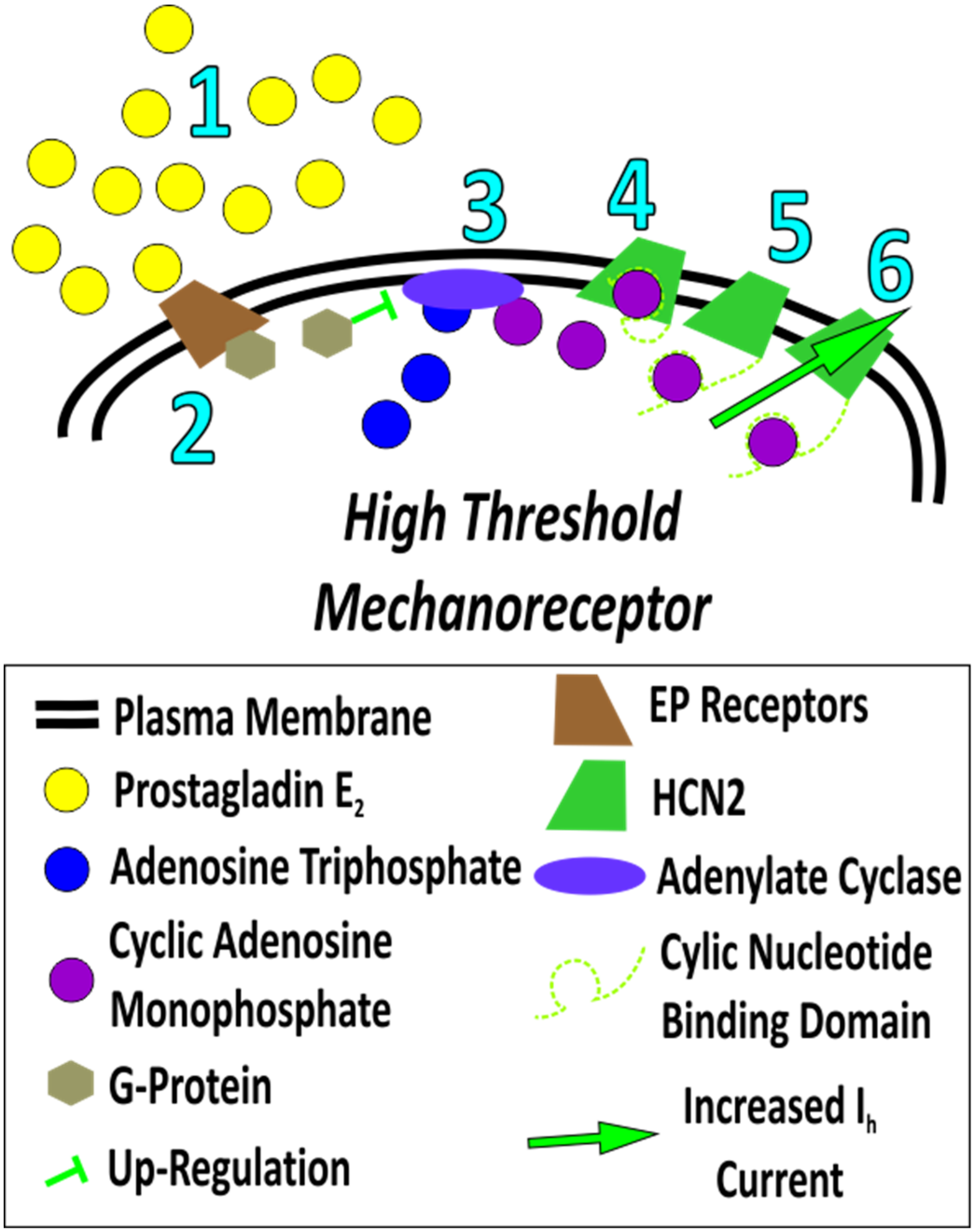

Figure 6.2: Possible Mechanism for the Effect of Prostaglandin E_2 on HCN2 in High Threshold Mechanoreceptors. PGE_2 acts on high threshold mechanoreceptors probably via an HCN2-driven mechanism. PGE_2 binds to EP receptors, resulting in increased activity of adenylate cyclase to convert adenosine triphosphate to cAMP. cAMP then binds to the cyclic nucleotide binding domain to remove the tonic inhibition of HCN2, resulting in a channel that is more active and results in less hyperpolarisation.

PGE_2 may mediate both mechanical and thermal hypersensitivity in specific DRG neuronal populations using different cellular pathways. The behavioural test results supports the role of different sub-populations of nociceptors being responsible for mechanical and thermal hypersensitivity (Lawson *et al.*, 2008; Cavanaugh *et al.*, 2009; Gold and Gebhart, 2010).

Heat hypersensitivity, in CIP and CNP, was not significantly reversed by ZD7288, although there was a reversal trend in CNP and this indicates that the I_h current in DRG neurons with receptive fields intact only plays a minor role in heat hypersensitivity. Therefore, PGE_2 may act indirectly through a specific **t**ransient **r**eceptor **p**otential {**TRP**} channel subunit, TRPV1, which is found in small- and medium-sized DRG neurons, as TRPV1 is essential for complete development of inflammatory thermal hypersensitivity (Caterina *et al.*, 2000; Davis *et al.*, 2000; Gavva *et al.*, 2005; Cui *et al.*, 2006). One proposed pathway may involve PGE_2-dependent activation of protein kinase A anchoring to TRPV1 due to the presence of A-Kinase anchoring protein 150 (Schnizler *et al.*, 2008; Brandao *et al.*, 2011). Furthermore, other TRP channel subunits, such as TRPV4, may also be responsible for heat hypersensitivity (Chen *et al.*, 2007).

Finally, PGE_2 serves important physiological functions in other regions of the body (Koeberle and Werz, 2009) and plays a role in helping the healing of various types of inflammation, such as allergy-induced inflammation (Kunikata *et al.*, 2005). Therefore, a synthetically produced PGE_2 antagonist at EP receptors may not alleviate CP without un-desirable side effects.

6.2.5. Adenylate Cyclase

Both PGE_2 and forskolin raise intracellular cAMP via adenylate cyclase activation (Seamon *et al.*, 1981). EP1 and 4 are G-Protein coupled receptors that are both up-regulated during the partial sciatic nerve ligation model of NP (Ma and Eisenach, 2003) and these receptors act via two different mechanisms to activate cAMP from adenosine tri-phosphate (Sugimoto and Narumiya, 2006). The EP1

mediated mechanism is thought to involve a currently un-identified G-protein that relies on **ca**lcium {$\mathbf{Ca^{2+}}$} (Sugimoto and Narumiya, 2006), while EP4 activation results in increased adenylate cyclase activity that directly converts adenosine triphosphate to cAMP (Wise, 2006). Furthermore, global knock-out of adenylate cyclase 5 inhibits the analgesic effects of morphine (Kim *et al.*, 2006).

6.2.6. Cyclic Adenosine Monophosphate

As a result of the activity of adenylate cyclase, intracellular cAMP within DRG neurons is raised and this could be the end-mediator of PGE_2-induced hypersensitivity (Cui and Nicol, 1995). Treating neurons with an adenylate cyclase inhibitor abolished prostaglandin induced increases in intracellular cAMP (Hingtgen *et al.*, 1995). PGE_2-induced hypersensitivity may produce varying degrees of involvement of I_h in the distinct pathways that are responsible for two types of hypersensitivity: mechanical (Kaupp and Seifert, 2001) and heat, which predominantly relies on capsaicin-sensitive currents (Lopshire and Nicol, 1998).

The chronic compression model of NP reported an increase in cAMP, and a related cyclic nucleotide, cyclic guanosine monophosphate (Song *et al.*, 2006). Furthermore, this hyperexcitability in DRG neurons following chronic compression is maintained by the presence of cAMP and cGMP (Zheng *et al.*, 2007). This enhanced neuronal activity may be mediated by cAMP's effects on the HCN channels and preventing the firing of these conducting, intact neurons in NP may result in CNP not developing (Wu *et al.*, 2001).

6.3. HCN Channel Modulation

The HCN channels are modulated by a variety of biological mediators (Biel *et al.*, 2009). In particular, HCN2 is sensitive to cAMP, whose presence produces a 20 **m**illi-**v**olt {**mV**} shift in the activation kinetics of HCN2 to more positive voltages (Wainger *et al.*, 2001). Furthermore, cAMP has a minimal effect, a few mVs, on

HCN1 and HCN3, whose activation kinetics are shifted slightly positively and negatively respectively (Kaupp and Seifert, 2001; Wainger *et al.*, 2001), making them less likely candidates to be affected by inflammatory mediators in either type of CP.

Another modulator of the activity of HCN channel subunits is **p**hosphatidyl**i**nositol 4,5,-bis**p**hosphate {**PIP_2**}, which shifts the activation voltage to more positive voltages with HCN2 affected by 20 mV (Zolles *et al.*, 2006), allowing activation at physiologically-relevant membrane voltages (Biel *et al.*, 2009). Furthermore, there is evidence that inflammatory heat hypersensitivity is partially mediated by PIP_2's effects on A-Kinase anchoring protein 150 (Jeske *et al.*, 2011).

PIP_2 concentration levels influence a vast array of ion channel subunits (Gamper and Shapiro, 2007; Suh and Hille, 2008), notably the TRP family (Hardie, 2003), and could contribute to the development of CP. In addition, PIP_2 is essential for the K_v-mediated M-current (Zhang et al., 2003) as the presence of PIP_2 drastically increases the open probability of the K_v7.2-7.4 subunits (Li et al., 2005). Additionally, there is evidence that both Ca_v channels (Hilgemann and Ball, 1996) and the TRP family, particularly TRPV1 (Lukacs et al., 2007), relies on an extremely complex relationship with PIP_2, as TRPV1 is sensitised when PIP_2 is hydrolysed and therefore depleted from the plasma membrane (Prescott and Julius, 2003), although interestingly this same reaction causes inactivation of TRPM7 (Runnels et al., 2002). Furthermore, TRPM8 can be activated solely through administration of PIP_2 (Liu and Qin, 2005). Finally, depleting PIP_2 by knocking out a pre-cursor protein reduced hypersensitivity in rodent models of IP and NP (Sowa *et al.*, 2010).

Finally, nitric oxide, which results in increased intracellular cyclic guanosine monophosphate, contributes to CP, particularly in spinal nociceptive processing (Meller and Gebhart, 1993), but also in the periphery where it plays a role in nociceptor sensitisation (Aley *et al.*, 1998). Like cAMP, but ten-fold less potent,

cyclic guanosine monophosphate also acts on the HCN channel subunits to alter their activation kinetics (Gauss *et al.*, 1998; Ludwig *et al.*, 1998). Two weeks after L5 and L6 SN ligation, nitric oxide synthase activity was increased and this might preclude changes in the **c**entral **n**ervous **s**ystem {**CNS**} (Choi *et al.*, 1996). Nitric oxide has a complex role, as high levels of nitric oxide facilitate cAMP-dependent, PGE_2-induced hypersensitivity, while low levels produce a cyclic guanosine-dependent hypersensitivity (Aley *et al.*, 1998). In addition, nitric oxide offers a neuroprotective role (Thippeswamy *et al.*, 2001). Disruption of neuronal nitric oxide synthase in the CNS attenuates both mechanical and thermal hypersensitivity in a CFA model of IP (Chu *et al.*, 2005). Nitric oxide has important physiological roles and often increases concentrations of cyclic guanosine monophosphate at multiple anatomical locations, although a possible connection to I_h has not been fully established.

6.4. Current Drugs that Alter via I_h

6.4.1. Current HCN Channel Blockers

The current HCN antagonists are I_h-specific, but not HCN-subunit selective (Postea and Biel, 2011). One of the problems with current I_h inhibitors is that patients taking zatebradine, which also inhibits $K_v1.5$ (Valenzuela *et al.*, 1995), complain of visual impairments such as spots of light and increased light sensitivity (Frishman *et al.*, 1995). Ivabradine, a specific blocker of I_h, is a bradycardic agent with a safer profile than zatebradine and other specific bradycardic agents (Thollon *et al.*, 1994). However, patients taking ivabradine still suffer from visual disturbances (Cervetto *et al.*, 2007) probably due to I_h blockade in rod cells, which occurs in mice (Demontis *et al.*, 2009). A further experiment might examine whether or not ZD7288 also affects vision.

6.4.2. Other Drugs that Alter I_h via Secondary Pharmacology

In addition, some commonly prescribed compounds that partially alleviate CP might act through physiological mechanisms involving I_h inhibition: 1) non-steroidal anti-inflammatory drugs; 2) opioids; and 3) anaesthetics.

6.4.2.1. Non-Steroidal Anti-Inflammatory Drugs

There is ample evidence that current pharmacological intervention involves modifying the proposed pathway involving macrophages, COX-2 and PGE_2 production, which further implicates the role of I_h in pain sensation. Non-steroidal anti-inflammatory drugs act on COX-2 (Seibert *et al.*, 1994), but not the constitutive COX-1 (Yaksh *et al.*, 2001). Decreasing the activity of the macrophage-mediated COX-2 has downstream effects that lower the sensitivity of DRG neurons in both IP (Broom *et al.*, 2004) and NP (Ma and Quirion, 2008). Lower concentrations of PGE_2 may reduce cAMP and the corresponding increase in activity of HCN2 (Emery *et al.*, 2012). Current front line treatment for NP involves COX inhibition (Gore *et al.*, 2007) and a significant number of patients self-medicate with non-steroidal anti-inflammatory drugs (Vo *et al.*, 2009).

6.4.2.2. Opioid Receptor Antagonists

Different subtypes of opioid receptors are important for hypersensitivity: δ-subclass involved in mechanical hypersensitivity (McKenzie and Milligan, 1990) and the μ-subclass in heat hypersensitivity (Scherrer *et al.*, 2009). Opioid receptor antagonists typically inhibit adenylate cyclase (Sharma *et al.*, 1977) and subsequently I_h (Ingram and Williams, 1994; 1996). Interestingly, despite being thought to have a CNS-mediated effect, topical application to the affected area of opioid receptor antagonists results in decreased excitability of DRG neurons (Sawynok, 2005) and reduced mechanical and thermal hypersensitivity in the chronic constriction injury of NP in rodents (Martinez *et al.*, 2002). loperamide,

which is a point mu-opioid receptor agonist, also blocks I_h in some types of DRG neurons with a high affinity (Vasilyev et al., 2007).

6.4.2.3. Anaesthetics

Both inhalational (Chen *et al.*, 2005; Budde *et al.*, 2008; Chen *et al.*, 2008) and general (Cacheaux *et al.*, 2005) anaesthetics inhibit I_h and this could mediate their analgesic effect. The inhalational anaesthetics may inhibit HCN2 as HCN1 knock-out mice were still transiently affected by isoflurane (Chen *et al.*, 2008). The general anaesthetic propofol has frequently been associated with bradycardia (Tramèr *et al.*, 1997), which is most likely a result of HCN4 blockade.

6.4.3. Development of a Novel HCN2 Antagonist

As this thesis and other work has shown, the HCN2 subunit appears to be specifically up-regulated in states of CIP (Weng *et al.*, 2012) and CNP. Furthermore, knocking out HCN2 in a specific subset of $Na_v1.8^+$ DRG neurons has a therapeutically beneficial impact on both the hyperexcitability of DRG neurons and hypersensitivity associated with CP (Emery *et al.*, 2011). Therefore, this subunit could be responsible for both the analgesic effects of the I_h blocker and the end-mediator of the macrophage driven COX-2 pathway.

However, drug specificity needs to be improved, as current I_h-specific compounds work in the micro-molar {**µM**}, but not nano-molar {**nM**}, range (Postea and Biel, 2011). Most of the current blockers, including ZD7288 (Shin *et al.*, 2001; Cheng *et al.*, 2007), require intra-cellular access to exert their effects, but extra-cellular binding is preferable and should be aided by the characterisation of the trans-membrane core of HCN channel subunits (Postea and Biel, 2011).

Attempts have been made to develop subunit-specific blockers and these have resulted in HCN1- and HCN4-subunit specific blockers (Melchiorre *et al.*, 2010).

While this is a promising start, HCN4 blockers will primarily provide therapeutic benefits for cardiovascular complications (Biel *et al.*, 2002).

6.4.4. Challenges of Novel Compound Development

The decade long dearth of novel drugs (Scannell *et al.*, 2012) is particularly concerning for patients suffering from CP, as only 30% of NP patients respond to current pharmaceutical treatment (Finnerup *et al.*, 2010). A significant portion of commercially available drugs act on membrane-bound proteins, primarily ion channels or G-Protein coupled receptors (Scholz and Woolf, 2002; Imming *et al.*, 2006). Although new research is providing novel targets, these are not currently reaching the clinic, which is surprising given that the NP pain market is expected to be worth £2.1 billion by 2020 (Nightingale, 2012).

6.4.4.1. Anatomical Location

A significant problem with most analgesics is their adverse side effects (Dworkin *et al.*, 2003), which complicates treatment and outweighs the beneficial effects. This problem is apparent because there are numerous potential targets, as during CP, especially CNP, anatomical, physiological and cytochemical changes occur at different levels of the somatosensory system: 1) Injured DRG neurons; 2) Intact DRG neurons; 3) 2^{nd} order neurons in the dorsal horn of the spinal cord; 4) 3^{rd} order neurons in the brain.

Neurons in these different physiological locations become hyperexcitable, which can be beneficial, as SA from the injured DRG neurons aids the up-regulation of genes that assist axonal regeneration (Mandolesi *et al.*, 2004; Abe and Cavalli, 2008; Rishal and Fainzilber, 2010). However, the physiological role of SA in un-injured DRG neurons with their receptive fields still intact is unclear. Determining exactly where a novel analgesic needs to act is difficult, nonetheless, given the evidence provided in this thesis, it is likely that SA in conducting DRG neurons

with their receptive fields intact needs to be blocked to at least partly alleviate CP by reducing hypersensitivity.

There are extremely complex interactions between the sensory nervous system and the immune system that are essential for healing (Benn and Woolf, 2004; Cafferty *et al.*, 2008; Costigan *et al.*, 2009). In the future, the best analgesic, with the fewest side effects, will target the precise mechanism that drives CP as basal pain thresholds need to remain un-altered, therefore, the specificity of any therapeutic intervention is paramount.

6.4.4.2. Targets other than HCN2

Over the last decade, progress has been made in understanding the physiological mechanisms responsible for pain sensation (Basbaum *et al.*, 2009) and, in particular, the changes that cause CP (Costigan *et al.*, 2009; Hehn *et al.*, 2012). However, this has largely failed to translate into novel analgesics with high profile failures of recent compounds such as a **Sub**stance **P** {**SubP**} antagonist (Patel and Lindley, 2003; Gold and Gebhart, 2010) and TRPV1 inhibitors (Gavva *et al.*, 2008). TRPV1, which despite a wide variety of antagonists in clinical trials (Szallasi *et al.*, 2007), is proving a problematic target (Patapoutian *et al.*, 2009), as antagonists cause a global increases in body temperature (Swanson *et al.*, 2005) that is likely due to modulation of $TRPV1^{+}$ cells in the CNS (Cui *et al.*, 2006; Starowicz *et al.*, 2008).

In addition, TRPA1 antagonists have been examined in rodent models of NP, such as the chronic constriction injury model where they show attenuation of cold, but not mechanical, hypersensitivity (Chen et al., 2011). However, a barrier to compound development is that there are species differences in TRPA1 as rodent and human versions share only 79% homology (Chen and Kym, 2009).

Even though Na_v channel blockers have been shown to reduce the persistent pain associated with CNP (Gold, 2008), these antagonists have encountered

problems (Theile and Cummins, 2011): 1) differences in activation kinetics between rodent and human subunits as human $Na_v1.8$ is less active at the resting membrane potential (Browne *et al.*, 2009); and 2) side effects that preclude usefulness (Campbell and Meyer, 2006).

A new direction may involve epigenetics (Denk and McMahon, 2012), which is growing in importance as the pathophysiological mechanisms behind NP can be different for each individual (Hehn *et al.*, 2012).

6.5. Challenges Facing Researchers of Pain Pathways

6.5.1. Advantages and Disadvantages of Animal Models

Scientific experiments to test hypotheses always require compromise and although animal models of CP are not perfect correlates of human conditions, they are currently the best alternative (Mogil, 2009). Despite successful 'backwards validation', or confirming the analgesic effects of compounds that alleviate hypersensitivity in humans, they have not been very successful in 'forwards validation', or predicting compounds that will show efficacy in humans (Whiteside *et al.*, 2008). This could be due to a number of reasons, including the extent of damage, output measures, and chronicity, which refers to the longer length of suffering in humans, which is ~ 4-5 years, compared to a rodent study, which is ~ 10 weeks (Rice *et al.*, 2008). The symptoms shown in these animal models needs to correlate with what is seen in the clinic (Blackburn-Munro, 2004; Vierck *et al.*, 2008) and pharmacokinetic differences also ought to be considered (Whiteside *et al.*, 2008).

One of the reasons why the underlying mechanisms of CP remain poorly understood is probably due to preclinical and clinical studies that measure different outputs. Indeed, clinical studies usually assess SP, which is the primary complaint of NP patients, whereas most preclinical animal studies focus on measuring the behavioural signs of evoked pain, including both mechanical and

thermal hypersensitivity (Mogil, 2009). An un-successful clinical trial should not instinctively be shouldered by the animal model as other important considerations include: poor clinical-trial design or execution, in addition to the lack of sufficiently sensitive toxicity screens for side effects (Mogil, 2009).

6.5.2. Choice of Methodology

There are still difficulties with classifying the many different types of DRG neurons (Baccaglini and Hogan, 1983), as researchers examining pain pathophysiology would benefit from a standardised, robust method (Jasmin and O'Hara, 2004). Classifying these neurons becomes particularly complicated when markers, such as neuropeptides are used (Hökfelt *et al.*, 1976).

6.5.2.1. *In Vitro* Techniques

Many researchers use *in vitro* studies (Burkey *et al.*, 2004) to record electrophysiological parameters of DRG neurons after inflammation or nerve injury, however, these studies require dissociation of DRG neurons, which produce axotomy-like phenotypes (Kerekes *et al.*, 1997). Identification of the receptive properties and **c**onduction **v**elocities {**CV**} of various types of DRG neurons is not possible in the majority of *in vitro* preparations. One such preparation where this is possible is the isolated skin-nerve preparation that can physiologically identify 16 different types of DRG neuron (Zimmermann *et al.*, 2009). To further complicate the issue, *in vitro* studies require neurons to be grouped, primarily, by their cell body size and this often ignores their important physiological properties as cell body size and phenotype are not reliable correlations (Gold and Gebhart, 2010), exemplified by the fact that 20% of large neurons are nociceptors (Djouhri and Lawson, 2004).

6.5.2.2. *In Vivo* Techniques

In vivo studies are also used to study the electrophysiological properties of DRG neurons (Bessou and Perl, 1969; Schäfers and Cain, 2004). Generally, *in vivo* studies are more apt to physiologically identify and categorise the different types of DRG neurons (Lawson *et al.*, 1997). Additionally, in these preparations, DRG neurons are in their natural environment, which is complex and changes with time during CP states in a way that is currently incompletely understood and therefore cannot be reproduced *in vitro*. For these reasons, it is extremely important to study DRG neurons *in vivo* (Vahle-Hinz and Detsch, 2002).

6.5.3. Plasticity of DRG Neurons

6.5.3.1. Cellular Environment

The extra-cellular environment around the DRG neurons has a pivotal role in determining which factors are present to act on ion channels in the plasma membrane and subsequently, affect excitability. Glial cells, which are responsible for interacting with neurons in both the periphery and CNS (Haydon, 2001), consist of both satellite and Schwann cells in the peripheral nervous system. During states of CP there is evidence that glial cells maintain an environment that contributes to the hyperexcitability of DRG neurons (McMahon *et al.*, 2005b; Scholz and Woolf, 2007; McMahon and Malcangio, 2009). In particular, glial cells release Ca^{2+}, which could be important in the initial stages of pain development, immediately after injury (Jahromi *et al.*, 1992; Reist and Smith, 1992; Rochon *et al.*, 2001). Finally, glial cells have important roles in Wallerian degeneration (Gaudet *et al.*, 2011) and the subsequent axonal regeneration (Fields and Stevens-Graham, 2002; Allodi *et al.*, 2012).

6.5.3.2. Plasticity is a Dynamic Process

Studying pain is particularly challenging as neuronal connections are dynamic (Zucker and Regehr, 2002) especially during the process of neuronal regeneration (Woolf and Salter, 2000), which requires a number of growth factors including neurotrophins (Rishal and Fainzilber, 2010). The presence of neurotrophins also changes neuronal plasticity (Thoenen, 1995) as NGF and BDNF exert their effects on different sub-populations of DRG neurons, both injured and un-injured. While this is beneficial for the injured DRG neurons that need to regenerate, the benefits for the un-injured DRG neurons are harder to discern.

Plasticity in the dorsal horn, which possess a wide range of neurons that are responsible for both excitatory and inhibitory roles, further complicates the already complex neuronal circuitry (Todd, 2010). Although experimental design is continuously improving, these challenges complicate the discovery of novel compounds analgesics to treat CP.

6.6. Final Statement

By continuing to explore and understand the complex interactions that result in the remarkable healing process that the body undertakes when injured, a novel analgesic is closer to being developed. However, during states of CP, there are such a myriad of changes that there may be a multitude of potential therapeutic interventions. Despite this, it appears likely that highly-specific targeting of ion channel subunits, such as the HCN2 channel subunit, that result in hyperexcitability of intact DRG neurons that are normally quiescent in the absence of stimuli, may result in achieving successful analgesia for clinical patients suffering from CP.

Bibliography

Abe, N., and Cavalli, V. (2008). Nerve Injury Signalling. Current Opinion in Neurobiology *18*, 276–283.

Abrahamsen, B., Zhao, J., Asante, C.O., Cendan, C.M., Marsh, S., Martinez-Barbera, J.P., Nassar, M.A., Dickenson, A.H., and Wood, J.N. (2008). The Cell and Molecular Basis of Mechanical, Cold, and Inflammatory Pain. Science *321*, 702–705.

Aderem, A., and Ulevitch, R.J. (2000). Toll-Like Receptors in the Induction of the Innate Immune Response. Nature *406*, 782–787.

Adrian, E.D., and Zotterman, Y. (1926). The Impulses Produced by Sensory Nerve-Endings. The Journal of Physiology *61*, 151–171.

Ahmad, S., Dahllund, L., Eriksson, A.B., Hellgren, D., Karlsson, U., Lund, P.-E., Meijer, I.A., Meury, L., Mills, T., Moody, A., et al. (2007). A Stop Codon Mutation in SCN9A Causes Lack of Pain Sensation. Human Molecular Genetics *16*, 2114–2121.

Akira, S., Tokeda, K., and Kaisho, T. (2001). Toll-Like Receptors: Critical Proteins Linking Innate and Acquired Immunity. Nature Immunology *2*, 675–680.

Akopian, A.N., Sivilotti, L., and Wood, J.N. (1996). A Tetrodotoxin-Resistant Voltage-Gated Sodium Channel Expressed by Sensory Neurons. Nature *379*, 257–262.

Aley, K.O., McCarter, G., and Levine, J.D. (1998). Nitric Oxide Signaling in Pain and Nociceptor Sensitization in the Rat. The Journal of Neuroscience *18*, 7008–7014.

Ali, Z., Ringkamp, M., Hartke, T.V., Chien, H.F., Flavahan, N.A., Campbell, J.N., and Meyer, R.A. (1999). Uninjured C-Fiber Nociceptors Develop Spontaneous Activity and α-Adrenergic Sensitivity Following L6 Spinal Nerve Ligation in Monkey. Journal of Neurophysiology *81*, 455–466.

Allen, J.W., and Yaksh, T.L. (2004). Assessment of Acute Thermal Nociception in Laboratory Animals. In Pain Research, Z.D. Luo, ed. (Totowa, New Jersey: Humana Press), pp. 11–23.

Allodi, I., Udina, E., and Navarro, X. (2012). Specificity of Peripheral Nerve Regeneration: Interactions at the Axon Level. Progress in Neurobiology *98*, 16–37.

Alreja, M., Mutalik, P., Nayar, U., and Manchanda, S.K. (1984). The Formalin Test: A Tonic Pain Model in the Primate. Pain *20*, 97–105.

Altier, C., and Zamponi, G.W. (2004). Targeting Ca^{2+} Channels to Treat Pain: T-Type versus N-Type. Trends in Pharmacological Sciences *25*, 465–470.

Altomare, C., Terragni, B., Brioschi, C., Milanesi, R., Pagliuca, C., Viscomi, C., Moroni, A., Baruscotti, M., and DiFrancesco, D. (2003). Heteromeric HCN1-HCN4 Channels: A Comparison with Native Pacemaker Channels from the Rabbit Sinoatrial Node. The Journal of Physiology *549*, 347–359.

Amaya, F., Decosterd, I., Samad, T.A., Plumpton, C., Tate, S., Mannion, R.J., Costigan, M., and Woolf, C.J. (2000). Diversity of Expression of the Sensory Neuron-Specific TTX-

Resistant Voltage-Gated Sodium Ion Channels SNS and SNS2. Molecular and Cellular Neuroscience *15*, 331–342.

Amaya, F., Samad, T.A., Barrett, L., Broom, D.C., and Woolf, C.J. (2009). Periganglionic Inflammation Elicits a Distally Radiating Pain Hypersensitivity by Promoting COX-2 Induction in the Dorsal Root Ganglion. Pain *142*, 59–67.

Amir, R., Kocsis, J.D., and Devor, M. (2005). Multiple Interacting Sites of Ectopic Spike Electrogenesis in Primary Sensory Neurons. The Journal of Neuroscience *25*, 2576–2585.

Amir, R., Michaelis, M., and Devor, M. (1999). Membrane Potential Oscillations in Dorsal Root Ganglion Neurons: Role in Normal Electrogenesis and Neuropathic Pain. The Journal of Neuroscience *19*, 8589–8596.

Andrade, E.L., Meotti, F.C., and Calixto, J.B. (2012). TRPA1 Antagonists as Potential Analgesic Drugs. Pharmacology and Therapeutics *133*, 189–204.

Antal, M., Papp, I., Bahaerguli, N., Veress, G., and Vereb, G. (2004). Expression of Hyperpolarization-Activated and Cyclic Nucleotide-Gated Cation Channel Subunit 2 in Axon Terminals of Peptidergic Nociceptive Primary Sensory Neurons in the Superficial Spinal Dorsal Horn of Rats. European Journal of Neuroscience *19*, 1336–1342.

Arévalo, M.I., Escribano, E., Calpena, A., Domenech, J., and Queralt, J. (2003). Thermal Hyperalgesia and Light Touch Allodynia After Intradermal. Inflammation *27*, 293–299.

Arnér, S., and Meyerson, B.A. (1988). Lack of Analgesic Effect of Opioids on Neuropathic and Idiopathic Forms of Pain. Pain *33*, 11–23.

Arnér, S., Lindblom, U., Meyerson, B.A., and Molander, C. (1990). Prolonged Relief of Neuralgia after Regional Anesthetic Blocks. A Call for Further Experimental and Systematic Clinical Studies. Pain *43*, 287–297.

Arvidsson, J., Ygge, J., and Grant, G. (1986). Cell Loss in Lumbar Dorsal Root Ganglia and Transganglionic Degeneration After Sciatic Nerve Resection in the Rat. Brain Research *373*, 15–21.

Attal, N., Cruccu, G., Haanpää, M., Hansson, P., Jensen, T.S., Nurmikko, T., Sampaio, C., Sindrup, S., and Wiffen, P. (2006). EFNS Guidelines on Pharmacological Treatment of Neuropathic Pain. European Journal of Neurology *13*, 1153–1169.

Attal, N., Jazat, F., Kayser, V., and Guilbaud, G. (1990). Further Evidence for "Pain-Related" Behaviours in a Model of Unilateral Peripheral Mononeuropathy. Pain *41*, 235–251.

Baccaglini, P.I., and Hogan, P.G. (1983). Some Rat Sensory Neurons in Culture Express Characteristics of Differentiated Pain Sensory Cells. Proceedings of the National Academy of Sciences *80*, 594–598.

Backonja, M.-M., and Stacey, B. (2004). Neuropathic Pain Symptoms Relative to Overall Pain Rating. The Journal of Pain *5*, 491–497.

Bajrović, F., and Sketelj, J. (1998). Extent of Nociceptive Dermatomes in Adult Rats Is Not Primarily Maintained by Axonal Competition. Experimental Neurology *150*, 115–121.

Banchet, von, G.S., Boettger, M.K., Fischer, N., Gajda, M., Bräuer, R., and Schaible, H.-G. (2009). Experimental Arthritis Causes Tumor Necrosis Factor-α-Dependent Infiltration of Macrophages into Rat Dorsal Root Ganglia which Correlates with Pain-Related Behavior. Pain *145*, 151–159.

Banks, M.I., Pearce, R.A., and Smith, P.H. (1993). Hyperpolarization-Activated Cation Current (Ih) in Neurons of the Medial Nucleus of the Trapezoid Body: Voltage-Clamp Analysis and Enhancement by Norepinephrine and CAMP Suggest a Modulatory Mechanism in the Auditory Brain Stem. The Journal of Neurophysiology *70*, 1420–1432.

Bankston, J.R., Camp, S.S., DiMaio, F., Lewis, A.S., Chetkovich, D.M., and Zagotta, W.N. (2012). Structure and Stoichiometry of an Accessory Subunit TRIP8b Interaction with Hyperpolarization-Activated Cyclic Nucleotide-Gated Channels. Proceedings of the National Academy of Sciences *109*, 7899–7904.

Baron, R., Binder, A., and Wasner, G. (2010). Neuropathic Pain: Diagnosis, Pathophysiological Mechanisms, and Treatment. The Lancet Neurology *9*, 807–819.

Barton, M.E., Eberle, E.L., and Shannon, H.E. (2005). The Antihyperalgesic Effects of the T-Type Calcium Channel Blockers Ethosuximide, Trimethadione, and Mibefradil. European Journal of Pharmacology *521*, 79–85.

Basbaum, A.I., Bautista, D.M., Scherrer, G., and Julius, D. (2009). Cellular and Molecular Mechanisms of Pain. Cell *139*, 267–284.

Bautista, D.M., Jordt, S.-E., Nikai, T., Tsuruda, P.R., Read, A.J., Poblete, J., Yamoah, E.N., Basbaum, A.I., and Julius, D. (2006). TRPA1 Mediates the Inflammatory Actions of Environmental Irritants and Proalgesic Agents. Cell *124*, 1269–1282.

Bautista, D.M., Movahed, P., Hinman, A., Axelsson, H.E., Sterner, O., Högestätt, E.D., Julius, D., Jordt, S.-E., and Zygmunt, P.M. (2005). Pungent Products from Garlic Activate the Sensory Ion Channel TRPA1. Proceedings of the National Academy of Sciences *102*, 12248–12252.

Bautista, D.M., Siemens, J., Glazer, J.M., Tsuruda, P.R., Basbaum, A.I., Stucky, C.L., Jordt, S.-E., and Julius, D. (2007). The Menthol Receptor TRPM8 is the Principal Detector of Environmental Cold. Nature *448*, 204–208.

Bender, R.A., Brewster, A., Santoro, B., Ludwig, A., Hofmann, F., Biel, M., and Baram, T.Z. (2001). Differential and Age-Dependent Expression of Hyperpolarization-Activated, Cyclic Nucleotide-Gated Cation Channel Isoforms 1-4 Suggests Evolving Roles in the Developing Rat Hippocampus. Neuroscience *106*, 689–698.

Benn, S.C., and Woolf, C.J. (2004). Adult Neuron Survival Strategies — Slamming on the Brakes. Nature Reviews: Neuroscience *5*, 686–700.

Bennett, G.J. (2012). What Is Spontaneous Pain and Who Has It? The Journal of Pain.

Bennett, G.J., and Xie, Y.-K. (1988). A Peripheral Mononeuropathy in Rat that Produces Disorders of Pain Sensation like those Seen in Man. Pain *33*, 87–107.

Berkley, K.J. (1997). Sex Differences in Pain. Behavioural and Brain Sciences *20*, 371–380.

Besson, J.-M., and Chaouch, A. (1987). Peripheral and Spinal Mechanisms of Nociception. Physiological Reviews *67*, 67–186.

Bessou, P., and Perl, E.R. (1969). Response of Cutaneous Sensory Units with Unmyelinated Fibers to Noxious Stimuli. Journal of Neurophysiology *32*, 1025–1043.

Biel, M., Schneider, A., and Wahl, C. (2002). Cardiac HCN Channels: Structure, Function, and Modulation. Trends in Cardiovascular Medicine *12*, 206–213.

Biel, M., Wahl-Schott, C., Michalakis, S., and Zong, X. (2009). Hyperpolarization-Activated Cation Channels: From Genes to Function. Physiological Reviews *89*, 847–885.

Billiau, A., and Matthys, P. (2001). Modes of Action of Freund's Adjuvants in Experimental Models of Autoimmune Diseases. Journal of Leukocyte Biology *70*, 849–860.

Birrell, G.J., McQueen, D.S., Iggo, A., and Grubb, B.D. (1993). Prostanoid-Induced Potentiation of the Excitatory and Sensitizing Effects of Bradykinin on Articular Mechanoreceptors in the Rat Ankle Joint. Neuroscience *54*, 537–544.

Birren, J.E., and Wall, P.D. (1956). Age Changes in Conduction Velocity, Refractory Period, Number of Fibers, Connective Tissue Space and Blood Vessels in Sciatic Nerve of Rats. The Journal of Comparative Neurology *104*, 1–16.

Bisby, M.A., and Chen, S. (1990). Delayed Wallerian Degeneration in Sciatic Nerves of C57BL/Ola Mice is Associated with Impaired Regeneration of Sensory Axons. Brain Research *530*, 117–120.

Black, J.A., Cummins, T.R., Plumpton, C., Chen, Y.H., Hormuzdiar, W., Clare, J.J., and Waxman, S.G. (1999). Upregulation of a Silent Sodium Channel After Peripheral, but not Central, Nerve Injury in DRG Neurons. Journal of Neurophysiology *82*, 2776–27762785.

Blackburn-Munro, G. (2004). Pain-Like Behaviours in Animals – How Human are They? Trends in Pharmacological Sciences *25*, 299–305.

Blackburn-Munro, G., and Jensen, B.S. (2003). The Anticonvulsant Retigabine Attenuates Nociceptive Behaviours in Rat Models of Persistent and Neuropathic Pain. European Journal of Pharmacology *460*, 109–116.

Bobker, D.H., and Williams, J.T. (1989). Serotonin Augments the Cationic Current Ih in Central Neurons. Neuron *2*, 1535–1540.

Boettger, M.K., Uceyler, N., Zelenka, M., Schmitt, A., Reif, A., Chen, Y., and Sommer, C. (2007). Differences in Inflammatory Pain in nNOS-, iNOS- and eNOS-Deficient Mice. European Journal of Pain *11*, 810–818.

Boivie, J., Leijon, G., and Johansson, I. (1989). Central Post-Stroke Pain -- A Study of the Mechanisms through Analyses of the Sensory Abnormalities. Pain *37*, 173–185.

BoSmith, R.E., Briggs, I., and Sturgess, N.C. (1993). Inhibitory Actions of ZENECA ZD7288 on Whole-Cell Hyperpolarization Activated Inward Current (If) in Guinea-Pig Dissociated Sinoatrial Node Cells. British Journal of Pharmacology *110*, 343–349.

Boucher, T.J., Okuse, K., Bennett, D.L.H., Munson, J.B., Wood, J.N., and McMahon, S.B. (2000). Potent Analgesic Effects of GDNF in Neuropathic Pain States. Science *290*, 124–127.

Bouldin, T.W., Earnhardt, T.S., and Goines, N.D. (1991). Restoration of Blood-Nerve Barrier in Neuropathy is Associated with Axonal Regeneration and Remyelination. Journal of Neuropathology and Experimental Neurology *50*, 719–728.

Bourinet, E., Alloui, A., Monteil, A., Barrère, C., Couette, B., Poirot, O., Pages, A., McRory, J., Snutch, T.P., Eschalier, A., et al. (2005). Silencing of the $Ca_V3.2$ T-type Calcium Channel Gene in Sensory Neurons Demonstrates its Major Role in Nociception. The EMBO Journal *24*, 315–324.

Brandao, K.E., Dell'Acqua, M.L., and Levinson, S.R. (2011). A-Kinase Anchoring Protein 150 Expression in a Specific Subset of TRPV1- and $Ca_V1.2$-Positive Nociceptive Rat Dorsal Root Ganglion Neurons. The Journal of Comparative Neurology *520*, 81–99.

Bráz, J.M., Nassar, M.A., Wood, J.N., and Basbaum, A.I. (2005). Parallel "Pain" Pathways Arise from Subpopulations of Primary Afferent Nociceptor. Neuron *47*, 787–793.

Brewster, A.L., Bernard, J.A., Gall, C.M., and Baram, T.Z. (2005). Formation of Heteromeric Hyperpolarization-Activated Cyclic Nucleotide-Gated (HCN) Channels in the Hippocampus is Regulated by Developmental Seizures. Neurobiology of Disease *19*, 200–207.

Broom, D.C., Samad, T.A., Kohno, T., Tegeder, I., Geisslinger, G., and Woolf, C.J. (2004). Cyclooxygenase 2 Expression in the Spared Nerve Injury Model of Neuropathic Pain. Neuroscience *124*, 891–900.

Brown, A.G., and Iggo, A. (1967). A Quantitative Study of Cutaneous Receptors and Afferent Fibres in the Cat and Rabbit. The Journal of Physiology *193*, 707–733.

Brown, H.F., DiFrancesco, D., and Noble, S.J. (1979). How Does Adrenaline Accelerate the Heart? Nature *280*, 236–237.

Brown, H.F., Giles, W., and Noble, S.J. (1977). Membrane Currents Underlying Activity in Frog Sinus Venosus. The Journal of Physiology *271*, 783–816.

Brown, S.M., Dubin, A.E., and Chaplan, S.R. (2004). The Role of Pacemaker Currents in Neuropathic Pain. Pain Practice *4*, 182–193.

Browne, L.E., Clare, J.J., and Wray, D. (2009). Functional and Pharmacological Properties of Human and Rat $Na_V1.8$ Channels. Neuropharmacology *56*, 905–914.

Brushart, T.M., Hoffman, P.N., Royall, R.M., Murinson, B.B., Witzel, C., and Gordon, T. (2002). Electrical Stimulation Promotes Motoneuron Regeneration without Increasing Its Speed or Conditioning the Neuron. The Journal of Neuroscience *22*, 6631–6638.

Buchwalow, I.B., and Böcker, W. (2010). Multiple Immunofluorescence Staining. In Immunohistochemistry: Basics and Methods, (London: Springer), pp. 69–76.

Budde, T., Coulon, P., Pawlowski, M., Meuth, P., Kanyshkova, T., Japes, A., Meuth, S.G., and Pape, H.-C. (2008). Reciprocal Modulation of I_h and I_{TASK} in Thalamocortical Relay

Neurons by Halothane. Pflugers Arch - European Journal of Physiology *456*, 1061–1073.

Burkey, T.H., Hingtgen, C.M., and Vasko, M.R. (2004). Isolation and Culture of Sensory Neurons From the Dorsal-Root Ganglia of Embryonic or Adult Rats. In Pain Research, Z.D. Luo, ed. (Totowa, New Jersey: Humana Press), pp. 189–202.

Cacheaux, L.P., Topf, N., Tibbs, G.R., Schaefer, U.R., Levi, R., Harrison, N.L., Abbott, G.W., and Goldstein, P.A. (2005). Impairment of Hyperpolarization-Activated, Cyclic Nucleotide-Gated Channel Function by the Intravenous General Anesthetic Propofol. Journal of Pharmacology and Experimental Therapeutics *315*, 517–525.

Cafferty, W.B.J., McGee, A.W., and Strittmatter, S.M. (2008). Axonal growth therapeutics: regeneration or sprouting or plasticity? Trends in Neurosciences *31*, 215–220.

Cai, D., Qui, J., Cao, Z., McAtee, M., Bregman, B.S., and Filbin, M.T. (2001). Neuronal Cyclic AMP Controls the Developmental Loss in Ability of Axons to Regenerate. The Journal of Neuroscience *21*, 4731–4739.

Calvino, B., Besson, J.-M., Boehrer, A., and Depaulis, A. (1996). Ultrasonic Vocalization (22-28 kHz) in a Model of Chronic Pain, the Arthritic Rat: Effects of Analgesic Drugs. Neuroreport *7*, 581–584.

Campbell, J.N., and Meyer, R.A. (2006). Mechanisms of Neuropathic Pain. Neuron *52*, 77–92.

Caterina, M.J., Leffler, A., Malmberg, A.B., Martin, W.J., Trafton, J., Petersen-Zeitz, K.R., Koltzenburg, M., Basbaum, A.I., and Julius, D. (2000). Impaired Nociception and Pain Sensation in Mice Lacking the Capsaicin Receptor. Science *288*, 306–313.

Caterina, M.J., Schumacher, M.A., Tominaga, M., Rosen, T.A., Levine, J.D., and Julius, D. (1997). The Capsaicin Receptor: A Heat-Activated Ion Channel in the Pain Pathway. Nature *389*, 816–824.

Catterall, W.A. (1984). The Molecular Basis of Neuronal Excitability. Science *223*, 653.

Cavanaugh, D.J., Lee, H., Lo, L., Shields, S.D., Zylka, M.J., Basbaum, A.I., and Anderson, D.J. (2009). Distinct Subsets of Unmyelinated Primary Sensory Fibers Mediate Behavioral Responses to Noxious Thermal and Mechanical Stimuli. Proceedings of the National Academy of Sciences *106*, 9075–9080.

Cervetto, L., Demontis, G.C., and Gargini, C. (2007). Cellular Mechanisms Underlying the Pharmacological Induction of Phosphenes. British Journal of Pharmacology *150*, 383–390.

Cesare, P., and McNaughton, P.A. (1996). A Novel Heat-Activated Current in Nociceptive Neurons and its Sensitization by Bradykinin. Proceedings of the National Academy of Sciences *93*, 15435–15439.

Cesare, P., Dekker, L.V., Sardini, A., Parker, P.J., and McNaughton, P.A. (1999). Specific Involvement of PKC-∈ in Sensitization of the Neuronal Response to Painful Heat. Neuron *23*, 617–624.

Chambers, M.R., Andres, K.H., Duering, von, M., and Iggo, A. (1972). The Structure and Function of the Slowly Adapting Type II Mechanoreceptor in Hairy Skin. Quarterly Journal of Experimental Physiology and Cognate Medical Sciences *57*, 417–445.

Chaney, M.A. (1995). Side Effects of Intrathecal and Epidural Opioids. Canadian Journal of Anaesthesia *42*, 891–903.

Chaplan, S.R., Guo, H.-Q., Lee, D.H., Luo, L., Liu, C., Kuei, C., Velumian, A.A., Butler, M.P., Brown, S.M., and Dubin, A.E. (2003). Neuronal Hyperpolarization-Activated Pacemaker Channels Drive Neuropathic Pain. The Journal of Neuroscience *23*, 1169–1178.

Chen, J., and Kym, P.R. (2009). TRPA1: The Species Difference. The Journal of General Physiology *133*, 623–625.

Chen, J., Joshi, S.K., DiDomenico, S., Perner, R.J., Mikusa, J.P., Gauvin, D.M., Segreti, J.A., Han, P., Zhang, X.-F., Niforatos, W., et al. (2011). Selective Blockade of TRPA1 Channel Attenuates Pathological Pain without Altering Noxious Cold Sensation or Body Temperature Regulation. Pain *152*, 1165–1172.

Chen, S., Wang, J., and Siegelbaum, S.A. (2001). Properties of Hyperpolarization-Activated Pacemaker Current Defined by Coassembly of HCN1 and HCN2 Subunits and Basal Modulation by Cyclic Nucleotide. The Journal of General Physiology *117*, 491–503.

Chen, X., Alessandri-Haber, N., and Levine, J.D. (2007). Marked Attenuation of Inflammatory Mediator-Induced C-Fiber Sensitization for Mechanical and Hypotonic Stimuli in TRPV4-/- Mice. Molecular Pain *3*, 31.

Chen, X., Shu, S., Kennedy, D.P., Willcox, S.C., and Bayliss, D.A. (2008). Subunit-Specific Effects of Isoflurane on Neuronal Ih in HCN1 Knockout Mice. The Journal of Neurophysiology *101*, 129–140.

Chen, X., Sirois, J.E., Lei, Q., Talley, E.M., Lynch, C., III, and Bayliss, D.A. (2005). HCN Subunit-Specific and cAMP-Modulated Effects of Anesthetics on Neuronal Pacemaker Currents. The Journal of Neuroscience *25*, 5803–5814.

Cheng, L., Khan, M., and Mudge, A.W. (1995). Calcitonin Gene-Related Peptide Promotoes Schwann Cell Proliferation. The Journal of Cell Biology *129*, 789–796.

Cheng, L., Kinard, K., Rajamani, R., and Sanguinetti, M.C. (2007). Molecular Mapping of the Binding Site for a Blocker of Hyperpolarization-Activated, Cyclic Nucleotide-Modulated Pacemaker Channels. Journal of Pharmacology and Experimental Therapeutics *322*, 931–939.

Cho, H.-J., Staikopoulos, V., Furness, J.B., and Jennings, E.A. (2009a). Inflammation-Induced Increase in Hyperpolarization-Activated, Cyclic Nucleotide-Gated Channel Protein in Trigeminal Ganglion Neurons and the Effect of Buprenorphine. Neuroscience *162*, 453–461.

Cho, H.-J., Staikopoulos, V., Ivanusic, J.J., and Jennings, E.A. (2009b). Hyperpolarization-Activated Cyclic-Nucleotide Gated 4 (HCN4) Protein is Expressed in a Subset of Rat Dorsal Root and Trigeminal Ganglion Neurons. Cell Tissue Res *338*, 171–177.

Choi, Y., Raja, S.N., Moore, L.C., and Tobin, J.R. (1996). Neuropathic Pain in Rats is

Associated with Altered Nitric Oxide Synthase Activity in Neural Tissue. Journal of the Neurological Sciences *138*, 14–20.

Chu, Y.-C., Guan, Y., Skinner, J., Raja, S.N., Johns, R.A., and Tao, Y.-X. (2005). Effect of Genetic Knockout or Pharmacologic Inhibition of Neuronal Nitric Oxide Synthase on Complete Freund's Adjuvant-Induced Persistent Pain. Pain *119*, 113–123.

Chung, J.M., Kim, H.K., and Chung, K. (2004). Segmental Spinal Nerve Ligation Model of Neuropathic Pain. In Pain Research, Z.D. Luo, ed. (Totowa, New Jersey: Humana Press), pp. 35–45.

Clark, A.K., D'Aquisto, F., Gentry, C., Marchand, F., McMahon, S.B., and Malcangio, M. (2006). Rapid Co-Release of Interleukin 1β and Caspase 1 in Spinal Cord Inflammation. The Journal of Neurochemistry *99*, 868–880.

Clarke, G.D., MacPherson, I.S., Petrone, G., and Spangler, R.S. (1994). Antinociceptive Effects of Non-Steroidal Anti-Inflammatory Drugs in a Rat Model of Unilateral Hindpaw Inflammation. European Journal of Pharmacology *257*, 103–108.

Coderre, T.J., and Wall, P.D. (1987). Ankle Joint Urate Arthritis (AJUA) in Rats: An Alternative Animal Model of Arthritis to that Produced by Freund's Adjuvant. Pain *28*, 379–393.

Cohan, C.S., and Kater, S.B. (1986). Suppression of Neurite Elongation and Growth Cone Motility by Electrical Activity. Science *232*, 1638–1640.

Colburn, R.W., Lubin, M.L., Stone, D.J., Jr, Wang, Y., Lawrence, D., D'Andrea, M.R., Brandt, M.R., Liu, Y., Flores, C.M., and Qin, N. (2007). Attenuated Cold Sensitivity in TRPM8 Null Mice. Neuron *54*, 379–386.

Cook, A.J., Woolf, C.J., Wall, P.D., and McMahon, S.B. (1987). Dynamic Receptive Field Plasticity in Rat Spinal Cord Dorsal Horn following C-Primary Afferent Input. Nature *325*, 151–153.

Correale, J., and Villa, A. (2004). The Neuroprotective Role of Inflammation in Nervous System Injuries. Journal of Neurology *251*, 1304–1316.

Costigan, M., Befort, K., Karchewski, L., Griffin, R.S., D'Urso, D., Allchorne, A., Sitarski, J., Mannion, J.W., Pratt, R.E., and Woolf, C.J. (2002). Replicate High-Density Rat Genome Oligonucleotide Microarrays Reveal Hundreds of Regulated Genes in the Dorsal Root Ganglion after Peripheral Root Injury. BMC Neuroscience *3*, 1–18.

Costigan, M., Scholz, J., and Woolf, C.J. (2009). Neuropathic Pain: A Maladaptive Response of the Nervous System to Damage. Annual Review of Neuroscience *32*, 1–32.

Coull, J.A.M., Beggs, S., Boudreau, D., Boivin, D., Tsuda, M., Inoue, K., Gravel, C., Salter, M.W., and De Koninck, Y. (2005). BDNF from Microglia Causes the Shift in Neuronal Anion Gradient Underlying Neuropathic Pain. Nature *438*, 1017–1021.

Coward, K., Plumpton, C., Facer, P., Birch, R., Carlstedt, T., Tate, S., Bountra, C., and Anand, P. (2000). Immunolocalization of SNS/PN3 and NaN/SNS2 Sodium Channels in Human Pain States. Pain *85*, 41–50.

Cox, J.J., Reimann, F., Nicholas, A.K., Thornton, G., Roberts, E., Springell, K., Karbani, G., Jafri, H., Mannan, J., Raashid, Y., et al. (2006). An SCN9A Channelopathy causes Congential Inability to Experience Pain. Nature *444*, 1–5.

Cui, M., and Nicol, G.D. (1995). Cyclic AMP Mediates the Prostaglandin E2-Induced Potentiation of Bradykinin Excitation in Rat Sensory Neurons. Neuroscience *66*, 459–466.

Cui, M., Honore, P., Zhong, C., Gauvin, D., Mikusa, J., Hernandez, G., Chandran, P., Gomtsyan, A., Brown, B., Bayburt, E.K., et al. (2006). TRPV1 Receptors in the CNS Play a Key Role in Broad-Spectrum Analgesia of TRPV1 Antagonists. The Journal of Neuroscience *26*, 9385–9393.

Cummins, T.R., Dib-Hajj, S.D., Black, J.A., Akopian, A.N., Wood, J.N., and Waxman, S.G. (1999). A Novel Persistent Tetrodotoxin-Resistant Sodium Current in SNS-Null and Wild-Type Small Primary Sensory Neurons. The Journal of Neuroscience *19*, RC43.

Dalle, C., and Eisenach, J.C. (2005). Peripheral Block of the Hyperpolarization-Activated Cation Current (Ih) Reduces Mechanical Allodynia in Animal Models of Postoperative and Neuropathic Pain. Regional Anesthesia and Pain Medicine *30*, 243–248.

Davis, J.B., Gray, J., Gunthorpe, M.J., Hatcher, J.P., Davey, P.T., Overend, P., Harries, M.H., Latcham, J., Clapham, C., Atkinson, K., et al. (2000). Vanilloid Receptor-1 is Essential for Inflammatory Thermal Hyperalgesia. Nature *405*, 183–187.

Davis, K.D., Meyer, R.A., and Campbell, J.N. (1993). Chemosensitivity and Sensitization of Nociceptive Afferents that Innervate the Hairy Skin of Monkey. Journal of Neurophysiology *69*, 1071–1081.

Deacon, R.M.J. (2006). Housing, Husbandry and Handling of Rodents for Behavioral Experiments. Nature Protocols *1*, 936–946.

Decosterd, I., and Berta, T. (2007). Animal Models and Neuropathic Pain. In The Senses: a Comprehensive Review, A.I. Basbaum, ed. (London: Academic Press), pp. 857–864.

del Camino, D., Murphy, S., Heiry, M., Barrett, L.B., Earley, T.J., Cook, C.A., Petrus, M.J., Zhao, M., D'Amours, M., Deering, N., et al. (2010). TRPA1 Contributes to Cold Hypersensitivity. The Journal of Neuroscience *30*, 15165–15174.

Delmas, P., Hao, J., and Rodat-Despoix, L. (2011). Molecular Mechanisms of Mechanotransduction in Mammalian Sensory Neurons. Nature Reviews: Neuroscience *12*, 139–153.

Demontis, G.C., Gargini, C., Paoli, T.G., and Cervetto, L. (2009). Selective Hcn1 Channels Inhibition by Ivabradine in Mouse Rod Photoreceptors. Invest. Ophthalmol. Vis. Sci. *50*, 1948–1955.

Denk, F., and McMahon, S.B. (2012). Chronic Pain: Emerging Evidence for the Involvement of Epigenetics. Neuron *73*, 435–444.

Devor, M. (2005). Clinical States: Neuropathic Pain. In Textbook of Pain, (Churchill Livingstone), pp. 903–928.

Devor, M. (2007). Ectopic Generators. In The Senses: a Comprehensive Review, A.I. Basbaum, ed. (London: Academic Press), pp. 83–88.

Devor, M. (2009). Ectopic Discharge in Aβ Afferents as a Source of Neuropathic Pain. Experimental Brain Research *196*, 115–128.

Dhaka, A., Murray, A.N., Mathur, J., Earley, T.J., Petrus, M.J., and Patapoutian, A. (2007). TRPM8 Is Required for Cold Sensation in Mice. Neuron *54*, 371–378.

Dhaka, A., Viswanath, V., and Patapoutian, A. (2006). TRP Ion Channels and Temperature Sensation. Annual Review of Neuroscience *29*, 135–161.

Dib-Hajj, S.D., Binshtok, A.M., Cummins, T.R., Jarvis, M.F., Samad, T., and Zimmermann, K. (2009). Voltage-Gated Sodium Channels in Pain States: Role in Pathophysiology and Targets for Treatment. Brain Research Reviews *60*, 65–83.

Dib-Hajj, S.D., Cummins, T.R., Black, J.A., and Waxman, S.G. (2010). Sodium Channels in Normal and Pathological Pain. Annual Review of Neuroscience *33*, 325–347.

DiFrancesco, D. (1981a). A New Interpretation of the Pace-Maker Current in Calf Purkinje Fibres. The Journal of Physiology *314*, 359–376.

DiFrancesco, D. (1981b). A Study of the Ionic Nature of the Pace-Maker Current in Calf Purkinje Fibres. The Journal of Physiology *314*, 377–393.

DiFrancesco, D., and Tortora, P. (1991). Direct Activation of Cardiac Pacemaker Channels by Intracellular Cyclic AMP. Nature *351*, 145–147.

Díaz Muñoz, M.D., Osma García, I.C., Fresno, M., and Iñiguez, M.A. (2012). Involvement of PGE_2 and the cAMP Signalling Pathway in the Up-Regulation of COX-2 and mPGES-1 Expression in LPS-Activated Macrophages. Biochemical Journal *443*, 451–461.

Djouhri, L., and Lawson, S.N. (1999). Changes in Somatic Action Potential Shape in Guinea-Pig Nociceptive Primary Afferent Neurones during Inflammation in vivo. Journal of Physiology *520*, 565–576.

Djouhri, L., and Lawson, S.N. (2004). Aβ-fiber Nociceptive Primary Afferent Neurons: A Review of Incidence and Properties in Relation to other Afferent A-Fiber Neurons in Mammals. Brain Research Reviews *46*, 131–145.

Djouhri, L., Dawbarn, D., Robertson, A., Newton, R., and Lawson, S.N. (2001). Time Course and Nerve Growth Factor Dependence of Inflammation-Induced Alterations in Electrophysiological Membrane Properties in Nociceptive Primary Afferent Neurons. The Journal of Neuroscience *21*, 8722–8733.

Djouhri, L., Fang, X., Koutsikou, S., and Lawson, S.N. (2012). Partial Nerve Injury Induces Electrophysiological Changes in Conducting (Uninjured) Nociceptive and Nonnociceptive DRG Neurons: Possible Relationships to Aspects of Peripheral Neuropathic Pain and Paresthesias. Pain *153*, 1824–1836.

Djouhri, L., Fang, X., Okuse, K., Wood, J.N., Berry, C.M., and Lawson, S.N. (2003). The TTX-Resistant Sodium Channel Nav1.8 (SNS/PN3): Expression and Correlation with Membrane Properties in Rat Nociceptive Primary Afferent Neurons. The Journal of

Physiology *550*, 739–752.

Djouhri, L., Koutsikou, S., Fang, X., McMullan, S., and Lawson, S.N. (2006). Spontaneous Pain, Both Neuropathic and Inflammatory, Is Related to Frequency of Spontaneous Firing in Intact C-Fiber Nociceptors. Journal of Neuroscience *26*, 1281–1292.

Djouhri, L., Newton, R., Levinson, S.R., Berry, C.M., Carruthers, B., and Lawson, S.N. (2002). Sensory and Electrophysiological Properties of Guinea-Pig Sensory Neurones Expressing Nav 1.7 (PN1) Na+ Channel Subunit Protein. The Journal of Physiology *546*, 565–576.

Dobler, T., Springauf, A., Tovornik, S., Weber, M., Schmitt, A., Sedlmeier, R., Wischmeyer, E., and Döring, F. (2007). TRESK Two-Pore-Domain K^+ Channels Constitute a Significant Component of Background Potassium Currents in Murine Dorsal Root Ganglion Neurones. The Journal of Physiology *585*, 867–879.

Dodt, E., and Zotterman, Y. (1952). The Discharge of Specific Cold Fibres at High Temperatures; The Paradoxical Cold. Acta Physiol. Scand. *26*, 358–365.

Dogrul, A., Gardell, L.R., Ossipov, M.H., Tulunay, F.C., Lai, J., and Porreca, F. (2003). Reversal of Experimental Neuropathic Pain by T-Type Calcium Channel Blockers. Pain *105*, 159–168.

Dong, X., Han, S.-K., Zylka, M.J., Simon, M.I., and Anderson, D.J. (2001). A Diverse Family of GPCRs Expressed in Specific Subsets of Nociceptive Sensory Neurons. Cell *106*, 619–632.

Drake, R.L., Vogl, A.W., and Mitchell, A.W.M. (2009). The Body. In Grey's Anatomy for Students, (Churchill Livingstone), pp. 1–53.

Dray, A. (1995). Inflammatory Mediators of Pain. British Journal of Anaesthesia *75*, 125–131.

Dray, A., Bettaney, J., Forster, P., and Perkins, M.N. (1988). Bradykinin-induced Stimulation of Afferent Fibres is Mediated through Protein Kinase C. Neuroscience Letters *91*, 301–307.

Dubuisson, D., and Dennis, S.G. (1977). The Formalin Test: A Quantitative Study of the Analgesic Effects of Morphine, Meperidine, and Brain Stem Stimulation in Rats and Cats. Pain *4*, 161–174.

Durrenberger, P.F., Facer, P., Casula, M.A., Yiangou, Y., Gray, R.A., Chessell, I.P., Day, N.C., Collins, S.D., Bingham, S., Wilson, A.W., et al. (2006). Prostanoid Receptor EP1 and Cox-2 in Injured Human Nerves and a Rat Model of Nerve Injury: A Time-Course Study. BMC Neurology *6*, 1.

Dworkin, R.H., Backonja, M., Rowbotham, M.C., Allen, R.R., Argoff, C.R., Bennett, G.J., Bushnell, C., Farrar, J.T., Galer, B.S., Haythornthwaite, J.A., et al. (2003). Advances in Neuropathic Pain. Neurological Review *60*, 1524–1534.

Dworkin, R.H., O'Connor, A.B., Backonja, M., Farrar, J.T., Finnerup, N.B., Jensen, T.S., Kalso, E.A., Loeser, J.D., Miaskowski, C., Nurmikko, T.J., et al. (2007). Pharmacologic Management of Neuropathic Pain: Evidence-based Recommendations. Pain *132*, 237–

251.

Eisemann, C.H., Jorgensen, W.K., Merritt, D.J., Rice, M.J., Cribb, B.W., Webb, P.D., and Zalucki, M.P. (1984). Do Insects Feel Pain? - A Biological View. Experientia *30*, 164–167.

Elmes, S.J.R., Jhaveri, M.D., Smart, D., Kendall, D.A., and Chapman, V. (2004). Cannabinoid CB2 Receptor Activation Inhibits Mechanically Evoked Responses of Wide Dynamic Range Dorsal Horn Neurons in Naïve Rats and in Rat Models of Inflammatory and Neuropathic Pain. European Journal of Neuroscience *20*, 2311–2320.

Emery, E.C., Young, G.T., and McNaughton, P.A. (2012). HCN2 Ion Channels: An Emerging Role as the Pacemakers of Pain. Trends in Pharmacological Sciences *33*, 456–463.

Emery, E.C., Young, G.T., Berrocoso, E.M., Chen, L., and McNaughton, P.A. (2011). HCN2 Ion Channels Play a Central Role in Inflammatory and Neuropathic Pain. Science *333*, 1462–1466.

England, S., Bevan, S., and Docherty, R.J. (1996). PGE2 Modulates the Tetrodotoxin-Resistant Sodium Current in Neonatal Rat Dorsal Root Ganglion Neurones via the Cyclic AMP-Protein Kinase A Cascade. The Journal of Physiology *495*, 439–440.

Er, F., Larbig, R., Ludwig, A., Biel, M., Hofmann, F., Beuckelmann, D.J., and Hoppe, U.C. (2003). Dominant-Negative Suppression of HCN Channels Markedly Reduces the Native Pacemaker Current If and Undermines Spontaneous Beating of Neonatal Cardiomyocytes. Circulation *107*, 485–489.

Erickson, K.R., Ronnekleiv, O.K., and Kelly, M.J. (1993). Electrophysiology of Guinea-Pig Supraoptic Neurones: Role of a Hyperpolarization-Activated Cation Current in Phasic Firing. The Journal of Physiology *460*, 407–425.

Esper, R.M., and Loeb, J.A. (2004). Rapid Axoglial Signaling Mediated by Neuregulin and Neurotrophic Factors. The Journal of Neuroscience *24*, 6218–6227.

Evans, A.R., Vasko, M.R., and Nicol, G.D. (1999). The cAMP Transduction Cascade Mediates the PGE_2-Induced Inhibition of Potassium Currents in Rat Sensory Neurones. The Journal of Physiology *516 (Pt 1)*, 163–178.

Fang, X., Djouhri, L., Black, J.A., Dib-Hajj, S.D., Waxman, S.G., and Lawson, S.N. (2002). The Presence and Role of the Tetrodotoxin-Resistant Sodium Channel Na(v)1.9 (NaN) in Nociceptive Primary Afferent Neurons. The Journal of Neuroscience *22*, 7425–7433.

Fang, X., Djouhri, L., McMullan, S., Berry, C., Waxman, S.G., Okuse, K., and Lawson, S.N. (2006). Intense Isolectin-B4 Binding in Rat Dorsal Root Ganglion Neurons Distinguishes C-Fiber Nociceptors with Broad Action Potentials and High Nav1.9 Expression. Journal of Neuroscience *26*, 7281–7292.

Fang, X., McMullan, S., Lawson, S.N., and Djouhri, L. (2005). Electrophysiological Differences Between Nociceptive and Non-Nociceptive Dorsal Root Ganglion Neurones in the Rat in vivo. The Journal of Physiology *565*, 927–943.

Faraday, M. (1834). Experimental Researches in Electricity: Seventh Series. Philosophical Transactions of the Royal Society of London *124*, 77–122.

Felix, R., Sandoval, A., Sánchez, D., Gómora, J.C., Vega-Beltrán, J.L.D.L., Treviño, C.L., and Darszon, A. (2003). ZD7288 Inhibits Low-Threshold Ca2+ Channel Activity and Regulates Sperm Function. Biochemical and Biophysical Research Communications *311*, 187–192.

Fields, R.D., and Stevens-Graham, B. (2002). New Insights into Neuron-Glia Communication. Science *298*, 556–562.

Fields, R.D., Neale, E.A., and Nelson, P.G. (1990). Effects of Patterned Electrical Activity on Neurite Outgrowth from Mouse Sensory Neurons. The Journal of Neuroscience *10*, 2950–2964.

Finn, J.T., Weil, M., Archer, F., Siman, R., Srinivasan, A., and Raff, M.C. (2000). Evidence That Wallerian Degeneration and Localized Axon Degeneration Induced by Local Neurotrophin Deprivation Do Not Involve Caspases. The Journal of Neuroscience *20*, 1333–1341.

Finnerup, N.B., Sindrup, S.H., and Jensen, T.S. (2010). The Evidence for Pharmacological Treatment of Neuropathic Pain. Pain *150*, 573–581.

Fjell, J., Hjelmström, P., Hormuzdiar, W., Milenkovic, M., Aglieco, F., Tyrrell, L., Dib-Hajj, S.D., Waxman, S.G., and Black, J.A. (2000). Localization of the Tetrodotoxin-Resistant Sodium Channel NaN in Nociceptors. Neuroreport *11*, 199–202.

Flecknell, P. (2009). Anaesthesia. In Laboratory Animal Anaesthesia, (Academic Press), pp. 19–78.

Frace, A.M., Maruoka, F., and Noma, A. (1992). Control of the Hyperpolarization-Activated Cation Current by External Anions in Rabbit Sino-Atrial Node Cells. The Journal of Physiology *453*, 307–318.

Frishman, W.H., Pepine, C.J., Weiss, R.J., and Baiker, W.M. (1995). Addition of Zatebradine, a Direct Sinus Node Inhibitor, Provides No Greater Exercise Tolerance Benefit in Patients With Angina Taking Extended-Release Nifedipine: Results of a Multicenter, Randomized, Double-Blind, Placebo-Controlled, Parallel-Group Study. Journal of the American College of Cardiology *26*, 305–312.

Funk, C.D. (2001). Prostaglandins and Leukotrienes: Advances in Eicosanoid Biology. Science *294*, 1871–1875.

Gagliese, L., and Melzack, R. (1997). Chronic Pain in Elderly People. Pain *70*, 3–14.

Gamper, N., and Shapiro, M.S. (2007). Regulation of Ion Transport Proteins by Membrane Phosphoinositides. Nature Reviews: Neuroscience *8*, 921–934.

Gaskin, D.J., and Richard, P. (2012). The Economic Costs of Pain in the United States. The Journal of Pain *13*, 715–724.

Gaudet, A.D., Leung, M., Poirier, F., Kadoya, T., Horie, H., and Ramer, M.S. (2009). A Role for Galectin-1 in the Immune Response to Peripheral Nerve Injury. Experimental Neurology *220*, 320–327.

Gaudet, A.D., Popovich, P.G., and Ramer, M.S. (2011). Wallerian Degeneration: Gaining Perspective on Inflammatory Events after Peripheral Nerve Injury. Journal of

Neuroinflammation *8*, 110.

Gauss, R., Seifert, R., and Kaupp, U.B. (1998). Molecular Identification of a Hyperpolarization-Activated Channel in Sea Urchin Sperm. Nature *393*, 583–587.

Gavva, N.R., Tamir, R., Qu, Y., Klionsky, L., Zhang, T.J., Immke, D., Wang, J., Zhu, D., Vanderah, T.W., Porreca, F., et al. (2005). AMG 9810 [(E)-3-(4-t-Butylphenyl)-N-(2,3-dihydrobenzo[b][1,4] dioxin-6-yl)acrylamide], a Novel Vanilloid Receptor 1 (TRPV1) Antagonist with Antihyperalgesic Properties. Journal of Pharmacology and Experimental Therapeutics *313*, 474–484.

Gavva, N.R., Treanor, J.J.S., Garami, A., Fang, L., Surapaneni, S., Akrami, A., Alvarez, F., Bak, A., Darling, M., Gore, A., et al. (2008). Pharmacological Blockade of the Vanilloid Receptor TRPV1 Elicits Marked Hyperthermia in Humans. Pain *136*, 202–210.

Geffeney, S.L., and Goodman, M.B. (2012). How We Feel: Ion Channel Partnerships that Detect Mechanical Inputsand Give Rise to Touch and Pain Perception. Neuron *74*, 609–619.

Gibbons, S.J., Núñez-Hernández, R., Mazé, G., and Harrison, N.L. (1996). Inhibition of a Fast Inwardly Rectifying Potassium Conductance by Barbiturates. Anesthesia & Analgesia *82*, 1241–1246.

Gilliatt, R.W., and Hjorth, R.J. (1972). Nerve Conduction during Wallerian Degeneration in the Baboon. The Journal of Neurology, Neurosurgery, and Psychiatry *35*, 335–341.

Gold, M.S. (2008). Na+ Channel Blockers for the Treatment of Pain: Context is Everything, Almost. Experimental Neurology *210*, 1–6.

Gold, M.S., and Caterina, M.J. (2007). Molecular Biology of the Nociceptor/Transduction. In The Senses: a Comprehensive Review, A.I. Basbaum, ed. (London: Academic Press), pp. 43–73.

Gold, M.S., and Gebhart, G.F. (2010). Nociceptor Sensitization in Pain Pathogenesis. Nature Medicine *16*, 1248–1257.

Goldberg, Y., MacFarlane, J., MacDonald, M., Thompson, J., Dube, M.-P., Mattice, M., Fraser, R., Young, C., Hossain, S., Pape, T., et al. (2007). Loss-of-Function Mutations in the Nav1.7 Gene Underlie Congenital Indifference to Pain in Multiple Human Populations. Clinical Genetics *71*, 311–319.

Goldin, A.L., Barchi, R.L., Caldwell, J.H., Hofmann, F., Howe, J.R., Hunter, J.C., Kallen, R.G., Mandel, G., Meisler, M.H., Netter, Y.B., et al. (2000). Nomenclature of Voltage-Gated Sodium Channels. Neuron *28*, 365–368.

Gore, M., Dukes, E., Rowbotham, D.J., Tai, K.-S., and Leslie, D. (2007). Clinical Characteristics and Pain Management Among Patients with Painful Peripheral Neuropathic Disorders in General Practice Settings. European Journal of Pain *11*, 652–664.

Gracely, R.H., Lynch, S.A., and Bennett, G.J. (1992). Painful Neuropathy: Altered Central Processing Maintained Dynamically by Peripheral Input. Pain *51*, 175–194.

Greenspan, J.D., Craft, R.M., LeResche, L., Arendt-Nielsen, L., Berkley, K.J., Fillingim, R.B., Gold, M.S., Holdcroft, A., Lautenbacher, S., Mayer, E.A., et al. (2007). Studying sex and gender differences in pain and analgesia: A consensus report. Pain *132*, S26–S45.

Hadley, J.K., Passmore, G.M., Tatulian, L., Al-Qatari, M., Wickenden, A.D., and Brown, D.A. (2003). Stoichiometry of Expressed KCNQ2/KCNQ3 Potassium Channels and Subunit Composition of Native Ganglionic M Channels Deduced from Block by Tetraethylammonium. The Journal of Neuroscience *23*, 5012–5019.

Halliwell, J.V., and Adams, P.R. (1982). Voltage-Clamp Analysis of Muscarinic Excitation in Hippocampal Neurons. Brain Research *250*, 71–92.

Hamberg, M., and Samuelsson, B. (1971). On the Metabolism of Prostaglandins E_1 and E_2 in Man. The Journal of Biological Chemistry *246*, 6713–6721.

Han, W., Bao, W., Wang, Z., and Nattel, S. (2002). Comparison of Ion-Channel Subunit Expression in Canine Cardiac Purkinje Fibers and Ventricular Muscle. Circulation Research *91*, 790–797.

Han, Y., Noam, Y., Lewis, A.S., Gallagher, J.J., Wadman, W.J., Baram, T.Z., and Chetkovich, D.M. (2011). Trafficking and Gating of Hyperpolarization-Activated Cyclic Nucleotide-Gated Channels Are Regulated by Interaction with Tetratricopeptide Repeat-Containing Rab8b-Interacting Protein (TRIP8b) and Cyclic AMP at Distinct Sites. The Journal of Biological Chemistry *286*, 20823–20834.

Handwerker, H.O., Kilo, S., and Reeh, P.W. (1991). Unresponsive Afferent Nerve Fibres in the Sural Nerve of the Rat. The Journal of Physiology *435*, 229–242.

Hannila, S.S., and Filbin, M.T. (2008). The Role of Cyclic AMP Signalling in Promoting Axonal Regeneration after Spinal Cord Injury. Experimental Neurology *209*, 321–332.

Hanz, S., and Fainzilber, M. (2006). Retrograde Signaling in Injured Nerve – the Axon Reaction Revisited. Journal of Neurochemistry *99*, 13–19.

Hara, S., Kamei, D., Sasaki, Y., Tanemoto, A., Nakatani, Y., and Murakami, M. (2010). Prostaglandin E Synthases: Understanding their Pathophysiological Roles through Mouse Genetic Models. Biochimie *92*, 651–659.

Hardel, N., Harmel, N., Zolles, G., Fakler, B., and Klöcker, N. (2008). Recycling Endosomes Supply Cardiac Pacemaker Channels for Regulated Surface Expression. Cardiovascular Research *79*, 52–60.

Hardie, R.C. (2003). Regulation of TRP Channels via Lipid Second Messengers. Annual Reviews of Physiology *65*, 735–759.

Hargreaves, K., Dubner, R., Brown, F., Flores, C., and Joris, J. (1988). A New and Sensitive Method for Measuring Thermal Nociception in Cutaneous Hyperalgesia. Pain *32*, 77–88.

Harris, N.C., and Constanti, A. (1995). Mechanism of Block by ZD 7288 of the Hyperpolarization-Activated Inward Rectifying Current in Guinea Pig Substantia Nigra Neurons In Vitro. The Journal of Neurophysiology *74*, 2366–2378.

Haydon, P.G. (2001). Glia: Listening and Talking to the Synapse. Nature Reviews:

Neuroscience *2*, 185–193.

Hehn, von, C.A., Baron, R., and Woolf, C.J. (2012). Deconstructing the Neuropathic Pain Phenotype to Reveal Neural Mechanisms. Neuron *73*, 638–652.

Heisler, A. (2007). Anatomy. In Rat Jugular Vein and Carotid Artery Catheterization for Acute Survival Studies: a Practical Guide, (Springer), pp. 29–33.

Hempenstall, K., Nurmikko, T.J., Johnson, R.W., A'Hern, R.P., and Rice, A.S.C. (2005). Analgesic Therapy in Postherpetic Neuralgia: A Quantitative Systematic Review. Plos Med *2*, e164.

Hensel, H., and Zotterman, Y. (1951). The Effect of Menthol on the Thermoreceptors. Acta Physiol. Scand. *24*, 27–34.

Herzog, R.I., Cummins, T.R., and Waxman, S.G. (2001). Persistent TTX-Resistant Na^+ Current Affects Resting Potential and Response to Depolarization in Simulated Spinal Sensory Neurons. Journal of Neurophysiology *86*, 1351–1364.

Hilgemann, D.W., and Ball, R. (1996). Regulation of Cardiac Na^+, Ca^{2+} Exchange and K_{ATP} Potassium Channels by PIP_2. Science *273*, 956–959.

Hingtgen, C.M., Waite, K.J., and Vasko, M.R. (1995). Prostaglandins Facilitate Peptide Release from Rat Sensory Neurons by Activating the Adenosine 3',5'-Cyclic Monophosphate Transduction Cascade. The Journal of Neuroscience *15*, 5411–5419.

Hogan, Q.H., and Poroli, M. (2008). Hyperpolarization-Activated Current (I_h) Contributes to Excitability of Primary Sensory Neurons in Rats. Brain Research *1207*, 102–110.

Honore, P., Rogers, S.D., Schwei, M.J., Salak-Johnson, J.L., Luger, N.M., Sabino, M.C., Clohisy, D.R., and Mantyh, P.W. (2000). Murine Models of Inflammatory, Neuropathic and Cancer Pain Each Generates a Unique Set of Neurochemical Changes in the Spinal Cord and Sensory Neurons. Neuroscience *98*, 585–598.

Horie, H., Inagaki, Y., Sohma, Y., Nozawa, R., Okawa, K., Hasegawa, M., Muramatsu, N., Kawano, H., Horie, M., Koyama, H., et al. (1999). Galectin-1 Regulates Initial Axonal Growth in Peripheral Nerves after Axotomy. The Journal of Neuroscience *19*, 9964–9974.

Horie, H., Kadoya, T., Hikawa, N., Sango, K., Inoue, H., Takeshita, K., Asawa, R., Hiroi, T., Sato, M., Yoshioka, T., et al. (2004). Oxidized Galectin-1 Stimulates Macrophages to Promote Axonal Regeneration in Peripheral Nerves after Axotomy. The Journal of Neuroscience *24*, 1873–1880.

Hökfelt, T., Elde, R., Johansson, O., Luft, R., Nilsson, G., and Arimura, A. (1976). Immunohistochemical Evidence for Separate Populations of Somatostatin-Containing and Substanc P-Containing Primary Afferent Neurons in the Rat. Neuroscience *1*, 131–136.

Hucho, T., and Levine, J.D. (2007). Signaling Pathways in Sensitization: Toward a Nociceptor Cell Biology. Neuron *55*, 365–376.

Hunt, S.P., and Mantyh, P.W. (2001). The Molecular Dynamics of Pain Control. Nature

Reviews: Neuroscience *2*, 83–91.

Hynes, M.A., Gitt, M., Barondes, S.H., Jessell, T.M., and Buck, L.B. (1990). Selective Expression of an Endogenous Lactose-Binding Lectin Gene in Subsets of Central and Peripheral Neurons. The Journal of Neuroscience *10*, 1004–1013.

Iggo, A., and Muir, A.R. (1969). The Structure and Function of a Slowly Adapting Touch Corpuscle in Hairy Skin. The Journal of Physiology *200*, 763–796.

Iggo, A., and Ogawa, H. (1977). Correlative Physiological and Morphological Studies of Rapidly Adapting Mechanoreceptors in Cat's Glabrous Skin. The Journal of Physiology *266*, 275–296.

Imming, P., Sinning, C., and Meyer, A. (2006). Drugs, their Targets and the Nature and Number of Drug Targets. Nature Reviews: Drug Discovery *5*, 821–834.

Indo, Y. (2001). Molecular Basis of Congenital Insensitivity to Pain With Anhidrosis (CIPA): Mutations and Polymorphisms in TRKA (NTRK1) Gene Encoding the Receptor Tyrosine Kinase for Nerve Growth Factor. Human Mutation *18*, 462–471.

Ingram, S.L., and Williams, J.T. (1994). Opioid Inhibition of Ih via Adenylyl Cyclase. Neuron *13*, 179–186.

Ingram, S.L., and Williams, J.T. (1996). Modulation of the Hyperpolarization-Activated Current (I_h) by Cyclic Nucleotides in Guinea-Pig Primary Afferent Neurons. The Journal of Physiology *492*, 97–106.

Ishii, T.M., Takano, M., and Ohmori, H. (2001). Determinants of Activation Kinetics in Mammalian Hyperpolarization-Activated Cation Channels. The Journal of Physiology *537*, 93–100.

Ishii, T.M., Takano, M., Xie, L.-H., Noma, A., and Ohmori, H. (1999). Molecular Characterization of the Hyperpolarization-Activated Cation Channel in Rabbit Heart Sinoatrial Node. The Journal of Biological Chemistry *274*, 12835–12839.

Jahromi, B.S., Robitaille, R., and Charlton, M.P. (1992). Transmitter Release Increases Intracellular Calcium in Perisynaptic Schwann Cells In Situ. Neuron *8*, 1069–1077.

Jakobsson, P.-J. (2010). How Macrophages Mediate Inflammatory Pain via ATP Signaling. Nature Publishing Group *6*, 679–681.

Jarvis, M.F., Honore, P., Shieh, C.-C., Chapman, M., Joshi, S.K., Zhang, X.-F., Fort, M., Carroll, W., Marron, B., Atkinson, R., et al. (2007). A-803467, a Potent and Selective $Na_v1.8$ Sodium Channel Blocker, Attenuates Neuropathic and Inflammatory Pain in the Rat. Proceedings of the National Academy of Sciences *104*, 8520–8525.

Jasmin, L., and O'Hara, P.T. (2004). Anatomical Identification of Neurons Responsive to Nociceptive Stimuli. In Pain Research, Z.D. Luo, ed. (Totowa, New Jersey: Humana Press), pp. 167–188.

Jensen, M.P., Karoly, P., and Braver, S. (1986). The Measurement of Clinical Pain Intensity: A Comparison of Six Methods. Pain *27*, 117–126.

Jensen, T.S., Baron, R., Haanpää, M., Kalso, E., Loeser, J.D., Rice, A.S.C., and Treede, R.-D. (2011). A New Definition of Neuropathic Pain. Pain *152*, 2204–2205.

Jeske, N.A., Por, E.D., Belugin, S., Chaudhury, S., Berg, K.A., Akopian, A.N., Henry, M.A., and Gomez, R. (2011). A-Kinase Anchoring Protein 150 Mediates Transient Receptor Potential Family V Type 1 Sensitivity to Phosphatidylinositol-4,5-Bisphosphate. The Journal of Neuroscience *31*, 8681–8688.

Jiang, Y.-Q., Xing, G.-G., Wang, S.-L., Tu, H.-Y., Chi, Y.-N., Li, J., Liu, F.-Y., Han, J.-S., and Wan, Y. (2008). Axonal Accumulation of Hyperpolarization-Activated Cyclic Nucleotide-Gated Cation Channels Contributes to Mechanical Allodynia after Peripheral Nerve Injury in Rats. Pain *137*, 495–506.

Jordt, S.-E., Bautista, D.M., Chuang, H.-H., McKemy, D.D., Zygmunt, P.M., Högestätt, E.D., Meng, I.D., and Julius, D. (2004). Mustard Oils and Cannabinoids Excite Sensory Nerve Fibres through the TRP Channel ANKTM1. Nature *427*, 260–265.

Jourdan, D., Ardid, D., and Eschalier, A. (2002). Analysis of Ultrasonic Vocalisation does not Allow Chronic Pain to be Evaluated in Rats. Pain *95*, 165–173.

Julius, D., and Basbaum, A.I. (2001). Molecular Mechanisms of Nociception. Nature *413*, 203–210.

Kaas, J.H. (2004). Somatosensory System. In The Human Nervous System, G. Paxinos, and J.K. Mai, eds. (Elseiver), pp. 1059–1092.

Kakigi, R., Endo, C., Neshige, R., Kuroda, Y., and Shibasaki, H. (1991). Estimation of Conduction Velocity of Aδ Fibers in Humans. Muscle Nerve *14*, 1193–1196.

Kang, D., and Kim, D. (2006). TREK-2 (K2P10.1) and TRESK (K2P18.1) are Major Background K^+ Channels in Dorsal Root Ganglion Neurons. American Journal of Physiology- Cell Physiology *291*, C138–C146.

Karashima, Y., Talavera, K., Everaerts, W., Janssens, A., Kwan, K.Y., Vennekens, R., Nilius, B., and Voets, T. (2009). TRPA1 Acts as a Cold Sensor in vitro and in vivo. Proceedings of the National Academy of Sciences *106*, 1273–1278.

Katikireddy, K.R., and O'Sullivan, F. (2011). Immunohistochemical and Immunofluorescence Procedures for Protein Analysis. In Gene Expression Profiling: Methods and Protocols, L. O'Driscoll, ed. (New York: Humana Press), pp. 155–167.

Kaupp, U.B., and Seifert, R. (2001). Molecular Diversity of Pacemaker Ion Channels. Annual Reviews of Physiology *63*, 235–257.

Kawate, T., Michel, J.C., Birdsong, W.T., and Gouaux, E. (2009). Crystal Structure of the ATP-Gated $P2X_4$ Ion Channel in the Closed State. Nature *460*, 592–598.

Kayser, V., and Guilbaud, G. (1987). Local and Remote Modifications of Nociceptive Sensitivity during Carrageenin-Induced Inflammation in the Rat. Pain *28*, 99–107.

Kehlet, H., Jensen, T.S., and Woolf, C.J. (2006). Persistent Postsurgical Pain: Risk Factors and Prevention. Lancet *367*, 1618–1625.

Kerekes, N., Landry, M., Rydh-Rinder, M., and Hökfelt, T. (1997). The Effect of NGF, BDNF and bFGF on Expression of Galanin in Cultured Rat Dorsal Root Ganglia. Brain Research *754*, 131–141.

Kim, K.-S., Lee, K.-W., Lee, K.-W., Im, J.-Y., Yoo, J.Y., Kim, S.-W., Lee, J.-K., Nestler, E.J., and Han, P.-L. (2006). Adenylyl Cyclase Type 5 (AC5) is an Essential Mediator of Morphine Action. Proceedings of the National Academy of Sciences *103*, 3908–3913.

Kim, K.J., Yoon, Y.W., and Chung, J.M. (1997). Comparison of Three Rodent Neuropathic Pain Models. Experimental Brain Research *113*, 200–206.

Kim, S.H., and Chung, J.M. (1992). An Experimental Model for Peripheral Neuropathy Produced by Segmental Spinal Nerve Ligation in the Rat. Pain *50*, 355–363.

King, T., Qu, C., Okun, A., Mercado, R., Ren, J., Brion, T., Lai, J., and Porreca, F. (2011). Contribution of Afferent Pathways to Nerve Injury-Induced Spontaneous Pain and Evoked Hypersensitivity. Pain *152*, 1997–2005.

King, T., Vera-Portocarrero, L., Gutierrez, T., Vanderah, T.W., Dussor, G., Lai, J., Fields, H.L., and Porreca, F. (2009). Unmasking the Tonic-Aversive State in Neuropathic Pain. Nature Neuroscience *12*, 1364–1366.

Kirschstein, T., Büsselberg, D., and Treede, R.-D. (1997). Coexpression of Heat-Evoked and Capsaicin-Evoked Inward Currents in Acutely Dissociated Rat Dorsal Root Ganglion Neurons. Neuroscience Letters *231*, 33–36.

Kitchener, P.D., Wilson, P., and Snow, P.J. (1993). Selective Labelling of Primary Sensory Afferent Terminals in Lamina II of the Dorsal Horn by Injection of Bandeiraea Simplicifolia Isolectin B4 into Peripheral Nerves. Neuroscience *54*, 545–551.

Klede, M., Handwerker, H.O., and Schmelz, M. (2003). Central Origin of Secondary Mechanical Hyperalgesia. Journal of Neurophysiology *90*, 353–359.

Knaus, A., Zong, X., Beetz, N., Jahns, R., Lohse, M.J., Biel, M., and Hein, L. (2007). Direct Inhibition of Cardiac Hyperpolarization-Activated Cyclic Nucleotide-Gated Pacemaker Channels by Clonidine. Circulation *115*, 872–880.

Knibestöl, M. (1973). Stimulus-Response Functions of Rapidly Adapting Mechanoreceptors in the Human Glabrous Skin Area. Journal of Physiology *232*, 427–452.

Kobayashi, K., Fukuoka, T., Obata, K., Yamanaka, H., Dai, Y., Tokunaga, A., and Noguchi, K. (2005). Distinct Expression of TRPM8, TRPA1, and TRPV1 mRNAs in Rat Primary Afferent Neurons with Aδ/c-Fibers and Colocalization with Trk Receptors. The Journal of Comparative Neurology *493*, 596–606.

Koch, U., Braun, M., Kapfer, C., and Grothe, B. (2004). Distribution of HCN1 and HCN2 in Rat Auditory Brainstem Nuclei. European Journal of Neuroscience *20*, 79–91.

Koeberle, A., and Werz, O. (2009). Inhibitors of the Microsomal Prostaglandin E2 Synthase-1 as Alternative to Non Steroidal Anti-Inflammatory Drugs (NSAIDs) - A Critical Review. Current Medicinal Chemistry *16*, 4274–4296.

Koltzenburg, M., Bennett, D.L.H., Shelton, D.L., and McMahon, S.B. (1999). Neutralization of Endogenous NGF Prevents the Sensitization of Nociceptors Supplying Inflamed Skin. European Journal of Neuroscience *11*, 1698–1704.

Koltzenburg, M., Torebjörk, H.E., and Wahren, L.K. (1994). Nociceptor Modulated Central Sensitization Causes Mechanical Hyperalgesia in Acute Chemogenic and Chronic Neuropathic Pain. Brain *117*, 579–591.

Komagiri, Y., and Kitamura, N. (2003). Effect of Intracellular Dialysis of ATP on the Hyperpolarization-Activated Cation Current in Rat Dorsal Root Ganglion Neurons. Journal of Neurophysiology *90*, 2115–2122.

Koschorke, G.M., Meyer, R.A., Tillman, D.B., and Campbell, J.N. (1991). Ectopic Excitability of Injured Nerves in Monkey: Entrained Responses to Vibratory Stimuli. Journal of Neurophysiology *65*, 693–701.

Kouranova, E.V., Strassle, B.W., Ring, R.H., Bowlby, M.R., and Vasilyev, D.V. (2008). Hyperpolarization-Activated Cylic Nucleotide-Gated Channel mRNA and Protein Expression in Large versus Small Diameter Dorsal Root Ganglion Neurons: Correlation with Hyperpolarization-Activated Current Gating. Neuroscience *153*, 1008–1019.

Krishtal, O. (2003). The ASICs: Signaling molecules? Modulators? Trends in Neurosciences *26*, 477–483.

Kunikata, T., Yamane, H., Segi, E., Matsuoka, T., Sugimoto, Y., Tanaka, S., Tanaka, H., Nagai, H., Ichikawa, A., and Narumiya, S. (2005). Suppression of Allergic Inflammation by the Prostaglandin E Receptor Subtype EP3. Nature Immunology *6*, 524–531.

Kwan, K.Y., Allchorne, A.J., Vollrath, M.A., Christensen, A.P., Zhang, D.-S., Woolf, C.J., and Corey, D.P. (2006). TRPA1 Contributes to Cold, Mechanical, and Chemical Nociception but Is Not Essential for Hair-Cell Transduction. Neuron *50*, 277–289.

Kwan, K.Y., Glazer, J.M., Corey, D.P., Rice, F.L., and Stucky, C.L. (2009). TRPA1 Modulates Mechanotransduction in Cutaneous Sensory Neurons. The Journal of Neuroscience *29*, 4808–4819.

Lai, H.C., and Jan, L.Y. (2006). The Distribution and Targeting of Neuronal Voltage-Gated Ion Channels. Nature Reviews: Neuroscience *7*, 548–562.

Lallemend, F., and Ernfors, P. (2012). Molecular Interactions Underlying the Specification of Sensory Neurons. Trends in Neurosciences *35*, 373–381.

LaMotte, R.H., and Campbell, J.N. (1978). Comparison of Responses of Warm and Nociceptive C-Fiber Afferents in Monkey with Human Judgments of Thermal Pain. Journal of Neurophysiology *41*, 509–528.

LaMotte, R.H., Shain, C.N., Simone, D.A., and Tsai, E.-F.P. (1991). Neurogenic Hyperalgesia: Psychophysical Studies of Underlying Mechanisms. Journal of Neurophysiology *66*, 190–211.

Lariviere, W.R., Chesler, E.J., and Mogil, J.S. (2001). Transgenic Studies of Pain and Analgesia: Mutation or Background Genotype? The Journal of Pharmacology and Experimental Therapeutics *297*, 467–473.

Larkman, P.M., Kelly, J.S., and Takahashi, T. (1995). Adenosine 3“:5” - Cyclic Monophosphate Mediates a 5-Hydroxytryptamine-Induced Response in Neonatal Rat Motoneurones. European Journal of Physiology *430*, 763–769.

Larson, A.A., Brown, D.R., el-Atrash, S., and Walser, M.M. (1986). Pain Threshold Changes in Adjuvant-Induced Inflammation: A Possible Model of Chronic Pain in the Mouse. Pharmacology, Biochemistry, and Behavior *24*, 49–53.

Lawson, J.J., McIlwrath, S.L., Woodbury, C.J., Davis, B.M., and Koerber, H.R. (2008). TRPV1 Unlike TRPV2 Is Restricted to a Subset of Mechanically Insensitive Cutaneous Nociceptors Responding to Heat. The Journal of Pain *9*, 298–308.

Lawson, S.N. (2002). Phenotype and Function of Somatic Primary Afferent Nociceptive Neurones with C-, Ad- or Aa/b-Fibres. Experimental Physiology *87*, 239–244.

Lawson, S.N., and Waddell, P.J. (1991). Soma Neurofilament Immunoreactivity is Related to Cell Size and Fibre Conduction Velocity in Rat Primary Sensory Neurons. Journal of Physiology *435*, 41–63.

Lawson, S.N., Crepps, B.A., and Perl, E.R. (1997). Relationship of Substance P to Afferent Characteristics of Dorsal Root Ganglion Neurones. Journal of Physiology *505*, 177–191.

Le Bars, D., and Cadden, S.W. (2007). What is a Wide-Dynamic-Range Cell? In The Senses: a Comprehensive Review, A.I. Basbaum, ed. (London: Academic Press), pp. 331–338.

Le Bars, D., Gozariu, M., and Cadden, S.W. (2001). Animal Models of Nociception. Pharmacological Reviews *53*, 597–652.

Lee, D.H., Chang, L., Sorkin, L.S., and Chaplan, S.R. (2005). Hyperpolarization-Activated, Cation-Nonselective, Cyclic Nucleotide-Modulated Channel Blockade Alleviates Mechanical Allodynia and Suppresses Ectopic Discharge in Spinal Nerve Ligated Rats. The Journal of Pain *6*, 417–424.

Lee, D.H., Iyengar, S., and Lodge, D. (2003). The Role of Uninjured Nerve in Spinal Nerve Ligated Rats Points to an Improved Animal Model of Neuropathic Pain. European Journal of Pain *7*, 473–479.

Leffler, A., Linte, R.M., Nau, C., Reeh, P., and Babes, A. (2007). A High-Threshold Heat-Activated Channel in Cultured Rat Dorsal Root Ganglion Neurons Resembles TRPV2 and is Blocked by Gadolinium. European Journal of Neuroscience *26*, 12–22.

Lev-Ram, V., and Ellisman, M.H. (1995). Axonal Activation-Induced Calcium Transients in Myelinating Schwann Cells, Sources, and Mechanisms. The Journal of Neuroscience *15*, 2628–2637.

Lever, I.J., Bradbury, E.J., Cunningham, J.R., Adelson, D.W., Jones, M.G., McMahon, S.B., Marvizón, J.C.G., and Malcangio, M. (2001). Brain-Derived Neurotrophic Factor Is Released in the Dorsal Horn by Distinctive Patterns of Afferent Fiber Stimulation. The Journal of Neuroscience *21*, 4469–4477.

Levitan, E.S., and Takimoto, K. (1998). Dynamic Regulation of K+ Channel Gene Expression in Differentiated Cells. Journal of Neurobiology *37*, 60–68.

Lewin, G.R., and Moshourab, R. (2004). Mechanosensation and Pain. Journal of Neurobiology *61*, 30–44.

Lewin, G.R., Rueff, A., and Mendell, L.M. (1994). Peripheral and Central Mechanisms of NGF-induced Hyperalgesia. European Journal of Neuroscience *6*, 1903–1912.

Lewis, A.S., Schwartz, E., Savio Chan, C., Noam, Y., Shin, M., Wadman, W.J., James Surmeier, D., Baram, T.Z., Macdonald, R.L., and Chetkovich, D.M. (2009). Alternatively Spliced Isoforms of TRIP8b Differentially Control h Channel Trafficking and Function. The Journal of Neuroscience *29*, 6250–6265.

Li, Y., Dorsi, M.J., Meyer, R.A., and Belzberg, A.J. (2000). Mechanical Hyperalgesia After an L5 Spinal Nerve Lesion in the Rat is not Dependent on Input from Injured Nerve Fibers. Pain 493–502.

Li, Y., Gamper, N., Hilgemann, D.W., and Shapiro, M.S. (2005). Regulation of Kv7 (KCNQ) K+ Channel Open Probability by Phosphatidylinositol 4,5-Bisphosphate. The Journal of Neuroscience *25*, 9825–9835.

Lima, D. (2007). Ascending Pathways: Anatomy and Physiology. In The Senses: a Comprehensive Review, A.I. Basbaum, ed. (London: Academic Press), pp. 477–526.

Lin, C.-R., Chuang, Y.-C., Cheng, J.-T., Wang, C.-J., and Yang, L.-C. (2002). Intrathecal Clonidine Decreases Spinal Nitric Oxide Release in a Rat Model of Complete Freund's Adjuvant Induced Inflammatory Pain. Inflammation *26*, 161–166.

Lin, M.T. (1981). Effects of Sodium Pentobarbital on Thermoregulatory Responses in the Rat. Neuropharmacology *20*, 693–698.

Liu, B., and Qin, F. (2005). Functional Control of Cold- and Menthol-Sensitive TRPM8 Ion Channels by Phosphatidylinositol 4,5-Bisphosphate. The Journal of Neuroscience *25*, 1674–1681.

Liu, C.-N., Wall, P.D., Ben-Dor, E., Michaelis, M., Amir, R., and Devor, M. (2000a). Tactile Allodynia in the Absence of C-Fiber Activation: Altered Firing Properties of DRG Neurons Following Spinal Nerve Injury. Pain *85*, 503–521.

Liu, X., Eschenfelder, S., Blenk, K.-H., Jänig, W., and Häbler, H.-J. (2000b). Spontaneous Activity of Axotomized Afferent Neurons After L5 Spinal Nerve Injury in Rats. Pain *84*, 309–318.

Lodish, H., Berk, A., Zipursky, S.L., Matsudaira, P., Baltimore, D., and Darnell, J. (2000). Chapter 21: Nerve Cells. In Molecular Cell Biology, (New York: W. H. Freeman and Company).

Loeser, J.D. IASP Taxonomy. International Association for the Study of Pain Press 209–214.

Lopshire, J.C., and Nicol, G.D. (1998). The cAMP Transduction Cascade Mediates the Prostaglandin E_2 Enhancement of the Capsaicin-Elicited Current in Rat Sensory Neurons: Whole-Cell and Single-Channel Studies. The Journal of Neuroscience *18*, 6081–6092.

Lörincz, A., Notomi, T., Tamás, G., Shigemoto, R., and Nusser, Z. (2002). Polarized and

Compartment-Dependent Distribution of HCN1 in Pyramidal Cell Dendrites. Nature Neuroscience *5*, 1185–1193.

Lubińska, L. (1977). Early Course of Wallerian Degeneration in Myelinated Fibres of the Rat Phrenic Nerve. Brain Research *130*, 47–63.

Ludwig, A., Zong, X., Jeglitsch, M., Hofmann, F., and Biel, M. (1998). A Family of Hyperpolarization-Activated Mammalian Cation Channels. Nature *393*, 587–591.

Ludwig, A., Zong, X., Steiber, J., Hullin, R., Hofmann, F., and Biel, M. (1999). Two Pacemaker Channels from Human Heart with Profoundly Different Activation Kinetics. The EMBO Journal *18*, 2323–2329.

Lukacs, V., Thyagarajan, B., Varnai, P., Balla, A., Balla, T., and Rohács, T. (2007). Dual Regulation of TRPV1 by Phosphoinositides. The Journal of Neuroscience *27*, 7070–7080.

Lumpkin, E.A., and Caterina, M.J. (2007). Mechanisms of Sensory Transduction in the Skin. Nature *445*, 858–865.

Luo, L., Chang, L., Brown, S.M., Ao, H., Lee, D.H., Higuera, E.S., Dubin, A.E., and Chaplan, S.R. (2007). Role of Peripheral Hyperpolarization-Activated Cyclic Nucleotide-Modulated Channel Pacemaker Channels in Acute and Chronic Pain Models in the Rat. Neuroscience *144*, 1477–1485.

Luo, W., Enomoto, H., Rice, F.L., Milbrandt, J., and Ginty, D.D. (2009). Molecular Identification of Rapidly Adapting Mechanoreceptors and Their Developmental Dependence on Ret Signaling. Neuron *64*, 841–856.

Lynn, B., and Carpenter, S.E. (1982). Primary Afferent Units from the Hairy Skin of the Rat Hind Limb. Brain Research *238*, 29–43.

Lyu, Y.S., Park, S.K., Chung, K., and Chung, J.M. (2000). Low Dose of Tetrodotoxin Reduces Neuropathic Pain Behaviors in an Animal Model. Brain Research *871*, 98–103.

Ma, C., Shu, Y., Zheng, Z., Chen, Y., Yao, H., Greenquist, K.W., White, F.A., and LaMotte, R.H. (2002). Similar Electrophysiological Changes in Axotomized and Neighboring Intact Dorsal Root Ganglion Neurons. Journal of Neurophysiology *89*, 1588–1602.

Ma, W., and Eisenach, J.C. (2002). Morphological and Pharmacological Evidence for the Role of Peripheral Prostaglandins in the Pathogenesis of Neuropathic Pain. European Journal of Neuroscience *15*, 1037–1047.

Ma, W., and Eisenach, J.C. (2003). Four PGE2 EP Receptors are Up-Regulated in Injured Nerve following Partial Sciatic Nerve Ligation. Experimental Neurology *183*, 581–592.

Ma, W., and Quirion, R. (2008). Does COX2-Dependent PGE2 Play a Role in Neuropathic Pain? Neuroscience Letters *437*, 165–169.

Ma, W., Chabot, J.-G., Vercauteren, F., and Quirion, R. (2010). Injured Nerve-Derived COX2/PGE2 Contributes to the Maintenance of Neuropathic Pain in Aged Rats. Neurobiology of Aging *31*, 1227–1237.

Ma, W., St-Jacques, B., and Cruz Duarte, P. (2012). Targeting Pain Mediators Induced by

Injured Nerve-Derived COX2 and PGE2 to Treat Neuropathic Pain. Expert Opinion on Therapeutic Targets *16*, 527–540.

Mabuchi, T., Kojima, H., Abe, T., Takagi, K., Sakurai, M., Ohmiya, Y., Uematsu, S., Akira, S., Watanabe, K., and Ito, S. (2004). Membrane-Associated Prostaglandin E Synthase-1 is Required for Neuropathic Pain. Neuroreport *15*, 1395–1398.

Maccaferri, G., Mangoni, M., Lazzari, A., and DiFrancesco, D. (1993). Properties of the Hyperpolarization-Activated Current in Rat Hippocampal CA1 Pyramidal Cells. The Journal of Neurophysiology *69*, 2129–2136.

MacFarlane, B.V., Wright, A., O'Callaghan, J., and Benson, H.A.E. (1997). Chronic Neuropathic Pain and Its Control by Drugs. Pharmacology and Therapeutics *75*, 1–19.

Macpherson, L.J., Dubin, A.E., Evans, M.J., Marr, F., Schultz, P.G., Cravatt, B.F., and Patapoutian, A. (2007). Noxious Compounds Activate TRPA1 Ion Channels Through Covalent Modification of Cysteines. Nature *445*, 541–545.

Malin, S.A., Molliver, D.C., Koerber, H.R., Cornuet, P., Frye, R., Albers, K.M., and Davis, B.M. (2006). Glial Cell Line-Derived Neurotrophic Factor Family Members Sensitize Nociceptors In Vitro and Produce Thermal Hyperalgesia In Vivo. The Journal of Neuroscience *26*, 8588–8599.

Mamet, J., Baron, A., Lazdunski, M., and Voilley, N. (2002). ProInflammatory Mediators, Stimulators of Sensory Neuron Excitability via the Expression of Acid-Sensing Ion Channels. The Journal of Neuroscience *22*, 10662–10670.

Mandolesi, G., Madeddu, F., Bozzi, Y., Maffei, L., and Ratto, G.M. (2004). Acute Physiological Response of Mammalian Central Neurons to Axotomy: Ionic Regulation and Electrical Activity. The FASEB Journal *18*, 1934–1936.

Marker, C.L., Stoffel, M., and Wickman, K. (2004). Spinal G-Protein-Gated K+ Channels Formed by GIRK1 and GIRK2 Subunits Modulate Thermal Nociception and Contribute to Morphine Analgesia. The Journal of Neuroscience *24*, 2806–2812.

Marsh, B., Acosta, C., Djouhri, L., and Lawson, S.N. (2012). Leak K+ Channel mRNAs in Dorsal Root Ganglia: Relation to Inflammation and Spontaneous Pain Behaviour. Molecular and Cellular Neuroscience *49*, 375–386.

Martinez, V., Christensen, D., and Kayser, V. (2002). The Glycine/NMDA Receptor Antagonist (+)-HA966 Enhances the Peripheral Effect of Morphine in Neuropathic Rats. Pain *99*, 537–545.

Matsuyoshi, H., Masuda, N., Chancellor, M.B., Erickson, V.L., Hirao, Y., de Groat, W.C., Wanaka, A., and Yoshimura, N. (2006). Expression of Hyperpolarization-Activated Cyclic Nucleotide-Gated Cation Channels in Rat Dorsal Root Ganglion Neurons Innervating Urinary Bladder. Brain Research *1119*, 115–123.

Maves, T.J., Pechman, P.S., Gebhart, G.F., and Meller, S.T. (1993). Possible Chemical Contribution from Chromic Gut Sutures Produces Disorders of Pain Sensation Like those Seen in Man. Pain *54*, 57–69.

Mayer, M.L., and Westbrook, G.L. (1983). A Voltage-Clamp Analysis of Inward

(Anomalous) Rectification in Mouse Spinal Sensory Ganglion Neurones. The Journal of Physiology *340*, 19–45.

McCarthy, P.W., and Lawson, S.N. (1990). Cell Type and Conduction Velocity of Rat Primary Sensory Neurons with Calcitonin Gene-Related Peptide-Like Immunoreactivity. Neuroscience *34*, 623–632.

McCleskey, E.W., and Gold, M.S. (1999). Ion Channels of Nociception. Annual Reviews of Physiology *61*, 835–856.

McKellar, G., Madhok, R., and Singh, G. (2007). The Problem with NSAIDs: What Data to Believe? Current Pain and Headache Reports *11*, 423–427.

McKemy, D.D., Neuhausser, W.M., and Julius, D. (2002). Identification of a Cold Receptor Reveals a General Role for TRP Channels in Thermosensation. Nature *416*, 52–58.

McKenzie, F.R., and Milligan, G. (1990). δ-Opioid-Receptor-Mediated Inhibition of Adenylate Cyclase is Transduced Specifically by the Guanine-Nucleotide-Binding Protein G_i2. Biochemical Journal *267*, 391.

McMahon, S.B., and Malcangio, M. (2009). Current Challenges in Glia-Pain Biology. Neuron *64*, 46–54.

McMahon, S.B., Bennett, D.L.H., and Bevan, S. (2005a). Inflammatory Mediators and Modulators of Pain. In Textbook of Pain, (Churchill Livingstone), pp. 49–72.

McMahon, S.B., Cafferty, W.B.J., and Marchand, F. (2005b). Immune and Glial Cell Factors as Pain Mediators and Modulators. Experimental Neurology *192*, 444–462.

Melchiorre, M., Del Lungo, M., Guandalini, L., Martini, E., Dei, S., Manetti, D., Scapecchi, S., Teodori, E., Sartiani, L., Mugelli, A., et al. (2010). Design, Synthesis, and Preliminary Biological Evaluation of New Isoform-Selective f-Current Blockers. Journal of Medicinal Chemistry *53*, 6773–6777.

Meller, S.T., and Gebhart, G.F. (1993). Nitric Oxide (NO) and Nociceptive Processing in the Spinal Cord. Pain *52*, 127–136.

Melzack, R., and Wall, P.D. (1965). Pain Mechanisms: A New Theory. Science *150*, 971–979.

Messinger, R.B., Naik, A.K., Jagodic, M.M., Nelson, M.T., Lee, W.Y., Choe, W.J., Orestes, P., Latham, J.R., Todorovic, S.M., and Jevtovic-Todorovic, V. (2009). *In Vivo* Silencing of the $Ca_V3.2$ T-Type Calcium Channels in Sensory Neurons Alleviates Hyperalgesia in Rats with Streptozocin-Induced Diabetic Neuropathy. Pain *145*, 184–195.

Meuth, S.G., Kanyshkova, T., Meuth, P., Landgraf, P., Munsch, T., Ludwig, A., Hofmann, F., Pape, H.-C., and Budde, T. (2006). Membrane Resting Potential of Thalamocortical Relay Neurons Is Shaped by the Interaction Among TASK3 and HCN2 Channels. Journal of Neurophysiology *96*, 1517–1529.

Meyer, R.A., Davis, K.D., Cohen, R.H., Treede, R.-D., and Campbell, J.N. (1991). Mechanically Insensitive Afferents (MIAs) in Cutaneous Nerves of Monkey. Brain Research *561*, 252–261.

Meyer, R.A., Ringkamp, M., Campbell, J.N., and Raja, S.N. (2005). Peripheral Mechanisms of Cutaneous Nociception. In Textbook of Pain, (Churchill Livingstone), pp. 1–34.

Miledi, R., and Slater, C.R. (1970). On the Degeneration of Rat Neuromuscular Junctions after Nerve Section. The Journal of Physiology *207*, 507–528.

Millan, M.J. (1999). The Induction of Pain: An Integrative Review. Progress in Neurobiology *57*, 1–164.

Milligan, C.J., Edwards, I.J., and Deuchars, J. (2006). HCN1 Ion Channel Immunoreactivity in Spinal Cord and Medulla Oblongata. Brain Research *1081*, 79–91.

Milligan, E.D., and Watkins, L.R. (2009). Pathological and Protective Roles of Glia in Chronic Pain. Nature Reviews: Neuroscience *10*, 23–36.

Ming, G.-L., Henley, J., Tessier-Lavigne, M., Song, H.-J., and Poo, M.-M. (2001). Electrical Activity Modulates Growth Cone Guidance by Diffusible Factors. Neuron *29*, 441–452.

Ming, G.-L., Song, H.-J., Berninger, B., Holt, C.E., Tessier-Lavigne, M., and Poo, M.-M. (1997). cAMP-Dependent Growth Cone Guidance by Netrin-1. Neuron *19*, 1225–1235.

Mire, E., Mezzera, C., Leyva-Díaz, E., Paternain, A.V., Squarzoni, P., Bluy, L., Castillo-Paterna, M., López, M.J., Peregrín, S., Tessier-Lavigne, M., et al. (2012). Spontaneous Activity Regulates Robo1 Transcription to Mediate a Switch in Thalamocortical Axon Growth. Nature Neuroscience 1–12.

Mitchell, S.W. (1872). Injuries of Nerves and their Consequences. The American Journal of Medical Sciences *64*, 229–232.

Mogil, J.S. (2009). Animal Models of Pain: Progress and Challenges. Nature Reviews: Neuroscience *10*, 283–294.

Mogil, J.S., and Chanda, M.L. (2005). The Case for the Inclusion of Female Subjects in Basic Science Studies of Pain. Pain *117*, 1–5.

Mogil, J.S., and Crager, S.E. (2004). What Should we be Measuring in Behavioral Studies of Chronic Pain in Animals? Pain *112*, 12–15.

Molliver, D.C., Wright, D.E., Leitner, M.L., Parsadanian, A.S., Doster, K., Wen, D., Yan, Q., and Snider, W.D. (1997). IB4-Binding DRG Neurons Switch from NGF to GDNF Dependence in Early Postnatal Life. Neuron *19*, 849–861.

Momin, A., Cadiou, H., Mason, A., and McNaughton, P.A. (2008). Role of the Hyperpolarization-Activated Current I_h in Somatosenosry Neurons. Journal of Physiology *586*, 5911–5929.

Montell, C. (2005). The TRP Superfamily of Cation Channels. Science STKE *272*, 1–24.

Mountcastle, V.B. (1957). Modality and Topographic Properties of Single Neurons of Cat's Somatic Sensory Cortex. Journal of Neurophysiology *20*, 408–434.

Much, B., Wahl-Schott, C., Zong, X., Schneider, A., Baumann, L., Moosmang, S., Ludwig, A., and Biel, M. (2003). Role of Subunit Heteromerization and N-Linked Glycosylation in

the Formation of Functional Hyperpolarization-Activated Cyclic Nucleotide-Gated Channels. The Journal of Biological Chemistry *278*, 43781–43786.

Munsch, T., and Pape, H.-C. (1999). Upregulation of the Hyperpolarization-Activated Cation Current in Rat Thalamic Relay Neurones by Acetazolamide. The Journal of Physiology *519*, 505–514.

Nagata, K., Duggan, A., Kumar, G., and García-Añoveros, J. (2005). Nociceptor and Hair Cell Transducer Properties of TRPA1, a Channel for Pain and Hearing. The Journal of Neuroscience *25*, 4052–4061.

Nagy, I., and Rang, H.P. (1999). Similarities and Differences Between the Responses of Rat Sensory Neurons to Noxious Heat and Capsaicin. The Journal of Neuroscience *19*, 10647–10655.

Nagy, J.I., and Hunt, S.P. (1982). Fluoride-Resistant Acid Phosphatase-Containing Neurones in Dorsal Root Ganglia are Separate from those Containing Substance P or Somatostatin. Neuroscience *7*, 89–97.

Namba, T., Sugimoto, Y., Negishi, M., Irie, A., Ushikubi, F., Kakizuka, A., Ito, S., Ichikawa, A., and Narumiya, S. (1993). Alternative Splicing of C-Terminal Tail of Prostaglandin E Receptor Subtype EP3 Determines G-protein Specificity. Nature *365*, 166–170.

Nassar, M.A., Baker, M.D., Levato, A., Ingram, R., Mallucci, G., McMahon, S.B., and Wood, J.N. (2006). Nerve Injury Induces Robust Allodynia and Ectopic Discharges in Nav1.3 Null Mutant Mice. Molecular Pain *2*, 33.

Nassar, M.A., Levato, A., Stirling, L.C., and Wood, J.N. (2005). Neuropathic Pain Develops Normally in Mice Lacking Both Nav1.7 and Nav1.8. Molecular Pain *1*, 24.

Nathan, C. (2002). Points of Control in Inflammation. Nature *420*, 846–852.

Nave, K.-A. (2010). Myelination and the Trophic Support of Long Axons. Nature Reviews: Neuroscience *11*, 275–283.

Nernst, W. (1888). Zur Kinetik der in Lösung Befindlichen Körper. Z Phys Chem.

Neumann, S., Bradke, F., Tessier-Lavigne, M., and Basbaum, A.I. (2002). Regeneration of Sensory Axons within the Injured Spinal Cord Induced by Intraganglionic cAMP Elevation. Neuron *34*, 885–893.

Nightingale, S. (2012). The Neuropathic Pain Market. Nature Reviews: Drug Discovery *11*, 101–102.

Nordin, M. (1990). Low-Threshold Mechanoreceptive and Nociceptive Units with Unmyelinated (C) Fibres in the Human Supraorbital Nerve. Journal of Physiology *426*, 229–240.

Notomi, T., and Shigemoto, R. (2004). Immunohistochemical Localization of I_h Channel Subunits, HCN1-4, in the Rat Brain. The Journal of Comparative Neurology *471*, 241–276.

Obata, K., Katsura, H., Mizushima, T., Yamanaka, H., Kobayashi, K., Dai, Y., Fukoka, T., Tokunaga, A., Tominaga, M., and Noguchi, K. (2005). TRPA1 Induced in Sensory Neurons

Contributes to Cold Hyperalgesia after Inflammation and Nerve Injury. Journal of Clinical Investigation *115*, 2393–2401.

Obreja, O., Klusch, A., Ponelies, N., Schmelz, M., and Petersen, M. (2008). A Subpopulation of Capsaicin-Sensitive Porcine Dorsal Root Ganglion Neurons is Lacking Hyperpolarization-Activated Cyclic Nucleotide-Gated Channels. European Journal of Pain *12*, 775–789.

Ocaña, M., Cendan, C.M., Cobos, E.J., Entrena, J.M., and Baeyens, J.M. (2004). Potassium Channels and Pain: Present Realities and Future Opportunities. European Journal of Pharmacology *500*, 203–219.

Olausson, H., Cole, J., Rylander, K., McGlone, F., Lamarre, Y., Wallin, B.G., Krämer, H., Wessberg, J., Elam, M., Bushnell, M.C., et al. (2007). Functional Role of Unmyelinated Tactile Afferents in Human Hairy Skin: Sympathetic Response and Perceptual Localization. Experimental Brain Research *184*, 135–140.

Olausson, H., Wessberg, J., Morrison, I., McGlone, F., and Vallbo, Å. (2010). The Neurophysiology of Unmyelinated Tactile Afferents. Neuroscience & Biobehavioral Reviews *34*, 185–191.

Olsson, Y. (1968). Topographical Differences in the Vascular Permeability of the Peripheral Nervous System. Acta Neuropathologica *10*, 26–33.

Omana-Zapata, I., Khabbaz, M.A., Hunter, J.C., Clarke, D.E., and Bley, K.R. (1997). Tetrodotoxin Inhibits Neuropathic Ectopic Activity in Neuromas, Dorsal Root Ganglia and Dorsal Horn Neurons. Pain *72*, 41–49.

Orio, P., Madrid, R., la Peña, de, E., Parra, A., Meseguer, V., Bayliss, D.A., Belmonte, C., and Viana, F. (2009). Characteristics and Physiological Role of Hyperpolarization Activated Currents in Mouse Cold Thermoreceptors. The Journal of Physiology *587*, 1961–1976.

Pakkenberg, B., Pelvig, D., Marner, L., Bundgaard, M.J., Gundersen, H.J.G., Nyengaard, J.R., and Regeur, L. (2003). Aging and the Human Neocortex. Experimental Gerontology *38*, 95–99.

Pape, H.-C., and McCormick, D.A. (1989). Noradrenaline and Serotonin Selectively Modulate Thalamic Burst Firing by Enhancing a Hyperpolarization-Activated Cation Current. Nature *340*, 715–718.

Papp, I., Holló, K., and Antal, M. (2010). Plasticity of Hyperpolarization-Activated and Cyclic Nucleotide-Gated Cation Channel Subunit 2 Expression in the Spinal Dorsal Horn in Inflammatory Pain. European Journal of Neuroscience *32*, 1193–1201.

Paré, M., Smith, A.M., and Rice, F.L. (2002). Distribution and Terminal Arborizations of Cutaneous Mechanoreceptors in the Glabrous Finger Pads of the Monkey. The Journal of Comparative Neurology *445*, 347–359.

Passmore, G.M., Selyanko, A.A., Mistry, M., Al-Qatari, M., Marsh, S.J., Matthews, E.A., Dickenson, A.H., Brown, T.A., Burbidge, S.A., Main, M., et al. (2003). KCNQ/M Currents in Sensory Neurons: Significance for Pain Therapy. The Journal of Neuroscience *23*, 7227–7236.

Patapoutian, A., Tate, S., and Woolf, C.J. (2009). Transient Receptor Potential Channels: Targeting Pain at the Source. Nature Reviews: Drug Discovery *8*, 55–68.

Patel, L., and Lindley, C. (2003). Aprepitant - A Novel NK1-Receptor Antagonist. Expert Opin on Pharmacotherapy *4*, 2279–2296.

Peier, A.M., Moqrich, A., Hergarden, A.C., Reeve, A.J., Andersson, D.A., Story, G.M., Earley, T.J., Dragoni, I., McIntyre, P., Bevan, S., et al. (2002). A TRP Channel that Senses Cold Stimuli and Menthol. Cell *108*, 705–715.

Pennacchio, L.A., Ahituv, N., Moses, A.M., Prabhakar, S., Nobrega, M.A., Shoukry, M., Minovitsky, S., Dubchak, I., Holt, A., Lewis, K.D., et al. (2006). In Vivo Enhancer Analysis of Human Conserved Non-Coding Sequences. Nature *444*, 499–502.

Perl, E.R. (1996). Cutaneous Polymodal Receptors: Characteristics and Plasticity. Progress in Brain Research *113*, 21–37.

Perl, E.R. (2007). Ideas About Pain, a Historical View. Nature Reviews: Neuroscience *8*, 71–80.

Perry, G.W., and Wilson, D.L. (1981). Protein Synthesis and Axonal Transport During Nerve Regeneration. Journal of Neurochemistry *37*, 1203–1217.

Perry, V.H., Brown, M.C., and Gordon, S. (1987). The Macrophage Response to Central and Peripheral Nerve Injury. A Possible Role for Macrophages in Regeneration. The Journal of Experimental Medicine *165*, 1218–1223.

Pian, P., Bucchi, A., Robinson, R.B., and Siegelbaum, S.A. (2006). Regulation of Gating and Rundown of HCN Hyperpolarization-activated Channels by Exogenous and Endogenous PIP2. The Journal of General Physiology *128*, 593–604.

Piccini, A., Carta, S., Tassi, S., Lasiglié, D., Fossati, G., and Rubartelli, A. (2008). ATP is Released by Monocytes Stimulated with Pathogen-Sensing Receptor Ligands and Induces IL-1β and IL-18 Secretion in an Autocrine Way. Proceedings of the National Academy of Sciences *105*, 8067.

Piskorowski, R., Santoro, B., and Siegelbaum, S.A. (2011). TRIP8b Splice Forms Act in Concert to Regulate the Localization and Expression of HCN1 Channels in CA1 Pyramidal Neurons. Neuron *70*, 495–509.

Pizzo, P.A., Clark, N.M., Carter-Pokras, O., Christopher, M., Farrar, J.T., Follett, K.A., Heitkemper, M.M., Inturrisi, C., Keefe, F., Kerns, R.D., et al. (2011). Relieving Pain in America. Institute of Medicine of the National Academies 1–4.

Poolos, N.P., Bullis, J.B., and Roth, M.K. (2006). Modulation of h-Channels in Hippocampal Pyramidal Neurons by p38 Mitogen-Activated Protein Kinase. The Journal of Neuroscience *26*, 7995–8003.

Porreca, F., Lai, J., Bian, D., Wegert, S., Ossipov, M.H., Eglen, R.M., Kassotakis, L., Novakovic, S., Rabert, D.K., Sangameswaran, L., et al. (1999). A Comparison of the Potential Role of the Tetrodotoxin-Insensitive Sodium Channels, PN3/SNS and NaN/SNS2, in Rat Models of Chronic Pain. Proceedings of the National Academy of Sciences *96*, 7640–7644.

Portanova, J.P., Zhang, Y., Anderson, G.D., Hauser, S.D., Masferrer, J.L., Seibert, K., Gregory, S.A., and Isakson, P.C. (1996). Selective Neutralization of Prostaglandin E_2 Blocks Inflammation, Hyperalgesia, and Interleukin 6 Production In Vivo. The Journal of Experimental Medicine *184*, 883–891.

Postea, O., and Biel, M. (2011). Exploring HCN Channels as Novel Drug Targets. Nature Reviews: Drug Discovery *10*, 903–914.

Prescott, E.D., and Julius, D. (2003). A Modular PIP_2 Binding Site as a Determinant of Capsaicin Receptor Sensitivity. Science *300*, 1284–1288.

Puig, S., and Sorkin, L.S. (1995). Formalin-Evoked Activity in Identified Primary Afferent Fibers: Systemic Lidocaine Suppresses Phase-2 Activity. Pain *64*, 345–355.

Rabert, D.K., Koch, B.D., Ilnicka, M., Obernolte, R.A., Naylor, S.L., Herman, R.C., Eglen, R.M., Hunter, J.C., and Sangameswaran, L. (1998). A Tetrodotoxin-Resistant Voltage-Gated Sodium Channel from Human Dorsal Root Ganglia, hPN3/SCN10A. Pain *78*, 107–114.

Rang, H.P., Bevan, S., and Dray, A. (1991). Chemical Activation of Nociceptive Peripheral Neurones. British Medical Bulletin *47*, 534–548.

Rasband, M.N., Park, E.W., Vanderah, T.W., Lai, J., Porreca, F., and Trimmer, J.S. (2001). Distinct Potassium Channels on Pain-Sensing Neurons. Proceedings of the National Academy of Sciences *23*, 13373–13378.

Ray, W.A., Stein, C.M., Daugherty, J.R., Hall, K., Arbogast, P.G., and Griffin, M.R. (2002). COX-2 Selective Non-Steroidal Anti-Inflammatory Drugs and Risk of Serious Coronary Heart Disease. Lancet *360*, 1071–1073.

Regan, L.J., Dodd, J., Barondes, S.H., and Jessell, T.M. (1986). Selective Expression of Endogenous Lactose-Binding Lectins and Lactoseries Glycoconjugates in Subsets of Rat Sensory Neurons. Proceedings of the National Academy of Sciences *83*, 2248–2252.

Reid, G., and Flonta, M.-L. (2001). Cold Current in Thermoreceptive Neurons. Nature *413*, 1–1.

Reist, N.E., and Smith, S.J. (1992). Neurally Evoked Calcium Transients in Terminal Schwann Cells at the Neuromuscular Junction. Proceedings of the National Academy of Sciences *89*, 7625–7629.

Renganathan, M., Cummins, T.R., and Waxman, S.G. (2001). Contribution of $Na_v1.8$ Sodium Channels to Action Potential Electrogenesis in DRG Neurons. Journal of Neurophysiology *86*, 629–640.

Rexed, B. (1952). The Cytoarchitectonic Organization of the Spinal Cord in the Cat. The Journal of Comparative Neurology *96*, 414–495.

Rice, A.S.C., and Hill, R.G. (2006). New Treatments for Neuropathic Pain. Annual Reviews of Medicine *57*, 535–551.

Rice, A.S.C., Cimino-Brown, D., Eisenach, J.C., Kontinen, V.K., Lacroix-Fralish, M.L., Machin, I., Mogil, J.S., and Stöhr, T. (2008). Animal Models and the Prediction of Efficacy

in Clinical Trials of Analgesic Drugs: A Critical Appraisal and Call for Uniform Reporting Standards. Pain *139*, 243–247.

Ringkamp, M., and Meyer, R.A. (2007). Physiology of Nociceptors. In The Senses: a Comprehensive Review, A.I. Basbaum, ed. (London: Academic Press), pp. 97–114.

Rishal, I., and Fainzilber, M. (2010). Retrograde Signaling in Axonal Regeneration. Experimental Neurology *223*, 5–10.

Rochon, D., Isabelle, R., and Robitaille, R. (2001). Synapse–Glia Interactions at the Mammalian Neuromuscular Junction. The Journal of Neuroscience *21*, 3819–3829.

Rodrigues, A.R.A., and Oertel, D. (2006). Hyperpolarization-Activated Currents Regulate Excitability in Stellate Cells of the Mammalian Ventral Cochlear Nucleus. Journal of Neurophysiology *95*, 76–87.

Runnels, L.W., Yue, L., and Clapham, D.E. (2002). The TRPM7 Channel is Inactivated by PIP_2 Hydrolysis. Nature Cell Biology *4*, 329–336.

Said, G., and Hontebeyrie-Joskowicz, M. (1992). Nerve Lesions Induced by Macrophage Activation. Research in Immunology *143*, 589–599.

Samuelsson, B., Morgenstern, R., and Jakobsson, P.-J. (2007). Membrane Prostaglandin E Synthase-1: A Novel Therapeutic Target. Pharmacological Reviews *59*, 207–224.

Sangameswaran, L., Delgado, S.G., Fish, L.M., Koch, B.D., Jakeman, L.B., Stewart, G.R., Sze, P., Hunter, J.C., Eglen, R.M., and Herman, R.C. (1996). Structure and Function of a Novel Voltage-Gated Tetrodotoxin-Resistant Sodium Channel Specific to Sensory Neurons. The Journal of Biological Chemistry *271*, 5953–5956.

Santoro, B., Chen, S., Lüthi, A., Pavlidis, P., Shumyatasky, G.P., Tibbs, G.R., and Siegelbaum, S.A. (2000). Molecular and Functional Heterogeneity of Hyperpolarization-Activated Pacemaker Channels in the Mouse CNS. The Journal of Neuroscience *20*, 5264–525275.

Santoro, B., Grant, S.G.N., Bartsch, D., and Kandel, E.R. (1997). Interactive Cloning with the SH3 Domain of N-src Identifies a New Brain Specific Ion Channel Protein, with Homology to Eag and Cyclic Nucleotide-Gated Channels. Proceedings of the National Academy of Science *94*, 14815–14820.

Santoro, B., Liu, D.T., Yao, H., Bartsch, D., Kandel, E.R., Siegelbaum, S.A., and Tibbs, G.R. (1998). Identification of a Gene Encoding a Hyperpolarization-Activated Pacemaker Channel of Brain. Cell *93*, 717–729.

Santoro, B., Piskorowski, R.A., Pian, P., Hu, L., Liu, H., and Siegelbaum, S.A. (2009). TRIP8b Splice Variants Form a Family of Auxiliary Subunits that Regulate Gating and Trafficking of HCN Channels in the Brain. Neuron *62*, 802–813.

Santoro, B., Wainger, B.J., and Siegelbaum, S.A. (2004). Regulation of HCN Channel Surface Expression by a Novel C-Terminal Protein-Protein Interaction. The Journal of Neuroscience *24*, 10750–10762.

Sato, A., Sato, Y., and Suzuki, H. (1985). Aging Effects on Conduction Velocities of

Myelinated and Unmyelinated Fibres of Peripheral Nerves. Neuroscience Letters *53*, 15–20.

Sawynok, J. (2005). Topical Analgesics in Neuropathic Pain. Current Pharmaceutical Design *11*, 2995–3004.

Scannell, J.W., Blanckley, A., Boldon, H., and Warrington, B. (2012). Diagnosing the Decline in Pharmaceutical R&D Efficiency. Nature Reviews: Drug Discovery *11*, 191–200.

Schabile, H.-G., and Schmidt, R.F. (1985). Effects of an Experimental Arthritis on the Sensory Properties. Journal of Neurophysiology *54*, 1109–1122.

Schaible, H.-G., and Schmidt, R.F. (1983a). Activation of Groups III and IV Sensory Units in Medial Articular Nerve. Journal of Neurophysiology *49*, 35–44.

Schaible, H.-G., and Schmidt, R.F. (1983b). Responses of Fine Medial Articular Nerve Afferents to Passive Movements of Knee Joint. Journal of Neurophysiology *49*, 1118–1126.

Schaible, H.-G., and Schmidt, R.F. (1988). Time Course of Mechanosensitivity Changes in Articular Afferents During a Developing Experimental Arthritis. Journal of Neurophysiology *60*, 2180–2195.

Schäfers, M., and Cain, D. (2004). Single-Fiber Recording: In Vivo and In Vitro Preparations. In Pain Research, Z.D. Luo, ed. (Totowa, New Jersey: Humana Press), pp. 155–166.

Schäfers, M., Lee, D.H., Brors, D., Yaksh, T.L., and Sorkin, L.S. (2003). Increased Sensitivity of Injured and Adjacent Uninjured Rat Primary Sensory Neurons to Exogenous Tumor Necrosis Factor-α After Spinal Nerve Ligation. The Journal of Neuroscience *23*, 3028–3038.

Schepelmann, K., MeBlinger, K., and Schmidt, R.F. (1993). The Effects of Phorbol Ester on Slowly Conducting Afferents of the Cat's Knee Joint. Experimental Brain Research *92*, 391–391398.

Schepelmann, K., MeBlinger, K., Schaible, H.-G., and Schmidt, R.F. (1992). Inflammatory Mediators and Nociception in the Joint: Excitation and Sensitization of Slowly Conducting Afferent Fibres of Cat's Knee by Prostaglandin I2. Neuroscience *50*, 237–247.

Scherrer, G., Imamachi, N., Cao, Y.-Q., Contet, C., Mennicken, F., O'Donnell, D., Kieffer, B.L., and Basbaum, A.I. (2009). Dissociation of the Opioid Receptor Mechanisms that Control Mechanical and Heat Pain. Cell *137*, 1148–1159.

Schmidt, R., Schmelz, M., Forster, C., Ringkamp, M., Torebjörk, E., and Handwerker, H. (1995). Novel Classes of Responsive and Unresponsive C Nociceptors in Human Skin. The Journal of Neuroscience *15*, 333–341.

Schnizler, K., Shutov, L.P., Van Kanegan, M.J., Merrill, M.A., Nichols, B., McKnight, G.S., Strack, S., Hell, J.W., and Usachev, Y.M. (2008). Protein Kinase A Anchoring via AKAP150 Is Essential for TRPV1 Modulation by Forskolin and Prostaglandin E_2 in Mouse Sensory Neurons. The Journal of Neuroscience *28*, 4904–4917.

Schnorr, S., Eberhardt, M., Reeh, P., Ludwig, A., and Herrmann, S. (2012). The Role of HCN2 in Neuropathic and Inflammatory Pain. Naunyn-Schmiedeberg's Arch Pharmacol *385*, 1–116.

Scholz, J., and Woolf, C.J. (2002). Can We Conquer Pain? Nature Neuroscience *5*, 1062–1067.

Scholz, J., and Woolf, C.J. (2007). The Neuropathic Pain Triad: Neurons, Immune Cells and Glia. Nature Neuroscience *10*, 1361–1368.

Scroggs, R.S., Todorovic, S.M., Anderson, E.G., and Fox, A.P. (1994). Variation in I_H, I_{IR}, and I_{LEAK} Between Acutely Isolated Adult Rat Dorsal Root Ganglion Neurons of Different Size. The Journal of Neurophysiology *71*, 271–279.

Seal, R.P., Wang, X., Guan, Y., Raja, S.N., Woodbury, C.J., Basbaum, A.I., and Edwards, R.H. (2009). Injury-Induced Mechanical Hypersensitivity Requires C-Low Threshold Mechanoreceptors. Nature *462*, 651–655.

Seamon, K.B., Padgett, W., and Daly, J.W. (1981). Forskolin: Unique Diterpene Activator of Adenylate Cyclase in Membranes and in Intact Cells. Proceedings of the National Academy of Sciences *78*, 3363–3367.

Seibert, K., Zhang, Y., Leahy, K., Hauser, S., Masferrer, J.L., Perkins, W., Lee, L., and Isakson, P. (1994). Pharmacological and Biochemical Demonstration of the Role of Cyclooxygenase 2 in Inflammation and Pain. Proceedings of the National Academy of Sciences *91*, 12013–12017.

Seifert, R., Scholten, A., Gauss, R., Mincheva, A., Lichter, P., and Kaupp, U.B. (1999). Molecular Characterization of a Slowly Gating Human Hyperpolarization-Activated Channel Predominantly Expressed in Thalamus, Heart, and Testis. Proceedings of the National Academy of Sciences *96*, 9391–9396.

Seijffers, R., Mills, C.D., and Woolf, C.J. (2007). ATF3 Increases the Intrinsic Growth State of DRG Neurons to Enhance Peripheral Nerve Regeneration. The Journal of Neuroscience *27*, 7911–7920.

Seltzer, Z., Dubner, R., and Shir, Y. (1990). A Novel Behavioural Model of Neuropathic Pain Disorders Produced in Rats by Partial Sciatic Nerve Injury. Pain *43*, 205–218.

Shamash, S., Reichert, F., and Rotshenker, S. (2002). The Cytokine Network of Wallerian Degeneration: Tumor Necrosis Factor-α, Interleukin-1α, and Interleukin-1β. The Journal of Neuroscience *22*, 3052–3060.

Sharma, S.K., Klee, W.A., and Nirenberg, M. (1977). Opiate-Dependent Modulation of Adenylate Cyclase. Proceedings of the National Academy of Sciences *74*, 3365.

Sherrington, C.S. (1906). The Integrative Action of the Nervous System (Yale University Press).

Shields, S.D., Ahn, H.-S., Yang, Y., Han, C., Seal, R.P., Wood, J.N., Waxman, S.G., and Dib-Hajj, S.D. (2012). Nav1.8 Expression is Not Restricted to Nociceptors in Mouse Peripheral Nervous System. Pain *153*, 2017–2030.

Shin, K.S., Rothberg, B.S., and Yellen, G. (2001). Blocker State Dependence and Trapping in Hyperpolarization-Activated Cation Channels: Evidence for an Intracellular Activation Gate. The Journal of General Physiology *117*, 91–101.

Shortland, P.J., Baytug, B., Krzyzanowska, A., McMahon, S.B., Priestley, J.V., and Averill, S. (2006). ATF3 Expression in L4 Dorsal Root Ganglion Neurons after L5 Spinal Nerve Transection. European Journal of Neuroscience *23*, 365–373.

Sievers, C., Platt, N., Perry, V.H., Coleman, M.P., and Conforti, L. (2003). Neurites Undergoing Wallerian Degeneration Show an Apoptotic-Like Process with Annexin V Positive Staining and Loss of Mitochondrial Membrane Potential. Neuroscience Research *46*, 161–169.

Silverman, J.D., and Kruger, L. (1990). Selective Neuronal Glycoconjugate Expression in Sensory and Autonomic Ganglia: Relation of Lectin Reactivity to Peptide and Enzyme Markers. Journal of Neurocytology *19*, 789–801.

Song, X.-J., Wang, Z.-B., Gan, Q., and Walters, E.T. (2006). cAMP and cGMP Contribute to Sensory Neuron Hyperexcitability and Hyperalgesia in Rats With Dorsal Root Ganglia Compression. Journal of Neurophysiology *95*, 479–492.

Song, Y., Li, H.-M., Xie, R.-G., Yue, Z.-F., Song, X.-J., Hu, S.-J., and Xing, J.-L. (2012). Evoked Bursting in Injured Aβ Dorsal Root Ganglion Neurons: A Mechanism Underlying Tactile Allodynia. Pain *153*, 657–665.

Southall, M.D., and Vasko, M.R. (2001). Prostaglandin Receptor Subtypes, EP3C and EP4, Mediate the Prostaglandin E2-induced cAMP Production and Sensitization of Sensory Neurons. The Journal of Biological Chemistry *276*, 16083–16091.

Sowa, N.A., Street, S.E., Vihko, P., and Zylka, M.J. (2010). Prostatic Acid Phosphatase Reduces Thermal Sensitivity and Chronic Pain Sensitization by Depleting Phosphatidylinositol 4,5-Bisphosphate. The Journal of Neuroscience *30*, 10282–10293.

Spitzer, N.C. (2006). Electrical Activity in Early Neuronal Development. Nature *444*, 707–712.

Starowicz, K., Cristino, L., and Di Marzo, V. (2008). TRPV1 Receptors in the Central Nervous System: Potential for Previously Unforeseen Therapeutic Applications. Current Pharmaceutical Design *14*, 42–54.

Stefanini, M., De Martino, C., and Zamboni, L. (1967). Fixation of Ejaculated Spermatozoa for Electron Microscopy. Nature *216*, 173–174.

Stein, C., and Machelska, H. (2011). Modulation of Peripheral Sensory Neurons by the Immune System: Implications for Pain Therapy. Pharmacological Reviews *63*, 860–881.

Stevens, D.R., Seifert, R., Bufe, B., Müller, F., Kremmer, E., Gauss, R., Meyerhof, W., Kaupp, U.B., and Lindemann, B. (2001). Hyperpolarization-Activated Channels HCN1 and HCN4 Mediate Responses to Sour Stimuli. Nature *413*, 631–635.

Stieber, J., Stöckl, G., Herrmann, S., Hassfurth, B., and Hofmann, F. (2005). Functional Expression of the Human HCN3 Channel. The Journal of Biological Chemistry *281*, 34635–34634643.

Stoll, G., Griffin, J.W., Li, C.Y., and Trapp, B.D. (1989). Wallerian Degeneration in the Peripheral Nervous System: Participation of Both Schwann Cells and Macrophages in Myelin Degradation. Journal of Neurocytology *18*, 671–683.

Story, G.M., Peier, A.M., Reeve, A.J., Eid, S.R., Mosbacher, J., Hricik, T.R., Earley, T.J., Hergarden, A.C., Andersson, D.A., Hwang, S.W., et al. (2003). ANKTM1, a TRP-like Channel Expressed in Nociceptive Neurons, Is Activated by Cold Temperatures. Cell *112*, 819–829.

Stucky, C.L., and Lewin, G.R. (1999). Isolectin B_4-Positive and -Negative Nociceptors are Functionally Distinct. The Journal of Neuroscience *19*, 6497–6505.

Stucky, C.L., Dubin, A.E., Jeske, N.A., Malin, S.A., McKemy, D.D., and Story, G.M. (2009). Roles of Transient Receptor Potential Channels in Pain. Brain Research Reviews *60*, 2–23.

Sugimoto, Y., and Narumiya, S. (2006). Prostaglandin E Receptors. Journal of Biological Chemistry *282*, 11613–11617.

Suh, B.-C., and Hille, B. (2008). PIP_2 Is a Necessary Cofactor for Ion Channel Function: How and Why? Annual Reviews of Biophysics *37*, 175–195.

Sukhotinsky, I., Ben-Dor, E., Raber, P., and Devor, M. (2004). Key Role of the Dorsal Root Ganglion in Neuropathic Tactile Hypersensibility. European Journal of Pain *8*, 135–143.

Swanson, D.M., Dubin, A.E., Shah, C., Nasser, N., Chang, L., Dax, S.L., Jetter, M., Breitenbucher, J.G., Liu, C., Mazur, C., et al. (2005). Identification and Biological Evaluation of 4-(3-Trifluoromethylpyridin-2-yl)piperazine-1-carboxylic Acid (5-Trifluoromethylpyridin-2-yl)amide, a High Affinity TRPV1 (VR1) Vanilloid Receptor Antagonist. Journal of Medicinal Chemistry *48*, 1857–1872.

Szallasi, A., Cortright, D.N., Blum, C.A., and Eid, S.R. (2007). The Vanilloid Receptor TRPV1: 10 Years from Channel Cloning to Antagonist Proof-of-Concept. Nature Reviews: Drug Discovery *6*, 357–372.

Taiwo, Y.O., Coderre, T.J., and Levine, J.D. (1989). The Contribution of Training to Sensitivity in the Nociceptive Paw-Withdrawal Test. Brain Research *487*, 148–151.

Takahashi, M., Kawaguchi, M., Shimada, K., Konishi, N., Furuya, H., and Nakashima, T. (2004). Cyclooxygenase-2 Expression in Schwann Cells and Macrophages in the Sciatic Nerve After Single Spinal Nerve Injury in Rats. Neuroscience Letters *363*, 203–206.

Takahashi, Y., Nakajima, Y., and Sakamoto, T. (1994). Dermatome Mapping in the Rat Hindlimb by Electrical Stimluation of the Spinal Nerves. Neuroscience Letters *168*, 85–88.

Takashima, Y., Daniels, R.L., Knowlton, W., Teng, J., Liman, E.R., and McKemy, D.D. (2007). Diversity in the Neural Circuitry of Cold Sensing Revealed by Genetic Axonal Labeling of Transient Receptor Potential Melastatin 8 Neurons. The Journal of Neuroscience *27*, 14147–14157.

Takasu, K., Ono, H., and Tanabe, M. (2010). Spinal hyperpolarization-activated cyclic nucleotide-gated cation channels at primary afferent terminals contribute to chronic

pain. Pain *151*, 87–96.

Talavera, K., Nilius, B., and Voets, T. (2008). Neuronal TRP Channels: Thermometers, Pathfinders and Life-Savers. Trends in Neurosciences *31*, 287–295.

Tandrup, T. (1993). A Method for Unbiased and Efficient Estimation of Number and Mean Volume of Specified Neuron Subtypes in Rat Dorsal Root Ganglion. The Journal of Comparative Neurology *329*, 269–276.

Taraska, J.W., and Zagotta, W.N. (2007). Structural Dynamics in the Gating Ring of Cyclic Nucleotide–Gated Ion Channels. Nature Structural and Molecular Biology *14*, 854–860.

Thacker, M.A., Clark, A.K., Marchand, F., and McMahon, S.B. (2007). Pathophysiology of Peripheral Neuropathic Pain: Immune Cells and Molecules. Anesthesia & Analgesia *105*, 838–847.

Theile, J.W., and Cummins, T.R. (2011). Recent Developments Regarding Voltage-Gated Sodium Channel Blockers for the Treatment of Inherited and Acquired Neuropathic Pain Syndromes. Frontiers in Pharmacology of Ion Channels and Channelopathies *2*, 1–14.

Thippeswamy, T., Jain, R.K., Mumtaz, N., and Morris, R. (2001). Inhibition of Neuronal Nitric Oxide Synthase Results in Neurodegenerative Changes in the Axotomised Dorsal Root Ganglion Neurons: Evidence for a Neuroprotective Role of Nitric Oxide In Vivo. Neuroscience Research *40*, 37–44.

Thoenen, H. (1995). Neurotrophins and Neuronal Plasticity. Science *270*, 593–598.

Thollon, C., Cambarrat, C., Vian, J., Prost, J.-F., Peglion, J.L., and Vilaine, J.P. (1994). Electrophysiological Effects of S 16257, a Novel Sino-Atrial Node Modulator, on Rabbit and Guinea-Pig Cardiac Preparations: Comparison with UL-FS 49. British Journal of Pharmacology *112*, 37–42.

Todd, A.J. (2010). Neuronal Circuitry for Pain Processing in the Dorsal Horn. Nature Reviews: Neuroscience *11*, 823–836.

Tokimasa, T., and Akasu, T. (1990). Cyclic AMP Regulates an Inward Rectifying Sodium-Potassium Current in Dissociated Bull-Frog Sympathetic Neurones. The Journal of Physiology *420*, 409–429.

Tominaga, M., and Caterina, M.J. (2004). Thermosensation and Pain. Journal of Neurobiology *61*, 3–12.

Tominaga, M., Caterina, M.J., Malmberg, A.B., Rosen, T.A., Gilbert, H., Skinner, K., Raumann, B.E., Basbaum, A.I., and Julius, D. (1998). The Cloned Capsaicin Receptor Integrates Multiple Pain-Producing Stimuli. Neuron *21*, 531–543.

Tramèr, M.R., Moore, R.A., and McQuay, H.J. (1997). Propofol and Bradycardia: Causation, Frequency and Severity. British Journal of Anaesthesia *78*, 642–651.

Trebino, C.E., Stock, J.L., Gibbons, C.P., Naiman, B.M., Wachtmann, T.S., Umland, J.P., Pandher, K., Lapointe, J.-M., Saha, S., Roach, M.L., et al. (2003). Impaired Inflammatory and Pain Responses in Mice Lacking an Inducible Prostaglandin E Synthase. Proceedings of the National Academy of Sciences *100*, 9044–9049.

Treede, R.-D., Jensen, T.S., Campbell, J.N., Cruccu, G., Dostrovsky, J.O., Griffin, J.W., Hansson, P., Hughes, R., Nurmikko, T., and Serra, J. (2008). Neuropathic Pain: Redefinition and a Grading System for Clinical and Research Purposes. Neurology *70*, 1630–1635.

Trelle, S., Reichenbach, S., Wandel, S., Hildebrand, P., Tschannen, B., Villiger, P.M., Egger, M., and Jüni, P. (2011). Cardiovascular Safety of Non-Steroidal Anti-Inflammatory Drugs: Network Meta-Analysis. British Medical Journal *342*, 1–11.

Trowbridge, H.O., and Emling, R.C. (1997a). Acute Inflammatory Process. In Inflammation, B. Solaro, ed. (London: Quintessence Publishing Co, Inc), pp. 1–18.

Trowbridge, H.O., and Emling, R.C. (1997b). Chronic Inflammatory Processes. In Inflammation, B. Solaro, ed. (London: Quintessence Publishing Co, Inc), pp. 129–145.

Tsujino, H., Konodo, E., Fukuoka, T., Dai, Y., Tokunaga, A., Miki, K., Yonenobu, K., Ochi, T., and Noguchi, K. (2000). Activating Transcription Factor 3 (ATF3) Induction by Axotomy in Sensory and Motoneurons: A Novel Neuronal Marker of Nerve Injury. Molecular and Cellular Neuroscience *15*, 170–182.

Turk, D.C. (2002). Clinical Effectiveness and Cost-Effectiveness of Treatments for Patients With Chronic Pain. The Clinical Journal of Pain *18*, 355–355365.

Udina, E., Furey, M., Busch, S., Silver, J., Gordon, T., and Fouad, K. (2008). Electrical Stimulation of Intact Peripheral Sensory Axons in Rats Promotes Outgrowth of their Central Projections. Experimental Neurology *210*, 238–247.

Ulens, C., and Tytgat, J. (2000). Functional Heteromerization of HCN1 and HCN2 Pacemaker Channels. The Journal of Biological Chemistry *276*, 6069–6072.

Ulmann, L., Hirbec, H., and Rassendren, F. (2010). $P2X_4$ Receptors Mediate PGE_2 Release by Tissue-Resident Macrophages and Initiate Inflammatory Pain. The EMBO Journal *29*, 2290–2300.

Vahle-Hinz, C., and Detsch, O. (2002). What Can *in vivo* Electrophysiology in Animal Models Tell us About Mechanisms of Anaesthesia? British Journal of Anaesthesia *89*, 123–142.

Valenzuela, C., Delpon, E., Tamkun, M.M., Tamargo, J., and Snyders, D.J. (1995). Stereoselective Block of a Human Cardiac Potassium Channel (Kv1.5) by Bupivacaine Enantiomers. Biophysical Journal *69*, 418–427.

Vane, J.R., Bakhle, Y.S., and Botting, R.M. (1998). Cyclooxygenases 1 and 2. Annual Review of Pharmacology and Toxicology *38*, 97–120.

Vasilyev, D.V., Shan, Q., Lee, Y., Mayer, S.C., Bowlby, M.R., Strassle, B.W., Kaftan, E.J., Rogers, K.E., and Dunlop, J. (2007). Direct Inhibition of Ih by Analgesic Loperamide in Rat DRG Neurons. Journal of Neurophysiology *97*, 3713–3721.

Vay, L., Gu, C., and McNaughton, P.A. (2012). The Thermo-TRP Ion Channel Family: Properties and Therapeutic Implications. British Journal of Pharmacology *165*, 787–801.

Vierck, C.J., Hansson, P.T., and Yezierski, R.P. (2008). Clinical and Pre-Clinical Pain

Assessment: Are we Measuring the Same Thing? Pain *135*, 7–10.

Vilceanu, D., and Stucky, C.L. (2010). TRPA1 Mediates Mechanical Currents in the Plasma Membrane of Mouse Sensory Neurons. PLoS ONE *5*, e12177.

Villière, V., and McLachlan, E.M. (2002). Electrophysiological Properties of Neurons in Intact Rat Dorsal Root Ganglia Classified by Conduction Velocity and Action Potential Duration. The Journal of Neurophysiology *76*, 1924–1941.

Vo, T., Rice, A.S.C., and Dworkin, R.H. (2009). Non-Steroidal Anti-Inflammatory Drugs for Neuropathic Pain: How do we Explain Continued Widespread Use? Pain *143*, 169–171.

Waddell, P.J., Lawson, S.N., and McCarthy, P.W. (1989). Conduction Velocity Changes Along the Processes of Rat Primary Sensory Neurons. Neuroscience *30*, 577–584.

Wahl-Schott, C., Baumann, L., Zong, X., and Biel, M. (2005). An Arginine Residue in the Pore Region Is a Key Determinant of Chloride Dependence in Cardiac Pacemaker Channels. The Journal of Biological Chemistry *280*, 13694–13700.

Wainger, B.J., DeGennaro, M., Santoro, B., Siegelbaum, S.A., and Tibbs, G.R. (2001). Molecular Mechanism of cAMP Modulation of HCN Pacemaker Channels. Nature *411*, 805–810.

Wall, P.D., and Gutnick, M. (1974). Properties of Afferent Nerve Impulses Originating from a Neuroma. Nature *248*, 740–743.

Walters, E.T. (2007). Evolutionary Aspects of Pain. In The Senses: a Comprehensive Review, A.I. Basbaum, ed. (London: Academic Press), pp. 175–184.

Wang, H., and Woolf, C.J. (2005). Pain TRPs. Neuron *46*, 9–12.

Wang, J., Chen, S., and Siegelbaum, S.A. (2001). Regulation of Hyperpolarization-Activated HCN Channel Gating and cAMP Modulation due to Interactions of COOH Terminus and Core Transmembrane Regions. The Journal of General Physiology *118*, 237–250.

Wang, Z., Van Den Berg, R.J., and Ypey, D.L. (1997). Hyperpolarization-Activated Currents in the Growth Cone and Soma of Neonatal Rat Dorsal Root Ganglion Neurons in Culture. Journal of Neurophysiology *78*, 177–186.

Watkins, L.R., and Maier, S.F. (2002). Beyond Neurons: Evidence That Immune and Glial Cells Contribute to Pathological Pain States. Physiological Reviews *82*, 891–1011.

Waxman, S.G. (2001). Transcriptional Channelopathies: An Emerging Class of Disorders. Nature Reviews: Neuroscience *2*, 652–659.

Waxman, S.G., Kocsis, J.D., and Black, J.A. (1994). Sodium Channel mRNA Is Expressed in Embryonic But Not Adult Spinal Sensory Neurons, and Is Reexpressed Following Axotomy. Journal of Neurophysiology *72*, 466–470.

Weidnar, C., Schmelz, M., Schmidt, R., Hansson, B., Handwerker, H.O., and Torebjörk, H.E. (1999). Functional Attributes Discriminating Mechano-Insensitive and Mechano-Responsive C Nociceptors in Human Skin. The Journal of Neuroscience *19*, 10184–10190.

Wells, J.E., Rowland, K.C., and Proctor, E.K. (2007). Hyperpolarization-Activated Channels in Trigeminal Ganglia Innervating Healthy and Pulp-Exposed Teeth. International Endodontic Journal *40*, 715–721.

Weng, X., Smith, T., Sathish, J., and Djouhri, L. (2012). Chronic Inflammatory Pain is Associated with Increased Excitability and Hyperpolarization-Activated Current (I_h) in C- but not Aδ-Nociceptors. Pain *153*, 900–914.

Werner, S., and Grose, R. (2003). Regulation of Wound Healing by Growth Factors and Cytokines. Physiolgical Reviews *83*, 836–870.

Whitaker, G.M., Angoli, D., Nazzari, H., Shigemoto, R., and Accili, E.A. (2007). HCN2 and HCN4 Isoforms Self-assemble and Co-assemble with Equal Preference to Form Functional Pacemaker Channels. The Journal of Biological Chemistry *282*, 22900–22909.

Whiteside, G.T., Adedoyin, A., and Leventhal, L. (2008). Predictive Validity of Animal Pain Models? A Comparison of the Pharmacokinetic–Pharmacodynamic Relationship for Pain Drugs in Rats and Humans. Neuropharmacology *54*, 767–775.

Wickenden, A.D., Maher, M.P., and Chaplan, S.R. (2009). HCN Pacemaker Channels and Pain: A Drug Discovery Perspective. Current Pharmaceutical Design *15*, 2149–2168.

Willis, W.D., and Westlund, K.H. (1997). Neuroanatomy of the Pain System and of the Pathways that Modulate Pain. Journal of Clinical Neurophysiology *14*, 2–31.

Willis, W.D., Trevino, D.L., Coulter, J.D., and Maunz, R.A. (1974). Responses of Primate Spinothalamic Tract Neurons to Natural Stimulation of Hindlimb. Journal of Neurophysiology *37*, 358–372.

Wilson, S.G., and Mogil, J.S. (2001). Measuring Pain in the (Knockout) Mouse: Big Challenges in a Small Mammal. Behavioural Brain Research *125*, 65–73.

Wise, H. (2006). Lack of Interaction Between Prostaglandin E_2 Receptor Subtypes in Regulating Adenylyl Cyclase Activity in Cultured Rat Dorsal Root Ganglion Cells. European Journal of Pharmacology *535*, 69–77.

Wolf, S.E., and Woodside, K.J. (2005). Transgenic and Gene Knock-out Techniques and Burn Research. Journal of Surgical Research *123*, 328–339.

Wolfe, F., and Hawley, D.J. (1985). Remission in Rheumatoid Arthritis. The Journal of Rheumatology *12*, 245–252.

Woolf, C.J., and Costigan, M. (1999). Transcriptional and Posttranslational Plasticity and the Generation of Inflammatory Pain. Proceedings of the National Academy of Sciences *96*, 7723–7730.

Woolf, C.J., and Ma, Q. (2007). Nociceptors—Noxious Stimulus Detectors. Neuron *55*, 353–364.

Woolf, C.J., and Salter, M.W. (2000). Neuronal Plasticity: Increasing the Gain in Pain. Science *288*, 1765–1768.

Woolf, C.J., and Wiesenfeld-Hallin, Z. (1986). Substance P and Calcitonin Gene-Related

Peptide Synergistically Modulate the Gain of the Nociceptive Flexor Withdrawal Reflex in the Rat. Neuroscience Letters *66*, 226–230.

Wu, G., Ringkamp, M., Hartke, T.V., Murinson, B.B., Campbell, J.N., Griffin, J.W., and Meyer, R.A. (2001). Early Onset of Spontaneous Activity in Uninjured C-Fiber Nociceptors after Injury to Neighboring Nerve Fibers. The Journal of Neuroscience *21*, 1–5.

Wu, G., Ringkamp, M., Murinson, B.B., Pogatzki, E.M., Hartke, T.V., Weerahandi, H.M., Campbell, J.N., Griffin, J.W., and Meyer, R.A. (2002). Degeneration of Myelinated Efferent Fibers Induces Spontaneous Activity in Uninjured C-Fiber Afferents. The Journal of Neuroscience *22*, 7746–7753.

Wu, J.-Y., and Cohen, I.S. (1997). Tyrosine Kinase Inhibition Reduces I_f in Rabbit Sinoatrial Node Myoctes. Pflügers Archive - European Journal of Physiology *434*, 509–514.

Xie, W., Strong, J.A., Meij, J.T.A., Zhang, J.-M., and Yu, L. (2005). Neuropathic Pain: Early Spontaneous Afferent Activity is the Trigger. Pain *116*, 243–256.

Xue, T., Marbán, E., and Li, R.A. (2002). Dominant-Negative Suppression of HCN1- and HCN2-Encoded Pacemaker Currents by an Engineered HCN1 Construct: Insights Into Structure-Function Relationships and Multimerization. Circulation Research *90*, 1267–1273.

Yagi, J., and Sumino, R. (1998). Inhibition of a Hyperpolarization-Activated Current by Clonidine in Rat Dorsal Root Ganglion Neurons. Journal of Neurophysiology *80*, 1094–1104.

Yaksh, T.L., Dirig, D.M., Conway, C.M., Svensson, C., Luo, Z.D., and Isakson, P.C. (2001). The Acute Antihyperalgesic Action of Nonsteroidal, Anti- Inflammatory Drugs and Release of Spinal Prostaglandin E_2 is Mediated by the Inhibition of Constitutive Spinal Cyclooxygenase-2 (COX-2) but not COX-1. The Journal of Neuroscience *21*, 5847–5853.

Yamakawa, K., Kamekura, S., Kawamura, N., Saegusa, M., Kamei, D., Murakami, M., Kudo, I., Uematsu, S., Akira, S., Chung, U.-I., et al. (2008). Association of Microsomal Prostaglandin E Synthase 1 Deficiency with Impaired Fracture Healing, but not with Bone Loss or Osteoarthritis, in Mouse Models of Skeletal Disorders. Arthritis Rheum *58*, 172–183.

Yanagihara, K., and Irisawa, H. (1980). Inward Current Activated During Hyperpolarization in the Rabbit Sinoatrial Node Cell. Pflügers Archive *385*, 11–19.

Yao, H., Donnelly, D.F., Ma, C., and LaMotte, R.H. (2003). Upregulation of the Hyperpolarization-Activated Cation Current after Chronic Compression of the Dorsal Root Ganglion. The Journal of Neuroscience *23*, 2069–2074.

Yoon, Y.W., Na, H.S., and Chung, J.M. (1996). Contributions of Injured and Intact Afferents to Neuropathic Pain in an Experimental Rat Model. Pain *64*, 27–36.

Yu, C.R., Power, J., Barnea, G., O'Donnell, S., Brown, H.E.V., Osborne, J., Axel, R., and Gogos, J.A. (2004). Spontaneous Neural Activity is Required for the Establishment and Maintenance of the Olfactory Sensory Map. Neuron *42*, 553–566.

Yu, F.H., Yarov-Yarovoy, V., Gutman, G.A., and Catterall, W.A. (2005). Overview of Molecular Relationships in the Voltage-Gated Ion Channel Superfamily. Pharmacological Reviews *57*, 387–395.

Zagotta, W.N., Olivier, N.B., Black, K.D., Young, E.C., Olson, R., and Gouaux, E. (2003). Structural Basis for Modulation and Agonist Specificity of HCN Pacemaker Channels. Nature *425*, 200–205.

Zerial, M., and McBride, H. (2001). Rab Proteins as Membrane Organizers. Nature Reviews: Molecular Cell Biology *2*, 107–117.

Zhang, H., Craciun, L.C., Mirshahi, T., Rohács, T., Lopes, C.M.B., Jin, T., and Logothetis, D.E. (2003). Activates KCNQ Channels, and Its Hydrolysis Underlies Receptor-Mediated Inhibition of M Currents. Neuron *37*, 963–975.

Zhang, X.-F., Chen, J., Faltynek, C.R., Moreland, R.B., and Neelands, T.R. (2008). Transient Receptor Potential A1 Mediates an Osmotically Activated Ion Channel. European Journal of Neuroscience *27*, 605–611.

Zheng, J.-H., Walters, E.T., and Song, X.-J. (2007). Dissociation of Dorsal Root Ganglion Neurons Induces Hyperexcitability That Is Maintained by Increased Responsiveness to cAMP and cGMP. Journal of Neurophysiology *97*, 15–25.

Zhou, L., and Siegelbaum, S.A. (2007). Gating of HCN Channels by Cyclic Nucleotides: Residue Contacts that Underlie Ligand Binding, Selectivity, and Efficacy. Structure *15*, 655–670.

Zimmermann, K., Hein, A., Hager, U., Kaczmarek, J.S., Turnquist, B.P., Clapham, D.E., and Reeh, P.W. (2009). Phenotyping Sensory Nerve Endings *in vitro* in the Mouse. Nature Protocols *4*, 174–196.

Zochodne, D.W., Levy, D., Zwiers, H., Sun, H., Rubin, I., Chen, C., and Lauritzen, M. (1999). Evidence for Nitric Oxide and Nitric Oxide Synthase Activity in Proximal Stumps of Transected Peripheral Nerves. Neuroscience *91*, 1515–1527.

Zolles, G., Klöcker, N., Wenzel, D., Weisser-Thomas, J., Fleischmann, B.K., Roeper, J., and Fakler, B. (2006). Pacemaking by HCN Channels Requires Interaction with Phosphoinositides. Neuron *52*, 1027–1036.

Zolles, G., Wenzel, D., Bildl, W., Schulte, U., Hofmann, A., MUller, C.S., Thumfart, J.-O., Vlachos, A., Deller, T., Pfeifer, A., *et al.* (2009). Association with the Auxiliary Subunit PEX5R/Trip8b Controls Responsiveness of HCN Channels to cAMP and Adrenergic Stimulation. Neuron *62*, 814–825.

Zong, X., Eckert, C., Yuan, H., Wahl-Schott, C., Abicht, H., Fang, L., Li, R., Mistrík, P., Gerstner, A., Much, B., et al. (2005). A Novel Mechanism of Modulation of Hyperpolarization-activated Cyclic Nucleotide-gated Channels by Src Kinase. The Journal of Biological Chemistry *280*, 34224–34232.

Zong, X., Stieber, J., Ludwig, A., Hofmann, F., and Biel, M. (2001). A Single Histidine Residue Determines the pH Sensitivity of the Pacemaker Channel HCN2. The Journal of Biological Chemistry *276*, 6313–6319.

Zucker, R.S., and Regehr, W.G. (2002). Short-Term Synaptic Plasticity. Annual Reviews of Physiology *64*, 355–405.

Zylka, M.J., Rice, F.L., and Anderson, D.J. (2005). Topographically Distinct Epidermal Nociceptive Circuits Revealed by Axonal Tracers Targeted to Mrgprd. Neuron *45*, 17–25.

Appendix 1

Approved Schedule 1 Methods

Animals (Scientific Procedures) Act 1986 (c. 14)
SCHEDULE 1 – APPROPRIATE METHODS OF HUMANE KILLING Document Generated: 2012-04-22
***Changes to legislation:** There are outstanding changes not yet made by the legislation.gov.uk editorial team to Animals (Scientific Procedures) Act 1986. Any changes that have already been made by the team appear in the content and are referenced with annotations. (See end of Document for details)*

Method	*Animals for which appropriate*
Animals other than foetal, larval and embryonic forms	
1.Overdose of an anaesthetic using a route and an anaesthetic agent appropriate for the size and species of animal.	All animals.
2. Exposure to carbon dioxide gas in a rising concentration.	Rodents, rabbits and birds up to 1.5kg
3. Dislocation of the neck.	Rodents up to 500g Rabbits up to 1kg Birds up to 3kg
4. Concussion of the brain by striking the cranium	Rodents and rabbits up to 1kg Birds up to 250g Amphibians and reptiles up to 1kg (with destruction of the brain before the return of consciousness) Fishes (with destruction of the brain before the return of consciousness)
5. One of the recognised methods of slaughter set out below which is appropriate to the animal and is performed by a registeredd veterinary surgeon, or, in the case of the methods described in paragraph (ii) below, performed by the holder of a current licence granted under the Welfare of Animals (Slaughter or Killing) Regulations 1995 i) Destruction of the brain by free bullet, or, ii) captive bolt, percussion or electrical stunning followed by destruction of the brain or exsanguination before return to consciousness	Ungulates

Method	*Animals for which appropriate*
For foetal, larval and embryonic forms	
1. Overdose of an anaesthetic using a route and anaesthetic agent appropriate for the size, stage of development and species of animal.	All animals.

2. Refrigeration, or disruption of membranes, or maceration in apparatus approved under appropriate slaughter legislation, or exposure to carbon dioxide in near 100% concentration until they are dead.	Birds Reptiles
3. Cooling of foetuses followed by immersion in cold tissue fixative	Mice, Rats and Rabbits
4. Decapitation	Mammals and birds up to 50g

Appendix 2

Immunofluorescent Study of DRG Neurons in Control and CFA

1. Remove the slides from the freezer (~ -20°C).
2. Insert the slides into a slide rack that fits into a 200 ml slide bath.
3. Then submerge the slide rack in 200 ml of 0.01 M PBS and wash for 10-25 minutes. *This step is to remove unbound fixative and excess Optimal Cutting Temperature (OCT) compound.*
    a. Phosphate Buffered Saline (3 L of 0.01 M):
        i. 3.45 g of Dibasic Sodium Phosphate (Na_2HPO_4; FW 142).
        ii. 0.76 g of Monobasic Sodium Phosphate ($NaH_2PO_4*H_2O$; FW 138).
        iii. 27.00 g of Sodium Chloride (NaCl; FW 58.44).
        iv. 0.6 g of Potassium Chloride (KCl; FW 74.55).
4. Repeat Step 3, 3 times.
5. If the tissue was cut 10 µm thick, submerge all of the slides in Triton solution for 20 minutes. *This step is to gently perforate the tissue by slightly dissolving the membrane to allow easier access for the antibodies.*
    a. Triton Solution (200 ml of 0.25% in 0.01 M PBS):
        i. 0.5 ml Triton X-100 ($C_{14}H_{22}O(C_2H_4O)$ n (n = 9-10); X100; Sigma-Aldrich, U.K.).
        ii. 199.5 ml of 0.01 M PBS.
6. Wash all of the slides 2 times for 10-20 minutes each, using fresh 0.01 M PBS each time.
7. Dry the back side of each slide using tissues and dry the front of the slide, if possible, making sure not to remove any of the tissue, but don't spend so long that the tissue dries out.
8. Use a hydrophobic barrier pen (H-4000; Vector Laboratories, CA) and draw a complete line around the outside of the slide, encompassing all of the tissue. *This step is to prevent the solution (typically the antibody) from dripping off of the slides and stay on top of the tissue.*
9. Individually apply the blocking solution to each slide and leave for 20 minutes. *This step is to prevent non-specific binding of either your primary or secondary antibody, by blocking the non-specific binding sites of your antibodies.*
    a. Blocking solution (5% natural donkey serum in 0.01 M PBS):
        i. 0.5 ml Donkey Serum (AS-228/100; Labtech International, U.K.)
        ii. 9.5 ml of 0.01 M PBS.
10. Wash 2 times for 10-20 minutes each, using fresh PBS each time.
11. Dilute the primary antibody for antigen 1 (HCN1-3) using a non-triton diluting solution:
    a. Non-Triton Diluting Solution:
        i. 0.01 M PBS.

ii. 0.25% Sodium Azide (71290; Sigma-Aldrich, U.K.).
iii. 2.5% natural donkey serum (see above from Labtech International).

b. HCN Antibodies (Alomone Laboratories, Israel):
i. HCN1 [1:1000] (APC-056).
ii. HCN2 [1:200] (APC-030).
iii. HCN3 [1:1000] (APC-057).

12. Prepare the humidifier by soaking the tissue at the bottom with distilled water. *This will help prevent the tissue from drying out.*
13. After the majority (but not all) of the PBS solution has dried from the slides, pipette 100-200 µl of primary antibody for antigen 1 onto the tissue and ensure that it stays within the barriers created by the hydrophobic pen.
14. Carefully place the slide in the humidifier, making sure it sits level so the antibody won't slide off.
15. Then, place the humidifier in the fridge (4°C), cover with a piece of blue roll and leave overnight. *This step is to protect and prevent the tissue from drying out.*
16. The following day, wash 4 times for 10-25 minutes each, using fresh PBS each time. *This step is to wash off any excess antibody.*
17. Apply 100 µl of secondary antibody to each slide and place each slide in the humidifier, in the fridge (4°C) for 1-2 hours.
    a. Secondary for A1: Anti-rabbit Dylight 594 [1:250] (711-515-152; Stratech Scientific Ltd., U.K.).
18. After 1-2 hours, wash 4 times for 10-25 minutes each, using fresh PBS each time.
19. If double staining, repeat steps 11-18 for Antigen 2 (A2).
    a. Primary for A2: IB4 [1:1000] (L2140; Sigma-Aldrich, U.K.).
    b. Secondary for A2: Streptavidin DTAF [1:400] (016-010-084; Stratech Scientific Ltd., U.K.).
20. If applying DAPI [1:5000] (D9542, Sigma-Aldrich, U.K.), then apply 100-200 µl onto the slide.
21. Wash 4 times for 10-25 minutes each, using fresh PBS each time.
22. Wash once in distilled water for 20 minutes. *This step is to wash the salts (PBS) off of the tissue.*
23. Allow the slides to almost completely air dry.
24. Then, apply one drop of Vectashield Mounting Medium (H-1000; Vector Laboratories, California) to the middle of the slide. *This medium enhances and preserves the fluorescent dyes.*
25. Use forceps to gently lower a cover-slip onto the top of the tissue to avoid creating air-bubbles and then view under the microscope.

Appendix 3

Immunofluorescent Study of Lumbar Enlargement of Spinal Cord in Control and CFA

1. The tissue, cut to 40 µm, should be in test tubes filled with 0.01 M PBS. *This step is to remove unbound fixative and excess Optimal Cutting Temperature (OCT) compound.*
    a. Phosphate Buffered Saline (3 L of 0.01 M):
        i. 3.45 g of Dibasic Sodium Phosphate (Na_2HPO_4; FW 142).
        ii. 0.76 g of Monobasic Sodium Phosphate ($NaH_2PO_4*H_2O$; FW 138).
        iii. 27.00 g of Sodium Chloride (NaCl; FW 58.44).
        iv. 60 g of Potassium Chloride (KCl; FW 74.55).
2. Repeat Step 1, 3 times.
3. Wash with 50% Ethanol in distilled water for 10 minutes. *This aids penetration of the antibody.*
4. Apply the blocking solution to each tube and leave for 20 minutes. *This step is to prevent non-specific binding of either your primary or secondary antibody, by blocking the non-specific binding sites of your antibodies.*
    a. Blocking solution (5% natural donkey serum in 0.01 M PBS):
        i. 0.5 ml Donkey Serum (AS-228/100; Labtech International, U.K.)
        ii. 9.5 ml of 0.01 M PBS.
5. Dilute the primary antibody for antigen 1 (HCN1-3) using a triton diluting solution:
    a. Triton Diluting Solution:
        i. 0.01 M PBS.
        ii. 0.25% Sodium Azide (71290; Sigma-Aldrich, U.K.).
        iii. 2.5% natural donkey serum (see above from Labtech International).
        iv. 0.5% Triton X-100 solution ($C_{14}H_{22}O(C_2H_4O)$ n (n = 9-10); X100, Sigma-Aldrich, U.K.).
    b. HCN Antibodies (Alomone Laboratories, Israel):
        i. HCN1 [1:1000] (APC-056).
        ii. HCN2 [1:200] (APC-030).
        iii. HCN3 [1:1000] (APC-057).
6. Pipette 100 µl of primary antibody for antigen 1 into the test tubes.
7. Place the test tube holder in the fridge (4°C), cover with a piece of blue roll and leave overnight. *This step is to protect the tissue.*
8. The following day, wash 3 times for 10-25 minutes each, using fresh PBS each time. *This step is to wash off any excess antibody.*
9. Apply 100 µl of secondary antibody to each test tube and place in the test tube holder, before covering this with blue roll and placing in the fridge (4°C) for 1-2 hours.
    a. Secondary for A1: Anti-rabbit Dylight 594 [1:250] (711-515-152; Stratech Scientific Ltd., U.K.)

10. After 1-2 hours, wash 3 times for 10-25 minutes each, using fresh PBS each time.
11. If double staining, repeat steps 5-10 for Antigen 2 (A2).
    a. Primary for A2:
        i. IB4 [1:1000] (L2140; Sigma-Aldrich, U.K.).
        ii. CGRP [1:500] (BML-CA1137; Biomol International, U.S.A.).
    b. Secondary for A2:
        i. Streptavidin DTAF [1:400] (016-010-084; Stratech Scientific Ltd., U.K.).
        ii. Anti-sheep FITC [1:500] (713-095-147; Jackson Immunoresearch, U.S.A.).
12. Wash once in distilled water for 20 minutes. *This step is to wash the salts (PBS) off of the tissue.*
13. Then, pour a single test tube into a petri dish and using fine brushes, carefully place the tissue on labelled slides.
14. Once all the tissue has been placed on the slide, apply one drop of Vectashield Mounting Medium (H-1000; Vector Laboratories, California) to the middle of the slide. *This medium enhances and preserves the fluorescent dyes.*
15. Using forceps, gently lower a cover-slip onto the top of the tissue to avoid creating air-bubbles and then view under the microscope.

Appendix 4

Immunofluorescent Study of DRG neurons after mSHAM and mSNA

1. Make up a stock Phosphate Buffered Saline (PBS) solution (1 L of x10 PBS):
    a. 2.0128 g of Potassium Chloride (KCl; FW 74.55)
    b. 2.0415 g of Monopotassium Phosphate (KH_2PO_4; FW 136.086)
    c. 80.0628 g of Sodium Chloride (NaCl; FW 58.44)
    d. 11.3568 g of Disodium Hydrogen Phosphate (Na_2HPO_4; FW 141.96)
2. Remove the slides from the freezer (~ -20°C).
3. Dry the back side of each slide using tissues and dry the front of the slide, if possible, making sure not to remove any of the tissue, but don't spend so long that the tissue dries out.
4. Use a hydrophobic barrier pen (H-4000; Vector Laboratories, CA) and draw a complete line around the outside of the slide, encompassing all of the tissue. *This step is to prevent the solution (typically the antibody) from dripping off of the slides and stay on top of the tissue.*
5. Add about 3 ml of permeabilising solution to each slide, ensuring that the hydrophobic barrier pen is not breached.
    a. Permeabilising solution (100 ml, pH = 7.4):
        i. 10 ml of x10 PBS
        ii. 0.1 ml of Triton X-11 ($C_{14}H_{22}O(C_2H_4O)$ n (n = 9-10); X100; Sigma-Aldrich, U.K.).
6. Leave for 10 minutes.
7. Rinse each slide with 3 ml of x1 PBS, 3 times, for 5 minutes each.
    a. PBS x1 (100 ml, pH 7.2):
        i. 10 ml of x10 PBS.
        ii. 90 ml of distilled water.
8. Incubate the slides with 200 µl of antibody diluting solution for 30 mins.
    a. Antibody Diluting Solution (10 ml, pH = 7.2):
        i. 9.8 ml of x10 PBS.
        ii. 0.2 ml of Goat Serum (total of 2%) (G9023; Sigma-Aldrich, U.K.).
        iii. 0.1 g Bovine Serum Album (total of 1%) (A2153; Sigma-Aldrich, U.K.).
        iv. 5 µl Triton X-100 (total of 0.05%) ($C_{14}H_{22}O(C_2H_4O)$ n (n = 9-10); X100; Sigma-Aldrich, U.K.).
9. While this 30 minute period is passing, dilute the antibodies in antibody diluting solution.
10. Then, remove the antibody diluting solution, but do not rinse.
11. Apply 100-150 µl of primary antibody pipette for antigen 1 (A1) onto each slide and ensure that the antibody solution stays within the barriers created by the hydrophobic pen.

12. Carefully place the slide in the humidifier, making sure it sits level so the antibody won't slide off.
13. Then, place the humidifier in the fridge (4°C), cover with a piece of blue roll and leave overnight. *This step is to protect and prevent the tissue from drying out.*
14. The following day, wash three times, for ten minutes each, with antibody wash solution:
    a. Antibody Wash Solution (250 ml, pH = 7.2)
        i. 25 ml of x10 PBS.
        ii. 0.125 ml of Triton X-100.
15. Dilute the secondary antibody to A1 in antibody diluting solution.
16. Apply 100-150 µl of secondary antibody pipette for antigen 1 (A1) onto each slide.
    a. Secondary for A1: Anti-rabbit AF 594 [1:500] (A-11037; Molecular Probes, U.K.)
17. Again, ensure that the antibody solution stays within the barriers created by the hydrophobic pen.
18. Carefully place the slide in the humidifier, making sure it sits level so the antibody won't slide off.
19. Cover with a piece of blue roll and leave, at room temperature (~ 23°C) for 1-2 hours.
20. Wash three times, for 10 minutes each, with antibody wash solution. While waiting for the 10 minutes to pass, keep foil on top of the slides. *This protects the secondary antibody from photobleaching. The slides need to be kept protected, for as much of the time as possible, from now until they are photographed under the microscope.*
21. If double staining, repeat steps 10-20 for Antigen 2 (A2).
    a. Primary for A2: IB4 [1:1000] (L2140; Sigma-Aldrich, U.K.).
    b. Secondary for A2: Streptavidin DTAF [1:400] (016-010-084; Stratech Scientific Ltd., U.K.).
22. If applying DAPI [1:5000] (D9542, Sigma-Aldrich, U.K.), then apply 100-200 µl onto the slide.
23. Repeat step 20.
24. Put the slides into a slider holder and dip into 200 ml of distilled water.
25. Repeat step 24.
26. Allow the slides to almost completely air dry.
27. Then, apply one drop of Vectashield Mounting Medium (H-1000; Vector Laboratories, California) to the middle of the slide. *This medium enhances and preserves the fluorescent dyes.*
28. Use forceps to gently lower a cover-slip onto the top of the tissue to avoid creating air-bubbles and then view under the microscope.